SHRP-P-394

Evaluation of the AASHTO Design Equations and Recommended Improvements

Jerome F. Daleiden
J. Brent Rauhut
Brian Killingsworth
Brent Rauhut Engineering Inc.
8240 North Mopac, #220
Austin, Texas 78759

Emmanuel Owusu Antwi
Michael I. Darter
Riaz Ahmad
ERES Consultants, Inc.
8 Dunlap Court
Savoy, Illinois 61874

Strategic Highway Research Program
National Research Council
Washington, DC 1994

SHRP-P-394
ISBN 0-309-05803-1
Product No.: 5000

Program Manager: *Neil F. Hawks*
Project Manager: *A. Robert Raab*
Program Area Secretary: *Cynthia Baker, Francine A. Burgess*
Production Editor: *Michael Jahr*

April 1994

key words:
evaluation of design procedures
flexible pavement design
performance equations
serviceability loss

Strategic Highway Research Program
National Research Council
2101 Constitution Avenue N.W.
Washington, DC 20418

(202) 334-3774

1.5M/NAP/494

Acknowledgments

We wish to acknowledge the valuable review, discussion, and suggestions by the Expert Task Group on Experimental Design and Analysis, the Pavement Performance Advisory Committee, the Strategic Highway Research Program (SHRP) staff, and the SHRP Contract P-001 staff. The many technical memoranda developed by Contract P-001 staff were especially valuable.

The research described herein was supported by SHRP. SHRP, a unit of the National Research Council, was authorized by Section 128 of the Surface Transportation and Uniform Relocation Assistance Act of 1987.

Contents

List of Figures

List of Tables

Abstract

One of the primary objectives of the Strategic Highway Research Program (SHRP) Long-Term Pavement Performance (LTPP) studies is to improve the ability of highway engineers to design new and overlaid pavement structures. The specific analyses discussed in this report were aimed at evaluation of the American Association of State Highway and Transportation Officials (AASHTO) pavement design equations (for both new and overlaid pavements), based on data currently available. These initial analyses confirm that although improvements have been made to the AASHTO design equations over the years, the equations still do not fully explain data from North American pavements.

The evaluation of the 1993 AASHTO overlay equation was severely limited by the lack of (1) distress and serviceability data prior to overlay, (2) knowledge as to design period and liability level sought, and (3) some of the input data required for the design equation (which had to approximate required data based on other available data). The evaluations were inconclusive for asphalt concrete (AC) overlays of AC and unbonded portland cement concrete (PCC) overlays of PCC. For the five test sections used in the evaluation, however, the design equation for AC overlays of PCC appeared to work reasonably well.

These analyses were accomplished on the LTPP data collected through December 1992.

Executive Summary

One of the primary objectives of the Strategic Highway Research Program (SHRP) Long-Term Pavement Performance (LTPP) studies is to improve the ability of highway engineers to design new and overlaid pavement structures. As part of this process, SHRP has contracted for the analysis of data collected to date for 770 in-service sections of highways in the United States and Canada. The specific analyses discussed in this report were aimed at evaluation of the American Association of State Highway and Transportation Officials (AASHTO) pavement design equations (for both new construction and overlaid pavements), based on currently available data.

These initial analyses confirm the belief that the use of the flexible pavement design equation printed in the 1986 AASHTO Design Guide generally represents a serious extrapolation outside the inference space from which the basic equation was derived and that its form does not fit the data from North American flexible pavements. In addition, the equation appears to predict much higher numbers of equivalent single axle loads (ESALs) needed to produce a specific Present Serviceability Index (PSI) loss than occur in reality. Based on backcalculated subgrade moduli, the equation predicted 100 times the estimated ESALs to produce the current loss of PSI for 112 (46%) of the 244 test sections and predicted between 2 and 100 times the estimated ESALs for 97 (40%) others. Based on subgrade resilient moduli available for 106 test sections from laboratory testing, the ratios of predicted to estimated ESALs were reduced to 3% above 100 and 41% between 2 and 100.

The AASHTO Design Guide's rigid pavement design equation was originally developed in 1960 at the conclusion of the American Association of State highway officials (AASHO) Road Test. This model predicts the number of axle loads for a given slab thickness and loss in serviceability. The original model has been extended to include several additional design factors over the last 30 years and has been used by many highway agencies for rigid pavement design. Owing to the limited inference space of the original Road Test model and the subjective nature of the extensions since that time, there is considerable interest in determining the adequacy of the model. The availability of the SHRP LTPP data has finally made an overall evaluation possible.

The evaluation centered around determining the ability of the equation to predict the number of 18 kip (80 kN) ESALs, needed to cause a given loss of serviceability. The results show that the original 1960 model generally overpredicts the number of ESALs necessary for a given loss of serviceability. The many extensions to the original model (drainage, load transfer, strength, etc.) generally improved the predictive accuracy, so the effect was

beneficial to the 1993 equation for design. Statistical studies indicate that the 1993 equation is a reasonably unbiased predictor of cumulative ESALs (about one-half of the predictions were over and one-half were under the estimates of ESALs experienced). However, comparisons with estimated ESALs by the State Highway Agencies (SHAs) showed that the range of predictions varied from a small fraction of the estimated ESALs to more than 10 times the estimates. These results were determined at the 50th percentile (mean) level. If a pavement is designed at a higher level of reliability (such as 95 percent), the 1993 AASHTO design equation will provide a conservative design for a majority of the test sections studied. However, many deficiencies still need to be improved.

The evaluation of the 1993 AASHTO overlay design equations was conducted by comparing the thickness designs from the AASHTO equation with constructed thicknesses. These comparisons also considered measured distress and serviceability levels at the time of comparison. These evaluations were limited by the lack of certain data and were considered inconclusive for asphalt concrete (AC) overlays of AC and unbonded portland cement concrete (PCC) overlays of PCC. For the limited data set of five test sections with sufficient data for evaluation, the design equation appeared to provide adequate overlay thicknesses for AC overlays of PCC.

A number of equations have been developed from the LTPP data for predicting distresses and increases in roughness for the various types of pavements under the traffic and environmental conditions applicable. The eventual uses for such equations are expected to be for design and in pavement management systems. However, the lack of time-sequence data over reasonable time periods (usually one or two data points for this analysis) and other data limitations preclude the use of these equations for design at a sufficient confidence level at this time. They are recommended for use only as design checks for pavement structures designed by other procedures and possibly as placeholders in pavement management systems until more reliable predictive equations become available.

A number of recommendations were provided for improvements to the design equations and for ancillary studies to improve the quality of the input values. However, the overall recommendation, apparently supported by the highway community at large, is to replace the present application of the serviceability concept for design with a comprehensive design system that provides direct consideration of the distress types expected to be significant. Pavement structures may then be designed to suitably minimize all distress types rather than just considering the composite index called PSI, which essentially considers only roughness in any meaningful way.

1

Introduction

Because of the diversity of the research activities and the bulk of the text required to describe them, this report has been produced in five volumes. The overall title is *Early Analyses of LTPP General Pavement Studies Data*, but each separate report has an additional title, as follows:

- SHRP-P-392 — *Executive Summary*;
- SHRP-P-684 — *Data Processing and Evaluation*;
- SHRP-P-393 — *Sensitivity Analyses for Selected Pavement Distresses*;
- SHRP-P-394 — *Evaluation of the AASHTO Design Equations and Recommended Improvements*; and
- SHRP-P-680 — *Lessons Learned and Recommendations for Future Analyses of LTPP Data.*

Each report can be used as a stand-alone document, but readers will find it useful to refer to other reports for additional detail.

This document reports the results from evaluations of the American Association of State Highway and Transportation Officials (AASHTO) design equations for flexible, rigid, and overlaid pavements and includes recommendations for improving the equations. This work was supported by the Strategic Highway Research Program (SHRP) Contract P-020, "Data Analysis," which served as the primary vehicle for harvesting the results from the first five years of the SHRP Long-Term Pavement Performance (LTPP) studies and transforming this new information into implementable products supporting the LTPP goal and objectives. The research was conducted by Brent Rauhut Engineering Inc. and ERES Consultants, Inc.

The goal for the LTPP studies, as stated in "Strategic Highway Research Plans," May 1986, is

> To increase pavement life by investigation of various designs of pavement structures and rehabilitated pavement structures, using different materials and under different loads, environments, subgrade soil and maintenance practices.

LTPP Objectives and Expected Products

The following six objectives were established by the SHRP Pavement Performance Advisory Committee in 1985 to contribute to accomplishment of the overall goal:

- Evaluate existing design methods.
- Develop improved design methods and strategies for pavement rehabilitation.
- Develop improved design equations for new and reconstructed pavements.
- Determine the effects of: (1) loading, (2) environment, (3) material properties and variability, (4) construction quality, and (5) maintenance levels on pavement distress and performance.
- Determine the effects of specific design features on pavement performance.
- Establish a national long-term pavement data base to support SHRP objectives and future needs.

This research was the first to utilize the National Pavement Performance Data Base (later renamed the LTPP Data Base) to pursue these objectives. The early products expected from this data analysis are listed below and are related to project tasks (to be described later):

- A better understanding of the effects of a broad range of loading, design, environmental, materials, construction and maintenance variables on pavement performance (Task 2).
- Evaluation of and improvements to the models included in the 1986 AASHTO Pavement Design Guide (Tasks 3 and 4).
- Evaluation and improvement of AASHTO overlay design procedures using data from the General Pavement Studies (GPS) (Task 5).

- Plans for future data analyses as time-sequence data for the GPS and Specific Pavement Studies (SPS) data enter the LTPP Data Base and the LTPP Traffic Data Base and offer opportunities for further insight and design improvements (Task 6).

This project began with the development of tentative plans for this initial analytical effort. These plans were presented on July 31, 1990, to the SHRP Expert Task Group on Experimental Design and Analysis and on August 2, 1990, to the highway community at a SHRP data analysis workshop. A detailed work plan was developed from the initial plans, in consideration of comments and guidance received from these and subsequent meetings. Guidance was furnished to the contractors throughout the research by a Data Analysis Working Group (composed of SHRP staff and SHRP contractors), the Expert Task Group on Experiment Design and Analysis, and the Pavement Performance Advisory Committee.

Research Tasks

The specified tasks for SHRP Contract P-020a were

- Task 1 — plan data evaluation procedure and present plans to workshop;
- Task 1A — process and evaluate data;
- Task 2 — conduct sensitivity analysis of explanatory variables in the National Pavement Performance Data Base;
- Task 3 — evaluate of the AASHTO design equations;
- Task 4 — improvement of the AASHTO design equations;
- Task 5 — evaluate and improve AASHTO overlay procedures based on GPS data; and
- Task 6 — plan future LTPP data analysis.

The relationships between the tasks and the general flow of the research appear in Figure 1.1. The tasks documented in this volume are Tasks 3, 4, and 5.

Data Bases Used in the Analyses

The National Information Management System (NIMS) will eventually include data for both GPS and SPS, but only the GPS data were even marginally adequate for these early analyses. In May 1993, the SPS data were only beginning to be entered into the NIMS for projects recently constructed, and most of the projects were not constructed. It should be noted that

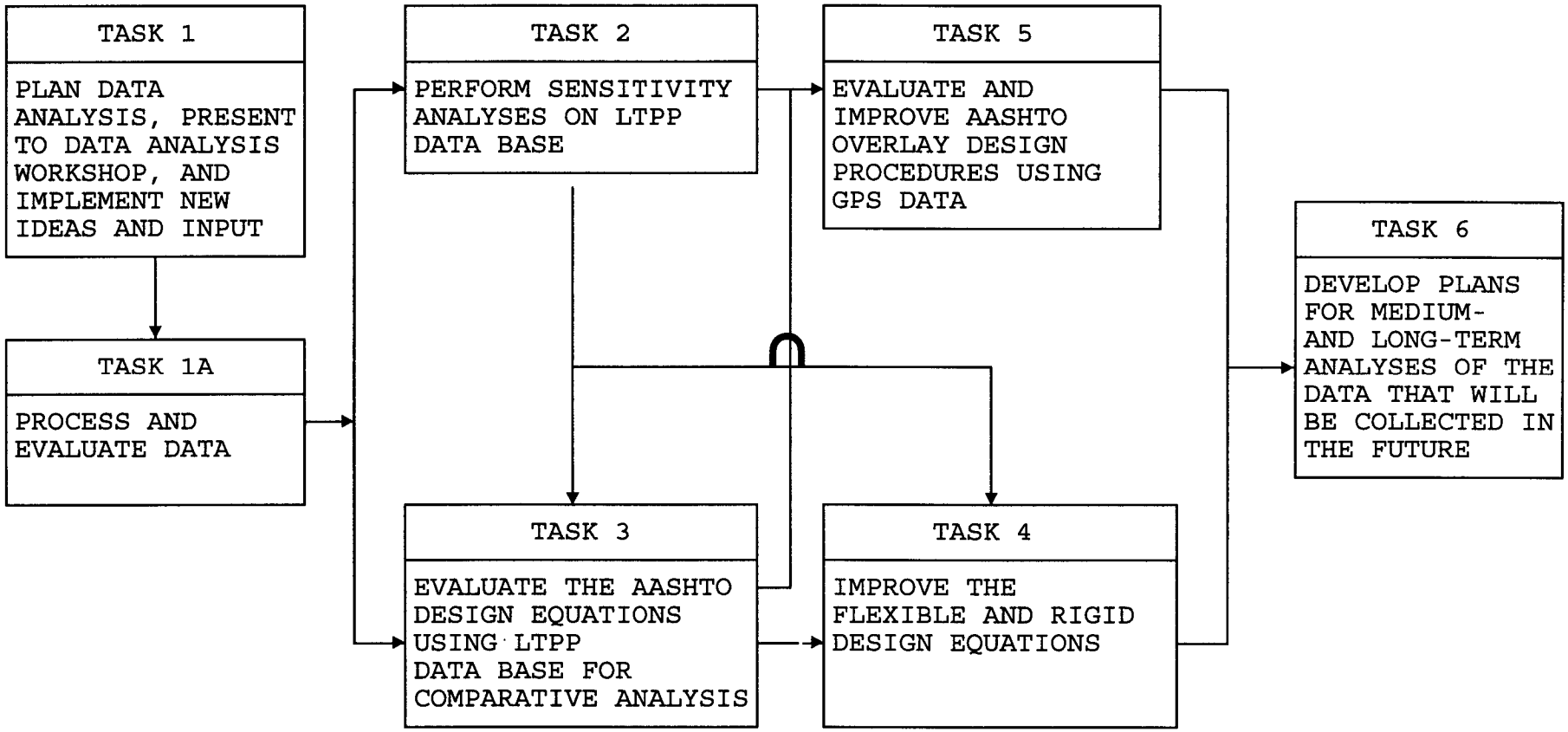

Figure 1.1. General Task Flow Diagram

all data collected for LTPP studies are for test sections 500 ft (152.4 m) in length and include only the outside traffic lane.

The GPS experiments are identified and briefly described in Table 1.1. The evaluations of the flexible pavement design equation used the GPS-1 and GPS-2 data sets, while the rigid pavement design equation used GPS-3, GPS-4, and GPS-5 data sets. The limited data bases available for the pavements with overlays were used for Task 5, evaluate and improve AASHTO overlay procedures based on GPS data (see SHRP-P-393 — Sensitivity Analyses for Selected Pavement Distresses).

It should be noted that some statisticians prefer to call the GPS experimental factorials "sampling templates" because existing in-service pavements were used instead of test sections that were constructed to satisfy rigorous experiment designs. However, the factorials were established to encourage reasonable distributions of parameters expected to be significant and test sections were sought to meet the factorial requirements. The SPS in fact follow the requirements of designed experiments.

Table 1.1. Listing of SHRP LTPP General Pavement Studies (GPS) Experiments

GPS Experiment	Brief Description	No. of Projects in the Data Base
1	Asphalt Concrete (AC) Pavement with Granular Base	253
2	AC Pavement with Bound Base	133
3	Jointed Plain Concrete Pavement (JPCP)	126
4	Jointed Reinforced Concrete Pavement (JRCP)	71
5	Continuously Reinforced Concrete Pavement (CRCP)	85
6A	AC Overlay of AC Pavement (Prior Condition Unknown)	61
6B	AC Overlay of AC Pavement (Prior Condition Known)	31
7A	AC Overlay of Concrete Pavement (Prior Condition Unknown)	34
7B	AC Overlay of Concrete Pavement (Prior Condition Known)	15
9	Unbonded PCC Overlays of Concrete Pavement	28

Work Plan

The work plan for the new design equations included the following:

- Accumulation of required data.
- Calculation of observed and predicted Present Serviceability Indices (PSIs) and traffic loadings, based on observed roughness and distress data in conformance with the procedures developed from the results of the AASHO Road Test and historical traffic and construction data as specified in the 1986 AASHTO Guide for Design of Pavement Structures (1), respectively.
- Initial evaluation based on graphical and statistical procedures.
- From the initial graphical evaluations, identification of specific detailed analyses to be conducted to obtain further insight into the causes of disparities between observed traffic and that predicted to cause the observed serviceability losses.
- Summarization of results and identification of potential improvements.

The work plan for evaluation of the overlay design procedure included the following:

- Accumulation of required data.
- Calculation of future overlay design equivalent single axle loads (ESALs) and overlay design serviceability.
- Calculation of an overlay design matrix based on future and effective structural capacities.
- Evaluation of the design procedure based on a graphical procedure of comparing current overlay serviceability to the terminal serviceability and overlay distress.
- Summarization of results and conclusions.

Data Limitations

The six primary limitations for the data are as follows:

- Measured initial values of PSI (when the pavements were opened to traffic) were not available because few State Highway Agencies (SHAs) measured roughness of new pavements in the past. It was necessary to utilize either estimates from the SHAs or estimates arrived at by other means.

- Actual traffic measurements were available for virtually none of the test sections; therefore, it was necessary to use estimates of cumulative ESALs developed by the SHAs, based on rules developed by SHRP.

- The only complete set of subgrade stiffness data available was that backcalculated from deflection data for the outer sensors, based on procedures specified in the AASHTO Guide. Very little laboratory and backcalculated subgrade moduli (from all falling weight deflectometer [FWD] sensors) were available for these studies.

- Sufficient information was not available to adequately address the potential loss in serviceability due to subgrade volume changes.

- Missing data for this early analysis limited the number of sections available for analysis.

- Some SHAs are believed to have reported when the overall project was paid for or when the formal "ribbon cutting" occurred, rather than when the pavement section was actually opened to traffic.

The current estimates of initial PSI are not expected to be improved for future studies, as continued test section monitoring will probably offer no basis for improving the estimates, with the exception of newer sections where the time sequence profile data could be backcalculated to estimate the initial PSI. However, future evaluations will be made with greater values of PSI loss as the pavements deteriorate in time. Also, compensation from estimates above and below the true values should reduce the effects of inaccurate estimates overall.

The cumulative traffic estimates should improve greatly for future analyses as monitoring continues because traffic data will be collected at the test section locations. Only the data for periods before traffic monitoring began will remain uncertain—a significant limitation for the older test sections that will soon require rehabilitation.

A more complete set of both laboratory and backcalculated subgrade resilient moduli will be available for future evaluations, so the effects of subgrade moduli may be better evaluated. The subgrade moduli used in these studies, however, are based on an estimation procedure provided in the AASHTO Guide, which will be discussed in greater detail in Chapter 2.

The data required by Appendix G of the 1986 AASHTO Design Guide for determination of serviceability loss (reduction in PSI) because of volume change in fine-grained subgrade soils are not available. Missing are data to determine the depths of frost penetration for estimating serviceability loss due to frost heave and the soil fabric data required for estimating the swell rate constant.

It was necessary to use the data available to estimate serviceability losses due to volume change in the subgrade. As most of the subgrade soils for the test sections used for these analyses were not fine grained, the application of the procedures from the Design Guide

produced minimal effects on study results.

While these data limitations will undoubtedly affect the evaluations of the design equations, the shortcomings of the design equation are sufficiently serious that the causes can readily be discerned. The limitations may have caused errors in the magnitude of the effects, but they are not believed to have seriously affected identification of the design equation shortcomings.

2

Data Sources

For the purposes of discussion, the data have been broken into two categories, observed and estimated. Observed data include those data that have been specifically collected from the SHRP test sections since the initiation of these studies. Estimated data are those for which site-specific observations preceding the initiation of these studies could not be documented. Separate discussions of the data required for flexible and rigid pavements are provided to highlight the specific data elements required for these two design procedures. The specific sections utilized in these evaluations of the AASHTO flexible and rigid equations are noted in Appendices A and B, respectively, along with their corresponding properties.

Flexible Pavement Data

Observed Data

In the Flexible Pavement Design Procedure, the three data elements classified as "observed" are as follows:

- Profile Data.
- Rut-Depth Data.
- Layer Thicknesses.

Longitudinal profile data were collected using the KJ Law Road profilometer, which records the surface profile at 6 in. (0.15 m) intervals throughout a pavement test section. The output from software operating on the measured profile includes the International Roughness Index (IRI), recorded in inches per mile, and slope variance, as well as other summary statistics of the pavement profile. IRI values were not used directly in these analyses, but slope variance results were used to calculate the observed Present Serviceability Index (PSI). It should be acknowledged that the slope variance data were not collected in the same fashion as those

collected at the AASHO Road Test and used in development of the AASHTO equation. There are undoubtedly some differences between the values of slope variance measured with the CHLOE profilograph (utilized in the AASHO Road Test) and the KJ Law Road profilometer. Research staff have not attempted to quantify this difference, which is primarily a function of the difference in wheel bases between the profilograph and the profilometer.

Rut depth data were measured from photographs of stringline projections on the pavement at a fixed angle from the horizontal, taken at 50 ft (15.2 m) intervals throughout each SHRP test section. The result is that a line on a photograph will vary from a straight line where ruts exist. Measurement of departures from a straight line provide transverse profiles of a test section at 50 ft (15.2 m) intervals. From these transverse profiles, rut depths have been established for either 4 ft (1.2 m) or 6 ft (1.8 m) straight edges. Since 4 ft (1.2 m) straight edges were used at the AASHO Road Test for the measurement of rut depth, the same were used for this analysis. These measurements have been averaged over the length of the section for use in the evaluations.

Layer thickness information has been documented through measurement of cores for bound materials and from logging of bore holes and test pits for unbound materials. Sampling was conducted just outside the test sections on the approach and leave ends, in the wheel paths and between wheel paths. The thicknesses of each layer in the pavement structure were recorded, and samples were recovered for testing the pertinent material properties in the laboratory. Because no material sampling was conducted within the test sections, researchers are not sure that the material layer thicknesses within the test sections are truly representative. However, extreme variations (greater than 30 percent) from end to end were rare, and deflection profiles (longitudinally through a test section) were available for review when variation within a test section was suspected.

The layer thicknesses from the approach and leave ends were averaged to establish a representative analysis section, unless differences in layer thicknesses and a review of deflection results indicated a different representation. The layer thicknesses included in the representative section were in turn utilized to calculate structural numbers for the test sections, based on the procedures recommended in the guide.

Estimated Data

Estimated data generally included two types: (1) historical data not available for a specific test section and (2) data to be collected in the future, but not yet available for these analyses.

The two data elements included under the first category were historical traffic data and initial PSI data. Although some State Highway Agencies (SHAs) did have documented data available, these data were rarely specific to the 500 foot (152.4 m) test sections included in the study.

Historical traffic data were collected from the SHAs by SHRP Regional Coordination Offices

(RCO's) personnel. The SHAs were asked to provide the average annual daily traffic (AADT) and total number of trucks for all lanes, as well as for the specific lane in which the test section resides (always an outer lane). The SHAs were also asked to provide the number of equivalent single axle loads (ESALs) per year for the General Pavement Studies (GPS) test lane. These traffic data were sought for each year from 1989 back to the year when each particular section of highway was opened to traffic. Most SHAs have records of the two-directional AADT for a given highway, but records have rarely been collected near an long-term pavement performance (LTPP) test section and are not lane-specific. All traffic data were screened to identify potential errors in the estimates. Specifically, section opening dates were compared to the first year of traffic data, and checks were made for random missing years of traffic. A check was also made to compare annual ESALs to the annual number of trucks to ensure that the truck factor remained reasonable. If the truck factor appeared unreasonable, the SHRP RCO was asked to verify the data. Site-specific traffic data will be collected in the future, so the precision of the traffic data may be expected to increase with time to the benefit of future analyses.

Since the SHAs are most familiar with the relative roughness of their newly constructed highways, the agencies were requested to provide initial PSI estimates specifically for this analysis. They were also asked to provide any historical roughness data (Mays Meter readings, Ride Quality Index [RQI] data, or Ride Comfort Index [RCI] data) that were considered representative of their LTPP test sections. Where historical roughness data had been collected, correlations were sought to tie this information to PSI and to backcast, where necessary, to the date of opening. Backcasting for a test section involved linear regression with the log of PSI versus time for the data values available, and extrapolation of the resulting line back to the date of opening. Where sufficient time series data were not available, the SHA estimates were used. The mean value of the initial PSI estimates for the 244 test sections used in the analysis was 4.25 and the standard deviation was 0.23.

Certain checks were applied while processing the historical roughness data to minimize the impact of suspect data. Considering that the range of PSI values is from 0 to 5.0 with 4.2 being the average initial PSI value for flexible pavements at the AASHO Road Test, no values were allowed to be less than 3.5 or greater than 5.0. When backcasting, the regression line was expected to have a negative slope, but a positive slope up to 0.01 was allowed to represent zero roughness change with time. Also, roughness data output from the SHRP GM profilometers were used as a check on those sections for which time series data were provided (to ensure that the trend was consistent with observations currently being collected). Where the procedures above resulted in reasonable PSI values, the values were used. Where the checks were not satisfied, a value of 4.2 was used.

Subgrade stiffness values fell into the second category of estimated data. Although measured resilient modulus data will ultimately be available from laboratory test results and stiffnesses will be backcalculated from deflection testing results for all the sections, both were only partially available for inclusion in these analyses. In lieu of these data, subgrade moduli were estimated from measured deflections at the outer sensor locations, in accordance with the guidelines set forth in the Guide.

The following equation provides for prediction of in situ subgrade layer moduli in Part III-5.2.3. of the 1986 Guide:

$$E_{sg} = \frac{PS_f}{d_r r} \quad (2.1)$$

Where:

E_{sg} = in situ moduli of elasticity of the subgrade layer,
P = the dynamic load (approximately 9,000 lbs or 40 kN) of the nondestructive testing (NDT) device used to obtain deflections,
d_r = the measured NDT deflection at a radial distance of r from the NDT plate load center,
r = radial distance from plate load center to point of d_r measurement (r = 60 in. or 1.5 m), and
S_f = the subgrade modulus prediction factor (a value of 0.2792 was assumed for this research).

Preliminary evaluations of these values versus laboratory resilient moduli available to date are discussed further in Chapter 4. As more laboratory and backcalculated values for subgrade stiffness become available, it will be possible to complete these evaluations of the Guide's recommendations for estimating these values, and to more thoroughly evaluate how use of any of the three affects the predictions of the design equation.

As shown in Figure 2.1, the mean value of those subgrade moduli estimates was 41.1 ksi (283 MPa) and the standard deviation was 24.0 ksi (166 MPa). As can be seen from the distribution, over 50% of the sections had moduli values between 20 and 40 ksi (138 and 276 MPa), which was considerably in excess of the 3 ksi (21 MPa) noted at the AASHO Road Test. The minimum value estimated for these LTPP test sections was 12.4 ksi (84.7 MPa). The maximum value was 195 ksi (1343 MPa), but such extremely high values were for sections with a rock subgrade.

Similarly, it can be seen from Figures 2.2, 2.3, and 2.4 that the mean asphalt thickness was 6.5 in. (16.5 cm), the mean age was 11 years, and the mean traffic loading was 208 KESALs (1000 ESALs) per year.

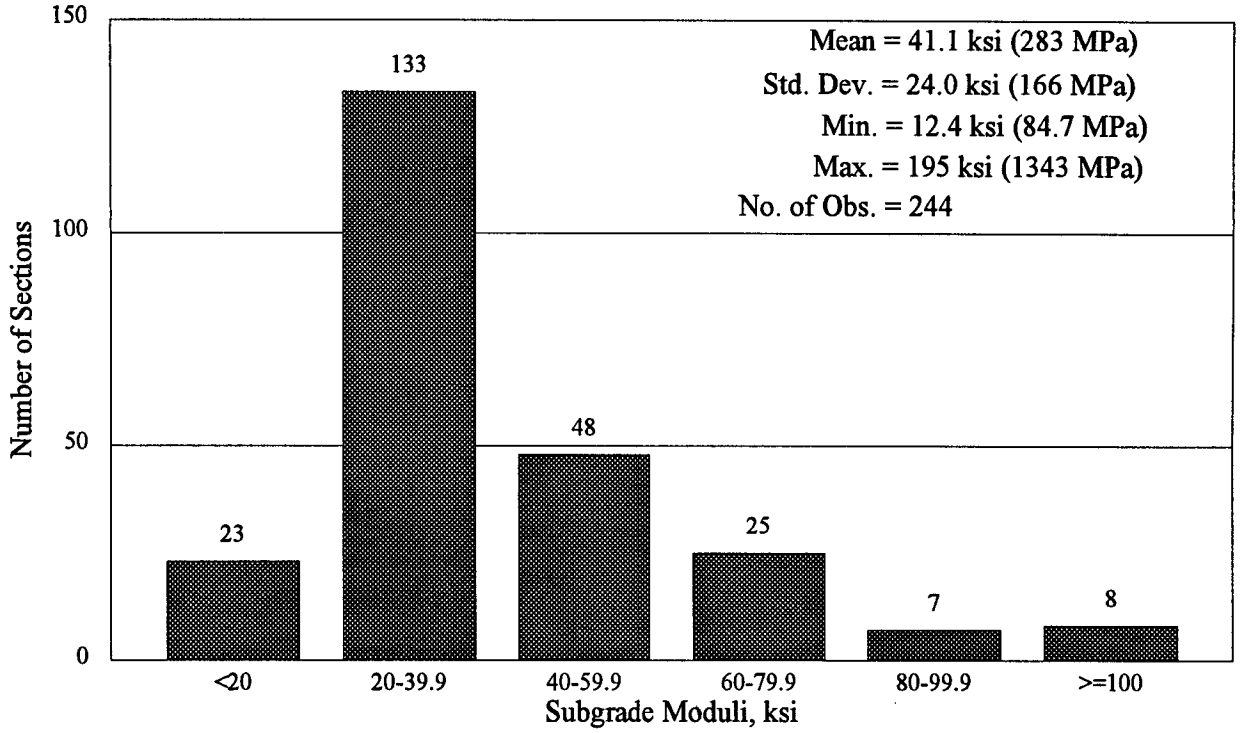

Figure 2.1. Distribution of Subgrade Moduli Estimates (From Backcalculation of FWD Data) in ksi

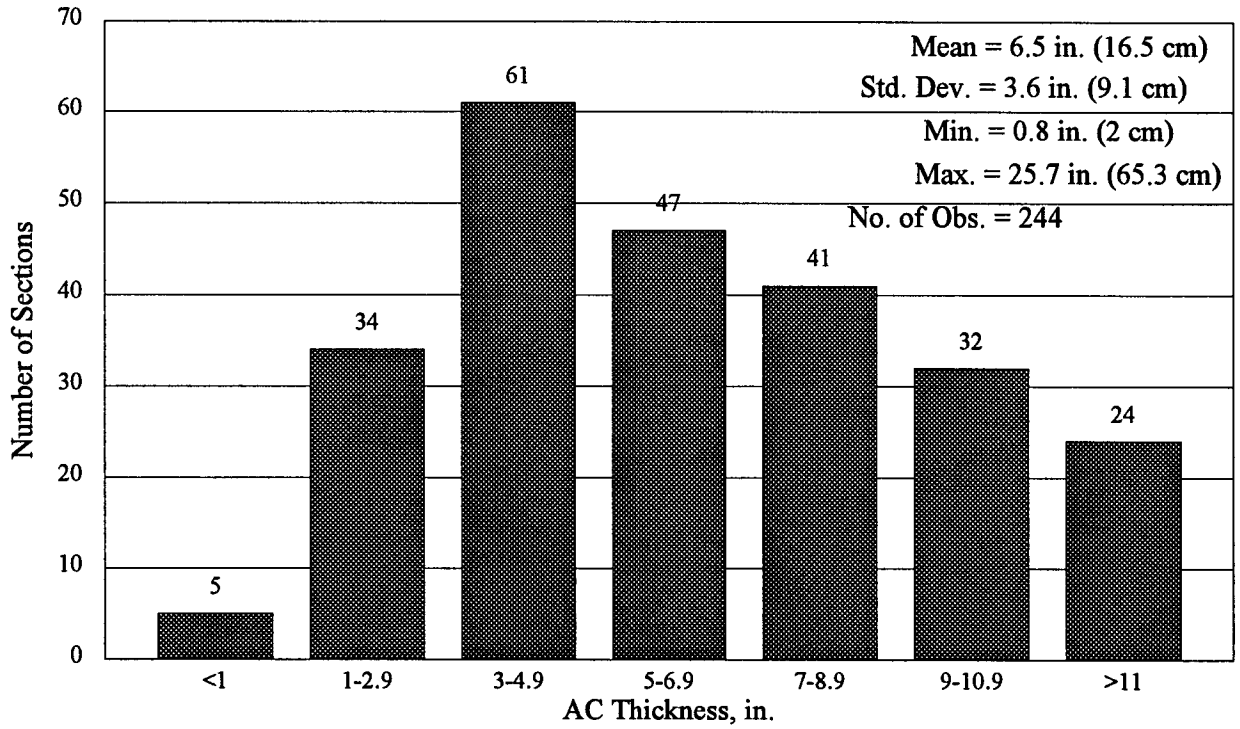

Figure 2.2. Distribution of AC Thicknesses in Inches

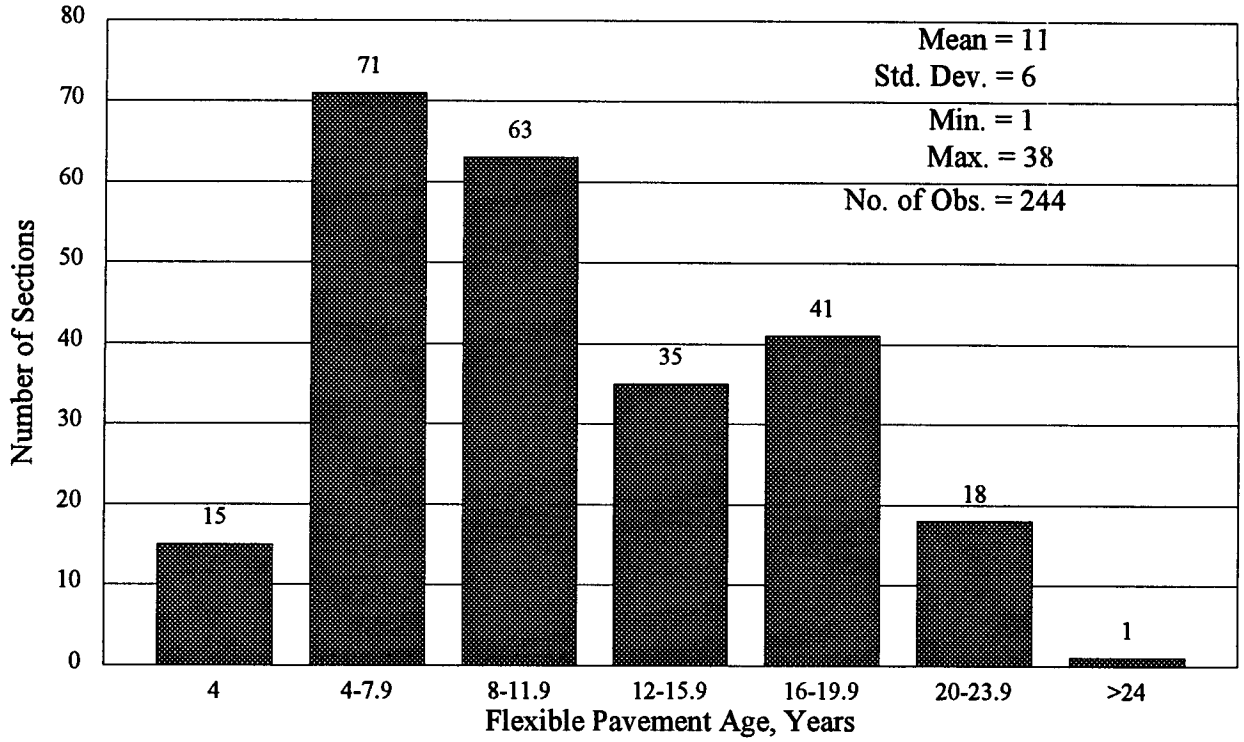

Figure 2.3. Distribution of Flexible Pavement Ages in Years

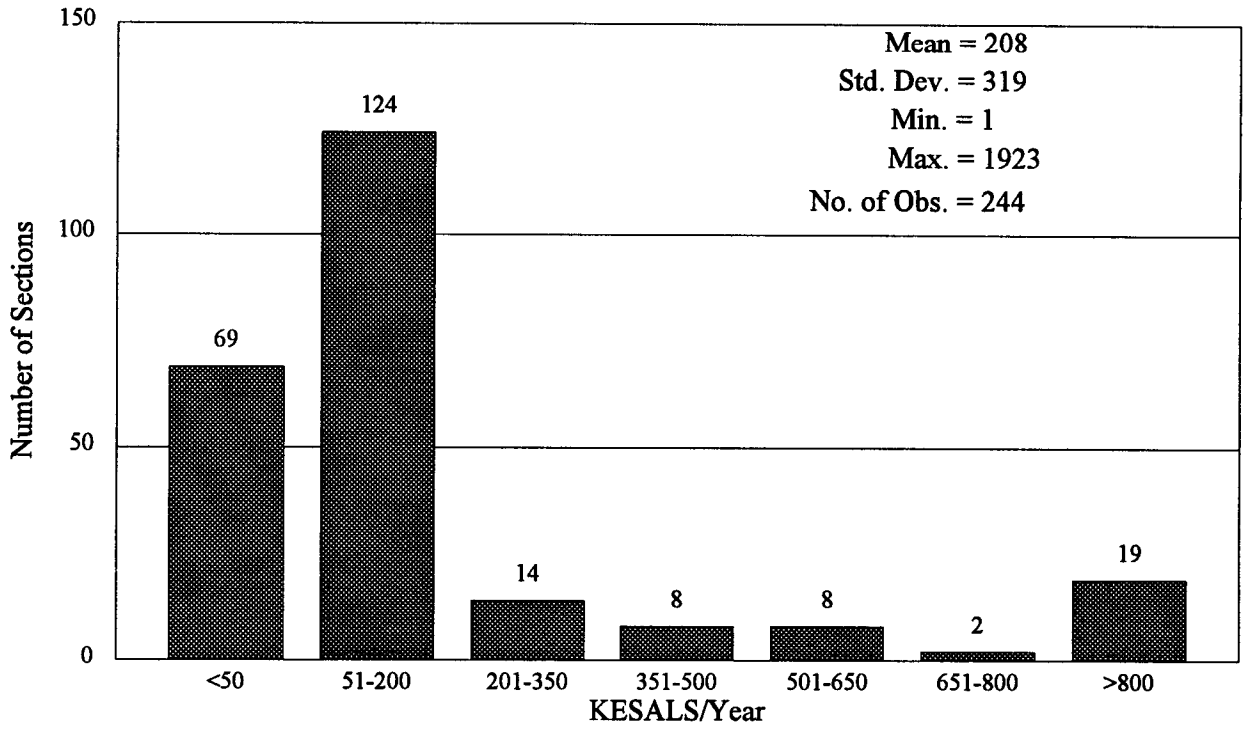

Figure 2.4. Distribution of Flexible Pavement Traffic Loadings in KESALs/Year

Rigid Pavement Data

Observed Data

PCC Slab Thickness

The mean slab thickness values available from the SHRP material testing data used for each section. The distribution of slab thicknesses for JPCP, JRCP, and CRCP considered in the evaluation data set is shown in Figure 2.5. It can be seen that the thicknesses in the data set are not uniformly distributed. Approximately 62% of the JRCP sections have a thickness range of 9 to 10 in. (22.9 to 25.4 cm) and 52% of CRCP sections have thicknesses of 8 to 9 in. (20.3 to 22.9 cm). Only JPCP sections are well distributed: 35 percent have thicknesses of 6 to 9 in. (15.2 to 22.9 cm); 35 percent, 9 to 10 in. (22.9 to 25.4 cm), and 30 percent, 10 in. (25.4 cm) and thicker.

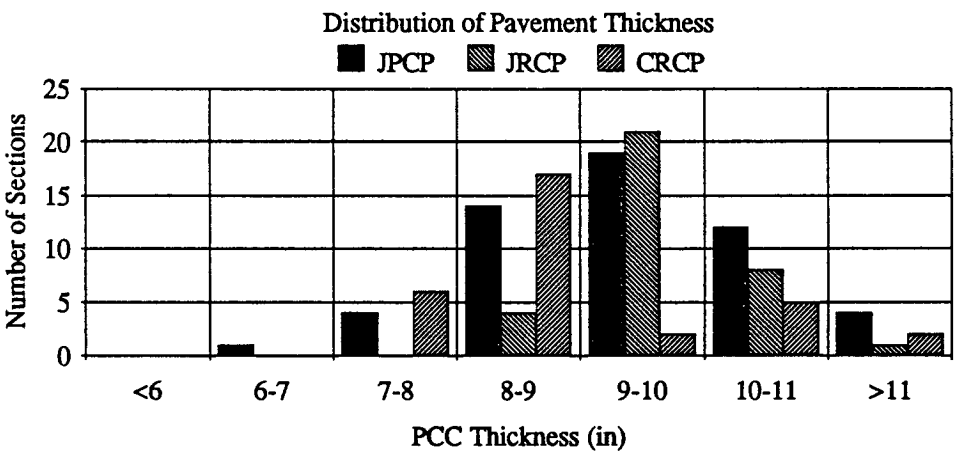

Figure 2.5. Distribution of PCC Thicknesses

PCC Modulus of Elasticity

The SHRP LTPP Data Base contains material testing data that include PCC compressive strength, split cylinder tensile strength, and modulus of elasticity. The moduli of elasticity obtained from the testing database were used in the analysis. The mean of all these tests was 4,600 ksi (31,700 MPa), while the values ranged from 2,800 to 6,800 ksi (19,300 to 46,900 MPa).

Pavement Age

The pavement age ranges from 2 to 27 years with a mean of 12 years. The pavement sections considered in the analysis data set are well distributed between 5 to 20 years. The distribution of pavement age is shown in Figure 2.6.

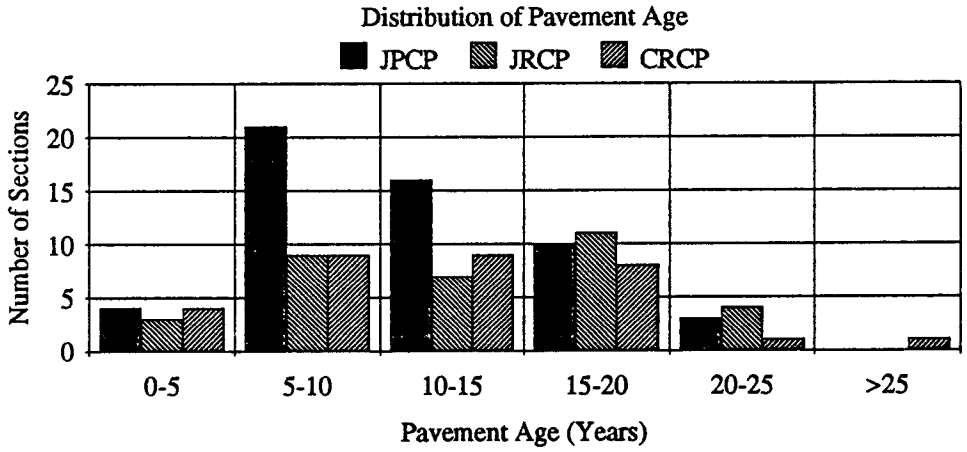

Figure 2.6. Distribution of Pavement Ages in the Analysis Data Set

Estimated Data

Estimates of actual cumulative KESALs as developed by the SHAs were used. The mean KESALs/year of age was computed for each section to provide an idea of the rate of loading on the sections. A distribution is shown in Figure 2.7 for all sections (mean = 352, range = 14 to 1813 KESALs/year).

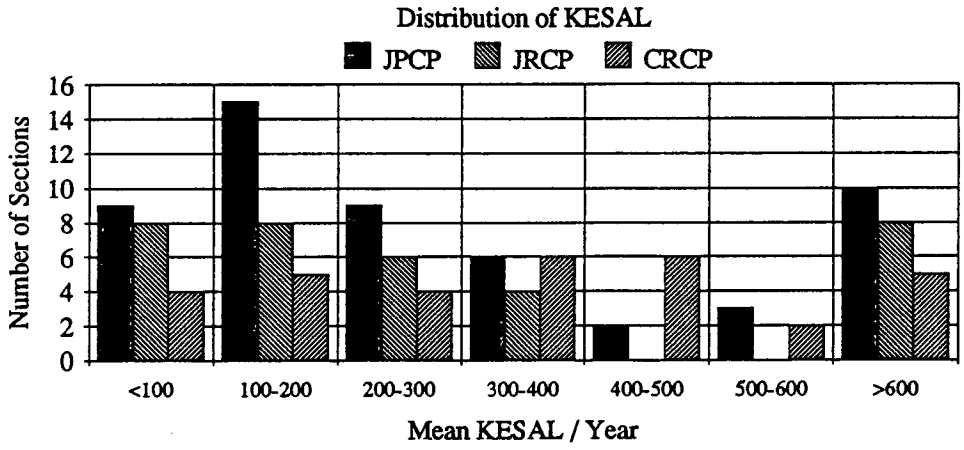

Figure 2.7. Distribution of Mean KESALs/Year in the Analysis Data Set

3

Data Processing

The data sources discussed in Chapter 2 were used to calculate the observed and predicted Present Serviceability Index (PSI) losses as well as predictions of traffic loadings based on observed PSI loss to date. Calculations for each of these will be discussed in greater detail in the following.

Flexible Pavement Data Processing

Observed PSI Loss

As noted in the AASHO Road Test Report 5 (2), the current PSI for a given section of flexible highway can be calculated from the average slope variance, average rut depth, and cracking and patching. The equation can be written as follows:

$$PSI = 5.03 - 1.91 \log (1 + \overline{SV}) - 1.38\ \overline{RD^2} - 0.01\ \sqrt{C+P} \qquad (3.1)$$

Where:

$\overline{SV}$ = average slope variance from both wheel paths as collected by the CHLOE profilograph;

$\overline{RD}$ = average rut depth from both wheel paths based on a 4 ft (1.22 m) straight edge, in inches;

C = square feet of Class 2 and Class 3 cracking per 1,000 ft^2 (92.9 m^2); and

P = patching in square feet per 1,000 ft^2 (92.9 m^2).

This equation, commonly used in the past to estimate PSI, was developed to model pavement serviceability ratings collected by a panel of raters at the AASHO Road Test.

The multiple squared correlation coefficient (r^2) for Equation 3.1 was 0.844, and the root mean square error (RMSE) of prediction was 0.38.

Cracking and patching were not included in the calculation of the current PSI for the test sections. Significant quantities of cracking and patching were noted on only a few of the test sections, and the impact of this term was not considered significant, because its coefficient is only 0.01. The mean value of current PSI was 3.53, with a standard deviation of 0.49.

Observed PSI loss is then the difference between the initial PSI and the results of Equation 3.1 above. The mean value for observed PSI loss was 0.70, and the standard deviation was 0.51.

Predicted PSI Loss

As the variables required to calculate G_t in the following equation developed from data at the Road Test are known, the equation can be used to calculate ΔPSI:

$$G_t = \text{Log}\left(\frac{\Delta PSI}{2.7}\right) \quad \textbf{(3.2)}$$

Where:

G_t	=	β (log W - logρ);
W	=	the number of 18 kip ESAL's;
ρ	=	$0.64\ (SN + 1)^{9.36}$;
β	=	$0.4 + 1094/(SN + 1)^{5.19}$;
SN	=	$a_1 D_1 + a_2 D_2 m_2 + A_3 D_3 m_3 + \ldots\ldots + a_n D_n m_n$;
D_i	=	thickness of layer i, in.;
a_i	=	structural coefficient for the material in Layer i; and
m_i	=	drainage coefficient for the material in Layer i.

Structural numbers (SNs) for these sections are based on the results of the materials testing data discussed in Chapter 2. From these data the thicknesses and material types for each layer in each section were determined. The structural layer coefficients a_i would ideally be based on resilient moduli from laboratory testing corrected for temperature effects. With no stiffness information available at the time of the analysis, the structural coefficients used in calculating the structural number were selected based on the material types noted from lab testing and the guidelines provided in the 1986 Guide for the associated material types (Table 3.1). Drainage coefficients (m_i) were selected based on drainability (as a function of material gradations) and exposure to moisture (as a function of the average annual rainfall), as later modified in the 1986 Guide.

Table 3.1. Structural Layer Coefficients Used In Analysis

Material Type	Coefficient (a_i)
Dense-graded Asphalt Concrete	0.44
Bituminous Bound Bases	0.34
Non-bituminous Bound Bases	0.23
Unbound Granular Bases	0.14
Subbases	0.07
Stabilized Subgrades	0.15

As noted under Section 2.4.1, "Drainage," of the 1986 AASHTO Guide, recommended values of m_i range from 1.4 (for sections with excellent drainage and less than 1% exposure to moisture levels approaching saturation) down to 0.4 (for sections with very poor drainage and levels approaching saturation more than 25 percent of the time). It should be noted that this drainage coefficient is only applied to unbound layers of the pavement structure, as noted in the 1986 Guide. Although specific information regarding the quality of drainage and/or the percentage of time the pavement structure is exposed to moisture levels approaching saturation is not available, the material gradation information and average annual rainfall data were used to approximate these values in the following fashion. If exposure to moisture varies from a value of 1.2 to 0.6, and the quality of drainage is similarly set for the same range, then the product of these two values will range from 1.44 to 0.36 (encompassing the range specified in Table 2.4 of the 1986 Guide). Utilizing the ranges noted above, a linear function can be established for calculating these values for each section as follows:

$$S_l = 1.2 - 0.6\ (AAR) \tag{3.3}$$

and

$$D_q = 1.2 - 0.6\ (P200) \tag{3.4}$$

Where:

S_l = the saturation level,
AAR = the average annual rainfall in inches/100,
D_q = the drainage quality, and
P200 = the percentage of material passing through a No. 200 sieve/100.

Based on the procedures outlined above, calculated values of m_i ranged from 1.44 to 0.56 with an average of 0.97 and a standard deviation of 0.2.

The AASHO equation, Equation 3.2, was further modified in 1972 (3,4) to accommodate variations in environmental region and soil support as follows:

$$\text{Log } W = \text{Log } \rho + \frac{G_t}{\beta} + \text{Log } \frac{1}{R} + 0.372\ (S-3) \tag{3.5}$$

Where:

R	=	regional factor (ranging from 0.5 to 3), and
S	=	soil support (ranging from 3 to 7).

The equation was again modified in 1986 (1) as follows:

$$\text{Log } W = Z_R * S_o + \text{Log } \rho + \frac{G_t}{\beta} + 2.32 \text{ Log } M_r - 8.07 \tag{3.6}$$

Where:

Z_R	=	standard normal deviate;
S_o	=	overall standard deviation; and
M_r	=	laboratory resilient modulus, psi.

As the equation was being used for research rather than design, a 50% reliability was selected as appropriate for mean predictions. At 50% reliability $Z_R = 0$, and this term drops out of the equation.

Equation 3.6 was used to predict the total KESALs (1000 ESALs) required to cause the observed losses in PSI.

Resilient moduli for the subgrade (M_r) were estimated based on the procedure provided in the 1986 Guide (see Equation 2.1). It should be noted that this procedure does not consider seasonal effects, so the subgrade moduli were not entirely consistent. However, the differences in magnitudes that would have occurred from seasonal adjustments would not have made an important difference in the results.

Historical traffic data provided by the State Highway Agencies (SHAs) (see "Estimated Data" in Chapter 2) were used for the traffic data (W) in these calculations. The cumulative KESALs for each section were divided by the number of years since the test section was opened to traffic to obtain average values per year. This allowed extrapolation of the extra year or two beyond 1989 to estimate a traffic level associated with the date of performance-monitoring activities. Most of the monitoring data used were obtained in 1990 or 1991.

Rigid Pavement Data Processing

The LTPP data base was used to obtain input data to predict KESALs carried for the measured loss of serviceability for each section under GPS-3, GPS-4 and GPS-5. Each data element used for this evaluation is described. The data limitations and their distribution in the evaluation data set are also discussed.

The pavement sections in the SHRP LTPP data base were divided into four broad climatic zones. These are wet-freeze (WF), wet-no freeze (WNF), dry-freeze (DF), and dry-no freeze (DNF) regions. The LTPP data base consists of 122 JPCP, 70 JRCP, and 85 CRCP sections located throughout the United States and Canada. A variety of information is collected for each section including climatic, material properties, traffic loads, profile, distress, and numerous other types of data. At the time of this analysis, the data required for the evaluation of the AASHTO concrete pavement design model were not available for all sections. Only 54 JPCP, 34 JRCP, and 32 CRCP sections existed for which all the required data for the evaluation of the AASHTO models were available. Tables 3.2, 3.3, and 3.4 show the distribution of the analysis data set based on the factorial design used to describe GPS-3, 4, and 5 experiments, respectively.

Initial Pavement Serviceability

The initial serviceability values (when the pavement was opened to traffic) for the specified 500 ft (152 m) sections were not measured at the time of construction. Estimates were obtained from SHAs of their typical initial serviceability values. Figure 3.1 shows the mean estimated initial serviceability for JPCP, JRCP, and CRCP in each of the climatic regions. The mean initial serviceability value obtained from all these estimates was 4.25. This value is slightly less than the 4.5 mean value used for all the original Road Test sections. Another consideration is that quite a number of the newer sections had current serviceability values higher than 4.25. The main analysis conducted herein used the 4.25 mean value for all sections since this value was the mean provided by the SHAs, but 4.5 was used later to show its impact on the results.

Current (or Terminal) Pavement Serviceability

The current pavement serviceability was calculated using the same regression equation developed by Carey and Irick (5) and used at the AASHO Road Test:

$$PSI = 5.41 - 1.80 \log (1 + \text{average } \overline{SV}) - 0.09 \sqrt{(C + P)} \qquad (3.7)$$

Table 3.2. Analysis Data Set Design for JPC Pavements.

Moisture			Wet								Dry							
Temperature			Freeze				No Freeze				Freeze				No Freeze			
Subgrade Type			F		C		F		C		F		C		F		C	
Traffic Rate			L	H	L	H	L	H	L	H	L	H	L	H	L	H	L	H
Base Type	PCC Thickness	Dowels	Number of JPCP Sections in the Analysis Data Set															
Granular	L	N		1	1	1			1					1				
		Y	2	2	2		2	1										
	H	N	1	2	1						1		1	1				
		Y	1	1	1			2										
Stabilized	L	N	1		1			1	2	2				1		1	2	
		Y	2	1			1	1		1								
	H	N									1					1	1	1
		Y	2	1		1		1	1	1								

Table 3.3. Analysis Data Set Design for JRC Pavements.

Moisture		Wet								Dry							
Temperature		Freeze				No Freeze				Freeze				No Freeze			
Subgrade Type		F		C		F		C		F		C		F		C	
Traffic Rate		L	H	L	H	L	H	L	H	L	H	L	H	L	H	L	H
PCC Thickness	Joint Spacing	Number of JRCP Sections in the Analysis Data Set															
L	L		2	1	2							1		-	-	-	-
	H	2	2	2			2							-	-	-	-
H	L		1	2	1	2	1			1				-	-	-	-
	H		2	1	1	2	2		2	1	1			-	-	-	-

Table 3.4. Analysis Data Set Design for CRC Pavements.

Moisture		Wet								Dry							
Temperature		Freeze				No Freeze				Freeze				No Freeze			
Subgrade Type		F		C		F		C		F		C		F		C	
Traffic Rate		L	H	L	H	L	H	L	H	L	H	L	H	L	H	L	H
PCC Thickness	% Reinforcement	Number of CRCP Sections in the Analysis Data Set															
L	L	1	1		1	1	2	1	1	1		1		1	2	2	
	H	1	1				1										
H	L	1			2	1	2							2	3	1	
	H								1				1				

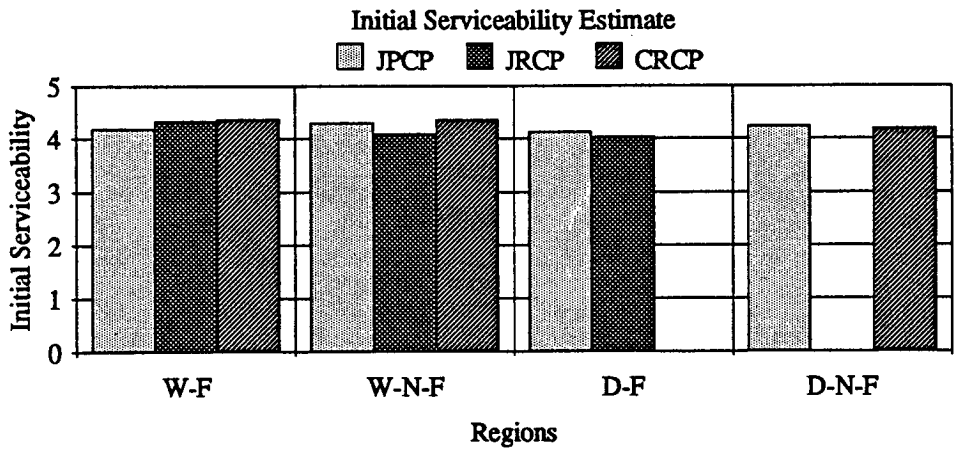

Figure 3.1. Mean Estimated Initial Serviceability for Each Climatic Region and Pavement Type

Where:

$\overline{SV}$ = average slope variance from both wheel paths as collected using the CHLOE profilograph,

C = sq ft of Class 3 and Class 4 cracking per 1,000 sq ft (92.9 m^2), and

P = AC and PCC patches in sq ft per 1,000 sq ft (92.9 m^2).

At the AASHO Road Test, Class 3 cracks were defined as those opened or spalled at the surface to a width of 1/4 in. (6.4 mm) or more, over a distance not less than half the length of the crack. Sealed cracks were defined as Class 4 cracks. Based on this definition, an estimate of cracking and patching for each section was obtained from the SHRP LTPP data base. The mean slope variance for each section was calculated with the profile data. The estimated current PSI was calculated from the data by Equation 3.7. In order to calculate the predicted KESALs for comparison with the actual KESALs, the current pavement serviceability was used as the terminal serviceability (p_t).

The distributions of cracking and patching in the analysis data set are shown in Figures 3.2 and 3.3 respectively. There is a relatively low amount of these distresses in most of the pavements. The distribution of current slope variance for different types of pavements is shown in Figure 3.4. With the mean initial serviceability and the current serviceability known, the measured loss in PSI can be calculated as follows:

$$\Delta PSI = \text{Mean Initial Serviceability} - \text{Current Serviceability}. \quad (3.8)$$

Mean existing serviceabilities and serviceability losses for JPCP, JRCP, and CRCP in different regions are shown in Figures 3.5 and 3.6. This measured loss in PSI is used in the AASHTO design equation to predict ESALs.

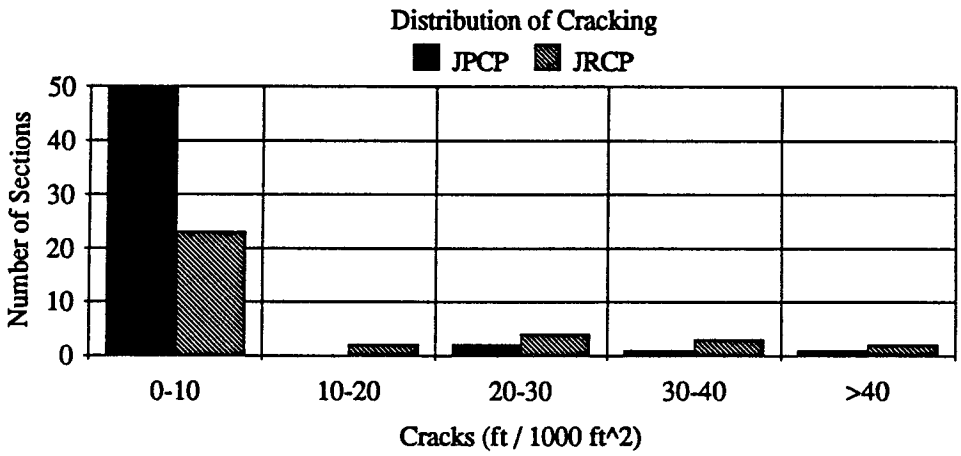

Figure 3.2. Distribution of cracking in the analysis data set

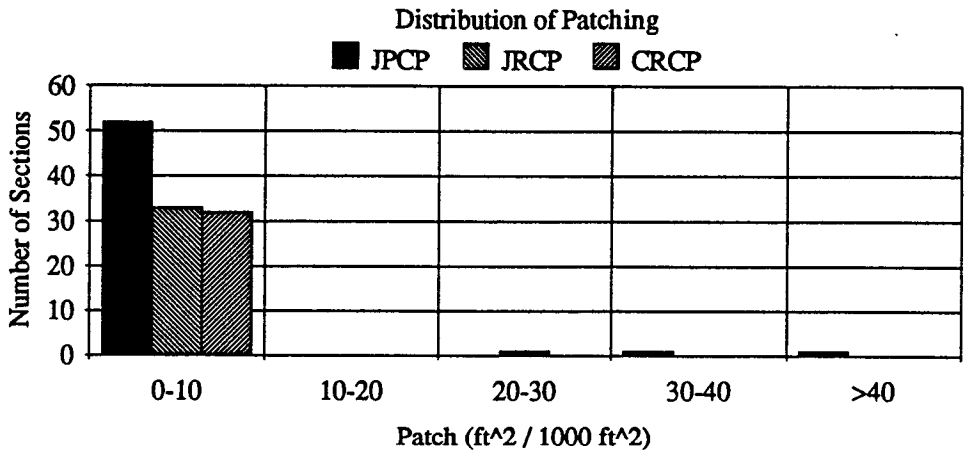

Figure 3.3. Distribution of patching in the analysis data set

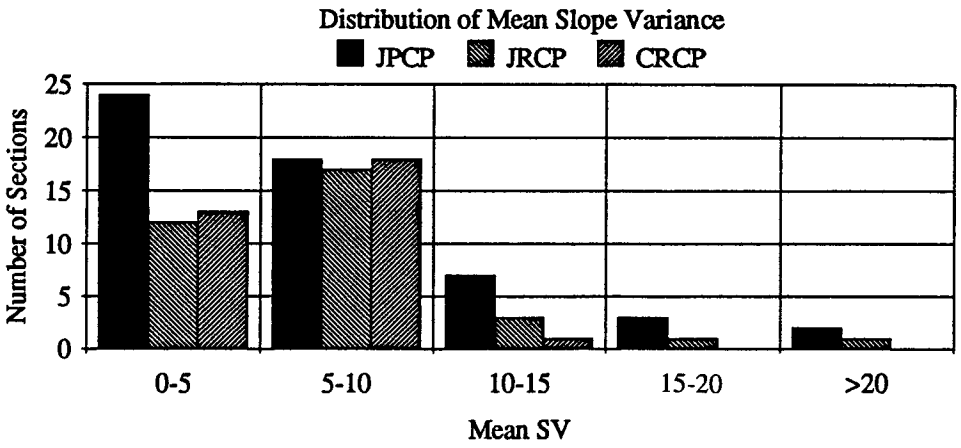

Figure 3.4. Distribution of mean slope variance (10^6)

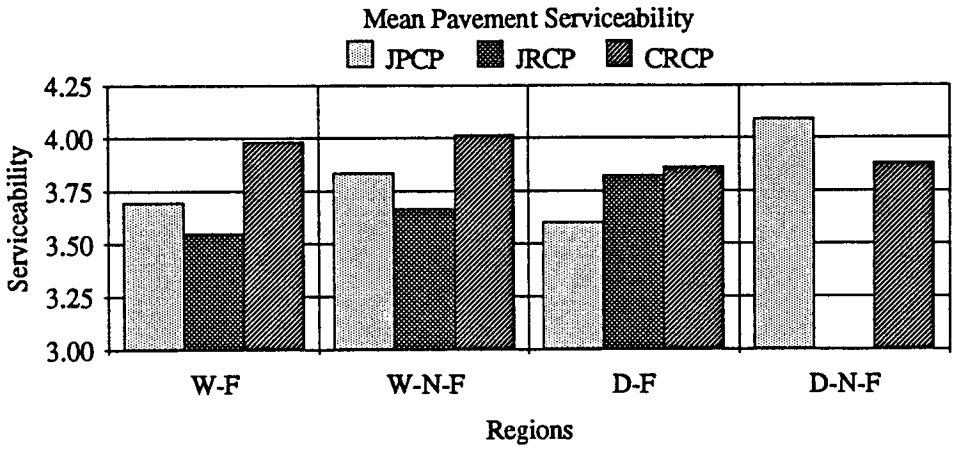

Figure 3.5. Mean Measured Current Serviceability by Climatic Regions in 1989-91

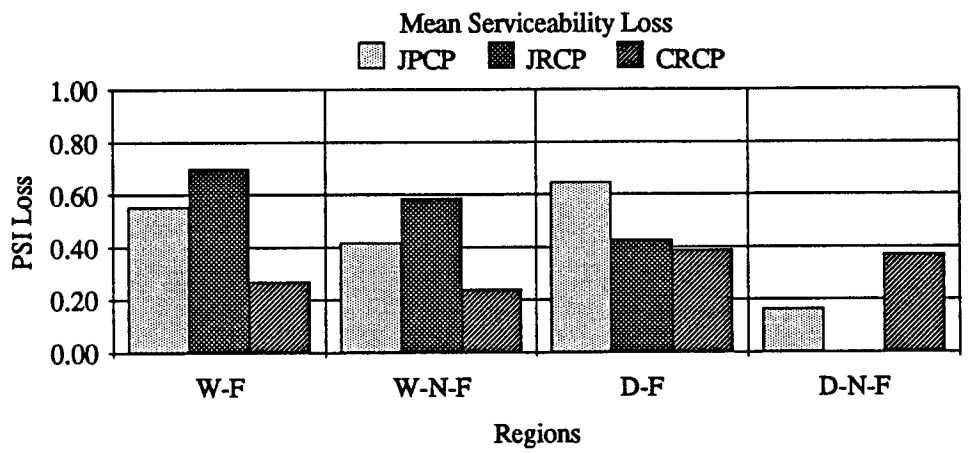

Figure 3.6. Mean Measured Loss in Serviceability by Climatic Regions

Modulus of Subgrade Reaction

Plate load-bearing tests were not conducted on the LTPP sections; therefore, for this analysis the measured deflections from falling weight deflectometer (FWD) testing were used to backcalculate the modulus of subgrade reaction k for all the sections. A computer program was developed for the backcalculation of concrete pavement layer properties based on equations from Hall (6), which were developed for application to the SHRP FWD seven-sensor arrangement. The mean dynamic k-value was obtained for each section with this computer program, and then reduced by a factor of two to estimate the static plate bearing k-value (7). The static k-value determined in this manner is essentially that on top of the subgrade since it is based on the maximum deflection measured. The principles behind this methodology are also described in Part III, Chapter 5 of the 1993 AASHTO Design Guide.

A distribution of the estimated static k-value on top of the subgrade determined for the LTPP sections is given in Figure 3.7.

In accordance with the AASHTO design procedure, in the cases where it was necessary, the estimated static k-value on top of the subgrade was adjusted to account for the presence of a stabilized base layer and/or loss of support (LOS). For the pavements with a stabilized base, the k-value on top of the base was determined with the equation that was used to develop Figure 3.3 of the AASHTO Design Guide (Equation LL.1, AASHTO Guide for Design of Pavement Structures, Volume 2, Appendix LL). Since the subgrade resilient modulus, M_R, is a required input for this equation and was not available in the data base at the time of this analysis, it was estimated from the backcalculated static k-values on top of the subgrade, using Equation 3.9 below. The development of Equation 3.9 is described in Appendix HH of Volume 2 of the AASHTO Guide.

$$k = \frac{M_R}{19.4} \tag{3.9}$$

For each of these sections, the estimated subgrade M_R and the typical stabilized base elastic modulus value were used to determine the composite k-value from Equation LL.1 of Volume 2 of the Guide. Where necessary, a loss of support (LOS) factor was then used to correct the composite k-value based on Figure 3.6 of the AASHTO Guide. Table 3.5 shows the typical base elastic modulus values (Ebase) and the LOS values that were used in these calculations. The values are based on guidelines provided in the AASHTO Guide.

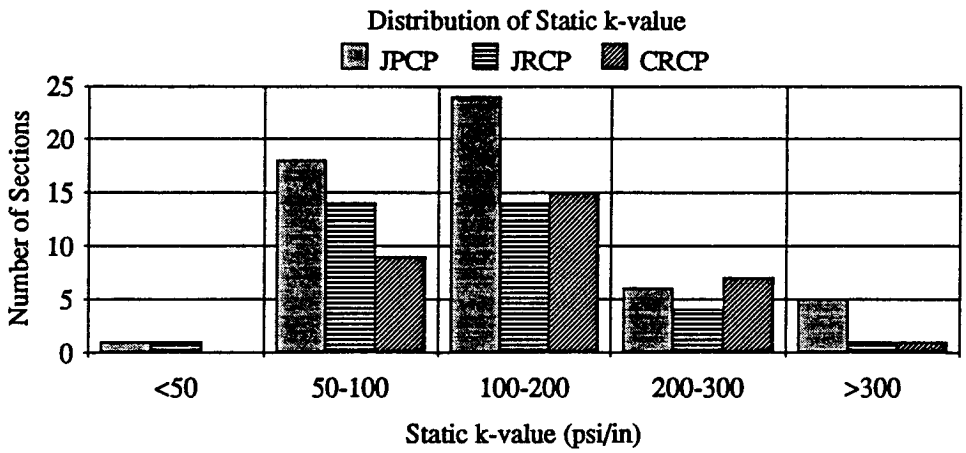

Figure 3.7. Distribution of Backcalculated Static k-Value of Subgrade

PCC Flexural Strength

The AASHTO model requires the mean flexural strength value determined at 28 days from a third-point loading test. This value, not available in the SHRP database, was estimated by first using Equation 3.10 to calculate the flexural strength from current core splitting tensile strength (7).

$$S_c = 1.02\ f_t + 210 \qquad \textbf{(3.10)}$$

Where:

f_t = splitting tensile strength of concrete core (at age of coring section), psi.

In order to obtain an estimate of the 28 day PCC flexural strength, multiple regression Equation 3.11 (based on data ranging from 3 days to 17 years) was used (8):

$$F_A = 1.22 + 0.17 \log_{10} T - .05 (\log_{10} T)^2 \qquad \textbf{(3.11)}$$

Where:

F_A = ratio of the flexural strength at time T to the flexural strength at 28 days; and

T = time since slab construction, years.

The flexural strength is then estimated at 28 days using the following expression:

$$S'_{c-28} = \left(\frac{S_c'}{F_A}\right) \qquad \textbf{(3.12)}$$

Where:

S'_c = flexural strength at time T; and

S'_{c-28} = flexural strength at 28 days (third-point loading).

The mean estimated 28 day flexural strength for all data was 735 psi (5.07 MPa), with a range of 543 to 1070 psi (3.74 to 7.38 MPa).

Load Transfer Coefficient

The appropriate load transfer coefficients, J, based on the type of load transfer device and shoulders in a section, were used. Recommended load transfer coefficients for various pavements and design conditions are given in Table 2.6 of the 1993 AASHTO Design Guide. Table 3.6 shows the load transfer coefficient values used for the analysis.

Table 3.5. Base Elastic Modulus and LOS Values Tested

Base Type	Permeable	LOS	Ebase (ksi)
Unbound	Yes	0.50	20
	No	1.00	20
Cement Treated	Yes	0.25	600
	No	0.75	1000
Asphalt Treated	Yes	0.25	800
	No	0.50	500
Lean Concrete	Yes	-	-
	No	0.25	1500

Table 3.6. Load Transfer Coefficients, J

Shoulder Type		AC	Tied PCC
Pavement Type	Dowels	Load Transfer Coefficient	
JPCP	N	4.10	3.90
	Y	3.20	2.80
JRCP	N	4.10	3.90
	Y	3.20	2.80
CRCP	-	3.05	2.60

Drainage Coefficient

The climatic zone in which a section is located and the quality of internal drainage was used to determine the value of the drainage coefficient, Cd. Recommended values of drainage coefficients for concrete pavements are given in Table 2.5 of the 1993 AASHTO Design Guide. Tables 3.7 and 3.8 were developed based on recommendations in the AASHTO Guide and procedures that were developed to best estimate the drainage coefficient for the sections (9).

General Comment

It is important to understand that all these inputs were selected as much as possible on the basis of AASHTO guidelines for design because these guidelines are used by pavement designers. Thus, many of these procedures were taken directly from the AASHTO Design Guide tables.

Table 3.7. Drainage Coefficient for Pavements With Permeable Blanket Drains

Moisture	Wet	Dry
Type of Drains	Drainage Coefficient	
Permeable Blanket Drains	1.10	1.20
No Permeable Blanket Drains	See Table 3.8	See Table 3.8

Table 3.8. Drainage Coefficients for Pavements Without Permeable Blanket Drains

Moisture		Wet				Dry			
Temperature		Freeze		No Freeze		Freeze		No Freeze	
Subgrade Type		F	C	F	C	F	C	F	C
Base Type	Type of Drains	Drainage Coefficient							
Granular	No Longitudinal	0.70	0.90	0.80	1.00	0.90	1.10	1.00	1.20
	Longitudinal	0.80	1.00	0.90	1.10	0.95	1.15	1.10	1.25
Stabilized	No Longitudinal	0.80	1.00	0.90	1.10	1.00	1.15	1.10	1.25
	Longitudinal	0.90	1.10	1.00	1.20	1.05	1.15	1.20	1.25

4

Evaluation of the Flexible Pavement Design Equation

Comparisons of Predicted Versus Observed Traffic

The work activities composing the evaluation consisted of a number of separate analyses, depicted in the flowchart in Figure 4.1. Data accumulation has been described in Chapters 2 and 3, so this discussion begins with calculation of the predicted KESALs (1000 ESALs) to cause the observed serviceability loss. Figure 4.2 provides a plot of predicted KESALs versus those estimated by the SHA's through 1989 and extrapolated through 1991. As can be seen, the traffic predicted by the AASHTO equation is consistently much higher than the estimates of historical traffic provided by the SHAs. From Figure 4.3, which provides the distribution of ratios of predicted to observed KESALs, it can be seen that only 9 of the 244 predictions were lower than the estimates by the State Highway Agencies. Almost half of the estimates (112) predicted traffic levels more than 100 times the SHA estimates. Note that the average ratio (8770) and standard deviation (51,800) are distorted by several sections where this ratio exceeded 100,000.

This extreme lack of fit of the design equation to the in-service data is not entirely due to shortcomings of the equation itself. Limitations of the input data (discussed in Chapters 1, 2, and 3) are also believed to have contributed to the apparent differences between predicted and estimated ESALs. The future availability of ESALs estimates that would include some years of measured data, plus higher values of Δ PSI (Present Serviceability Index), should allow a somewhat more accurate evaluation of the deficiencies in the equation itself.

Studies to Examine Fit of the AASHTO Design Equation to Observed Data

As one of six separate studies to explain the causes of the poor predictions, linear regressions were conducted using the AASHTO equation form shown in Equation 3.6 and the pertinent data for the 244 test sections. No significant fit could be obtained for this equation form. The coefficient of determination (R^2) never exceeded 0.25 and the root mean square error never went below 0.4.

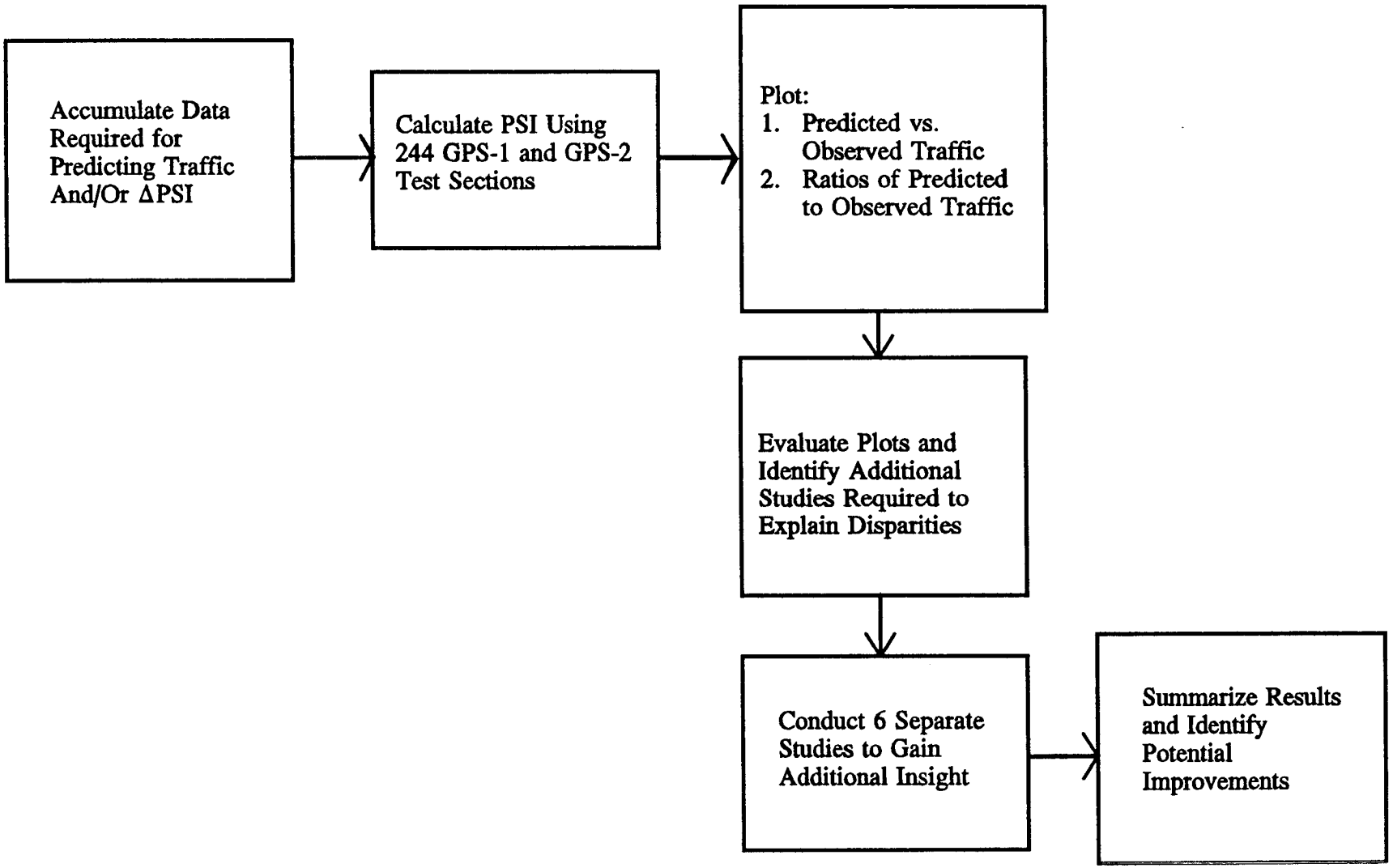

Figure 4.1. Work Plan for Evaluating the AASHTO Flexible Pavement Design

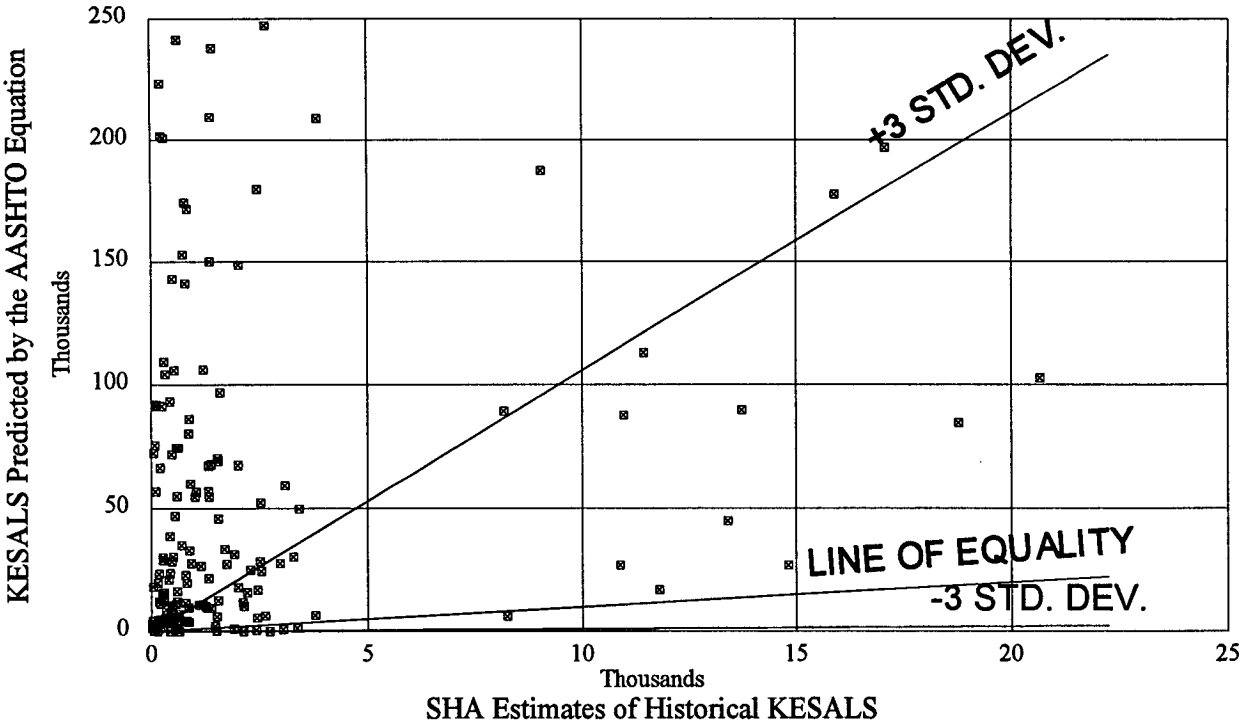

Figure 4.2. SHA Estimates of Historical Traffic Versus AASHTO Predicted Traffic

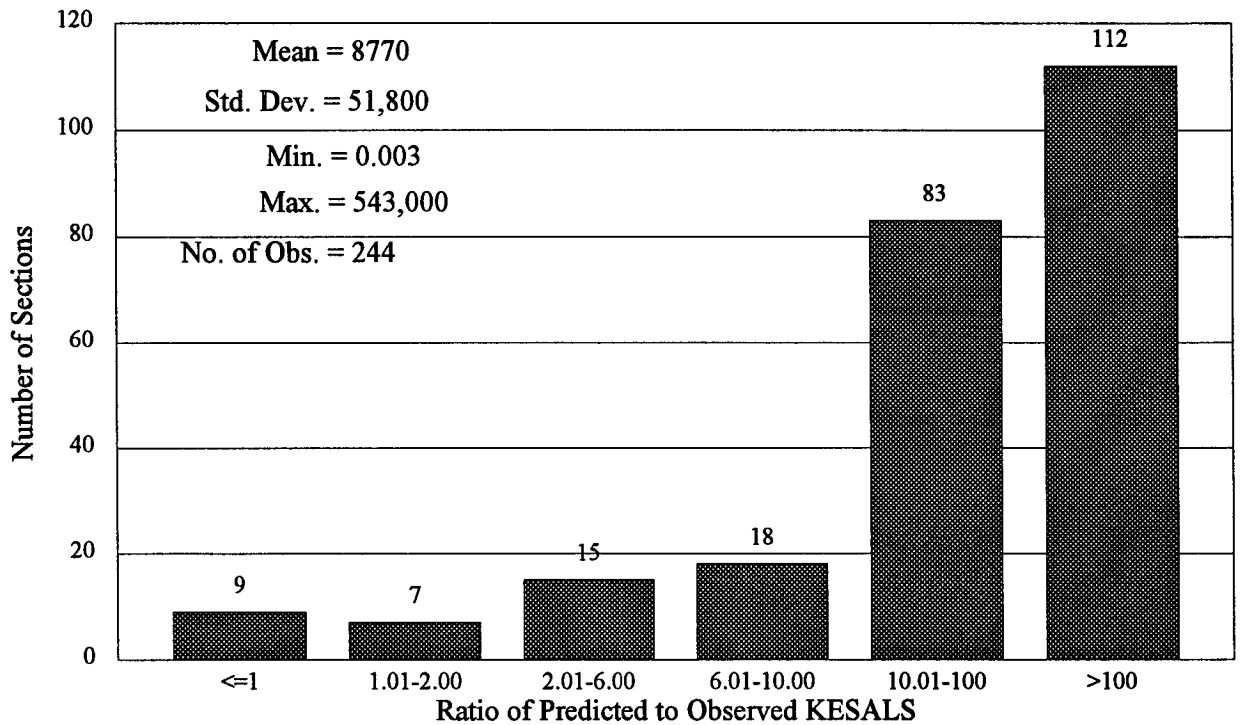

Figure 4.3. Distribution of Ratios of Predicted to Observed Traffic

Comparisons of Inference Spaces for the AASHO Road Test and the LTPP Data Base

From the evaluations of fit, however, it was established that there were several influential observations (sections for which the properties at those locations and their impact on predictions of traffic and/or serviceability loss at those locations significantly affected evaluations of the AASHTO model's ability to fit these data). Further evaluation of these influential observations indicated that some characteristics of these test sections fell outside of the inference space of the original AASHO equation. Modifications to the AASHTO flexible design equation over the years were intended to broaden the inference space for the AASHTO design equation.

Table 4.1 presents calculated values of PSI loss, using the AASHTO flexible pavement design equation for a factorial of subgrade resilient moduli, cumulative KESALs, and structural numbers. Because the resilient modulus of 3,000 psi for the subgrade is that used for the road test analyses, the group of results for this resilient modulus should best represent the inference space for the Road Test data. As can be seen, unreasonable results were obtained for structural numbers of 2 or 3, both of which are within the inference space of the Road Test. Although also well within the inference space, values of cumulative KESALs of 500 and 1,000 gave unreasonable predictions for structural numbers of 2 or 3.

Although out of the inference space for the Road Test, an increase of the subgrade resilient modulus to 10,000 psi decreased the magnitudes of the unreasonable predictions, as might be expected, but these predictions are still unreasonable. Use of 50,000 psi reduced the predictions to unreasonably small magnitudes. From this simple study, it was apparent that the design equation is capable of unreasonable predictions, even when the variable magnitudes fall within the inference space for the data used for its development.

Similarly, it can be seen from Figure 4.4 that most of the test sections in the SHRP Data Base (180 or 74% of the sections) have currently experienced a loss in PSI of 1 or less. This loss is obviously much less than the PSI loss experienced by similar pavements at the road test, which were trafficked to failure (with PSI losses of 2 to 3). Further, the average absolute deviation of observed PSI from the computed curves at the AASHO Road Test was 0.46 (10), so it can be seen from Figure 4.4 that 95 of the 244 test sections (39%) have currently experienced losses in PSI within the "noise" at the Road Test.

Effects of Extrapolation Beyond the AASHO Road Test Inference Space

Recognizing the potential impact of these inference space limitations, the data set was pared down and regressions rerun to see if better fits could be established. The three data sets (including the full data set as No. 1) were

Data Set	Test Section Exclusions	Included in Data Set
1	None	244
	SN < 2	
2	SN > 6	168
	ESALs > 5,000,000	
3	Avg. Ann. Rainfall < 25 in.	37
	Avg. Ann. Rainfall > 60 in.	
	Avg. Ann. Freeze Days < 100	

These exclusions were made to better approximate the environmental conditions at the AASHO Road Test. Even with these limitations, however, no significant improvements in the fit resulted. The R^2 continued to be less than 25%.

Table 4.1. Factorial of Solutions for Predicted PSI Loss From Equation 3.6

Mr (PSI)	Cumulative KESALs	Structural Number (SN)				
		2	3	5	7	10
3000	100	2483	0.79	0.24	0.11	0.04
	500	1,692,438	6	0.55	0.22	0.07
	1000	28,110,062	13	0.77	0.30	0.10
	5000	1.92E+10	93	1.73	0.59	0.19
	10,000	3.18E + 11	218	2.44	0.80	0.25
10,000	100	0.03	0.03	0.06	0.03	0.01
	500	20	0.19	0.14	0.07	0.02
	1000	340	0.43	0.19	0.09	0.03
	5000	231,585	3.09	0.43	0.18	0.06
	10,000	3,846,446	7.19	0.60	0.24	0.08
50,000	100	0.00	0.00	0.01	0.01	0.00
	500	0.00	0.00	0.02	0.01	0.01
	1000	0.00	0.00	0.03	0.02	0.01
	5000	0.06	0.03	0.07	0.04	0.01
	10000	1.03	0.08	0.09	0.05	0.02

Note: Shaded copy represents suspect loss values.

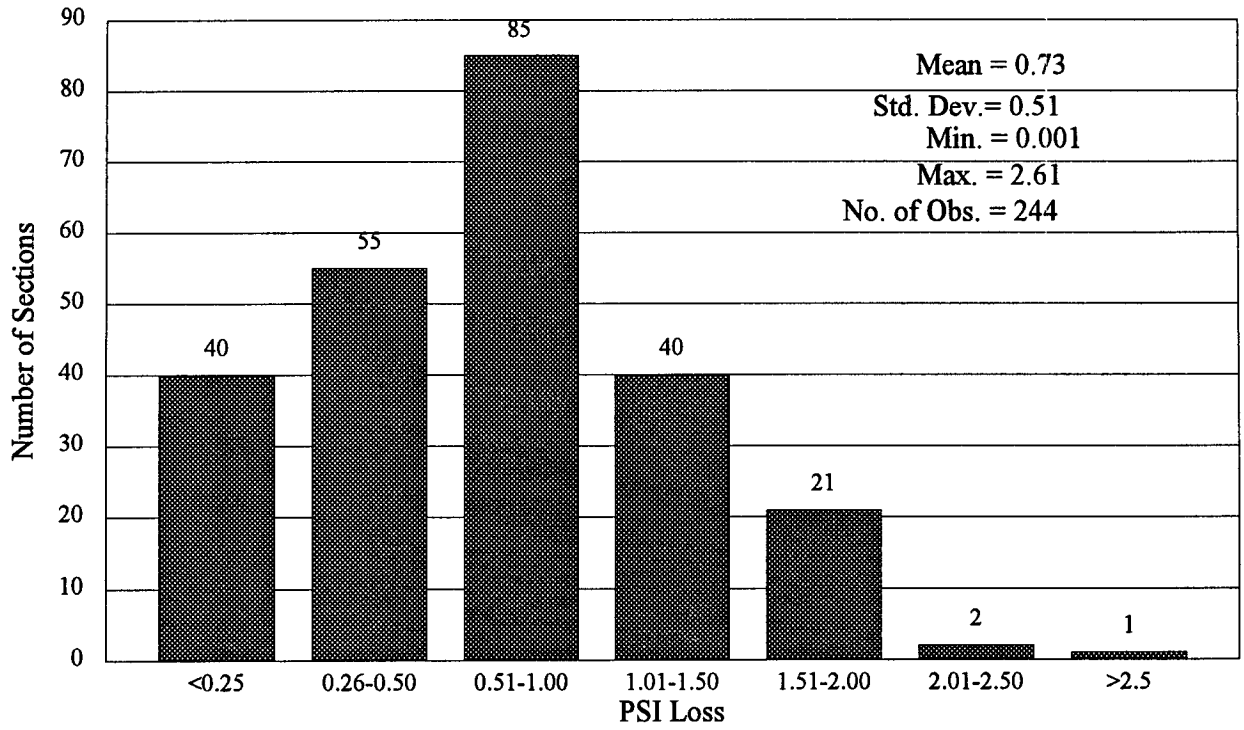

Figure 4.4. Distribution of Observed PSI Loss

Regressions of Ratios of Predicted to Observed Traffic

In an effort to identify why a better fit could not be obtained, linear regressions were conducted to model the ratio of predicted to observed traffic (R). This step allowed identification of variables not included in the AASHTO design equation that are needed to better predict the traffic required to cause the observed serviceability losses. The resulting model for R (the coefficient of determination $R^2 = 0.77$) was a function of average annual rainfall, average annual number of days below freezing, subgrade modulus, serviceability loss, structural number, and the thickness of existing seal coats. From previous discussions in this report and others, the significance of environmental variables is not surprising. Attempts have been made through the years since the Road Test to include environmental effects through various revisions to the original equations, but these attempts do not appear to have been sufficient, and some additional environmental variables are needed.

The subgrade moduli were estimated using only Sensor 7, as discussed in Chapter 2. Also, the relatively minor serviceability losses experienced by test sections included in the database thus far, as compared to the much higher serviceability losses at the Road Test overall, should be expected to play a significant role in this lack of fit. At the AASHO Road Test, most of the sections experienced serviceability losses in the range of 2 to 3, whereas the SHRP data base only includes three such sections (see Figure 4.4). Because few highway pavements are currently allowed in practice to deteriorate to the levels at the Road Test, it appears clear that the experience of the Road Test does not represent today's in-service North American highways.

It is generally recognized that the structural number concept has some theoretical flaws. For example, with a structural coefficient of 0.44 for an asphalt layer and a structural coefficient of 0.14 for an unbound granular base, it is implied that 1 in. (2.54 cm) of asphalt is equivalent to 3.14 in. (7.98 cm) of granular base. This ratio is, in fact, affected by many factors, not the least of which are the stresses to which the layer is exposed (i.e., its position within the total pavement structure).

Effects of Subgrade Moduli

Although resilient modulus testing of the subgrade was just getting underway at the time of the analysis, enough data were available to explore this subject a little further. It can be seen from Figure 4.5 that backcalculated moduli are considerably higher than the resilient moduli measured in the laboratory at a deviator stress of 2 psi (0.014 MPa) and a confining pressure of 2 psi (0.014 MPa). This stress state was selected for these comparisons as being the one utilized in the testing that was most representative for the first three feet of subgrade under a 9 kip (40 KN) wheel load. The mean ratio of estimated values to laboratory values is 4.48 for the 106 observations available. Assuming that subgrade moduli estimated from only the Sensor 7 deflections will generally average around 4.5 times the laboratory resilient moduli for the same materials tested at a similar stress state, it is fairly obvious that this extrapolates the design equation far outside its inference space. (A laboratory resilient modulus of 3,000 psi [20.7 MPa] was identified for the subgrade soils at the Road Test and was used in the extension of the 1986 Flexible Design Equation.) In order to learn whether use of resilient moduli obtained from laboratory moduli would improve the predictive capabilities, the estimated moduli were divided by 4.48 and the predictions repeated. Figure 4.6 displays the distributions of the ratios of predicted to observed traffic when the estimated subgrade moduli were used (identified as "Unmodified" — same distribution as in Figure 4.3) and when the backcalculated moduli were divided by 4.48 to approximate laboratory resilient moduli.

It can be seen from Figure 4.6 that use of the approximations to laboratory moduli considerably reduced the differences between the SHA estimates and the predictions of traffic from the AASHTO equation. The predictions for 40% of the 244 test sections were less than the SHA estimates and predictions for 12% ranged from one to two times their SHA estimates, but the predictions for the remaining 48% of the test sections ranged from two to over 100 times the SHA estimates. Although it appears clear that use of the resilient moduli obtained from laboratory testing could be expected to greatly improve the predictive capabilities of the design equation, the AASHTO equation still does not appear to adequately model the serviceability loss for the North American pavements in the SHRP LTPP Data Base.

Later, when subgrade moduli data were available for 106 of the 244 test sections being studied, these data were utilized to evaluate the various sources of subgrade moduli information available and their impact on the design equation. By limiting the analysis to these 106 sections, it can be seen from Figure 4.7 that the use of the laboratory subgrade moduli data considerably reduced the overpredictions produced by the use of the estimated subgrade moduli from deflection data. The use of the laboratory subgrade moduli data also

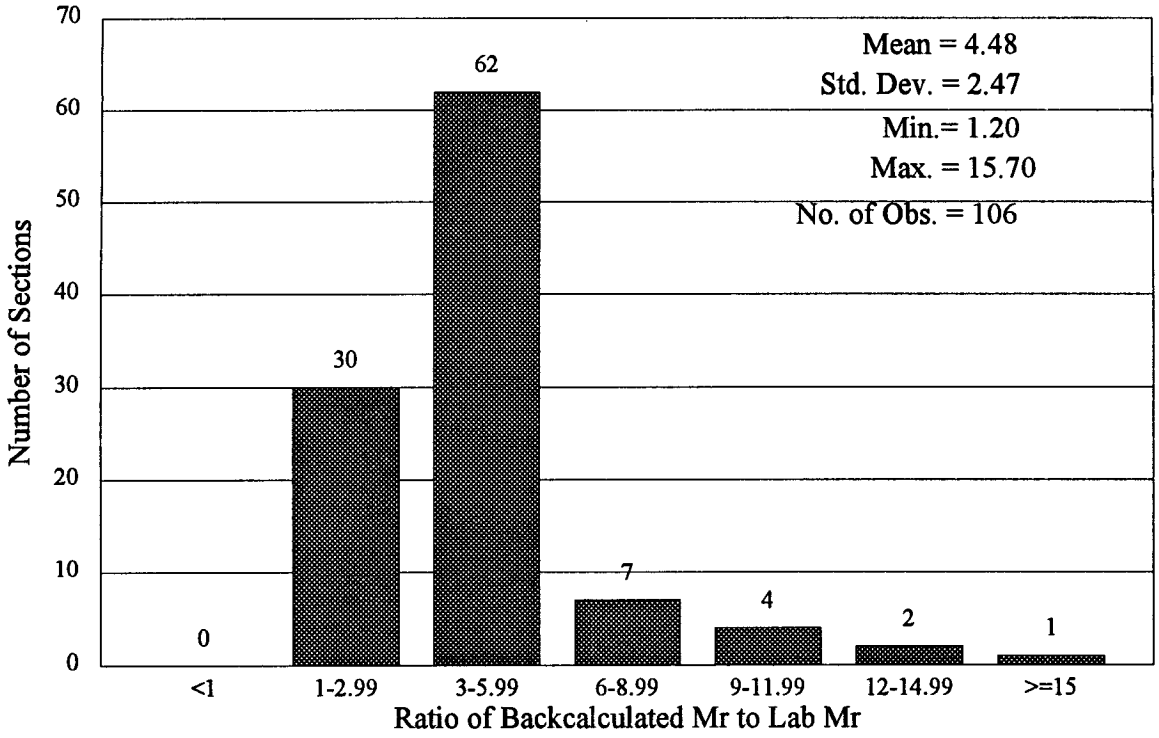

Figure 4.5. Distribution of Ratios of Backcalculated Subgrade Moduli to Resilient Moduli From Laboratory Testing

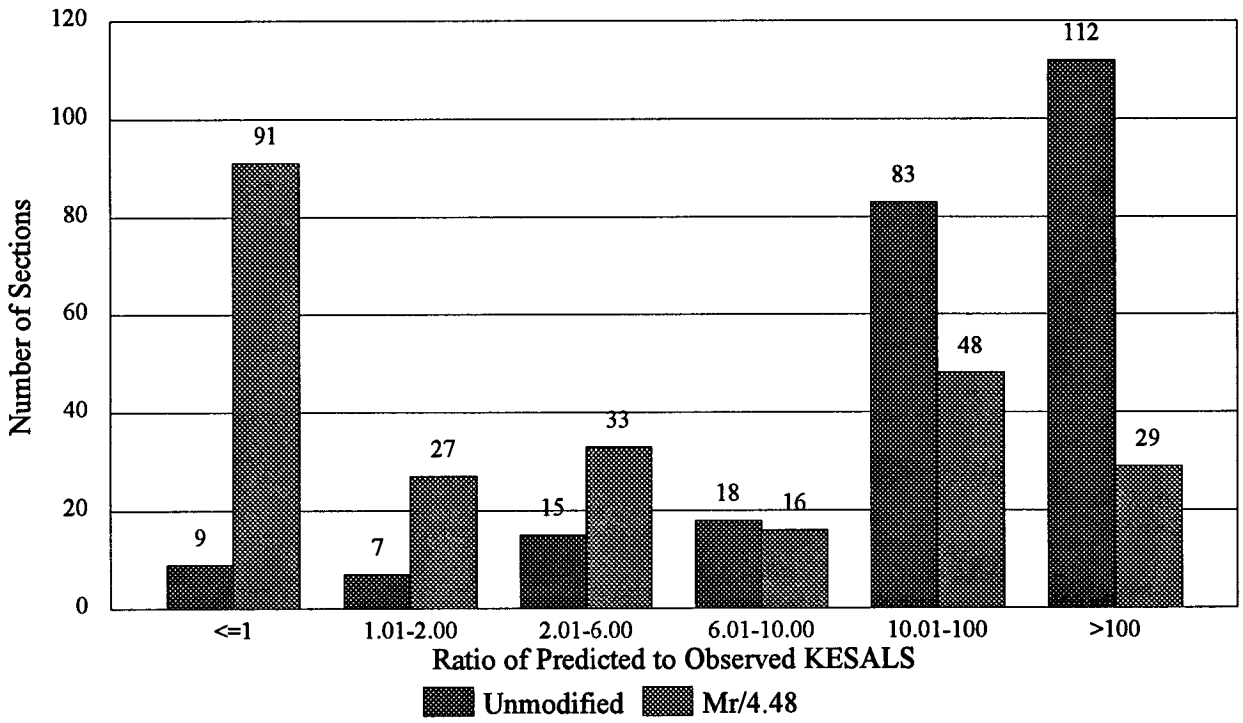

Figure 4.6. Distribution of Predicted to Observed Traffic Based on Estimated Subgrade Moduli and an Approximation of Laboratory Resilient Moduli

reduced the number of underpredictions. As expected, there are fewer sections with a ratio of less than one based on actual laboratory data than those identified by the scalar shift of subgrade moduli (by a factor of 4.48). The laboratory values appeared to provide the most reasonable evaluation of the design equation, but even with laboratory data it is still evident that many (almost 50 percent) of these test sections with laboratory subgrade moduli have predicted traffic levels in excess of a factor of two above those observed. Even with the best subgrade moduli data available, the equation still appeared to significantly overpredict.

Impact of Subgrade Volume Changes

In a final attempt at explaining the discrepancies in fit, steps were taken to estimate the loss in PSI due to subgrade volume changes and subtract them from the observed losses, based on the following equations from Appendix G of the 1986 Guide:

$$\Delta PSI_{sw} = 0.00335 * V_R * P_S * (1 - e^{-\theta t}) \quad (4.1)$$

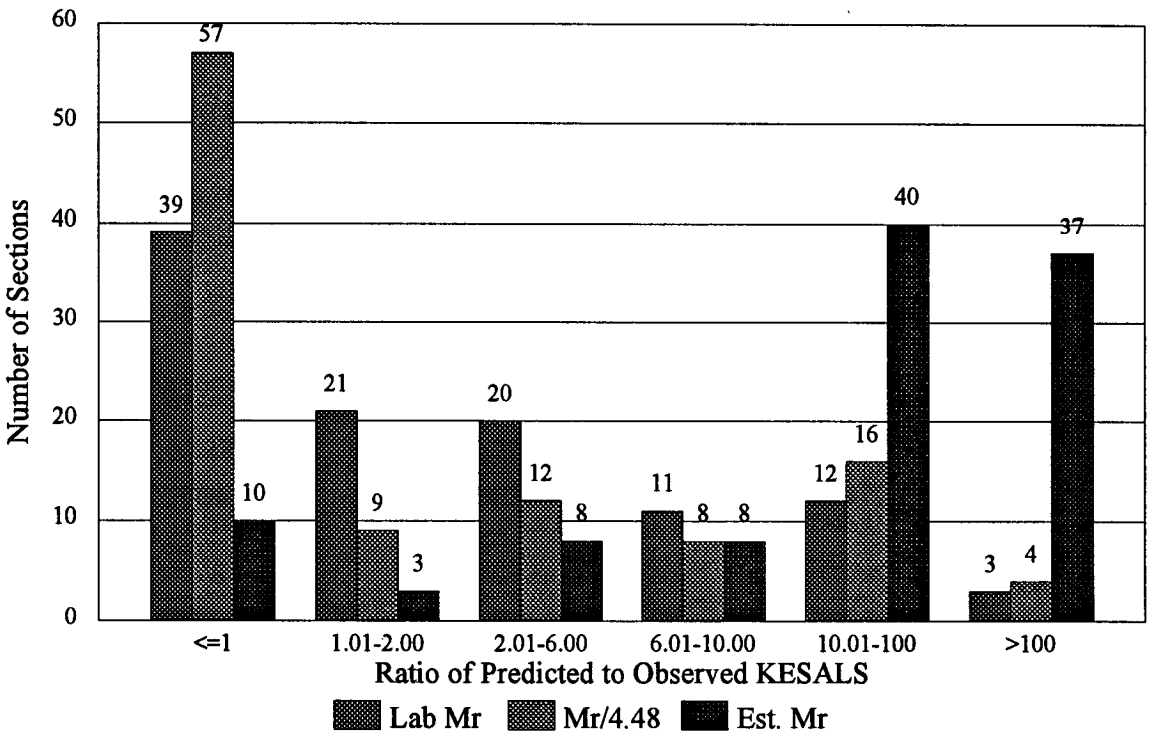

Figure 4.7. Distribution of Predicted to Observed Traffic Comparing Laboratory Subgrade Moduli to Estimates From Various Sources

Where:

ΔPSI_{sw}	=	serviceability loss due to roadbed swelling;
V_R	=	potential vertical rise, inches;
P_S	=	swell probability, % of total area subject to swell;
θ	=	swell rate constant; and
t	=	time, years.

Similarly, it is noted in Appendix G that:

$$\Delta PSI_{FH} = 0.01 * P_F * \Delta PSI_{MAX} (1 - e^{-0.02 \phi t}) \quad \textbf{(4.2)}$$

Where:

ΔPSI_{FH}	=	serviceability loss due to frost heave;
P_F	=	frost heave probability, (% of total area subject to frost heave);
ΔPSI_{MAX}	=	maximum potential serviceability loss;
ϕ	=	frost heave rate, mm/day;
t	=	time, years.

As discussed in Chapter 1, under "Data Limitations," all the data necessary to fully address these volume change phenomena are not available. Attempts have been made, however, to estimate these values based on the information available (plasticity index, average annual rainfall, average annual number of days below freezing, and soil gradations). As can be seen from Figure 4.8, the subgrade soil volume change corrections affect only a few sections.

Only 14 test sections were identified that would be expected to experience serviceability loss due to roadbed swelling. The highest serviceability loss due to swelling was 0.5, leaving only 0.3 due to traffic. The mean serviceability loss was 0.17 for the 14 test sections, and the mean effect for the entire data set of 244 test sections was a serviceability loss of 0.01.

For the 99 test sections estimated to be susceptible to roughness due to frost heave, the highest serviceability loss calculated was 0.14; the mean for these 99 test sections was 0.03, and the mean for the 244 test sections was 0.01.

Considerable time was spent applying the procedures in Appendix G of the Design Guide as well as they could be applied with the data available, but the effects appear to be insignificant for this evaluation of the AASHTO flexible design equation.

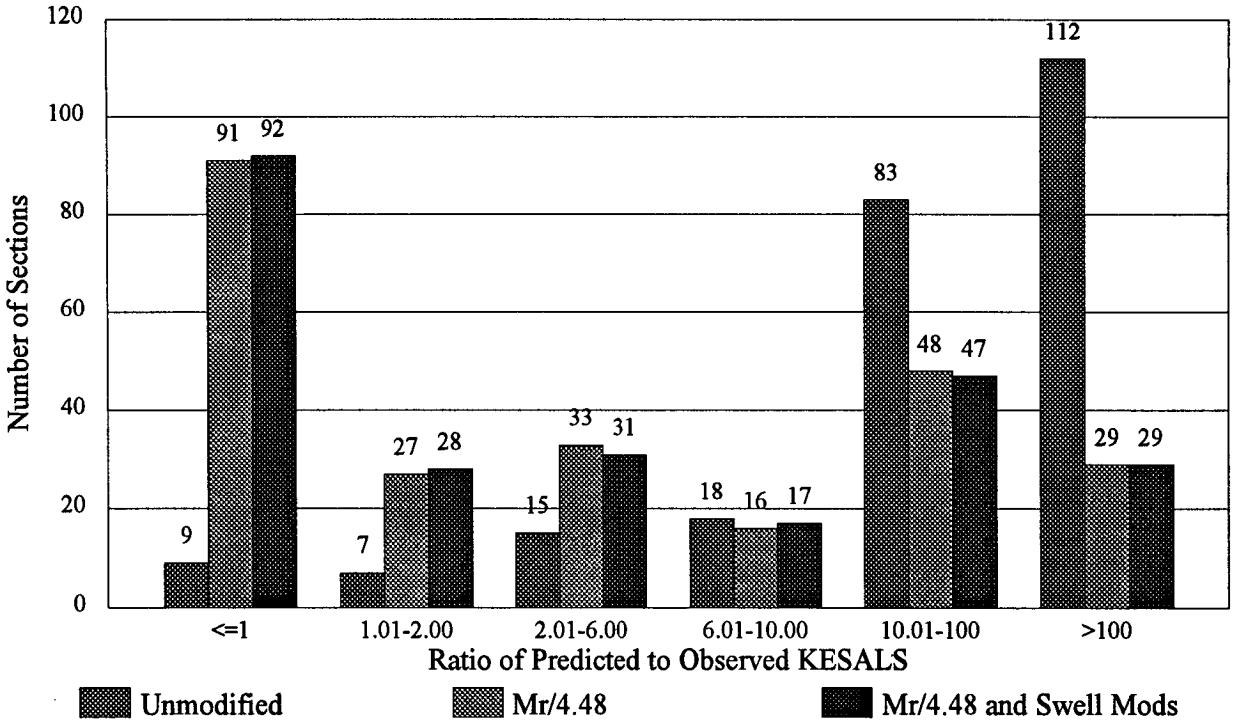

Figure 4.8. Distribution of Predicted to Observed Traffic, Based on Estimated Subgrade Moduli and an Approximation of Laboratory Moduli, With and Without Subgrade Volume Change Modifications

Recommendations

If serviceability loss is to be used as a basis for future design procedures, attempts should be made to improve the handling or incorporation of environmental and pavement structure data in pavement performance models. Several variables were identified in studies conducted here that significantly contribute to the disparity between predicted and observed performance. These specific variables were average annual rainfall, average annual number of days below freezing, subgrade moduli, and structural number (or some other means of representing pavement structure).

It should be noted that these early evaluations are based on only one round of measured roughness and rutting for each of the 244 test sections. Similarly, these evaluations are based on estimates of historical traffic and of initial PSI. Although there does not appear to be any opportunity for improving the estimates of initial PSI, there is a possibility for improving the historical traffic estimates through a technique called backcasting. As monitored traffic data accumulates, studies should be conducted to check and improve the historical traffic estimates. By calibrating the historical traffic estimates in this fashion based on monitored traffic data, potential errors in some of these estimates may be identified and adjusted. Also, as measured traffic data are added in time to the historical estimates, the magnitude of errors in the overall ESAL estimates will be reduced.

Similarly, as laboratory resilient modulus testing is completed, the results can be used to

replace the estimated subgrade stiffnesses currently included in these analyses. Initial analyses indicate that the estimated subgrade moduli established with Sensor 7 (as described in the 1986 Guide) appear to result in subgrade moduli estimates five times as high as the results from laboratory testing.

If future design equations are to be based on the serviceability concept, additional studies of slope variance (SV) are needed to quantify the difference between SV from the profilograph used at the Road Test and SV from the profilometer. These studies will allow a more accurate prediction of PSI as defined at the AASHO Road Test. By utilizing some of the sections that are fairly new, observation of how these values truly change with time would also be possible.

It is recommended, however, that future design equations be based on contemporary methods for measuring subgrade moduli and roughness. Different design equations will be required for backcalculated subgrade moduli and those moduli obtained from laboratory testing, unless suitable relationships between them can be developed.

It has long been recognized that the great majority of serviceability loss is due to increasing roughness and that rutting, cracking, and patching contribute little to the calculated serviceability loss (other than contributing to roughness). Many in the highway community believe that a better approach is to model roughness instead. Roughness would then become a separate concern, along with permanent deformation, fatigue cracking and thermal cracking for consideration by designers and pavement managers as noted in Figure 4.9, which was adapted from Figure 1 of Professor Carl Monismith's 1992 distinguished lecture (11). Figure 4.9 simply adds roughness (shown in dashed lines) to Monismith's diagram.

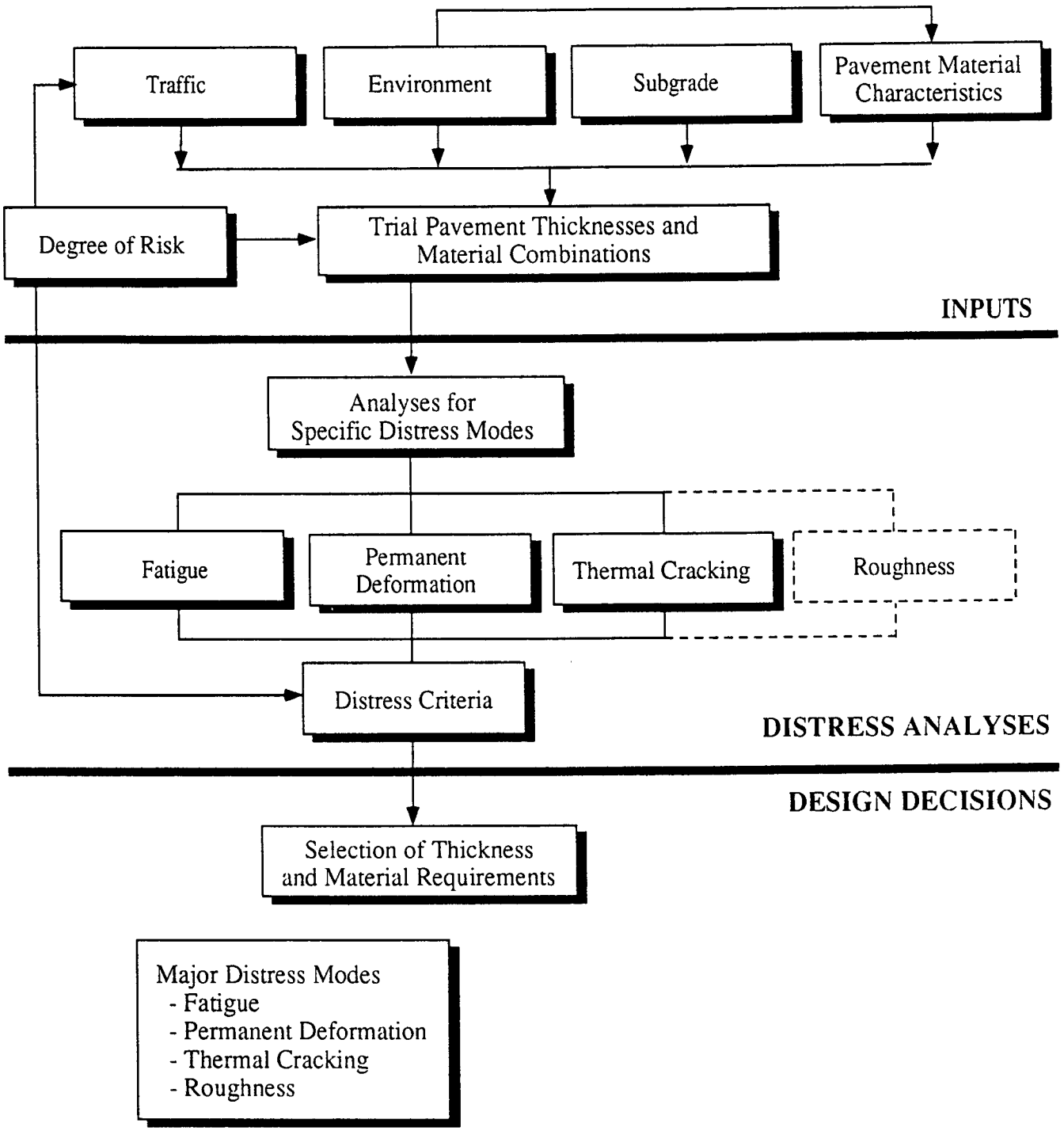

Figure 4.9. Simplified Framework for Pavement Analysis and Design

5

Improvements to the Flexible Pavement Design Equation

A number of different mechanisms affect the performance of a flexible pavement. These mechanisms, operating both individually and interactively, eventually lead to one or more types of pavement distresses (observed as distress manifestations such as cracks or ruts). Researchers at the AASHO Road Test elected to lump multiple distresses into one composite index—the Present Serviceability Index—which really emphasizes ride quality and virtually ignores the individual distresses that frequently dictate maintenance or rehabilitation strategies. Most members of the highway community agree that such pooling of distress types into one composite index is no longer necessary or desirable. By predicting the individual distresses and roughness separately, as shown in Figure 4.9, a flexible pavement design process can be optimized to meet a given agency's specific needs. For example, if for a given facility rutting is predicted to be the predominant distress of concern, a pavement design can be developed to minimize the occurrence of this particular distress. However, this design should be checked to be sure that unacceptable levels of roughness change, fatigue cracking, or transverse cracking would not be expected.

Another approach would be to generate separate designs for each of the individual distresses. From this grouping of pavement designs, an optimum could be selected based on one of the mathematical procedures currently available for this type of operation (e.g., linear programming, dynamic programming, or possibly even simple weighted averages). Still another approach to utilizing this set of distress prediction models would simply be to program an iterative process by which a pavement design would be sought to ensure that each of the distresses fell below a given level specified by the designer. Again, as an example, the designer would specify the applicable materials and traffic constraints, along with maximum distress levels tolerable for the traffic specified, and the program would be able to respond with the thicknesses required.

The thrust here is not toward the details of precisely how this optimum design would be reached, but rather to emphasize the flexibility provided to the designer through the use of unique predictive models for each individual distress. In this chapter, we will highlight the predictive models that have been developed from these early analyses of the SHRP data and how they might ultimately be refined and utilized in the pavement design process.

Results From Statistical Evaluations of Data

These results will compose an entire volume in the data analysis report, but only the most important results are included here. At this early stage of the long-term studies, the distresses experienced by the pavements in the studies are very limited. Only three distresses existed in the General Pavement Studies (GPS) test sections in sufficient quantity for reasonable evaluation. These distresses were change in roughness, rutting (or permanent deformation), and transverse cracking. Only 18 test sections displayed fatigue cracking at any severity level, so predictive equations for this distress must await future analyses when more test sections have experienced fatigue cracking. The mean value of rut depth was only 0.28 in. (0.71 cm) and the mean of International Roughness Index (IRI) was 97 in./mi (1.54 m/km). The estimated mean change in IRI was 44 in./mi (0.70 m/km).

Predictive Equations From the Sensitivity Analyses

Based on all data available at the time of these analyses, studies were conducted to evaluate the impact of the numerous pavement properties on the prediction of the distresses observed. The sensitivity analyses were conducted on several data sets gleaned from the GPS-1 and GPS-2 data. One data set included "HMAC [Hot Mix Asphalt Pavement] on granular base." Test sections in this data set could have an HMAC base, as well as an HMAC surface, as long as the combination rested on a granular (unbound) base, subbase, or both. A second data set included test sections with HMAC layers resting directly on untreated or treated subgrade. A third data set included test sections with HMAC resting on a bound base other than HMAC. The bound bases were either asphalt- or cement-treated.

The sensitivity analyses required equations to predict the occurrence of distress, and these equations had to be *statistically linear* (however, transformed variables such as logarithms or inverses, as well as variable combinations could be used) and have minimum collinearity between the independent variables. These requirements precluded use of nonlinear regression techniques and independent variable combinations with strong correlations.

The initial predictive models had an inference space that included the entire United States and parts of Canada. It was found that a single model to predict a distress across such a broad range of environmental conditions could not be developed that would sufficiently explain the effects from variations of the independent variables. This could possibly be a result of insufficient environmental data to explain the regional distinctions, but it is more likely a reflection of the different ways in which distress mechanisms manifest themselves in different environmental regions, as well as differences in interactions of distresses. Although the research staff continued to produce these North American models, models were also

developed separately for the four environmental regions (wet-no freeze, dry-no freeze, wet-freeze, and dry-freeze). The approximate boundaries for these environmental regions appear in Figure 5.1. These regional models were much better and are considered statistically sufficient for limited use until additional data become available for future analyses. Their interim use could include (1) acting as checks for individual distresses of pavement designs produced by existing procedures and (2) predicting pavement management systems for which more reliable predictive equations are not available.

The equations developed for HMAC over granular base appear in Tables 5.1 through 5.3 as examples. Separate equations were produced for combinations of pavement type, distress type, and environmental region. Because there are three distress types (rutting, transverse cracking, and change in roughness), four environmental regions, and three types of pavements; the potential for 36 regional equations exists. While this may seem an overwhelming number of equations, project location quickly restricts the search to a particular environmental region, and selection of type of pavement (HMAC over granular base, HMAC over PC [portland cement] treated base, or full-depth) immediately leads to one equation each for rutting, transverse cracking, and change in roughness. The North American equations developed from full data sets are not recommended for general use.

The array of independent variables differs between equations because the relative significance of individual data elements to prediction of distresses vary from one environmental region to another. This variation reflects differences in environmental effects, mechanisms leading to distress occurrence, and design and construction practices, and probably other differences or biases as well. Each predictive equation selected was the best of several hundred trial equations in terms of statistical parameters and minimization of collinearities between independent variables.

One glaring omission is the lack of equations to predict fatigue cracking. Although this important distress should be considered, there were not enough test sections with alligator cracking to support statistical analyses (as discussed above).

Specific details on how these analyses were conducted, how the model forms were developed, additional predictive equations, and additional details on the sensitivity analysis results appear in SHRP-P-393, "Sensitivity Analyses for Selected Pavement Distresses."

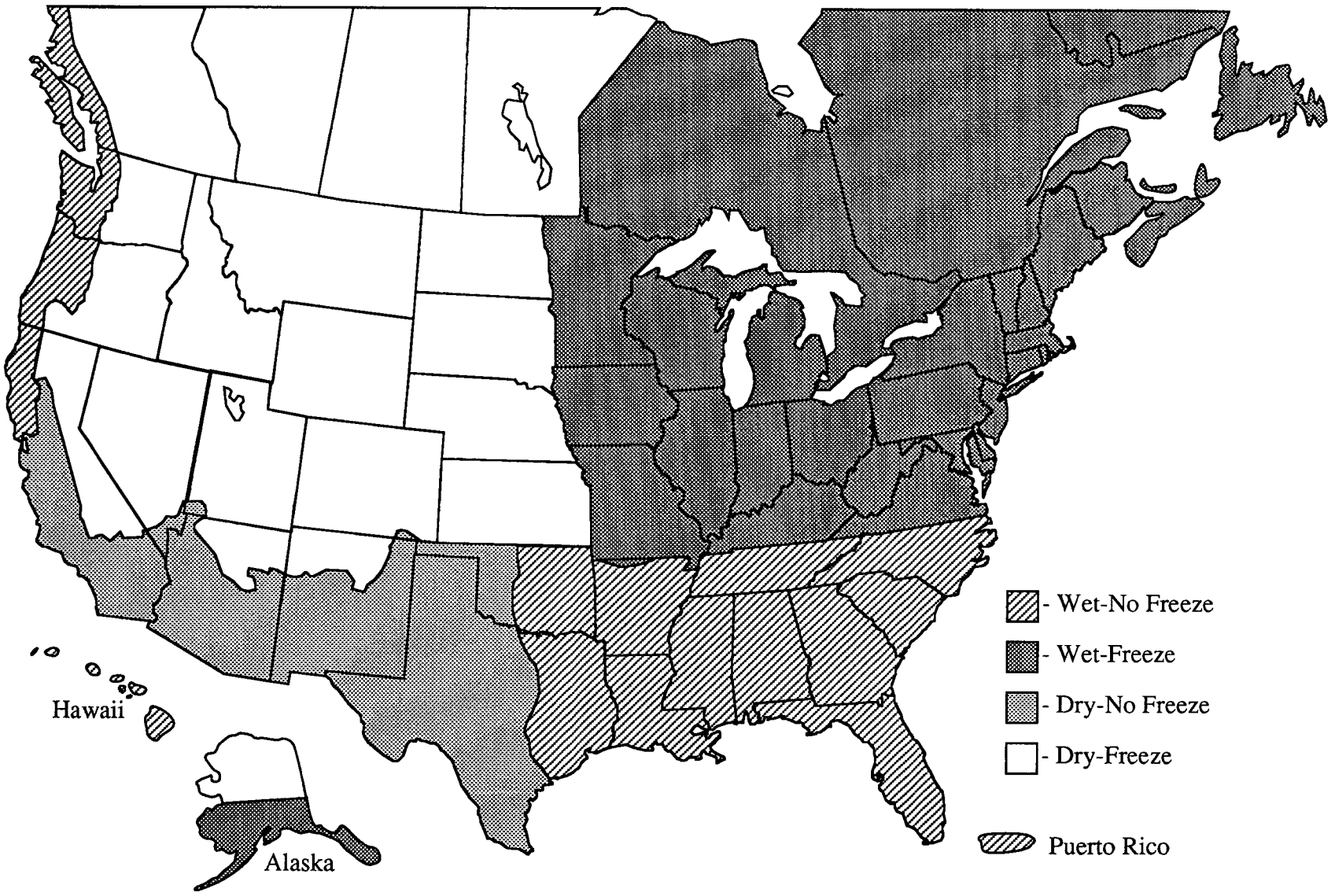

Figure 5.1. Environmental Zones for SHRP-LTPP Studies

Table 5.1. Coefficients for Regression Equations Developed to Predict Rutting in HMAC Pavements on Granular Base

Rut Depth (Inches) $= N^B 10^C$

Where: N = Number of Cumulative KESALs

$B = b_0 + b_1 x_1 + b_2 x_2 + \ldots + b_n x_n$

$C = c_0 + c_1 x_1 + c_2 x_2 + \ldots + c_n x_n$

a. Entire Data Set

Explanatory Variable or Interaction (x_i)	Units	Coefficients for Terms in	
		b_i	c_i
Constant Term	-	0.151	-0.00475
Log (HMAC Aggregate < No. 4 Sieve)	% by Weight	0	-0.596
Log (Air Voids in HMAC)	% by Volume	-0.0726	0
Log (Base Thickness)	Inches	0	0.190
Subgrade < No. 200 Sieve	% by Weight	0	0.00582
Freeze Index	Degree-Days	8.49×10^{-6}	0
(Log (HMAC Thickness) * Log (Base Thickness))	Inches Inches	0	-0.161

n = 152 R^2 = 0.45 Adjusted R^2 = 0.41 RMSE in Log_{10} Rut Depth = 0.18

b. Wet-No Freeze Data Set

Explanatory Variable or Interaction (x_i)	Units	Coefficients for Terms in	
		b_i	c_i
Constant Term	-	0.0739	0.00998
Log (HMAC Aggregate < No. 4 Sieve)	% by Weight	0	-0.373
Log (Air Voids in HMAC)	% by Volume	0	-0.215
Subgrade < No. 200 Sieve	% by Weight	-0.00056	0
Annual Number of Days > 90°F (32.2°C)	Number	0	-0.00022
Log (Annual Freeze-Thaw Cycles +1)	Number	0	0.0337
Log (HMAC Thickness) * Log (Base Thickness)	Inches Inches	0	-0.135

n = 41 R^2 = 0.72 Adjusted R^2 = 0.66 RMSE in Log_{10} Rut Depth = 0.18

Table 5.1. Coefficients for Regression Equations Developed to Predict Rutting in HMAC Pavements on Granular Base (continued)

Rut Depth = N^B 10^C (Inches)

Where: N = Number of Cumulative KESALs

$B = b_0 + b_1 x_1 + b_2 x_2 + ... + b_n x_n$

$C = c_0 + c_1 x_1 + c_2 x_2 + ... + c_n x_n$

c. Wet-Freeze Data Set

Explanatory Variable or Interaction (x_i)	Units	Coefficients for Terms in	
		b_i	c_i
Constant Term	-	0.183	0.0289
Log (Air Voids in HMAC)	% by Volume	0	-0.189
Log (HMAC Thickness)	Inches	0	-0.181
Log (HMAC Aggregate No. 4 Sieve)	% by Weight	0	-0.592
Asphalt Viscosity at 140°F (60°C)	Poise	0	1.80×10^{-5}
Log (Base Thickness)	Inches	0	-0.0436
(Annual Precipitation * Freeze Index)	Inches Degree-Days	0	3.23×10^{-6}

n = 41 R^2 = 0.73 Adjusted R^2 = 0.68 RMSE in Log_{10} Rut Depth = 0.19

d. Dry-No Freeze Data Set

Explanatory Variable or Interaction (x_i)	Units	Coefficients for Terms in	
		b_i	c_i
Constant Term	-	0.156	-0.00163
Log (HMAC Aggregate < No. 4 Sieve)	% by Weight	0	-0.628
Log (HMAC Thickness)	Inches	0	0.0918
Log (Air Voids in HMAC)	% by Volume	-0.0988	0
Base Thickness	Inches	0	0.00257
Subgrade < No. 200 Sieve)	% by Weight	0	0.00153
(Annual Precipitation * Annual Number of Days > 90°F [32.2°C])	Inches Number	0	6.588×10^{-5}

n = 36 R^2 = 0.75 Adjusted R^2 = 0.70 RMSE in Log_{10} Rut Depth = 0.16

Table 5.1. Coefficients for Regression Equations Developed to Predict Rutting in HMAC Pavements on Granular Base (continued)

Rut Depth (Inches) $= N^B 10^C$

Where: N = Number of Cumulative KESALs

$B = b_0 + b_1 x_1 + b_2 x_2 + \ldots + b_n x_n$

$C = c_0 + c_1 x_1 + c_2 x_2 + \ldots + c_n x_n$

e. Dry-Freeze Data Set

Explanatory Variable or Interaction (x_i)	Units	Coefficients for Terms in	
		b_i	c_i
Constant Term	-	0.0394	0.00451
Log (HMAC Thickness)	Inches	0	0.0600
Mod. AASHTO Base Compaction	% of Max. Density	0	-0.00849
(Base Thickness * Log (HMAC Thickness))	Inches Inches	0	0.00875
(Log (Subgrade < #200 Sieve) * Log (Freeze Index +1))	% by Weight Degree-Days	0	0.0107
(Log (Subgrade < #200 Sieve) * Log (Air Voids in HMAC))	% by Weight % by Volume	0	-0.00567

n = 34 R^2 = 0.85 Adjusted R^2 = 0.81 RMSE in Log_{10} (Rut Depth) = 0.11

Table 5.2. Coefficients for Regression Equations Developed to Predict Change in Roughness in HMAC Pavements on Granular Base

$\Delta IRI = N^B 10^C$ (Inches/Mile)

Where:

N = Number of Cumulative KESALs

$B = b_0 + b_1 x_1 + b_2 x_2 + \ldots + b_n x_n$

$C = c_0 + c_1 x_1 + c_2 x_2 + \ldots + c_n x_n$

a. Entire Data Set

Explanatory Variable or Interaction (x_i)	Units	Coefficients for Terms in	
		b_i	c_i
Constant Term	-	0.153	-0.000543
Asphalt Content	% by Weight	0	-0.0160
Annual Precipitation	Inches	0	0.000359
Asphalt Viscosity at 140°F (60°C)	Poise	0	3.634×10^{-5}
Base Thickness	Inches	0	-0.00335
Base Compaction (Mod. AASHTO)	% of Max. Density	0	0.0113
Subgrade < #200 Sieve	% by Weight	0	0.00062
Freeze Index	Degree-Days	0	8.107×10^{-5}
(Ann. No. Days > 90°F (32.2°C) * HMAC Thickness)	Number Inches	0	-0.000437
(Ann. No. Days > 90°F (32.2°C) * Air Voids in HMAC)	Number % by Volume	0	0.000178

n = 108 R^2 = 0.65 Adjusted R^2 = 0.62 RMSE in Log_{10} (ΔIRI) = 0.34

Table 5.2. Coefficients for Regression Equations Developed to Predict Change in Roughness in HMAC Pavements on Granular Base (continued)

$\Delta IRI = N^B 10^C$ (Inches/Mile) Where: N = Number of Cumulative KESALs

$B = b_0 + b_1 x_1 + b_2 x_2 + \ldots + b_n x_n$

$C = c_0 + c_1 x_1 + c_2 x_2 + \ldots + c_n x_n$

b. Wet-No Freeze Data Set

Explanatory Variable or Interaction (x_i)	Units	Coefficients for Terms in	
		b_i	c_i
Constant Term	-	0.210	0.0233
Base Thickness	Inches	0	-0.0372
Annual Number of Days > 90°F (32.2°C)	Number	0	0.00249
Annual Precipitation	Inches	0	0.0214
(HMAC Thickness * Base Compaction (Mod AASHTO))	Inches % of Max. Density	0	-0.000761
(Log (Air Voids in HMAC) * Daily Temperature Range	% by Volume °F	0	0.0322
(Asphalt Viscosity at 140°F [60°C] * Log (Annual Freeze-Thaw Cycles +1))	Poise Number	0	-0.000299
(Asphalt Viscosity at 140°F [60°C] * Daily Temperature Range)	Poise °F	0	1.702×10^{-5}

n = 32 R^2 = 0.85 Adjusted R^2 = 0.81 RMSE in Log_{10} (ΔIRI) = 0.31

c. Wet-Freeze Data Set

Explanatory Variable or Interaction (x_i)	Units	Coefficients for Terms in	
		b_i	c_i
Constant Term	-	0.250	0.0403
Asphalt Viscosity at 140°F (60°C)	Poise	0	0.00014
Air Voids in HMAC	% by Volume	0	0.0704
Log (HMAC Thickness)	Inches	0	0.314
Base Thickness	Inches	0	-0.00162
Annual Number of Days > 90°F (32.2°C)	Number	0	-0.00165
(Freeze Index * Air Voids in HMAC)	Degree-Days % by Volume	0	1.628×10^{-5}

n = 35 R^2 = 0.87 Adjusted R^2 = 0.84 RMSE in Log_{10} (ΔIRI) = 0.27

Table 5.2. Coefficients for Regression Equations Developed to Predict Change in Roughness in HMAC Pavements on Granular Base (continued)

$\Delta IRI = N^B 10^C$ (Inches/Mile) Where: N = Number of Cumulative KESALs

$B = b_0 + b_1 x_1 + b_2 x_2 + \ldots + b_n x_n$

$C = c_0 + c_1 x_1 + c_2 x_2 + \ldots + c_n x_n$

d. Dry-No Freeze Data Set

Explanatory Variable or Interaction (x_i)	Units	Coefficients for Terms in	
		b_i	c_i
Constant Term	-	0.406	-0.00994
HMAC Thickness	Inches	0	0.0255
Asphalt Viscosity at 140°F (60°C)	Poise	0	0.00024
Base Thickness	Inches	0	-0.0329
Annual Precipitation	Inches	0	0.0124
(Annual Number of Days > 90°F (32.2°C) * HMAC Thickness)	Number Inches	0	-0.00114
(Subgrade < #200 Sieve * Annual Precipitation)	% by Weight Inches	0	0.000268

n = 27 R^2 = 0.95 Adjusted R^2 = 0.93 RMSE in Log_{10} (ΔIRI) = 0.18

e. Dry-Freeze Data Set

Explanatory Variable or Interaction (x_i)	Units	Coefficients for Terms in	
		b_i	c_i
Constant Term	-	0.271	0.00393
Asphalt Viscosity at 140°F (60°C)	Poise	0	0.000317
Base Thickness	Inches	0	0.0240
Annual Number of Days > 90°F (32.2°C)	Number	0	-0.0125
(Log (Air Voids in HMAC) * HMAC Thickness)	% by Volume Inches	0	-0.00197
(Freeze Index * Annual Number of Days > 90°F [32.2°C])	Degree-Days Number	0	1.451×10^{-5}

n = 14 R^2 = 0.94 Adjusted R^2 = 0.92 RMSE in Log_{10} (ΔIRI) = 0.21

Table 5.3. Coefficients for Regression Equations Developed to Predict Transverse Crack Spacing in HMAC Pavements on Granular Base and Full-Depth HMAC Pavements

Crack Spacing = $N^B 10^C$ (Feet)

Where: N = Age, Years

$B = b_0 + b_1 x_1 + b_2 x_2 + \ldots + b_n x_n$

$C = c_0 + c_1 x_1 + c_2 x_2 + \ldots + c_n x_n$

a. Entire Data Set

Explanatory Variable or Interaction (x_i)	Units	Coefficients for Terms in	
		b_i	c_i
Constant Term	-	-0.205	0.282
Log (HMAC Thickness)	Inches	0	0.341
Air Voids in HMAC	% by Volume	0	0.00686
Log (Base Thickness +1)	Inches	0	-0.00310
Base Compaction (Mod. AASHTO)	% of Max. Density	0	0.00646
(Asphalt Viscosity at 140°F [60°C] * Log (Base Thickness +1))	Poise Inches	0	0.00013
(Log (Annual Precipitation) * Log (Base Thickness +1))	Inches Inches	0	0.301

n = 118 R^2 = 0.37 Adjusted R^2 = 0.33 RMSE in Log_{10} Crack Spacing = 0.53

b. Wet-No Freeze Data Set

Explanatory Variable or Interaction (x_i)	Units	Coefficients for Terms in	
		b_i	c_i
Constant Term	-	-1.12	0.0131
Log (Freeze Index +1)	°F - Days	0	0.733
Log (Annual Precipitation)	Inches	0	0.534
(HMAC Thickness * Log (Asphalt Viscosity at 140°F [60°]))	Inches Poise	0	0.0109
(Base Thickness * Asphalt Content)	Inches % by Weight	0	-0.00587
(Base Compaction * Daily Temperature Range)	% of Max. Density °F	0	0.000295

n = 17 R^2 = 0.85 Adjusted R^2 = 0.75 RMSE in Log_{10} Crack Spacing = 0.52

Table 5.3. Coefficients for Regression Equations Developed to Predict Transverse Crack Spacing in HMAC Pavements on Granular Base and Full-Depth HMAC Pavements (continued)

Crack Spacing (Feet) $= N^B 10^C$ Where: N = Age, Years

$B = b_0 + b_1 x_1 + b_2 x_2 + \ldots + b_n x_n$

$C = c_0 + c_1 x_1 + c_2 x_2 + \ldots + c_n x_n$

c. Wet Freeze Data Set

Explanatory Variable or Interaction (x_i)	Units	Coefficients for Terms in	
		b_i	c_i
Constant Term	-	-0.106	-0.0201
HMAC Aggregate < No. 4	% by Weight	0	-0.0131
HMAC Thickness	Inches	-0.00474	0
Log (Annual Precipitation)	Inches	0	1.84
Annual No. of Days > 90°F (32.2°C)	Number	-0.0540	0
(Base Thickness * Log (Annual Precipitation))	Inches Inches	0	-0.0159
(Base Thickness * Annual No. of Days > 90°F [32.2°C])	Inches Number	0	0.00240
(Subgrade < No. 200 * Log (Annual Precipitation))	% by Weight Inches	0	0.00408

n = 44 R^2 = 0.86 Adjusted R^2 = 0.83 RMSE in Log_{10} Crack Spacing = 0.30

d. Dry-No Freeze Data Set

Explanatory Variable or Interaction (x_i)	Units	Coefficients for Terms in	
		b_i	c_i
Constant Term	-	-0.241	-0.00155
HMAC Thickness	Inches	0	-0.0282
Log (Base Thickness +1)	Inches	-0.147	0
Log (Annual Precipitation)	Inches	0	1.89

n = 23 R^2 = 0.86 Adjusted R^2 = 0.83 RMSE in Log_{10} Crack Spacing = 0.35

Table 5.3. Coefficients for Regression Equations Developed to Predict Transverse Crack Spacing in HMAC Pavements on Granular Base and Full-Depth HMAC Pavements (continued)

Crack Spacing (Feet) $= N^B 10^C$

Where: N = Age, Years

$B = b_0 + b_1 x_1 + b_2 x_2 + \ldots + b_n x_n$

$C = c_0 + c_1 x_1 + c_2 x_2 + \ldots + c_n x_n$

e. Dry Freeze Data Set

Explanatory Variable or Interaction (x_i)	Units	Coefficients for Terms in	
		b_i	c_i
Constant Term	-	-0.425	0.0468
Log (Annual Traffic)	KESALs	0	0.854
Base Thickness	Inches	0	-0.00853
Freeze Index	°F - Days	0	0.00013
(HMAC Thickness * Base Thickness)	Inches Inches	0	0.00398
(HMAC Thickness * Asphalt Viscosity at 140°F [60°C])	Inches Poise	0	1.64×10^{-5}
(HMAC Thickness * Log (Subgrade < No. 200 +1))	Inches % by Weight	0	-0.0350
(Asphalt Viscosity at 140°F [60°C] * Log (Subgrade < No. 200 +1))	Poise % by Weight	0	0.000109

n = 34 $R^2 = 0.78$ Adjusted $R^2 = 0.72$ RMSE in Log_{10} Crack Spacing = 0.44

Studies to Adapt Predictive Equations for Use in Design

The predictive equations from the sensitivity analyses discussed above were generated with a great number of data elements available in the LTPP Data Base. It must be recognized, however, that designers frequently do not have all these data at their disposal. For example, HMAC mix properties and base compaction can only be accurately established during construction. However, it is anticipated that most agencies select a set of assumed or specified values for these factors and simplify the equations accordingly. Those variables that may require assumed or specified values during design are

- HMAC air voids,
- asphalt viscosity,
- asphalt content,
- HMAC aggregate passing a No. 4 sieve, and
- base compaction (percentage of modified AASHTO maximum density).

Figures 5.2, 5.3, and 5.4 graphically display relative sensitivities of the regional prediction equations for HMAC over granular base to each of the significant independent variables incorporated in them. The most significant variable appears at the top of each plot, and the relative significance of variables decreases with position below, as indicated by the width of the bars that represent each variable. The procedure used for the sensitivity analyses involved setting all explanatory variables in a predictive equation at their means, and then varying each one independently from one standard deviation below the mean to one standard deviation above the mean. The relative sensitivity of the distress prediction for that variable is the change in the predicted distress across the range of two standard deviations, as compared to the changes when other explanatory variables were varied in the same manner. The vertical lines through the bars are located at the predicted mean values for each data set. The arrows within the bars indicate whether an increase in that variable increases or decreases the predicted value. As an example, increasing KESALs in Figure 5.2 increases rut depth. Using the results of the sensitivity analyses, a designer can establish the relative significance of a given variable to the prediction of a given distress mechanism. This determination allows a designer to establish how inaccuracies in an assumed value of any given variable will affect prediction of a given distress.

Table 5.4 is an example of the statistical data prepared to help designers who are utilizing these equations, or researchers who wish to use the LTPP data base, understand and appreciate the inference spaces from which the equations were developed. Included in this table are the mean, minimum, maximum, standard deviation, and other significant properties associated with each of the variables included in the rutting equations from the entire data set for HMAC over a granular base. The use of these equations for data outside the ranges of data elements including the inference space should be approached with caution and may not provide satisfactory results. The majority of the test sections had coarse subgrades, so the equations should be used more conservatively for projects with fine-grained subgrades. Similar tables are available for all the predictive equations and appear in the "Data Processing and Evaluation" section of this report.

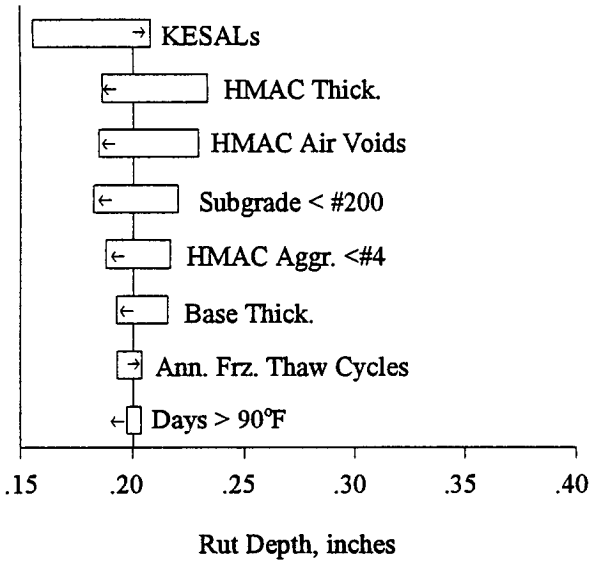

a. Wet-No Freeze Data Set

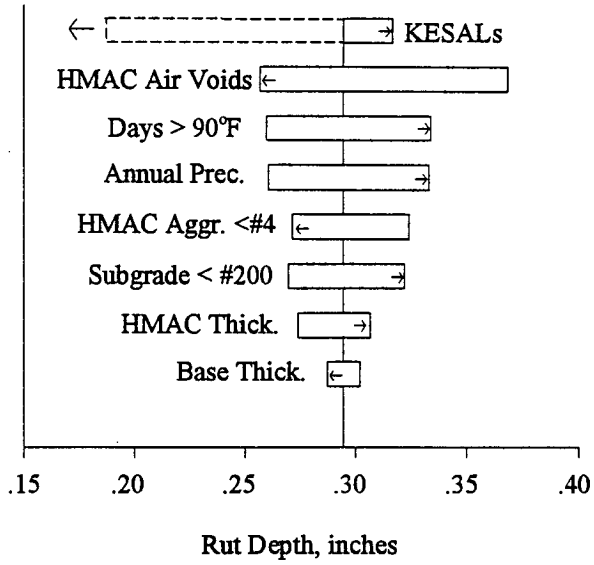

b. Dry-No Freeze Data Set

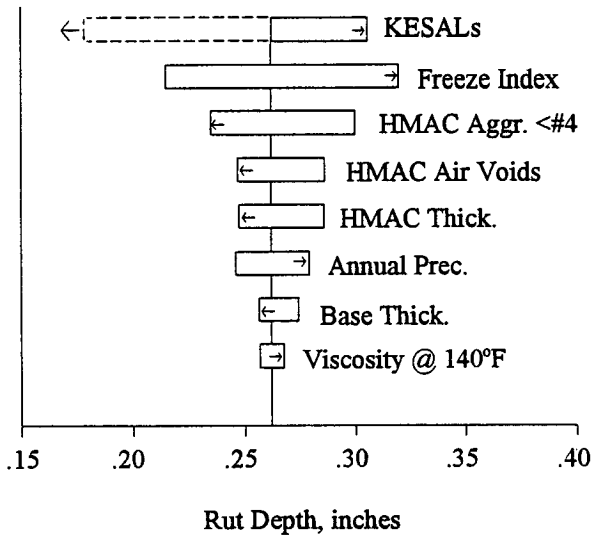

c. Wet-Freeze Data Set

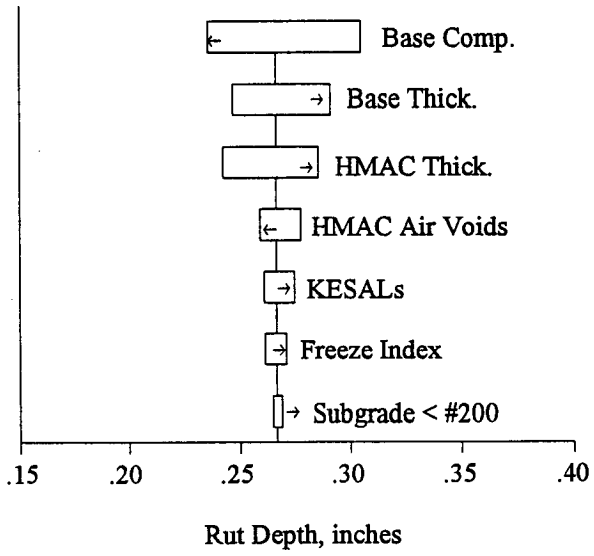

d. Dry-Freeze Data Set

Figure 5.2. Results From Sensitivity Analyses for Rutting in HMAC Pavements on Granular Base, by Environmental Zone

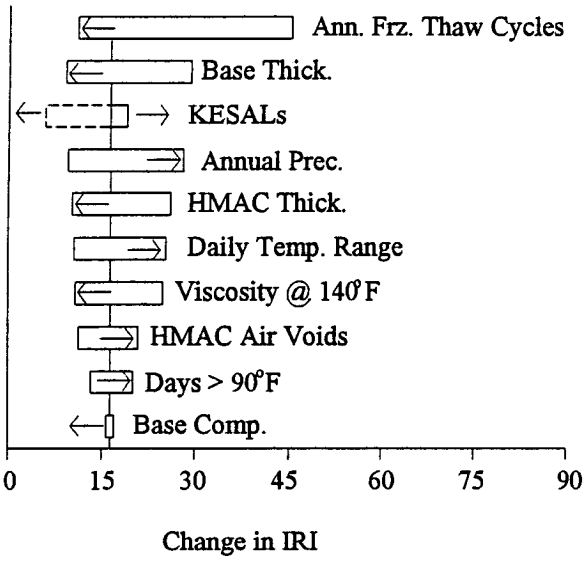

a. **Wet-No Freeze Data Set**

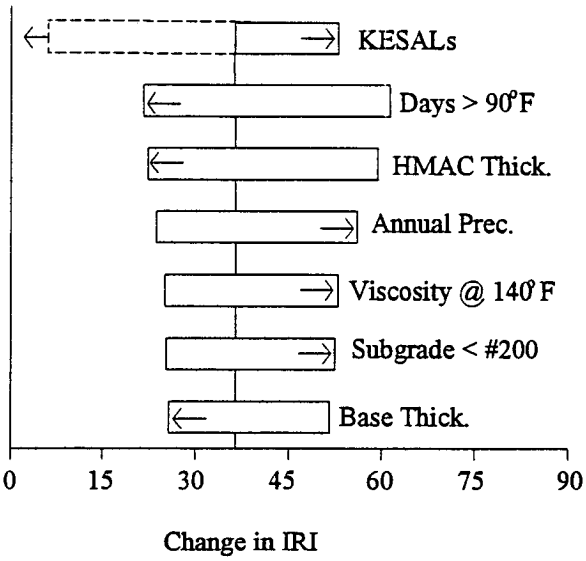

b. **Dry-No Freeze Data Set**

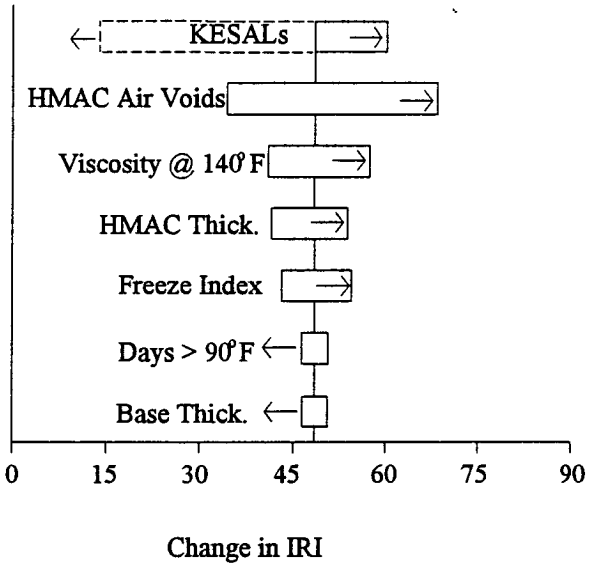

c. **Wet-Freeze Data Set**

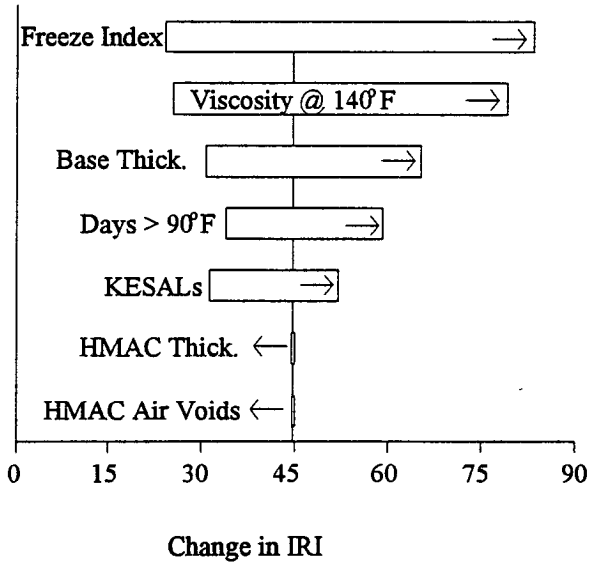

d. **Dry-Freeze Data Set**

Figure 5.3. Results From Sensitivity Analyses for Change in IRI in HMAC Pavements on Granular Base, by Emotional Zone

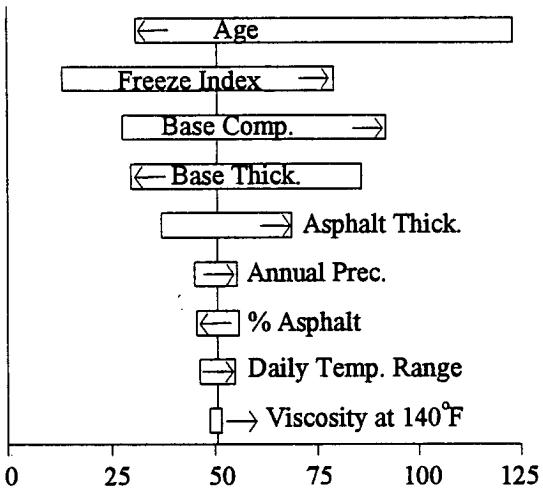

a. Wet-No Freeze Data Set

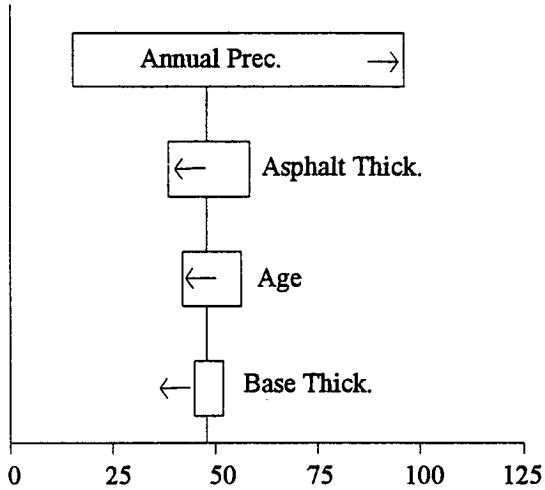

b. Dry-No Freeze Data Set

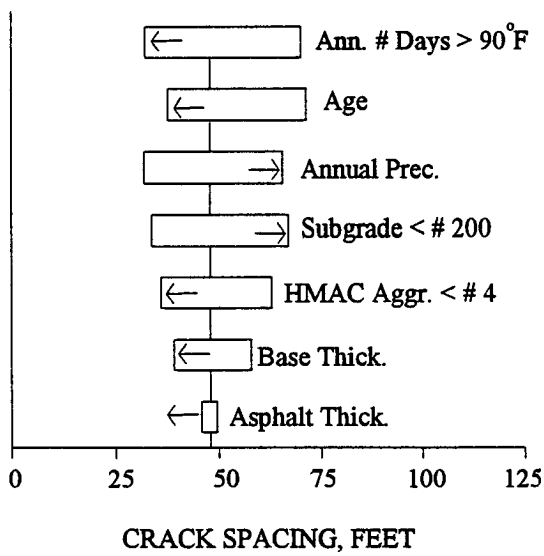

c. Wet-Freeze Data Set

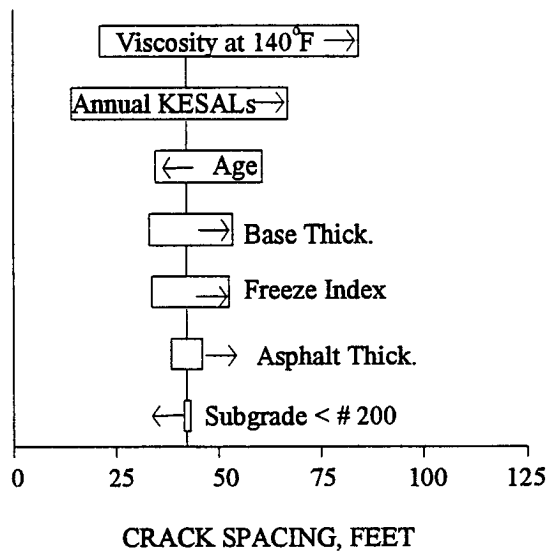

d. Dry-Freeze Data Set

Figure 5.4. Results From Sensitivity Analyses of Transverse Crack Spacing for HMAC Pavements on Granular Base and Full-Depth HMAC, by Environmental Zone

Table 5.4. Numbers of Values in the Data Set and Statistical Values of Interest for Significant Variables in the Rutting Data Set for HMAC Pavements Over Granular Base (All Regions)

Variable	Units	No. of Values	Mean Value	Standard Deviation	Low Value	Median Value	High Value	Range
Rut Depth	Inches	153	0.28	0.14	0.05	0.25	0.85	0.80
HMAC Surface Thickness	Inches	153	5.56	2.88	1.2	5.2	13.6	12.4
Asphalt Content Surface	% by weight	153	5.15	0.81	2.66	5.12	7.44	4.77
Air Void Surface	% by weight	153	4.82	2.20	1.05	4.49	13.60	12.55
HMAC Aggregate Passing No. 4 Sieve	% by weight	153	54.9	9.4	27.4	55.0	75.0	47.6
Asphalt Viscosity at 140°F (60°C)	Poise	152	16-64.4	745.1	414	1707	5316	4901
Base Thickness	Inches	153	13.8	8.5	3.0	10.9	47.1	44.1
Base Compaction	%	152	95.7	5.7	76.0	95.5	117.0	41.0
Plasticity Index of Subgrade	%	153	7.6	9.2	0	4	44	44
In Situ Moisture of Subgrade	% by weight	153	11.7	7.0	0	10.7	32	32
Subgrade Soil Passing No. 200 Sieve	% by weight	153	36.3	26.9	0	30.6	97.2	97.2
Age of Pavement	Years	153	9.3	5.8	1	8	25	24
Cumulative KESALs	No.	153	19-56.2	3714.4	5	740	21445	21440
Annual Precipitation	Inches	153	32.3	16.8	3.8	31.7	84.2	80.4

Table 5.4. Numbers of Values in the Data Set and Statistical Values of Interest for Significant Variables in the Rutting Data Set for HMAC Pavements Over Granular Base (All Regions)

Variable	Units	No. of Values	Mean Value	Standard Deviation	Low Value	Median Value	High Value	Range
No. of Days Max. Temp > 90°F (32.2°C)	No.	153	46.7	43.5	0	37	180	180
No. of Days Min. Temp < 32°F (0°C)	No.	153	94.4	61.6	0	95	226	226
Number of Air Freeze-Thaw Cycles	No.	153	77.9	44.5	0	86	178	178
Freeze-Thaw Index	°F-Days <32°F (0°C)	153	520.6	678.2	0	182	3012	3012
Avg. Max. Temp. (Daily Max. Temps. for June, July and Aug.)	°F	153	68.10	10.77	46.97	69.32	88.54	41.57
Avg. Min. Temp. (Daily Min. Temps. for Dec., Jan. and Feb.)	°F	153	43.89	10.48	22.90	43.54	68.69	45.79
Average Daily Temp. Range	°F	153	24.18	4.15	15.33	23.56	34.51	19.18
Avg. Max. Temp. By Month	°F	153	86.69	7.43	71.38	87.95	109.01	37.63
Avg. Min. Temp By Month	°F	153	26.17	13.45	-2.14	26.26	60.76	62.90

By utilizing the information in these tables in a slightly different fashion for those variables with minimal sensitivity, a designer could reasonably fix these variables. The selection of input values would then be simplified without significantly jeopardizing the prediction capabilities of an equation.

A predictive equation should ideally include HMAC thickness, base thickness, and KESALs if it is to be used for design. HMAC thickness includes all HMAC layers, while base thickness includes unbound base and subbase. With this in mind, layer thicknesses were forced into all equations. A review of the sensitivity analyses results, however, indicates that the layer thicknesses have little or no significance in some equations. This finding probably reflects the adequacy of the pavement structures for most pavement sections offered by the State Highway Agencies (SHAs), such that layer thicknesses did not in fact explain much of the variations in distress occurrence.

Of particular interest, however, are those instances where the impact of these thicknesses is contrary to normal expectations. As an example, when predicting rutting in the dry-freeze region, greater layer thicknesses (either HMAC or base) result in greater rut depth predictions. It is not difficult to visualize how such a situation could occur. However, for design purposes, such trends confuse the process.

Particularly problematic was the fact that separate consideration of HMAC and base thicknesses created conflicting effects for some distress types in some regions. That is, increasing the thickness of one did not necessarily result in a decreased required thickness for the other. As a result, other equations were developed to utilize structural numbers to control those effects; however, this strategy was not effective in improving the use of the equations for selecting layer thicknesses.

For each of the rutting and roughness equations for HMAC over granular base, the equations were inverted to predict asphalt concrete (AC) thickness and a factorial of solutions was generated to evaluate the use of these equations for design purposes. Three levels of each variable were selected to establish how these equations would predict AC thickness for the various potential combinations of factors.

In several instances the factorial included values for some factors that were outside the inference space of the model (but within practical limits for the variable). As expected, in many of these instances unreasonable design thicknesses were generated. The use of factorials in this fashion provided an opportunity to further evaluate the sensitivity of these distress mechanisms to the various factors incorporated and reemphasized the importance of the inference space on which the equations were developed. In one instance, for selecting an AC thickness based on roughness data from the dry-freeze region, the equation was so sensitive to the freeze index that only a narrow band of conditions provided reasonable AC thickness results. Similarly, when evaluating the equations based on rutting, it was noted that the average rut depth for all these sections was only 0.28 in. (0.71 cm). Attempts to utilize the equations with a rut depth of 0.50 in. (1.27 cm) occasionally produced AC thickness values that were impractical. This example should serve to emphasize that caution is required when employing these (or any) equations for conditions outside the inference space from which they were developed.

Use of Distress Equations for Design

The distress types considered significant were alligator cracking, rutting, transverse (or thermal) cracking, increases in roughness, and loss of surface friction. However, alligator fatigue cracking could not be studied at this early stage because there were only 16 pavements displaying medium- or high-severity alligator cracking, and the data collected were not considered adequate for modeling the loss of surface friction.

The distress equations presented in this chapter were developed specifically for predicting the individual distresses rather than for use as design equations, although it was expected that they could satisfy both needs. The original intent was to rearrange the models developed for the sensitivity analyses (SHRP-P-393) as design equations, but separate consideration of HMAC and unbound base thicknesses was a problem because the separate effects for some distress types and environmental zones were not additive. That is, increasing the thickness of one did not necessarily result in a decreased required thickness for the other. Consequently, it was decided to try structural number, in lieu of HMAC and unbound base thicknesses separately, to develop models that were better behaved.

The models were developed again in essentially the same equation form except with structural number representing base and HMAC thicknesses. However, the results discussed above were still reflected in the design models. These models for separate environmental zones had adjusted R^2 values that varied from 0.69 to 0.88.

The following is a generic basis for transforming equations predicting distress into equations to estimate layer thickness requirements; it is assumed that this knowledge may prove useful in the future. The equations to predict distresses (see Tables 5.1, 5.2, and 5.3 for examples) are in the form:

$$D = N^B 10^C \quad \textbf{(5.1)}$$

Where:

- D = distress in appropriate units (e.g., inches of rutting or in./mi of roughness increase),
- N = number of cumulative KESALs,
- $B = b_0 + b_1 x_1 + b_2 x_2 + ...b_n x_n$, and
- $C = c_0 + c_1 x_1 + c_2 x_2 + ...c_n x_n$.

By designating some new variables and taking common logarithms of each side of the equation, Equation 5.1 can be transformed to estimate required layer thicknesses when allowable levels of distress are established and other independent variables (such as asphalt

viscosity, environmental variables, other layer thicknesses, etc.) are defined. The transformed equation is

$$X_T = \frac{(\text{Log } D/N^B) - C_X}{C_T} \quad (5.2)$$

Where:

X_T = thickness of the base or HMAC,
C_X = C (as shown in Tables 5.1 through 5.3) - C_T X_T, and
C_T = coefficient of the term c_i x_i that includes the layer thickness of interest X_T.

Figure 5.5 is a nomograph developed for one of the new equations to illustrate the frustration encountered in attempting to use the distress equations for layer thickness designs. Two examples are shown on Figure 5.5 that differ only in the number of ESALs "N." Both limit changes in IRI to 100 in./mi (16.1 m/km), assume air voids of 5 percent, use AC-10 asphalt, have a freeze index of 500, and expect an average of 70 days each year with temperatures greater than 90°F (32.2°C). The unexpected result, however, is that the structural number required for 1,000,000 ESALs is 11, while that for 10,000,000 ESALs is 5.1. The immediate response to such a result is that something is wrong with the nomograph or the equation. The nomograph is correct for the equation, so that leaves the equation (with an adjusted R^2 of 0.88) in question, or could it be that the pavements are trying to communicate something that we do not yet understand?

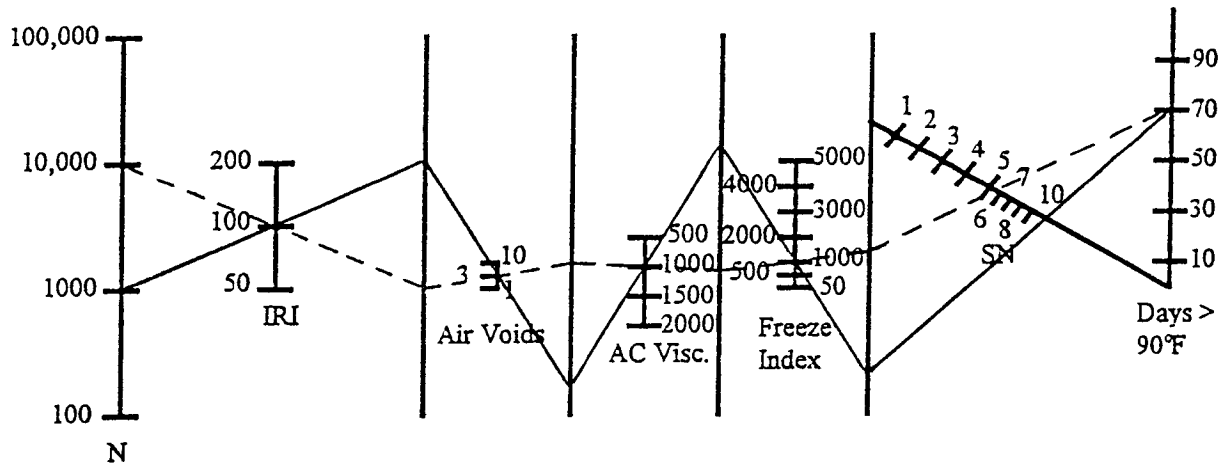

Figure 5.5. Design Nomograph to Limit Roughness in the Dry-Freeze Climate

However, the research staff does know from the sensitivity analyses that increasing base thickness for the dry-freeze data set strongly indicates increasing roughness. When the base compaction provided for these pavements is assumed to be insufficient or to later deteriorate due to environmental or other effects, it can be seen that increasing the depth of the base could result in more differential rutting and thus roughness. Future studies will be needed to gain an understanding of unexpected results, such as in this example.

Because the approach of rearranging the regression equations and establishing limiting levels of distress was not working out, it was decided to simply use the equations directly to predict distresses for several trial designs. To explore this approach, a factorial experiment was initiated for HMAC over granular base pavements to study predicted distresses over a range of pavement structures and ESALs (ages for transverse cracking), with material properties fixed at reasonable values and climatic variables set at their regional means. This approach required 144 solutions each for predictions of rut depths, changes in IRI, and transverse crack spacing. The results from these calculations appear in Tables 5.5 through 5.7.

If the goal is to restrict rut depths to 0.50 in. (1.27 cm) or less for an estimated 25 million ESALs, a review of Table 5.5 indicates that this limiting rut depth would be exceeded only for pavements with only 2 in. (5.08 cm) of HMAC in the wet-freeze climatic zone (see shaded cells).

Similarly, if the goal is to limit the change in roughness to 100 in./mi (1.59 m/km) for an estimated 25 million ESALs, review of the shaded cells in Table 5.6 indicates the following:

- More than 8 in. (20.2 cm) of base would be required for the pavement with 2 in. of HMAC for the wet-no freeze zone. Any of the other pavement designs for the wet-no freeze zone would be adequate to limit rutting.

- Any of the pavement designs would satisfy this limitation for the dry-no freeze zone.

- All the pavement designs would be satisfactory for the wet-freeze zone, even though the designs with 10 in. (25.4 cm) of HMAC and 8 in. (20.3 cm) of base slightly exceed the limitation.

- Only the designs with 8 in. (20.3 cm) of base were satisfactory for the dry-freeze zone (see the explanation above for the similar result illustrated by Figure 5.5).

Table 5.5. Predicted Rut Depths in Inches Based on Regional Predictive Equations, Ranges of Layer Thicknesses, and ESALs, With Climatic Variables at Their Regional Means, HMAC Pavements Over Granular Base (Also Predictive Equation Statistics)

HMAC Thickness, Inches	Base Thickness, Inches	Climatic Zones and ESALs in Millions															
		Wet-No Freeze				Dry-No Freeze				Wet-Freeze				Dry-Freeze			
		1	6	12	25	1	6	12	25	1	6	12	25	1	6	12	25
2	8	.26	.29	.30	.31	.22	.26	.27	.29	.30	.42	.47	.54	.23	.25	.25	.26
	16	.25	.28	.29	.30	.21	.24	.26	.28	.29	.41	.46	.53	.24	.26	.27	.27
	24	.24	.27	.29	.30	.20	.23	.25	.26	.29	.40	.45	.52	.25	.27	.28	.29
6	8	.22	.25	.26	.27	.24	.28	.30	.32	.25	.34	.39	.45	.26	28	.29	.30
	16	.21	.23	.24	.25	.23	.27	.29	.31	.24	.33	.38	.43	.30	.32	.33	.34
	24	.20	.22	.23	.24	.22	.26	.27	.29	.23	.33	.37	.42	.34	.36	.37	.39
10	8	.21	.23	.24	.26	.25	.30	.31	.34	.23	.31	.36	.41	.28	.30	.31	.32
	16	.19	.21	.22	.23	.24	.28	.30	.32	.22	.30	.34	.39	.33	.36	.37	.38
	24	.18	.20	.21	.22	.23	.27	.29	.31	.21	.30	.34	.39	.39	.42	.43	.44
R^2		0.72				0.75				0.73				0.85			
Adj. R^2		0.66				0.70				0.68				0.81			
RMSE in Log Rutting		0.18				.016				0.19				0.11			

Fixed values of variables: HMAC Air Voids = 5%
Asphalt Content = 5%
AC Viscosity = 1,000 Poise
HMAC Aggregate < No. 4 Sieve = 55%
Base Compaction = 95%-Modified AASHTO
Subgrade Soil < No. 200 Sieve = 20%

Table 5.6. Predicted Change in Roughness (IRI) in Inches/Mile Based on Regional Predictive Equations, Ranges of Layer Thicknesses, and ESALs, With Climatic Data at Their Regional Means, HMAC Pavements Over Granular Base (Also Predictive Equation Statistics)

HMAC Thickness, Inches	Base Thickness, Inches	Climatic Zones and ESALs in Millions															
		Wet-No Freeze				Dry-No Freeze				Wet-Freeze				Dry-Freeze			
		1	6	12	25	1	6	12	25	1	6	12	25	1	6	12	25
2	8	55	80	92	107	26	53	71	95	28	43	52	62	31	50	60	73
	16	28	40	46	54	14	29	39	52	27	42	50	60	48	77	93	114
	24	14	20	23	27	8	16	21	28	26	41	49	58	74	120	145	177
6	8	28	25	47	55	12	25	33	44	39	61	73	87	30	49	59	72
	16	14	21	24	29	7	14	18	24	38	59	71	85	47	76	92	112
	24	7	10	12	14	4	7	10	13	37	58	69	82	73	119	143	175
10	8	14	21	24	28	6	12	15	21	46	72	85	103	30	49	58	71
	16	7	11	12	14	3	6	8	11	45	70	83	100	46	75	91	111
	24	4	5	6	7	2	3	5	6	43	68	80	97	72	117	141	173
R^2		0.85				0.95				0.87				0.94			
Adj. R^2		0.81				0.93				0.84				0.92			
RMSE in Log ΔIRI2		0.31				0.18				0.27				0.21			

Fixed values of variables:
HMAC Air Voids = 5%
HMAC Aggregate < No. 4 Sieve = 55%
AC Viscosity = 1,000 poise
Base Compaction = 95%-modified AASHTO
Asphalt Content = 5%
Subgrade Soil < No. 200 Sieve = 20%

Table 5.7. Predicted Transverse Crack Spacing in Feet Based on Regional Predictive Equations, Ranges of Layer Thicknesses, and Ages, With Climatic Variables at Their Regional Means, HMAC Pavements Over Granular Base (Also Predictive Equation Statistics)

HMAC Thickness, Inches	Base Thickness, Inches	Climatic Zones and Age in Years															
		Wet-No Freeze				Dry-No Freeze				Wet-Freeze				Dry-Freeze			
		5	10	15	20	5	10	15	20	5	10	15	20	5	10	15	20
2	8	113	52	33	24	89	68	59	52	80	55	44	38	40	30	25	22
	16	66	30	19	14	83	62	52	46	71	49	39	33	39	29	25	22
	24	38	18	11	8	80	59	49	36	63	43	35	30	39	29	24	22
6	8	153	71	45	33	69	53	45	40	78	53	42	36	41	30	25	23
	16	89	41	26	19	64	48	40	36	69	47	37	32	54	40	34	30
	24	52	24	15	11	62	45	38	33	61	41	33	28	71	53	45	40
10	8	206	95	61	44	53	41	35	31	75	50	40	34	41	31	26	23
	16	120	55	35	26	50	37	31	28	67	45	35	30	74	55	46	41
	24	70	32	21	15	48	35	29	26	59	40	31	26	131	97	82	73
R^2		0.85				0.86				0.86				0.78			
Adj. R^2		0.75				0.83				0.83				0.72			
RMSE in Log ΔIRI2		0.52				0.35				0.30				0.44			

Notes:
1. Increasing transverse crack spacing means decreased cracking.
2. The predictive equation for the dry-freeze region includes KESALs/year, which were set at the regional mean of 83.1 KESALs/year.

- The closest crack spacing (most cracks) was generally predicted in all climatic zones for the thicker base layers, except that the opposite was true for the dry-freeze zone.

- Closer crack spacings were predicted for pavements with thick bases in the wet-no freeze climate than in the other climatic zones.

- The crack spacings predicted for all pavement designs and climatic zones appear to be acceptable except those in the wet-no freeze zone for pavements with 2 to 6 in. (5.08 to 20.3 cm) of HMAC over 24 in. (60.96 cm) of base.

It can be seen from the discussion above that it would not be difficult to select pavement designs that would limit distresses to satisfactory levels, based on specific predictive equations to estimate the levels of distress that may be expected for a trial pavement design and specified traffic and climatic conditions. This approach is proposed for future design procedures. Longitudinal and fatigue cracking should be included as predictive equations become available.

Table 5.8 indicates the effects on predicted distresses by increasing HMAC or base thicknesses. These tabulated general effects are consistent with those indicated graphically in Figures 5.2, 5.3, and 5.4.

Improved Design Equations

One objective of Task 4 was to develop improved design equations for flexible pavements, but the research staff is unable to claim success in this effort. Although the distress models developed for the sensitivity analyses (SHRP-P-393 in this report) are believed to have served that purpose, transforming them to estimate thicknesses of HMAC and base materials was not successful.

While these models may prove reasonable over time, they are based for this early analysis on limited time sequence data (generally an initial point and another in 1990 or 1991 for the distresses) and should be used with care and only as design checks in concert with other design procedures. While a good distribution of pavement ages undoubtedly helped explain curvature in the relationship, which will be enhanced by future time sequence data, the research staff does not wish to promote these models for general use at this time.

Table 5.8. Effects on Predicted Distresses of Increasing HMAC or Base Thicknesses, by Climatic Region for HMAC Pavements over Granular Base

Distress Type	Variable Increasing	Effects			
		Wet-No Freeze	Dry-No Freeze	Wet-Freeze	Dry-Freeze
Rutting	HMAC Thickness	Decreased	Increased Slightly	Decreased	Increased
	Base Thickness	Decreased Slightly	Decreased Slightly	Decreased Slightly	Increased
Roughness	HMAC Thickness	Substantially Decreased	Substantially Decreased	Increased	Very Slightly Decreased
	Base Thickness	Substantially Decreased	Substantially Decreased	Slightly Decreased	Substantially Increased
Transverse Cracking	HMAC Thickness	Decreased	Increased	Slightly Increased	Decreased *
	Base Thickness	Increased	Slightly Increased	Increased	Decreased *

* For HMAC = 2 in. (5.08 cm), predicted crack spacing is essentially independent of HMAC or base thicknesses.

Note: Increased transverse cracking results in decreased crack spacing and vice versa.

6

Evaluation of the Rigid Pavement Design Equation

This chapter describes the evaluation of the original 1960 American Association of State Highway Officials (AASHO) Road Test equation and the extended 1993 American Association of State Highway and Transportation Officials (AASHTO) design equation (12) based on data obtained from the LTPP Data Base for experiments GPS-3, GPS-4, and GPS-5, which provided data for JPCP, JRCP, and CRCP, respectively.

The AASHTO design equations were evaluated by comparing the predicted 18 Kip (80 kN) equivalent single axle loads (ESALs) for each test section determined from the design equation to the observed ESALs (estimated from traffic data) carried by the section. The predicted ESALs are calculated from the concrete pavement equations from the original Road Test and the latest extended form in the 1993 AASHTO Design Guide for Pavement Structures.

Examination of the AASHTO Concrete Pavement Design Equation

The AASHTO design model for concrete pavement structures was originally derived from data obtained during the two year AASHO Road Test. The original model has been extended by theoretical analysis and engineering judgment several times over the past 30 years. The original 1960 AASHTO design equation is a relationship between serviceability loss, axle loads and types, and slab thickness:

$$G_t = \beta(\log W_t - \log\rho) = \log\left(\frac{4.5-p_t}{4.5-1.5}\right) \qquad (6.1)$$

Where:

G_t	=	the logarithm of the ratio of loss in serviceability at time t to the potential loss taken to a point where serviceability equals 1.5.
β	=	a function of design and load variables that influence the shape of the p-versus-W serviceability curve.
W_t	=	cumulative 18 kip ESALs applied at end of time t.
ρ	=	a function of design and load variables that denotes the expected number of axle load applications to a terminal serviceability index.
$\log \rho$	=	7.35 log (D+1) - 0.06
D	=	slab thickness, inches
4.5	=	mean initial serviceability value of all sections
p_t	=	terminal serviceability.

This equation was extended to apply to a broader set of conditions, using a variety of analytical and subjective methods to make it more useful in design. Table 6.1 shows a summary of concrete pavement design factors included in the original and extended performance prediction models used in the AASHTO Guide. There was no validation data to support most of these extensions.

In the 1993 AASHTO Guide, the rigid pavement design model is given as:

$$\log W_{18} = Z_R S_o + 7.35 \log (D+1) - 0.06 + \frac{\log\left(\frac{\Delta PSI}{4.5-1.5}\right)}{1+\frac{1.624*10^7}{(D+1)^{8.46}}}$$

$$+ (4.22 - 0.32 p_t) \log \left(\frac{S_c' C_d (D^{0.75} - 1.132)}{215.63\ J\ (D^{0.75} - \frac{18.42}{(E/k)^{0.25}})} \right) \qquad \textbf{(6.2)}$$

Where:

ΔPSI	=	loss of serviceability (p_i - p_t);
D	=	thickness of PCC pavement, inches;
S'_c	=	modulus of rupture of concrete, psi;
Cd	=	drainage coefficient;

Ec = elastic modulus of concrete, psi;
k = modulus of subgrade reaction, psi/inch;
J = joint load transfer coefficient;
W_{18} = cumulative 18-kip ESALs at end of time t;
p_i = initial serviceability; and
p_t = terminal serviceability.

Table 6.1. Factors Included in AASHTO Concrete Pavement Design Model

Model		Design Factor
1960 Original AASHO Road Test	1.	Slab Thickness
	2.	Number and magnitude of single or tandem axle loads
	3.	Initial serviceability index
	4.	Terminal serviceability index
1961 Extension	5.	Modulus of subgrade reaction
	6.	PCC Modulus of Elasticity
	7.	PCC Poisson's ratio
	8.	PCC modulus of rupture
	9.	Axle load equivalency factor
1972 Extension	10.	J factor recommended for CRCP and unprotected corner design
	11.	Joint design recommendations
	12.	Reinforcement design procedure
1981 Extension	13.	Safety factor to reduce design M_R
1986 Extension	14.	Drainage adjustment factor
	15.	Loss of support adjustment factor
	16.	J factor for different load transfer systems
	17.	Design reliability factor
	18.	Resilient modulus for subgrade
	19.	Environmental serviceability loss

For this evaluation, the reliability factor is set to 50% (Z_R = 0). In order to evaluate the AASHTO models, it was necessary to ensure that the traffic, climatic, material and other design input variables were determined by the same procedures specified in the AASHTO Guide or used in the Road Test, which was accomplished to the extent possible.

Comparative Analysis of Predicted Versus Actual ESALs

The AASHTO design model was used differently for this analysis than it would typically be used in designing. When designing, the engineer determines the design slab thickness based on the traffic forecasted over the design life and on a specific loss in the Present Index Serviceability (ΔPSI). In this analysis, the thickness, ΔPSI, and other variables for a specific section were known and the predicted cumulative KESALs were calculated. The ΔPSI is calculated as the difference between the initial serviceability and the serviceability at the time of distress and roughness measurements. An estimate of the traffic carried from the time the pavement was opened to traffic to the time of survey is also known for each test section. If the AASHTO design equation is to be considered adequate and accurate, its predictions of the ESALs needed to reach the PSI loss should approximate the cumulative ESALs estimated by the State Highway Agencies.

Five sets of analyses were performed individually for the GPS-3, GPS-4, and GPS-5 experiments to examine the equation's ability to predict the amount of traffic actually sustained by each test section. Initially, analyses were conducted on all available data for each experiment. Then the data sets for each pavement type (JPCP, JRCP, and CRCP) were further separated by environmental regions. Analyses were then performed for each of the four environmental regions for each of the pavement types.

The analyses were carried out based on the original AASHTO design equation and the 1993 extension of that equation. The analysis based on the AASHTO original equation was mainly done to determine if the improvements to the prediction model were beneficial.

The predicted KESALs were plotted against the estimated KESALs on scattergrams to visually examine the scatter of the data. If the AASHTO model should predict the estimated KESALs exactly, then all the data would fall on the line of equality shown in each figure.

The results are also presented using bar graphs showing the ratio of predicted to actual KESALs. If the predicted to actual KESALs ratio is less than 1, then the AASHTO equation can be said to be conservative. If the ratio is greater than 1, the predicted KESAL capacity of the pavement is greater than the actual KESALs carried to cause the specified loss in PSI, and the equation would produce an inadequate design (at the 50% reliability level).

Comparison at 50 Percent Reliability

The plots of predicted versus actual KESALs based on the original AASHTO model (Equation 6.1) are shown in Figure 6.1 for JPCP and JRCP sections. The plots for individual climatic regions are shown in Figures 6.2 and 6.4. If the predictions were unbiased for all regions, approximately 50 percent of the points would be on each side of the line of equality. CRCP was not included in this evaluation of the original AASHTO

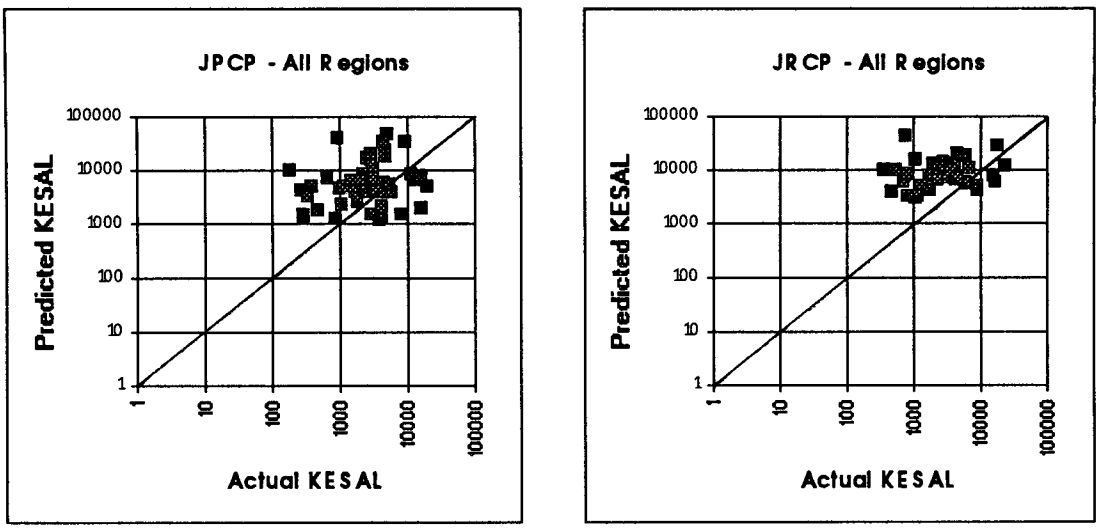

Figure 6.1. Predicted KESALs versus Actual KESALs for JPCP and JRCP Based on Original AASHTO Prediction Model

model because the Road Test did not include CRCP. It can be seen that the original AASHTO model overpredicts KESALs for a majority of test sections (78% of JPCP and 82% of JRCP).

The distributions of the ratios of predicted to actual KESALs for JPCP and JRCP sections, based on the original AASHTO equation are shown in Figures 6.3 and 6.5. The mean ratio for all test sections is approximately 4. The original AASHTO equation was developed based on data from a wet-freeze region (Illinois). The results from this analysis of data from the wet-freeze region only show that the AASHTO model overpredicts KESALs for 92% of the JPCP sections and 74% of the JRCP sections. These results are not surprising since the Road Test inference space included only two years of aging and one million axle loadings (8 million total ESALs on heaviest loops).

The predicted versus actual KESALs plots, based on the 1993 AASHTO model, are shown in Figure 6.6 for JPCP, JRCP, and CRCP sections. The plots for individual climatic regions are shown in Figures 6.7, 6.9, and 6.11. The 1993 model was a much better predictor for these analysis data sets than the original AASHTO model, which suggests that the addition of several design factors considerably improved the performance prediction capability of the model. Compared to the original model, the 1993 AASHTO model (at 50% reliability) overpredicts KESALs for only 49% of the JPCP sections, 68% of the JRCP sections and 47% of the CRCP sections. However, large amounts of scatter exist about the lines of equality, indicating poor precision. The standard error of prediction approaches 0.6 (of log N) for several of these plots. This results in a factor of about plus or minus 4 for predicted versus estimated ESALs. This scatter may be due to several causes, including inadequacies in the model, errors in the inputs, and random performance variations (or pure error). These data sets do not permit the determination of how much variation is due to each of these sources. A considerable amount of variation is believed to be due to model inadequacies, such as the inability of the model to show the effects of different climates on performance.

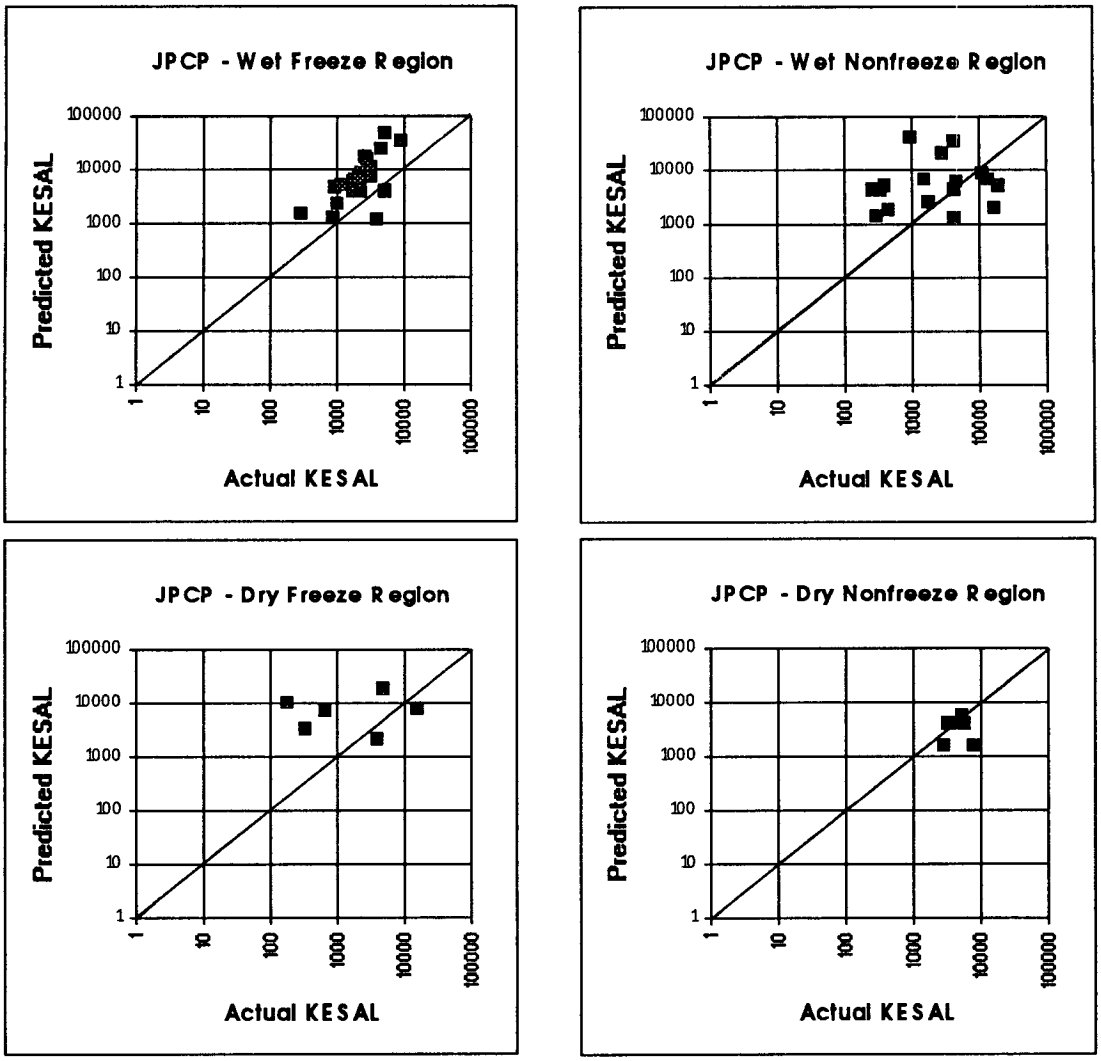

Figure 6.2. Predicted KESALs Versus Actual KESALs for JPCP Based on the Original AASHTO Prediction Model

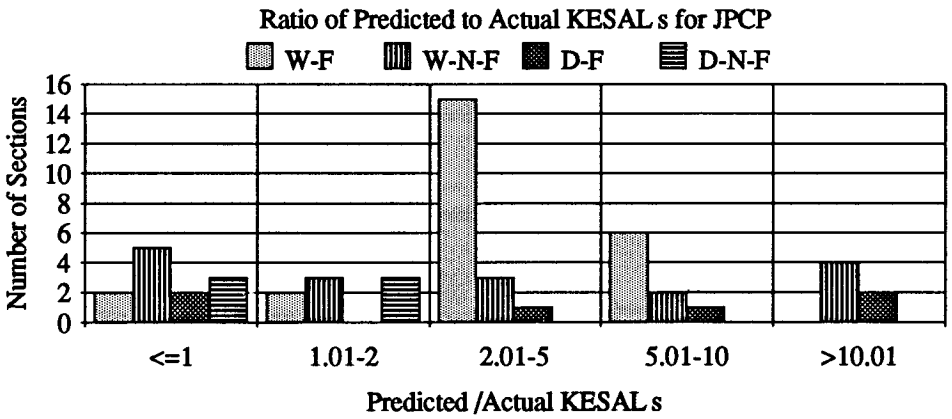

Figure 6.3. Ratio of Predicted KESALs to Actual KESALs for JPCP Based on the Original AASHTO Prediction Model

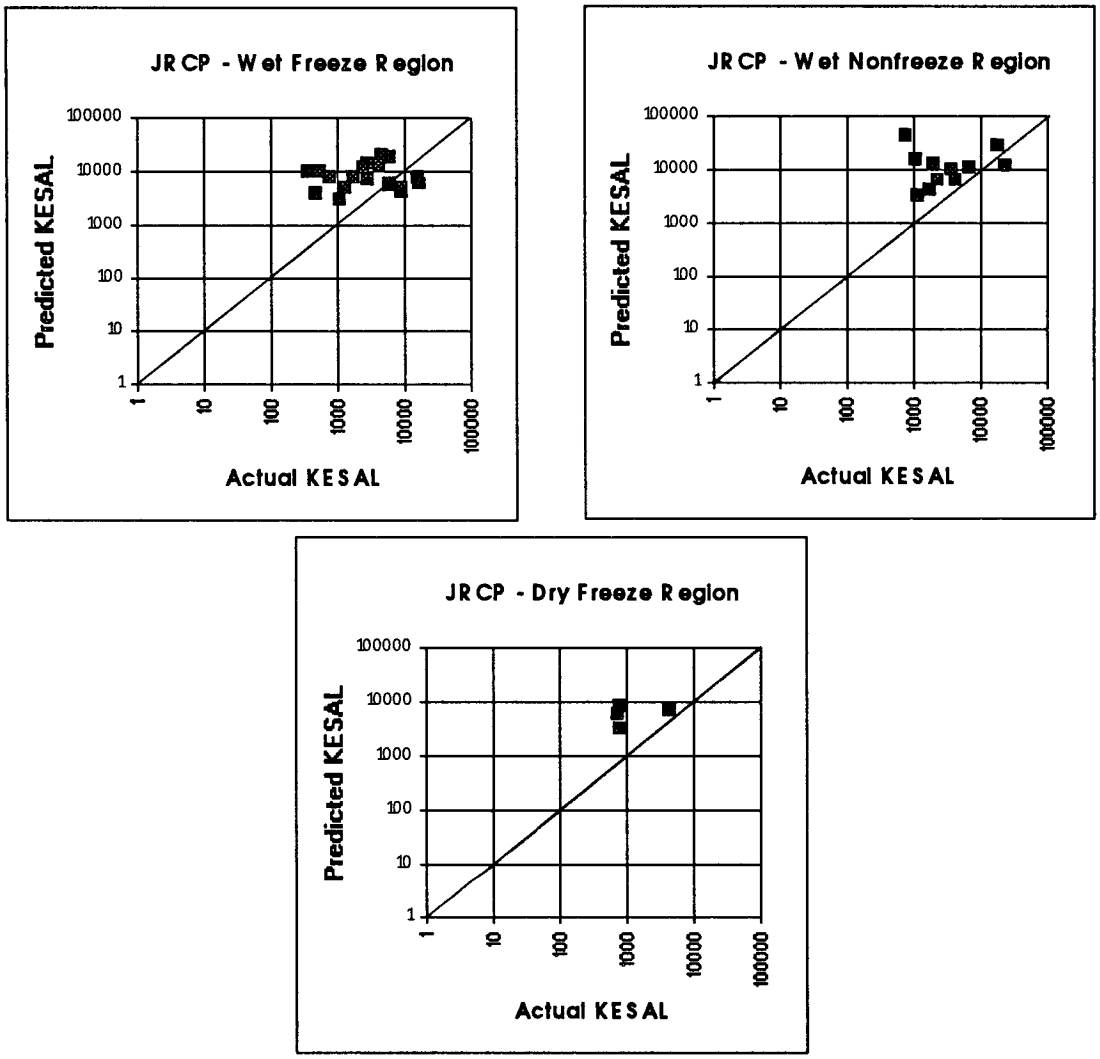

Figure 6.4. Predicted KESALs versus Actual KESALs for JRCP Based on the Original AASHTO Prediction Model

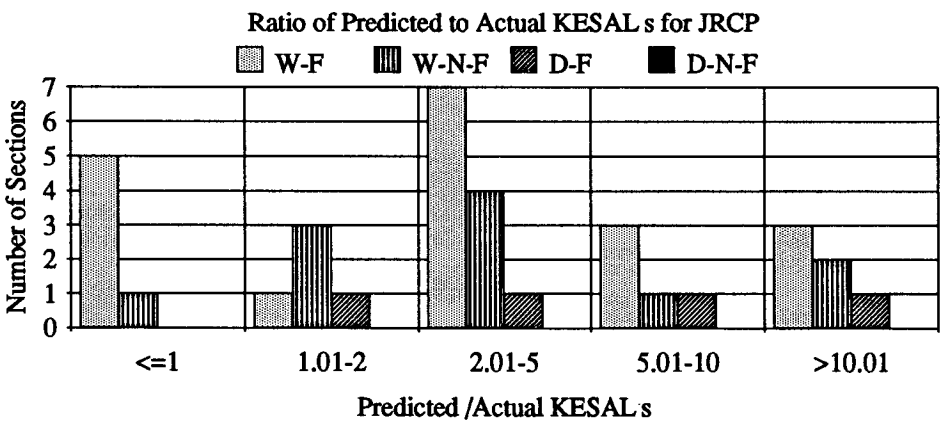

Figure 6.5. Ratio of Predicted KESALs to Actual KESALs for JRCP Based on the Original AASHTO Prediction Model

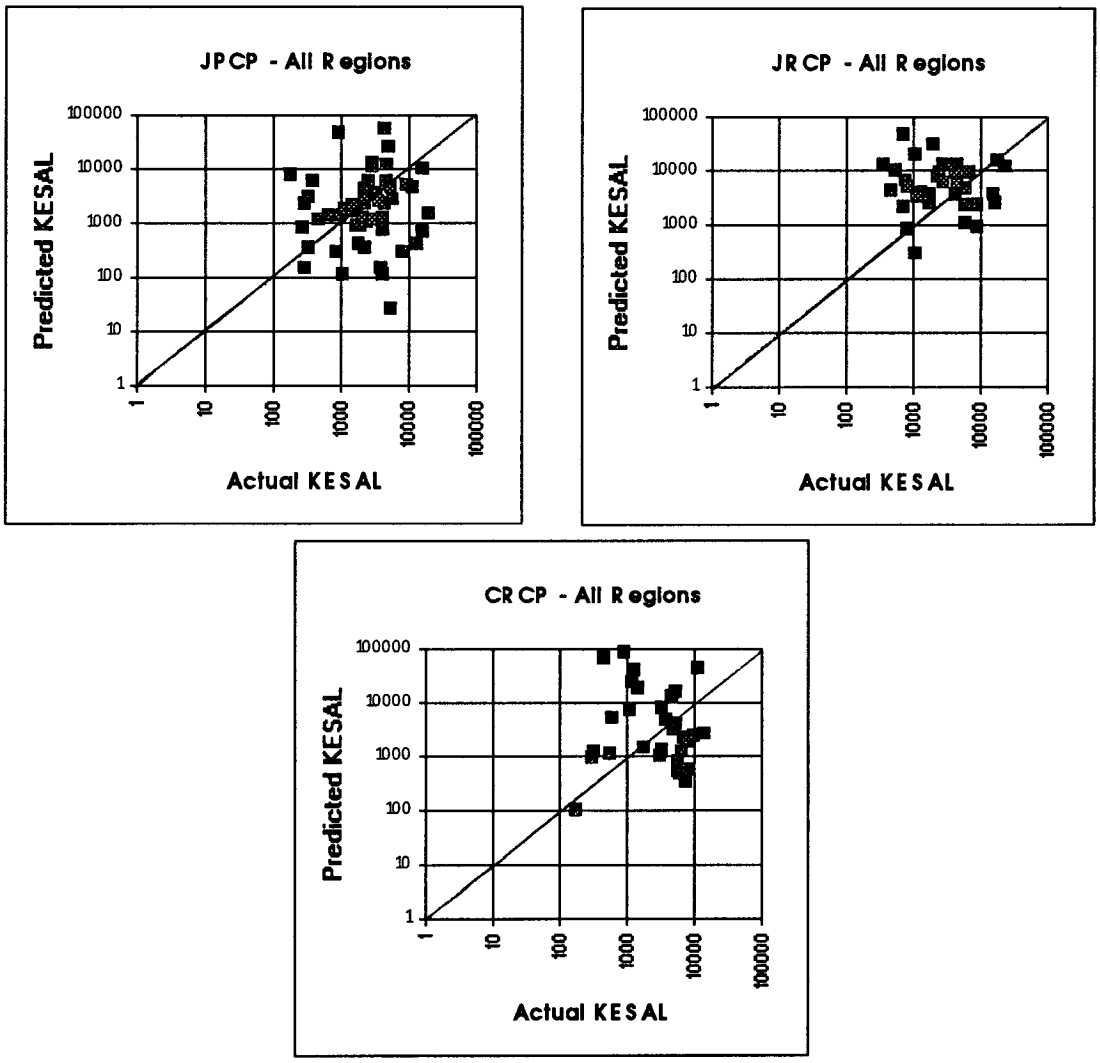

Figure 6.6. Predicted KESALs Versus Actual KESALs for JPCP, JRCP and CRCP Based on the 1993 AASHTO Prediction Model

The distribution of the ratios of predicted to actual KESALs for JPCP, JRCP, and CRCP test sections, based on the 1993 AASHTO equation, are shown in Figures 6.8, 6.10, and 6.12. The improved performance prediction of the 1993 AASHTO model, compared to the original AASHTO equation, can be seen from these plots. However, there remains a considerable scatter about the line of equality. This scatter is believed to be due to three causes: (1) deficiencies in the model, (2) errors in inputs, and (3) random performance variation (noise).

In order to analytically determine the ability of the AASHTO concrete pavement design model to predict the actual KESALs observed for the pavement sections, a statistical procedure is followed which determines whether two sample data sets (actual and predicted) are from the same population. The paired-difference method, based on the student t-distribution, was used to determine if the KESALs as predicted by the AASHTO equation were statistically from the same population as the estimated KESALs.

The Microsoft® EXCEL™ statistical analysis tools (13) were used to compare the observed KESALs to those predicted by the AASHTO equations. The calculated t-statistic (t-calc) is compared with a tabulated t-statistic (t-table) for a specific confidence level. If t-calc > t-table, then the null hypothesis (that they are from the same population) is rejected with a 5 percent chance of error, since the confidence level selected for this analysis is 95 percent.

A summary of the statistical analysis is presented in Tables 6.2 and 6.3. It is observed that t-calc is greater than t-table for one-half the data sets when the original AASHTO model is used, which indicates that the original AASHTO model does not reliably predict the ESALs actually sustained by the pavement sections. However, for the 1993 AASHTO model, the results show that the design estimates are statistically similar to the observed values. This finding holds true for all climatic regions. These results show that the improvements to the original AASHTO model were beneficial in increasing the accuracy of the design equation.

Use of a 4.5 PSI Value as the Initial Serviceability

For all the pavement sections in the original AASHTO equation, the mean initial PSI was set at 4.5. In this analysis, however, the mean estimated initial PSI from all the data was set at 4.25. This 0.25 PSI loss reduction causes a reduction in predicted KESALs by the model. Therefore, an analysis using an initial PSI of 4.5 (the same as the original AASHO Road Test) was carried out. The statistical results from this analysis are shown in Table 6.4. The results from this analysis show that the model for JPCP, JRCP, or CRCP generally overpredicts numbers of axle loads. Because the initial PSI of the LTPP sections were not measured after construction, it is impossible to know the exact loss of PSI with time or traffic.

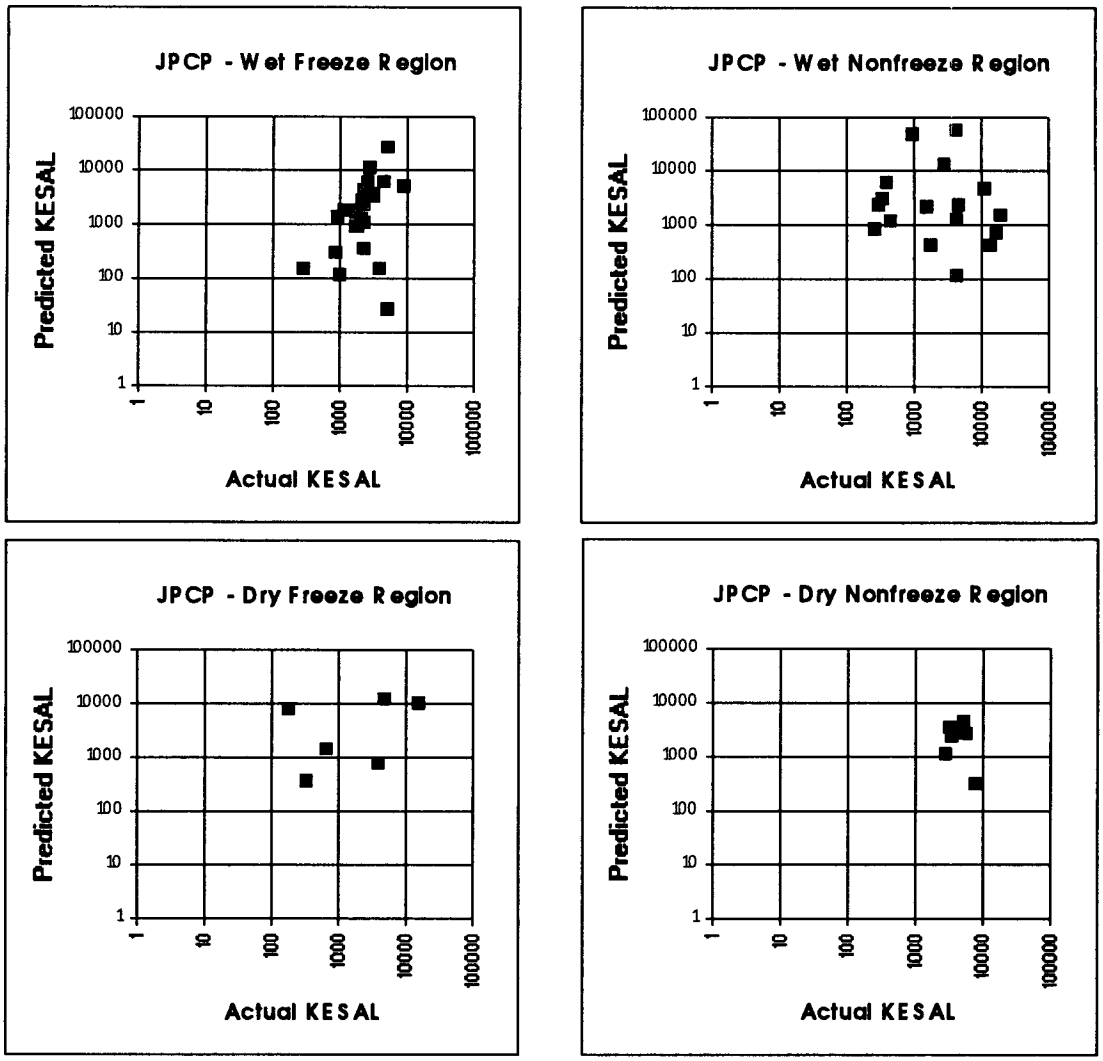

Figure 6.7. Predicted KESALs Versus Actual KESALs for JPCP Based on the 1993 AASHTO Prediction Model

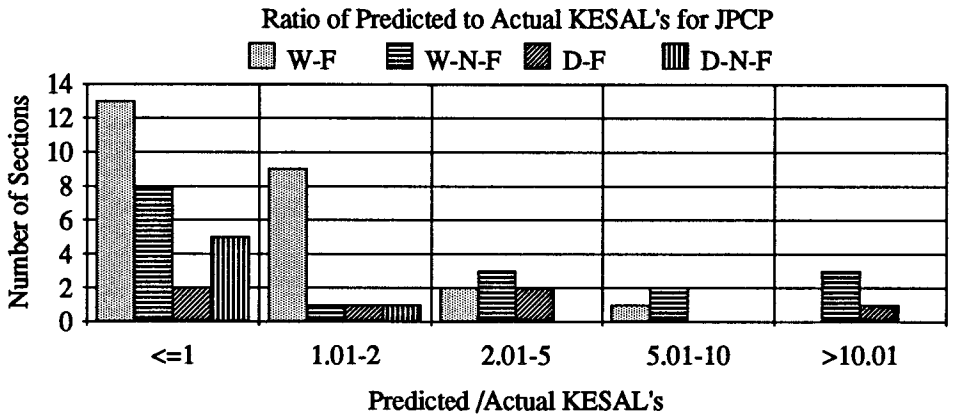

Figure 6.8. Ratio of Predicted KESALs to Actual KESALs for JPCP Based on the 1993 AASHTO Prediction Model

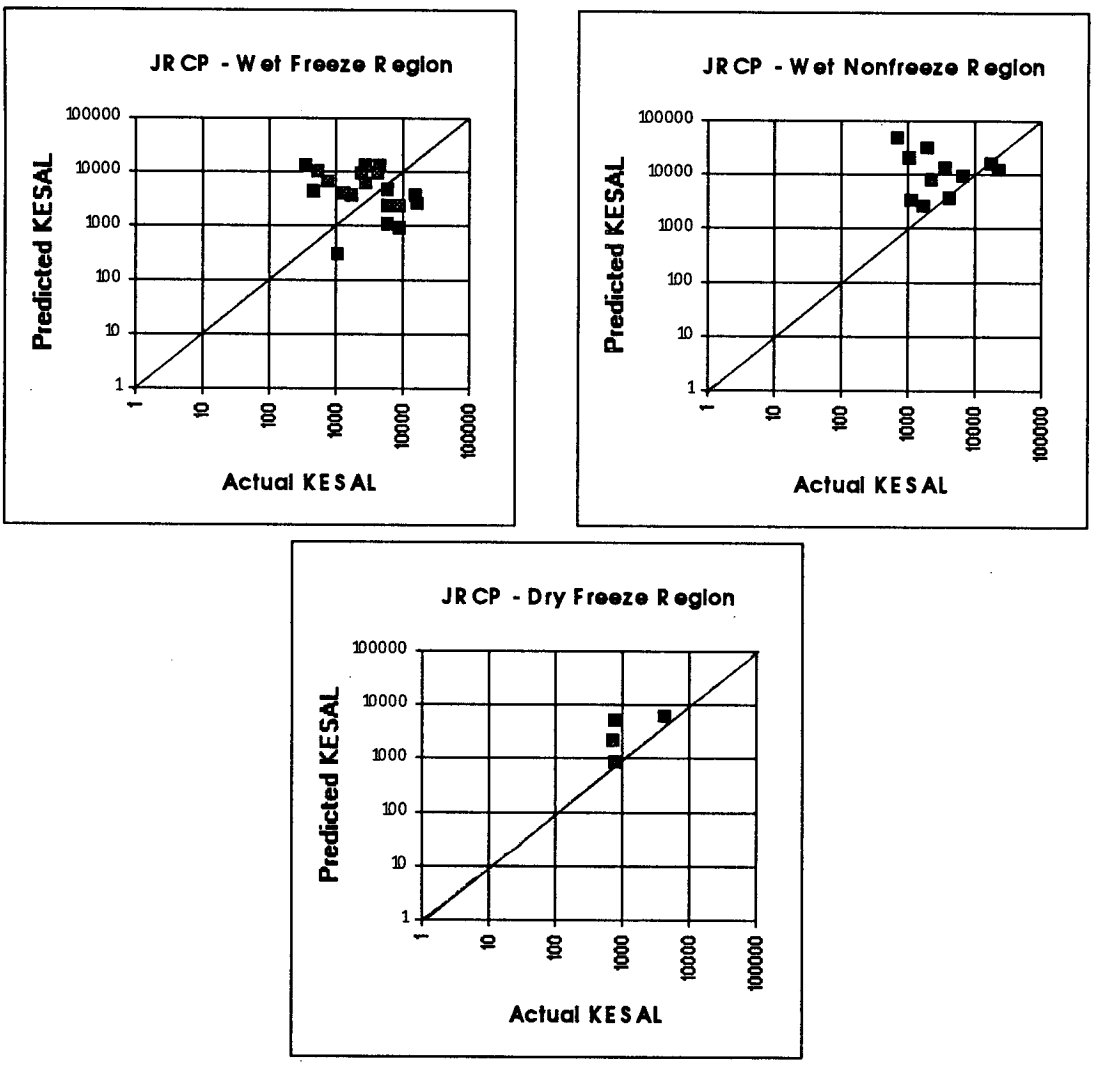

Figure 6.9. Predicted KESALs Versus Actual KESALs for JRCP Based on the 1993 AASHTO Prediction Model

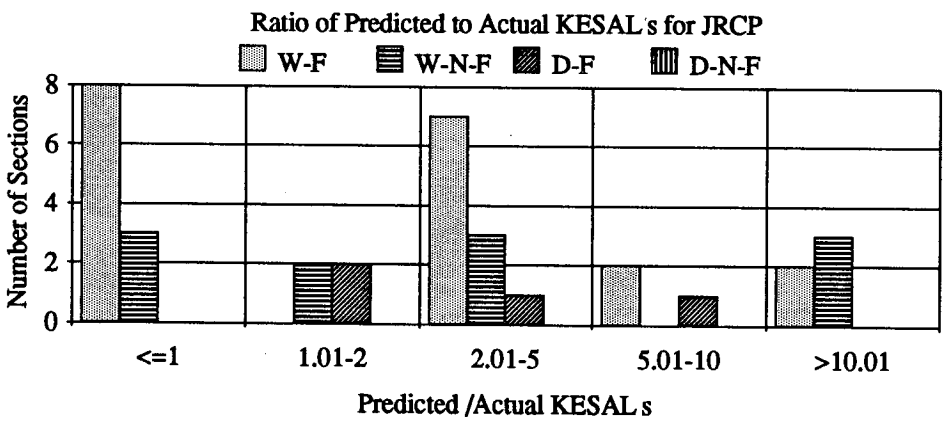

Figure 6.10. Ratio of Predicted KESALs to Actual KESALs for JRCP Based on the 1993 AASHTO Prediction Model

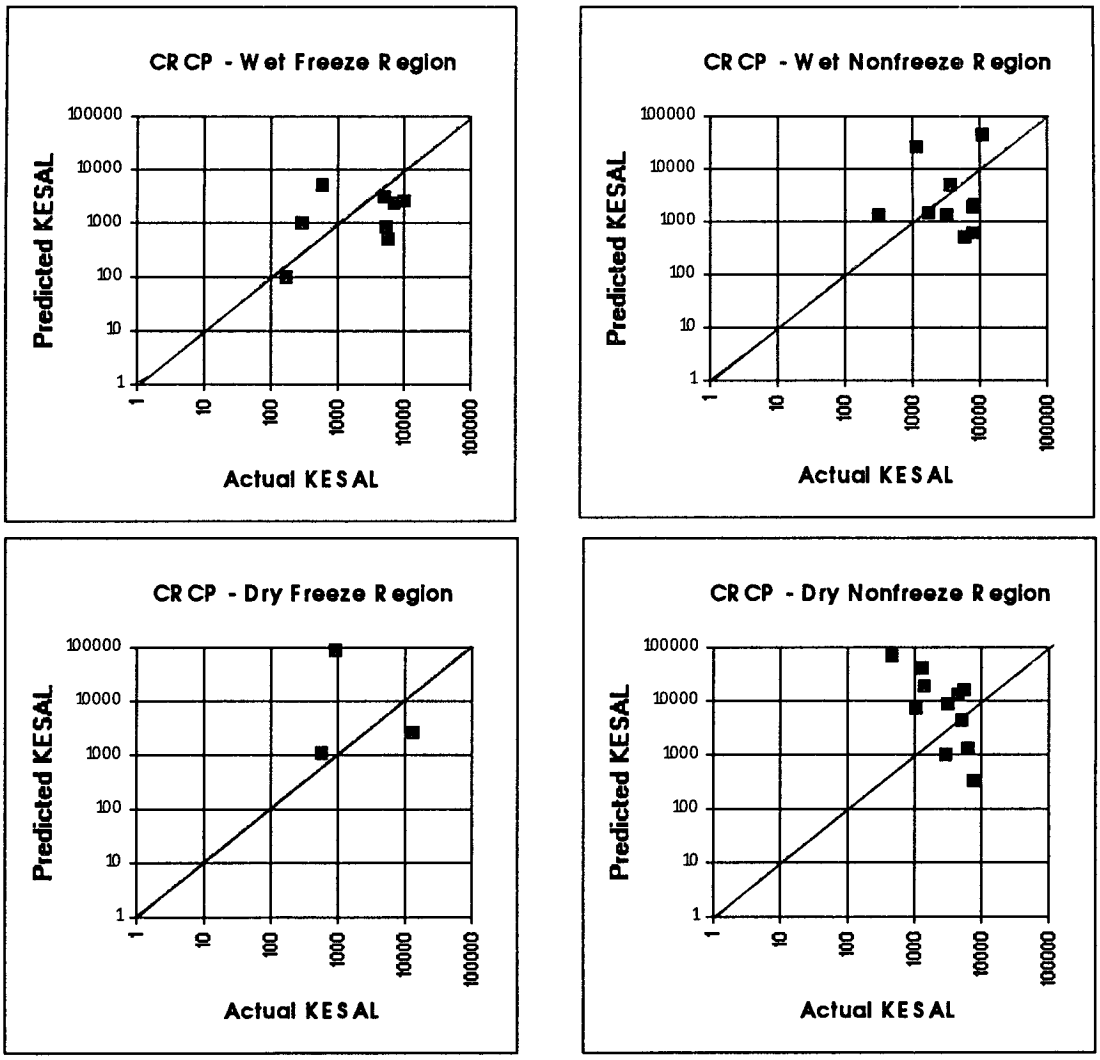

Figure 6.11. Predicted KESALs Versus Actual KESALs for CRCP Based on the 1993 AASHTO Prediction Model

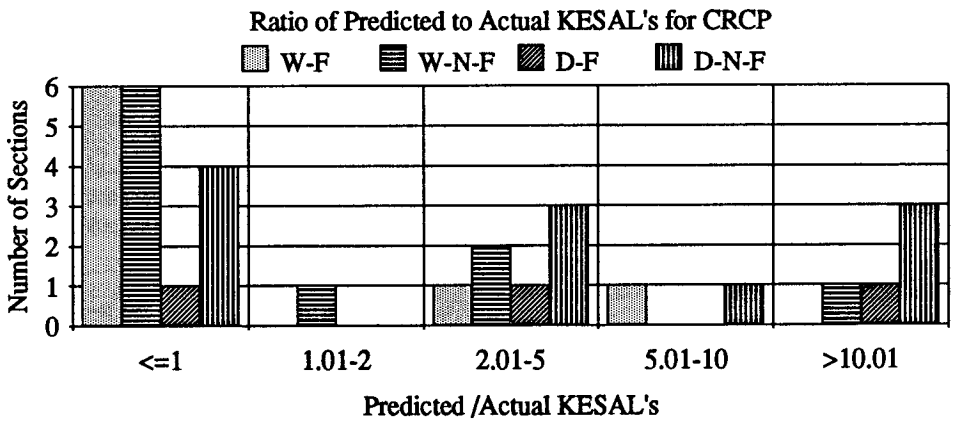

Figure 6.12. Ratio of Predicted KESALs to Actual KESALs for CRCP Based on the 1993 AASHTO Prediction Model

Comparison at 95 Percent Reliability Level

Thus far, all comparisons of predicted versus actual KESALs discussed above have been based on the mean 50th percentile model prediction. Another comparison was made of actual KESALs to predicted KESALs at a particular level of design reliability. Thus, the mean $\log W_{50\%}$ prediction is reduced by $Z_R S_o$ (where Z_R = 1.64 for 95% reliability, and S_o = 0.35). The predicted KESALs (at 95% reliability) versus actual KESALs are shown in Figure 6.13. Here, most of the points are below the line of equality, which indicates that the consideration of design reliability definitely results in a large proportion of sections (77%) having a conservative design, which is desired. However, 77% is considerably less than 95% design reliability.

Table 6.2. Results of t-Test for the Analysis Data Set Based on the Original AASHTO Equation

Type	Region	Number of Observations	t-calc	t-table	t-calc>t-table	Adequately Predict Performance?
JPCP	ALL	54	3.53	2.00	YES	NO
	WF	25	3.62	2.06	YES	NO
	WNF	17	1.27	2.12	NO	YES
	DF	6	1.20	2.57	NO	YES
	DNF	6	-1.11	2.57	NO	YES
JRCP	ALL	34	3.55	2.03	YES	NO
	WF	19	2.53	2.10	YES	NO
	WNF	11	2.12	2.23	NO	YES
	DF	4	3.91	3.18	YES	NO
	DNF	-	-	-	-	-

Table 6.3. Results of t-Test for the Analysis Data Set Based on the 1993 AASHTO Equation for Initial PSI = 4.25

Pavement Type	Region	Number of Observations	t-calc	t-table	t-calc>t-table	Adequately Predict Performance?
JPCP	ALL	54	0.89	2.00	NO	YES
	WF	25	0.76	2.06	NO	YES
	WNF	17	0.78	2.12	NO	YES
	DF	6	0.56	2.57	NO	YES
	DNF	6	-1.96	2.57	NO	YES
JRCP	ALL	34	1.99	2.03	NO	YES
	WF	19	0.64	2.10	NO	YES
	WNF	11	1.90	2.23	NO	YES
	DF	4	2.05	3.18	NO	YES
	DNF	-	-	-	-	-
CRCP	ALL	32	1.86	2.04	NO	YES
	WF	8	-1.95	2.36	NO	YES
	WNF	10	0.72	2.26	NO	YES
	DF	3	2.00	4.30	NO	YES
	DNF	11	1.87	2.23	NO	YES

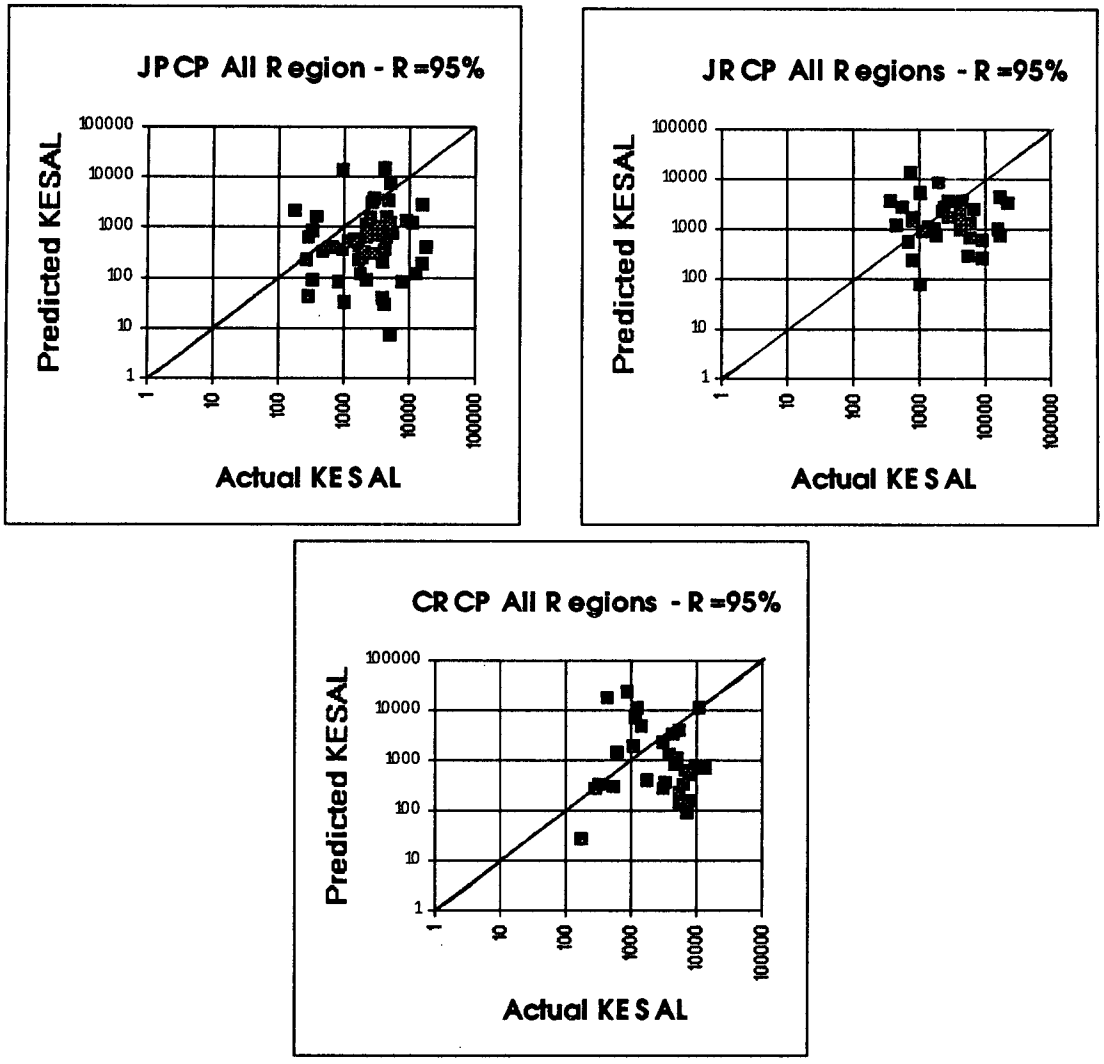

Figure 6.13. Predicted KESALs Versus Actual KESALs for JPCP, JRCP, and CRCP Based on the 1993 AASHTO Prediction Model With 95% Design Reliability

Summary

The original AASHTO rigid pavement model was based on empirical field data from the Road Test, collected over a two-year period, and basically reflects the effects of axle load, axle type, number of load applications, and slab thickness on serviceability loss. Therefore, its inference space is specifically that of the Road Test site. To use the original model for different conditions, adjustments are required to account for each significant difference introduced. As a result, over the years adjustments have been made to the original model to account for differences such as mixed traffic, pavement age greater than two years, climate (moisture, temperature, freeze-thaw), joint load transfer, concrete strength, base and subbase, subgrade, drainage, shoulders, joint spacing, widened lanes, and reinforcement.

Table 6.4. Results of t-Test for the Analysis Data Set With Initial PSI = 4.5 Based on the 1993 AASHTO Equation

Pavement Type	Region	Number of Observations	t-calc	t-table	t-calc>t-table	Adequately Predict Performance?
JPCP	ALL	54	2.14	2.00	YES	NO
	WF	25	1.72	2.06	NO	YES
	WNF	17	1.41	2.12	NO	YES
	DF	6	1.32	2.57	NO	YES
	DNF	6	1.15	2.57	NO	YES
JRCP	ALL	34	3.12	2.03	YES	NO
	WF	19	1.65	2.10	NO	YES
	WNF	11	2.68	2.23	YES	NO
	DF	4	2.51	3.18	NO	YES
	DNF	-	-	-	-	-
CRCP	ALL	32	2.51	2.04	YES	NO
	WF	8	-0.29	2.36	NO	YES
	WNF	10	1.26	2.26	NO	YES
	DF	3	0.91	4.30	NO	YES
	DNF	11	2.24	2.23	YES	NO

An evaluation was conducted to check the adequacy of the original AASHTO model and the current 1993 AASHTO model. Of importance was the need to determine the adequacy of the adjustment factors added to obtain the 1993 model and the need for any new improvements to the model. The results of the evaluation show that, for the LTPP data used, the original AASHTO model overpredicts ESALs for JPCP and JRCP sections. This finding is not surprising in view of the limited inference space of the data used to develop the original model, as indicated previously.

The results of the evaluation of the 1993 model indicate that, in general, the model is an unbiased predictor of KESALs. A statistical analysis of the results obtained show there is no significant difference between the predicted and actual KESALs for the JPCP, JRCP, and CRCP sections evaluated. However, a closer examination of the results shows a large scatter of the data about the line of equality that points to deficiencies in the model and/or the inputs used. For example, when the value of the estimated initial PSI used was changed from 4.25 to 4.5 in a sensitivity analysis, the results of a statistical analysis of the same sections show that the 1993 AASHTO model overpredicts KESALs in some instances (compare Table 6.3 to Table 6.4). Thus, even though collectively the adjustments to the 1993 model seem to have improved prediction capabilities in comparison to the original AASHTO model, the evaluation points to the obvious need for further improvements.

7

Improvements to the Rigid Pavement Design Equation

An evaluation of the 1993 AASHTO rigid pavement design equation in this study shows that, although the current model appears to be an unbiased predictor of cumulative ESALs, further refinements are needed to improve the precision of the model's predictions. This chapter describes several recommended improvements to the AASHTO rigid pavement design equation. It also describes a more fundamental approach to improve the rigid pavement design based on results from the LTPP analysis.

Design Improvements Based on LTPP Data

This section describes a more fundamental way to improve rigid pavement design that utilizes the results obtained from current and future LTPP data analyses. The general approach is shown in Figure 7.1. Key distress and roughness indicators that trigger rehabilitation needs and user comfort and safety are used as the measures of performance rather than only the Present Serviceability Index (PSI) used in the current AASHTO design method. The design procedure can be formulated in a variety of ways, however, for simplicity's sake it is assumed that a given design has been proposed for a given project based on agency design standards and thickness design procedure.

For any proposed pavement structure, the key distress and roughness indicators are predicted based on the best available LTPP models of the design traffic and life. The adequacy of the design is judged by the predicted performance of joints, the slab, and roughness. Design modifications can be made if any aspect of performance is found to be deficient. This sequence can then be repeated until an acceptable design is obtained.

The approach that directly considers key distress types and roughness is believed to be an improvement over the existing AASHTO procedure, which only considers the PSI as the performance indicator. Direct consideration of key distress types provides the opportunity to examine various components of the pavement design (joint load transfer, joint spacing, subgrade support, slab thickness, and edge support) for adequacy. In addition, the LTPP

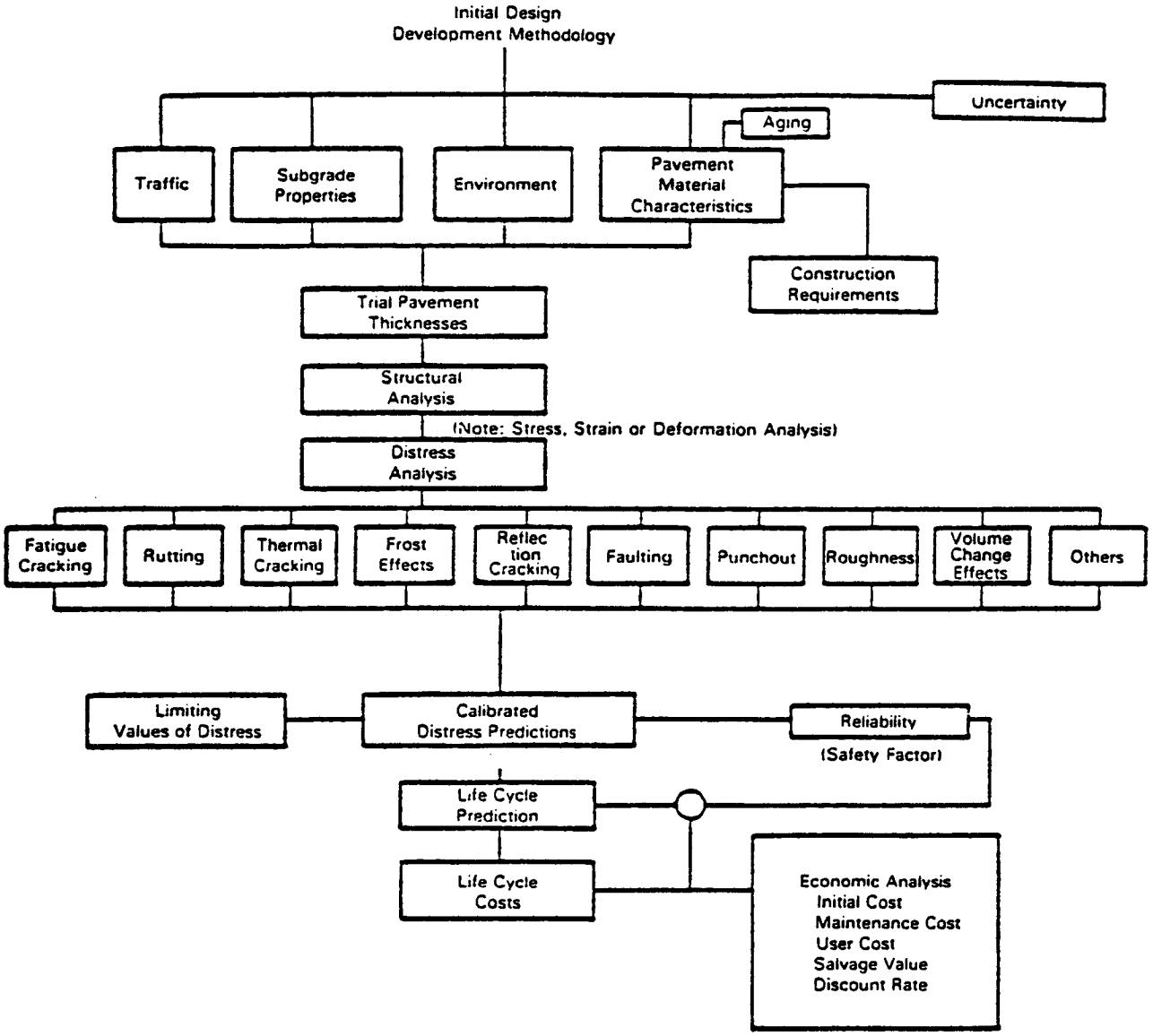

Figure 7.1. Improved AASHTO Design Concept for Pavements (AASHTO Guide for Design of Pavement Structures 1993)

models more directly consider climatic variables such as precipitation, freeze-thaw cycles, temperature range, and freezing index, and their effects on pavement performance.

An example of this approach is given at the end of this chapter, based on the preliminary prediction models developed. This design approach/procedure can be continuously improved as more reliable prediction equations become available from LTPP data analyses in the future.

Predictive Equations From the Sensitivity Analyses

The development of several predictive models was documented in SHRP-P-393 for JPCP, JRCP and CRCP. It is emphasized that these models are preliminary in nature, based on inadequate data, and should not be utilized for pavement design at this stage. They are presented here only to demonstrate their potential use in an improved design approach. It is important that this point be kept in mind when observing the models included in this section.

The following models were developed for each key distress type and each type and design of pavement:

Joint faulting:	JPCP non-doweled joint model
	JPCP/JRCP doweled joint model
Transverse cracking:	JPCP model (all severities)
	JRCP model (medium/high severities)
Joint spalling:	JPCP model (all severities)
	JRCP model (all severities)

International Roughness Index (IRI) roughness:

- JPCP doweled joint model
- JPCP non-doweled joint model
- JRCP model
- CRCP model

One important model that is missing is localized failures for CRCP (i.e., punchouts). There were only a few sections with punchouts, and no model could be developed using the current LTPP data. Such a model may be developed in the future when further deterioration and time series data are available. Note also that only the existing IRI could be predicted since the initial IRI of the sections was not measured. All these models were developed based on available LTPP data from the entire North American database. Unfortunately, there were insufficient data to develop regional models (i.e., pavements located in wet-freeze areas). However, in the future much additional data will become available, permitting regional models to be developed that will likely be considerably improved over those based on the entire North American database.

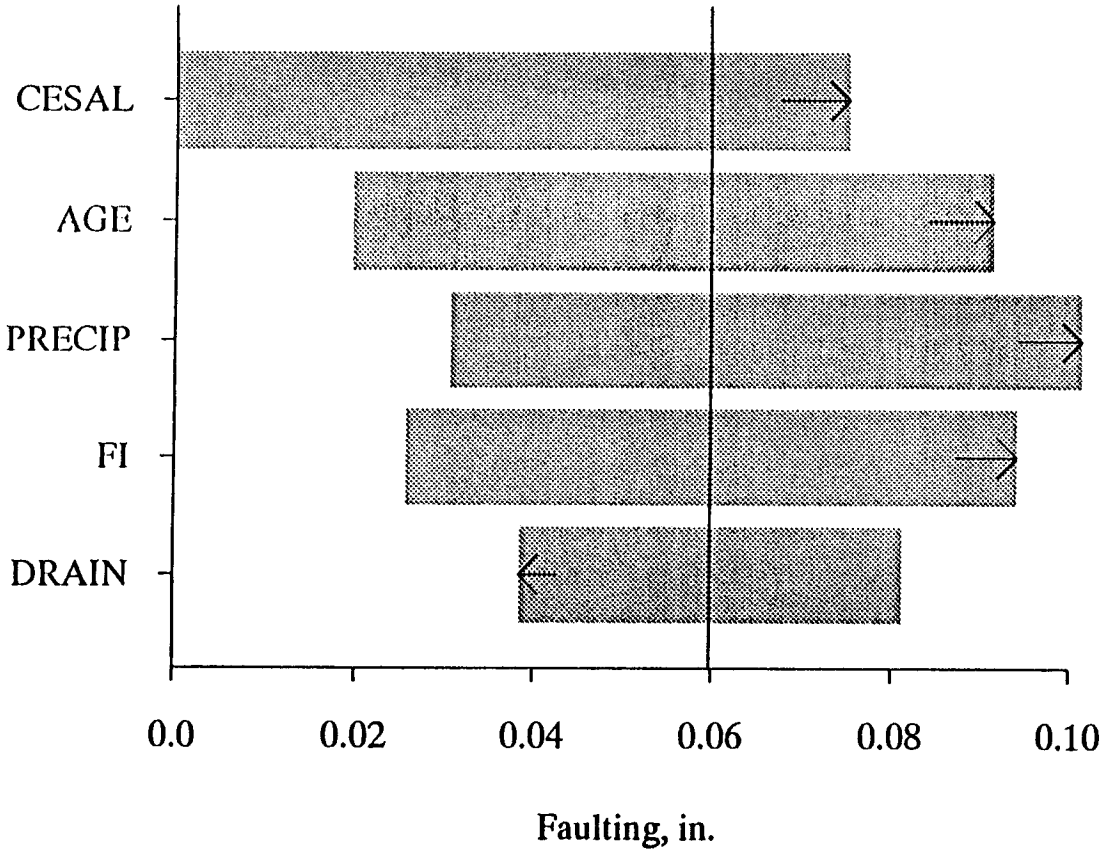

Figure 7.2. Sensitivity Analysis for Non-doweled Joint Faulting Model

A sensitivity analysis was conducted for each model similar to that described in Chapter 4 of this volume and in more detail in SHRP-P-393. A figure was prepared for each equation that shows the sensitivity of each variable in the model. The relative sensitivity of the distress or IRI prediction for a variable is the change in the prediction while the variable of interest is varied from one standard deviation below its mean to one standard deviation above its mean. All other variables were held at their mean value. The wider the bar the greater the relative sensitivity of the variable. In addition, the arrow shown in each bar represents the direction of the prediction of distress or IRI when the variable itself is increased in magnitude.

Joint Faulting — JPCP Non-doweled Equation

The following predictive equation was developed for transverse joint faulting, based on only data for non-doweled JPCP sections from GPS-3.

$$FAULTND = CESAL^{0.25} * \left[-0.0757 + 0.0251 * \sqrt{AGE} + 0.0013 * \left(\frac{PRECIP}{10} \right)^2 + 0.0012 * \left(\frac{FI * PRECIP}{1000} \right) - 0.0378 * DRAIN \right] \quad (7.1)$$

Where:

FAULTND	=	predicted mean transverse non-doweled joint faulting, inches;
CESAL	=	cumulative 18,000 lbs (80 kN) ESALs in traffic lane, millions;
PRECIP	=	mean annual precipitation, inches;
FI	=	mean freezing index, °F days < freezing;
AGE	=	age since construction, years; and
DRAIN	=	1 if longitudinal subdrainage exists; 0 if otherwise.

Statistics:	N	=	25 sections
	R^2	=	0.550
	MSE	=	mean square error = 0.047 in. (1.2 mm)

A detailed description of development of the predictive equation and its sensitivity to individual independent variables is provided in SHRP-P-393. Results from the sensitivity analysis of the model are shown in Figure 7.2. All variables significantly affect joint faulting. The form of the model matches the physical development of faulting with traffic loadings. Faulting is known to increase rapidly at first and then level off with continued traffic loadings (14,15). In addition, this form matches boundary conditions of zero faulting at zero loadings.

As CESAL increases, faulting increases rapidly at first and then levels off. Age was included in the model due to its apparent strong individual effect. There was very little correlation between AGE and CESAL. Here, AGE probably represents cycles of climatic changes such as joint opening and closing, thermal curling cycles, cold-hot cycles, etc. Two climatic variables were sufficiently strong enough to enter the model. Increased annual precipitation is known to result in increased faulting. Pavements located in areas having a higher freezing index (FI) fault more than those in warmer climates, which is consistent with previous studies. Most of these sections did not include subdrainage and thus had high potential for erosion and pumping, especially with no dowel bars to limit corner deflections. The subdrainage variable is included in the model, although only five sections had subdrainage in the form of longitudinal pipes. There were no permeable base sections in this analysis.

The model includes several variables known from previous studies to affect faulting and the directions of these variables are explainable. However, several potential variables are missing. For example, base type (untreated versus treated) did not show much significance even though other studies have shown it to be significant. Joint spacing did not show much significance even though previous studies have shown it to be significant. The R^2 is only 0.55 and the residual standard error (MSE) is fairly high which indicates that there is considerable room for improvement.

Joint Faulting — JPCP/JRCP Doweled Model

The following equation was developed to predict transverse joint faulting in JPCP and JRCP with dowels, using data from GPS-3 and GPS-4:

$$FAULTD = CESAL^{0.25} * \left[0.0238 + 0.0006 * \left(\frac{JTSPACE}{10} \right)^2 + 0.0037 * \left(\frac{100}{KSTATIC} \right)^2 + 0.0039 * \left(\frac{AGE}{10} \right)^2 - 0.0037 * EDGESUP - 0.0218 * DOWDIA \right] \quad (7.2)$$

Where:

FAULTD	=	predicted mean transverse doweled joint faulting, inches;
CESAL	=	cumulative 18,000 lbs (80 kN) ESALs in traffic lane, millions;
JTSPACE	=	mean transverse joint spacing, ft;
KSTATIC	=	mean backcalculated static k-value, psi/inch;
AGE	=	age since construction, years;
EDGESUP	=	1 if tied concrete shoulder; 0 if any other shoulder type; and
DOWDIA	=	diameter of dowels in transverse joints, inches.

Statistics:	N	=	59 sections
	R^2	=	0.534
	MSE	=	0.028 in. (0.7 mm)

A detailed description of the development of this predictive equation is provided in SHRP-P-393. The results of the sensitivity analysis for the equation are shown in Figure 7.3. CESAL, JTSPACE, AGE, and KSTATIC have the greatest effects on doweled joint faulting. The form of the model matches the physical development of faulting with traffic loadings (14,15). Faulting is known to increase rapidly at first and then level off with continued traffic loadings. In addition, this form matches boundary conditions of zero faulting at zero loadings.

As CESAL increases, faulting increases rapidly at first and then levels off. Faulting increases considerably as joint spacing increases — a trend found in several previous studies. Joint spacing ranged from 13.5 to 65 ft (4.1 to 19.8 m). As the static k-value increases, faulting decreases. This variable shows the effect of subgrade stiffness on the development of faulting. AGE was included in the model due to its apparent strong individual effect. There was very little correlation between AGE and CESAL. Here, AGE probably represents cycles of climatic changes: joint opening and closing, thermal curling cycles, cold-hot cycles, etc. None of the climatic variables were strong enough to enter the model by themselves. Edge support shows slight reduced faulting when a tied concrete shoulder is present. Faulting decreases as dowel diameter increases, reflecting a reduction in dowel/concrete bearing stress with larger dowel bars.

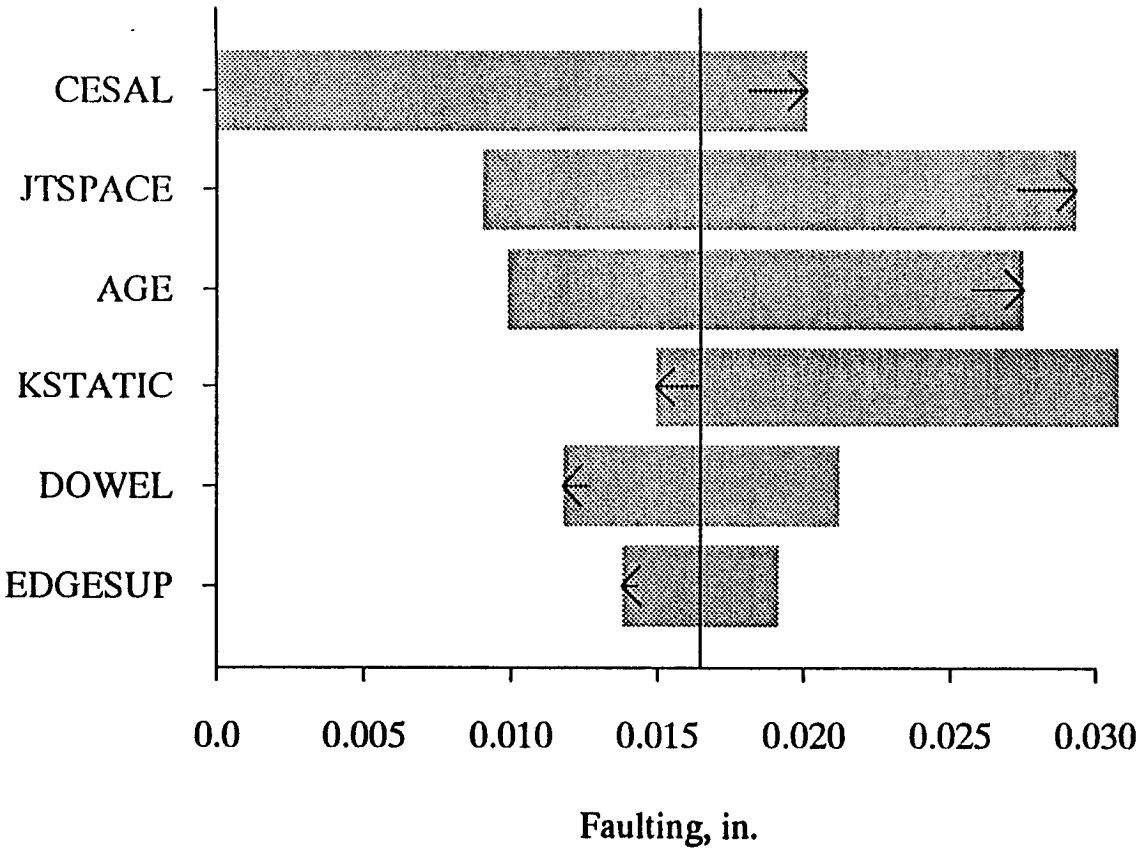

Figure 7.3. Sensitivity Analysis for Doweled Joint Faulting Model

The model includes several variables known from previous studies to affect faulting, and the effects (increase or decrease of faulting) are logical. However, several variables not found to significantly affect faulting for this data set are generally considered significant. For example, base type (untreated versus treated) and climate did not show much significance. The R^2 is only 0.53 and the MSE is 0.028 in. (0.7 mm), which is fairly high, indicating that there is considerable room for improvement.

Transverse Cracking — JPCP Model

A model for transverse cracking (all severities) of JPCP was developed using all data for the GPS-3 sections. However, this database included only a few sections that had transverse cracking. Efforts to develop predictive models based on the procedures used for all the other models were unsuccessful for transverse cracking. Therefore, a mechanistic procedure was used to calculate the accumulated fatigue damage over the life of each section, and attempts were then made to correlate this damage with transverse cracking based on procedures applied in previous studies (4,14). A detailed description of the model development is provided in SHRP-P-393.

Miner's fatigue damage model was used to determine the accumulated fatigue damage (n/N) over the life of each pavement section. The details of the procedure used to determine the fatigue damage parameters n and N for the pavement sections are given in SHRP-P-393. The numerator n is a function of the cumulative ESAL loadings and was calculated as the expected number of applied edge stresses due to traffic ESAL loadings and thermal daytime curling. The denominator N is the mean number of allowable edge stress loads required to cause failure or slab cracking and is a function of the stress to strength ratio of the pavement sections.

The mean 28 day flexural strengths of the concrete pavements were estimated from the split tensile strength data from the LTPP data base. Finite element techniques (ILLISLAB) were used to calculate the edge stress. The edge stress was calculated to account for the combined effects of loading and positive temperature gradient curling. The stress prediction equations are included in "Mechanistic Design Models of Loading and Curling in Concrete Pavement" (16). Several variables are included in the edge stress calculation, including slab thickness, modulus of elasticity, Poisson's ratio, and length; thermal gradients through the slab; subgrade k-values; single axle load at edge of slab; and the thermal coefficient of expansion of concrete.

Temperature gradients were based on mean positive gradients during daylight hours. Values used are as follows:

Climatic Region	Slab Thickness, in.	Mean Annual Thermal Gradient, °F/in.
Nonfreeze	8	1.40
	9	1.30
	10	1.21
	11	1.11
	12	1.01
Freeze	8	1.13
	9	1.05
	10	0.96
	11	0.87
	12	0.79

(1 in. = 2.54 cm; °F/in. = 0.0458 °C/m)

The free edge stress was adjusted for load transfer from a tied concrete shoulder (approximately 75 percent deflection transfer, which results in a 15 percent reduction in edge stress).

Both n and N were computed for each section in the database and the fatigue damage ratio determined as the total estimated fatigue damage from the time the section was opened to traffic to the time when transverse cracking was measured. A plot of percentage of cracked slabs versus $\log_{10}(n/N)$ was prepared to show the relationship between cumulative fatigue damage and percentage of cracked slabs. Figure 7.4 shows these results. This plot shows

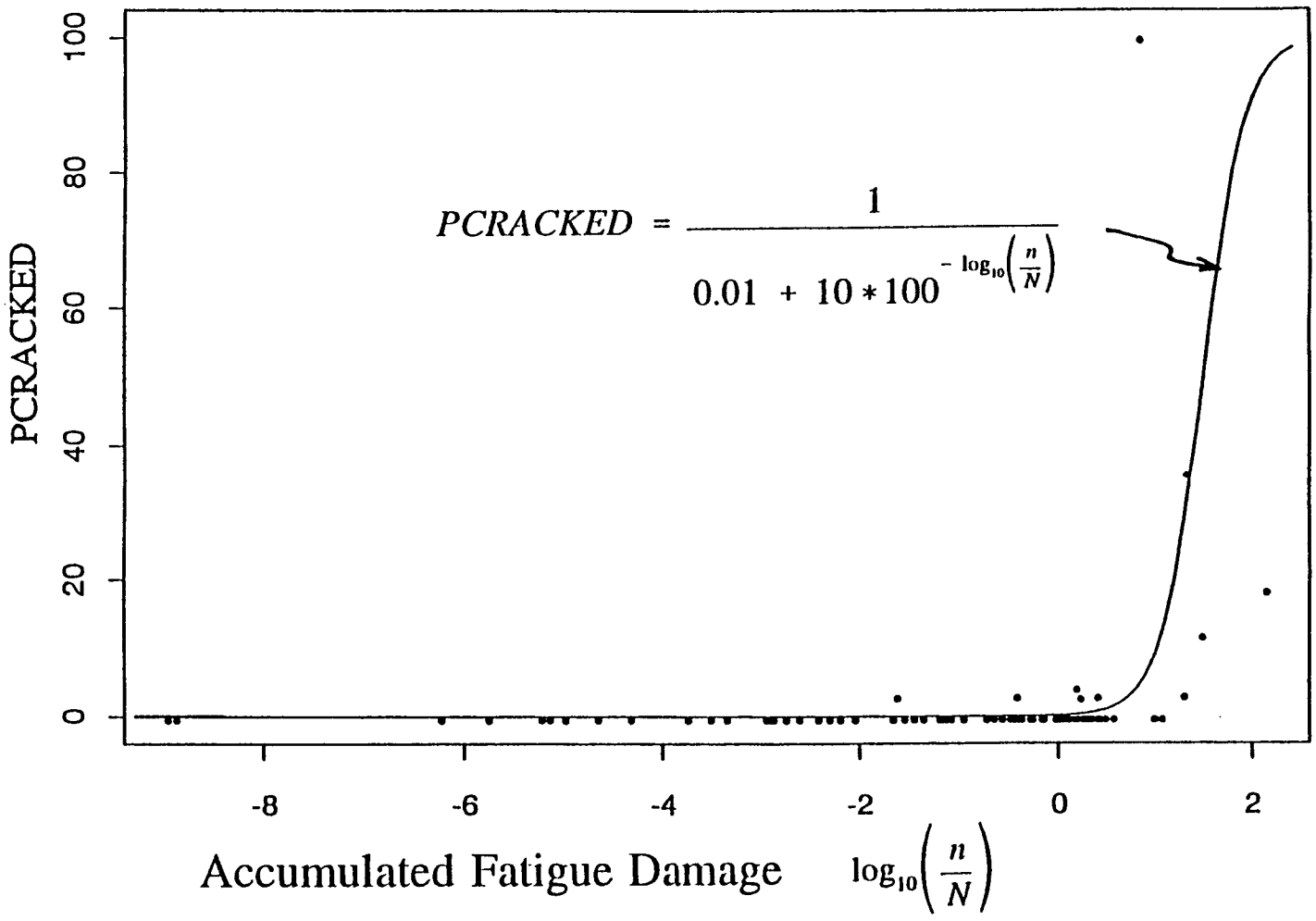

Figure 7.4. Percentage of Slabs Cracked Versus Accumulated Fatigue Damage for JPCP

no cracking for fatigue damages less than about 0.1 and then some cracking developing as fatigue damage increases beyond 1.0. Although there are a limited number of cracked sections, a general trend can be seen. Previous studies with far more data than were available for this study have shown similar results (8,15).

Conceptually, an s-shaped curve should be fitted through these data to consider boundary conditions. However, fitting such a curve by regression techniques was not successful due to the scatter of data. Therefore, for illustrative purposes only, an s-shaped curve was fitted by eye through the data and is shown in Figure 7.4. The equation for this curve is given below:

$$PCRACKED = \frac{1}{0.01 + 10 * 100^{-\log_{10}\left(\frac{n}{N}\right)}} \quad (7.3)$$

Where:

PCRACK	=	percentage of cracked slabs,
n	=	expected number of applied edge stresses based on traffic ESAL loadings and thermal daytime curling,
N	=	mean number of allowable edge stress loads that causes slab cracking, and
	=	f(slab thickness, modulus of elasticity, Poisson's ratio, slab length, thermal gradients, subgrade k-value, single axle load at edge of slab, and thermal coefficient of expansion of concrete).

A sensitivity analysis of this equation, with the equations for n and N included, is described in SHRP-P-393, and the results are shown in Figure 7.5. Thickness (THICK) has by far the strongest effect on cracking, followed by the concrete modulus of rupture at 28 days (MR28). This model is based on too few data points and should only be considered approximate. This type of model has been derived with far more data under several previous studies (8,14). As more LTPP data become available, it will be possible to develop a much more reliable model for slab cracking for JPCP. A more comprehensive fatigue damage analysis should also be developed and applied. Such an analysis should consider axle load spectra, increases in concrete strength over time, and variations in thermal gradient over seasons and days.

Transverse Cracking — JRCP Model

The model below was developed for transverse cracking from data for JRCP test sections from GPS-4. Only deteriorated transverse cracks were considered, because low-severity transverse cracks are a normal design occurrence in JRCP where reinforcement is supposed to hold them tight and prevent deterioration.

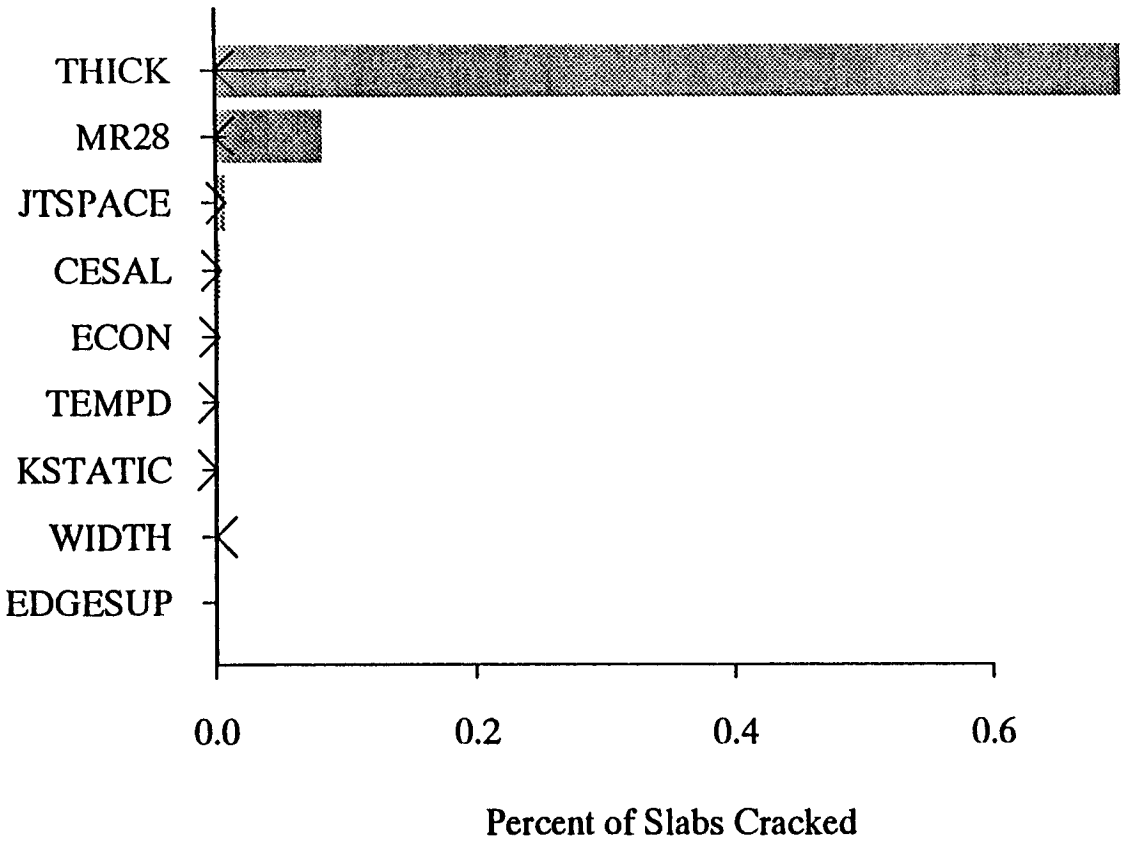

Figure 7.5. Sensitivity Analysis for Transverse Cracking of JPCP Model

$$CRACKJR = -72.95 + 1.907\ CESAL + 0.182\left(\frac{1}{PSTEEL^2}\right) + 2474\left(\frac{1}{KSTATIC}\right) + 0.697\ PRECIP \quad (7.4)$$

Where:

CRACKJR	=	number of transverse cracks (medium-high severity)/mile;
CESAL	=	cumulative 18,000 lbs (80 kN) ESALs in traffic lane, millions;
PSTEEL	=	percentage of steel (longitudinal reinforcement);
PRECIP	=	annual precipitation, inches; and
KSTATIC	=	mean backcalculated k-value, psi/inch

Statistics:			
	N	=	27 sections
	R^2	=	0.48
	MSE	=	20.8 cracks/mi (12.5 cracks/km)

A detailed description of the development of this predictive equation is provided in SHRP-P-393. The results of the sensitivity analysis for the model are shown in Figure 7.6. All variables significantly affect crack deterioration in JRCP. It can be seen that the modulus of subgrade reaction k was predicted to have the greatest influence on the occurrence of

deterioration of transverse cracks in JRCP. The next most significant variable was percentage of steel, while the form of the equation shows deteriorated cracks developing at a uniform rate with increased traffic loadings. The model shows that as steel percentage increases, the number of deteriorated transverse cracks is reduced greatly. The exact amount of reinforcement to prevent crack deterioration may depend on climatic factors. JRCPs in areas with relatively high precipitation levels experience more crack deterioration than those in drier climates.

All variables recommended by the experts and available in the data base were evaluated, but only these were found to be significant. However, several variables which are generally considered to significantly affect transverse crack deterioration did not surface as significant for this data set. These include base type (untreated versus treated), slab thickness, joint spacing, and other climatic variables (14). The R^2 is only 0.48 and the MSE is 21 cracks/mi (13 cracks/km), which is fairly high, indicating that there is considerable room for improvement in predictive ability.

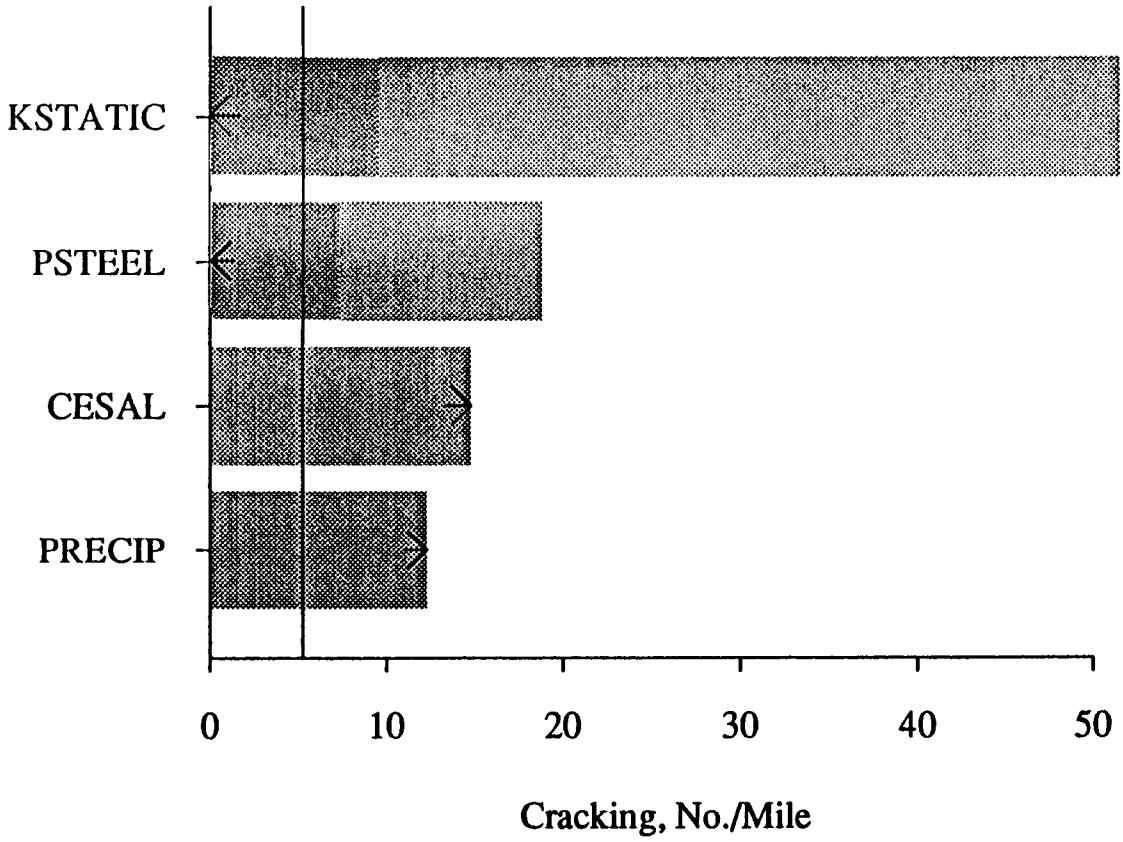

Figure 7.6. Sensitivity Analysis for Transverse Cracking of JRCP Model

Joint Spalling — JPCP Model

The following equation was developed to predict transverse joint spalling (all severities), based on a data set that included data from all JPCP sections in GPS-3:

$$SPALLJP = 9.79 + 10.01 * [-1.227 + 0.0022 * (0.985 * AGE + 0.171 * FTCYCLE)] \quad \textbf{(7.5)}$$

Where:

SPALLJP	=	predicted mean percentage of transverse joint spalling (all severities), percentage of total joints;
FTCYCLE	=	mean annual air freeze-thaw cycles; and
AGE	=	Age since construction, years.

Statistics:	N	=	56 sections
	R^2	=	0.335
	MSE	=	11.05 percent of joints

A detailed description of the model development is provided in SHRP-P-393. The results from a sensitivity analysis for this equation are shown in Figure 7.7. Both FTCYCLE and AGE have a significant effect on JPCP joint spalling. The form of the model generally matches the physical development of spalling with age (14,15). Spalling generally increases slowly at first and then increases more rapidly after several years due to a variety of design and climatic conditions. Over time, incompressibles infiltrate into joints with inadequate seals, causing increased compressive stresses in hot weather. The freeze-thaw cycle of saturated concrete may weaken concrete near the joints over time. Dowel bar corrosion and subsequent lockup may also contribute to joint spalling.

All variables recommended by the experts and available in the data base were evaluated but few were found to have any significance. Only two variables were included in the final model. As AGE increases, spalling increases slowly at first and then increases more rapidly. Here, AGE probably represents cycles of climatic changes such as joint opening and closing, thermal curling cycles, cold-hot cycles, etc. Only one climatic variable was strong enough to enter the model. An increased annual number of air freeze-thaw cycles result in prediction of increased joint spalling. This variable may indicate that freeze-thaw cycles cause a weakening in the (often-saturated) concrete near the joint, which eventually spalls over time.

The model includes only two of several variables known from previous studies to affect spalling, and their effects (increase spalling) are logical. Variables believed from other studies to be significant to joint spalling but not found to be significant for this data set include joint seal type and joint spacing. Joint spacing is inherent in the model because the dependent variable is the percentage of joints spalled. However, its absence from the model indicates that it apparently does not affect the percentage of joints spalled. Joint spacing only

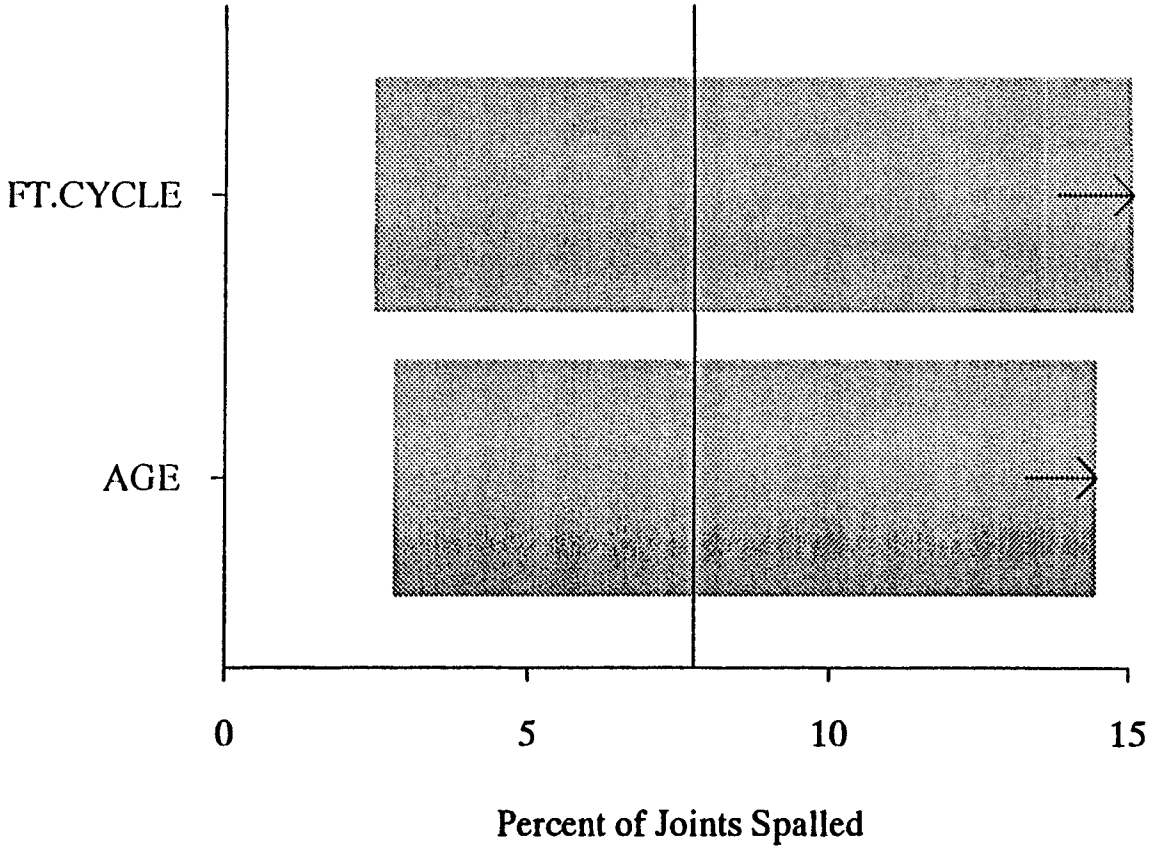

Figure 7.7. Sensitivity Analysis for Joint Spalling of JPCP Model

ranged from 13 to 30 ft (3.9 to 9 m) in this data set, so within this limited range it may not have contributed significantly to joint spalling. The R^2 is only 0.34, and the MSE is 11 percent, which indicates that there is considerable room for improvement in the predictive capability of this equation.

Joint Spalling — JRCP Model

The following model was developed for transverse joint spalling (all severities) from a data set that included all JRCP test sections in GPS-4:

$$SPALLJR = -79.01 + 0.603 * (AGE)^{1.5} + 0.129 * (TRANGE)^{1.5} \quad \textbf{(7.6)}$$

Where:

SPALLJR	=	predicted mean percentage of transverse joints spalled (all severities), percentage of total joints;
TRANGE	=	mean monthly temperature range (mean maximum daily temperature minus mean minimum daily temperature for each month over each year); and
AGE	=	age since construction, years.

Statistics:	N	=	25 sections
	R^2	=	0.644
	MSE	=	16.6 percent of joints

A detailed description of the model development is provided in SHRP-P-393. The results from a sensitivity analysis of the model are shown in Figure 7.8. Both AGE and TRANGE have a significant effect on joint spalling in JRCP. The form of the model shows a curvilinear increase in spalling with age and more severe temperature conditions (14,15).

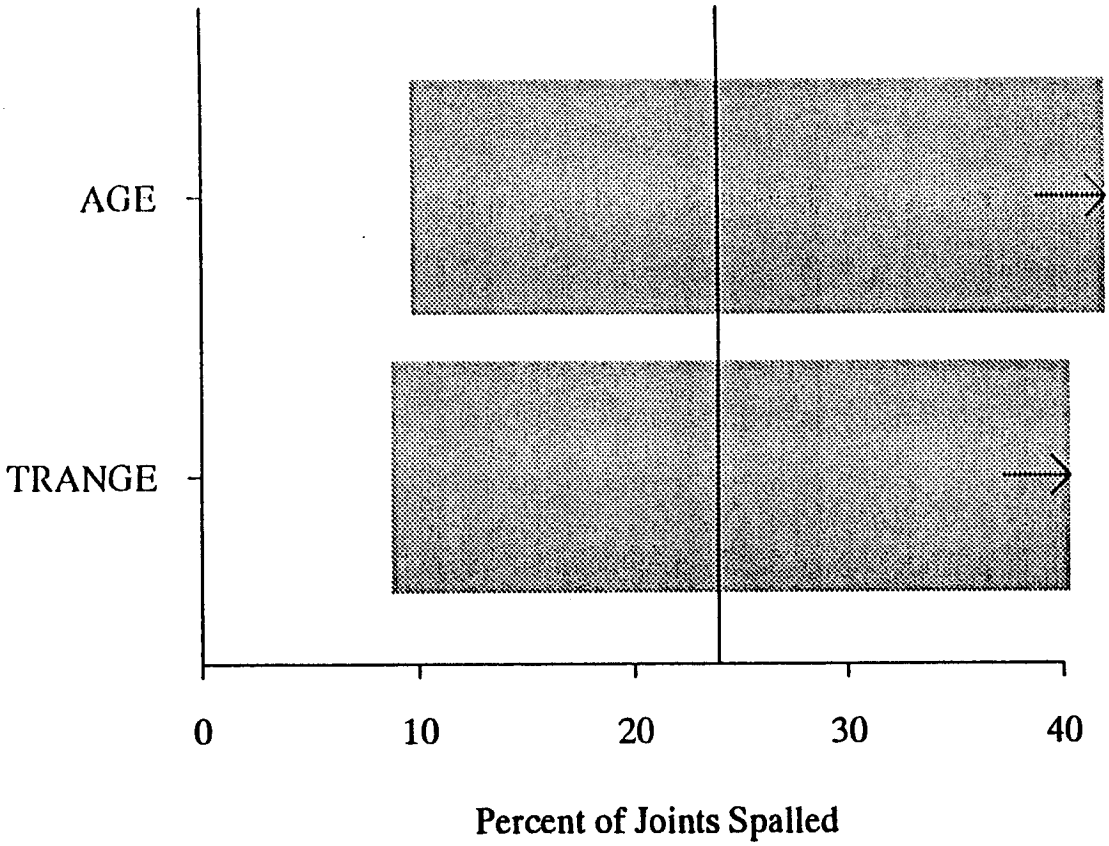

Figure 7.8. Sensitivity Analysis for Joint Spalling of JRCP Model

All variables recommended by the experts and available in the data base were evaluated but few were found to have any significance. Only two variables were included in the final model. As AGE increases, spalling increases in a curvilinear manner, according to this model. AGE here is believed to represent cycles of climatic changes such as joint opening and closing, thermal curling cycles, cold-hot cycles, freeze-thaw cycles, progressive corrosion of dowels, etc. The TRANGE variable reflects daily and monthly temperature ranges to which the pavement is subjected. The higher the TRANGE (northern United States and Canada), the greater the joint spalling. A greater temperature range would generally cause increased joint openings, and increase the infiltration of incompressibles in winter and high compressive stresses in summer. TRANGE also correlates strongly with other thermal variables, including the number of freeze-thaw cycles, number of days above 90°F (32.2°C), and the freezing index.

The model includes only two of several variables known from other studies to affect spalling. The effects from these two variables (increases in joint spalling) appear logical. There are, however, several variables believed from other studies to be significant to joint spalling that were not found to be significant for this data set. For example, joint seal type did not show significant effect. Joint spacing is inherent in the model because the dependent variable is a percentage of joints spalled. However, its apparent lack of significance indicates that it does not affect the percentage of joints spalling. Pavements with longer joint spacing would conceivably have the same percentage of joint failures as similar pavements with shorter joint spacing. Pavements with closer joint spacing would be expected to have more spalled joints per mile than pavements with longer joint spacing. The R^2 is only 0.64, and the MSE is 17 percent, which indicates that there is considerable room for improvement in this predictive equation.

Roughness (IRI) — JPCP Doweled Joint Model

The equation below was developed for roughness (IRI) of doweled JPCP, based on the entire data set for GPS-3. The current IRIs of the pavements were used for prediction, rather than the increase in IRI, since the initial IRI after construction was not generally measured.

$$IRI = 105.9 + 159 * \left(\frac{AGE}{KSTATIC}\right) + 2.17 * JTSPACE - 7.13 * THICK + 13.50 * EDGESUP \quad (7.7)$$

Where:

IRI	=	International Roughness Index, inches/mile;
AGE	=	age since construction, years;
THICK	=	concrete slab thickness, inches;
KSTATIC	=	mean backcalculated static k-value, psi/inch;
EDGESUP	=	1 if tied concrete shoulder, 0 for any other shoulder type; and
JTSPACE	=	mean transverse joint spacing, feet.

Statistics:	N	=	21 sections
	R^2	=	0.548
	MSE	=	19.06 in./mi (30.6 cm/km)

A detailed description of the model development is provided in SHRP-P-393. The results from a sensitivity analysis for the model are shown in Figure 7.9. JTSPACE has the largest effect on the occurrence of roughness, followed by THICK, EDGESUP, AGE, and KSTATIC. The form of the model provides for a linear increase in IRI over time. Here, AGE probably represents a combination of factors that include traffic loadings and the effect of cycles of climatic changes on the pavement, such as joint opening and closing, thermal curling cycles, cold-hot cycles, etc. AGE may also represent time-dependent settlements or heaves of the foundation. No climatic variables were strong enough to be included in the

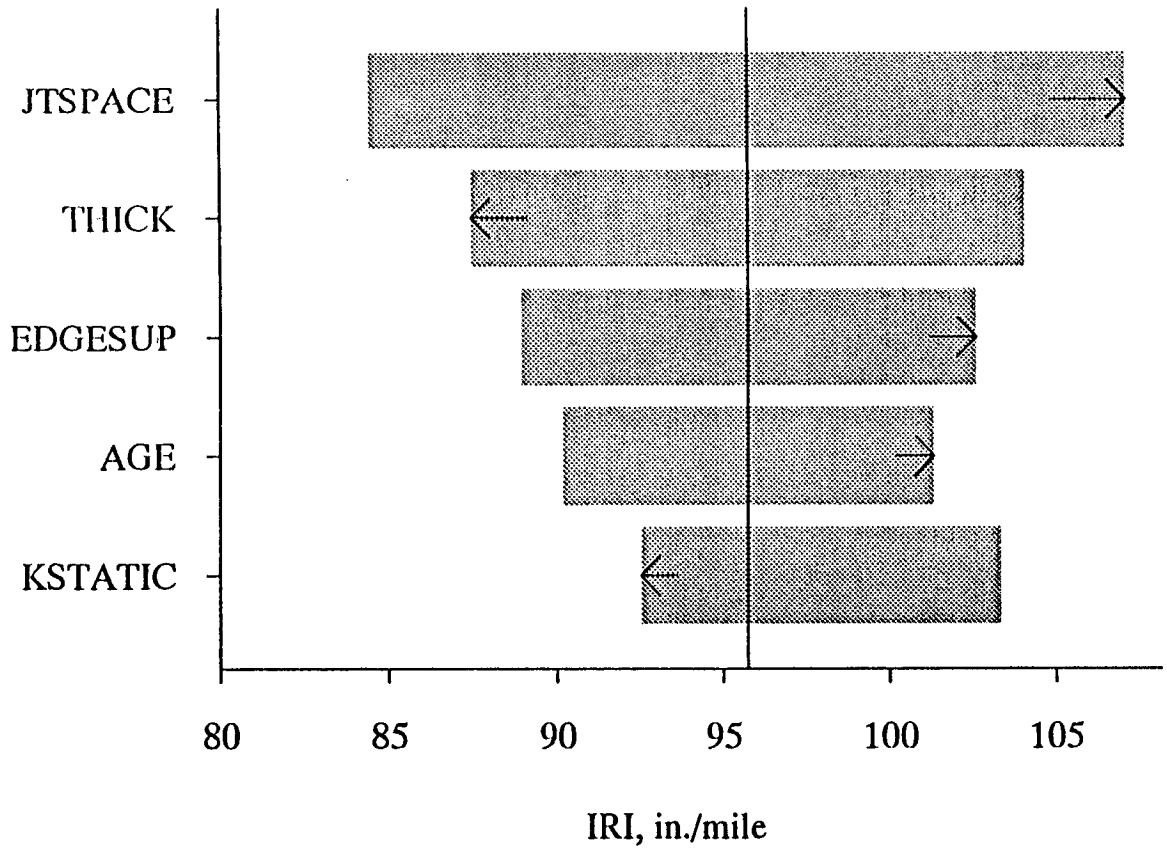

Figure 7.9. Sensitivity Analysis for IRI Roughness for Doweled Joint Model

model. The stiffer the subgrade, as measured by the backcalculated KSTATIC, the lower the IRI. As joint spacing decreases, the IRI increases. As slab thickness increases, IRI decreases. The presence of a tied concrete shoulder appears to increase the IRI slightly.

The model for doweled JPCP includes several variables known from previous studies to affect roughness, and the effects of these variables (increase or decrease in roughness) appear logical. However, several variables that were expected to have an effect were not significant for this data set, including base type (untreated versus treated) and several climatic variables. The R^2 is only 0.55, and the MSE is 19 in./mi (30.6 cm/km), which indicates that there is considerable room for improvement in the predictive ability of this equation.

Roughness (IRI) — JPCP Non-doweled Model

The predictive equation below was developed for roughness (IRI) of non-doweled JPCP from the GPS-3 data set. The current IRIs of the pavements were used for prediction, rather than the increase in IRI, since the initial IRI after construction was not measured.

$$IRI = 38.85 + 12.9 * CESAL + 0.222 * FT + 1.50 * PRECIP$$
$$-10.97 * BASE - 13.7 * SUBGRADE \quad \textbf{(7.8)}$$

Where:

IRI	=	International Roughness Index, inches/mile;
CESAL	=	cumulative 18,000 lbs (80 kN) ESALs in traffic lane, millions;
PRECIP	=	mean annual precipitation, inches;
FT	=	mean annual air freeze-thaw cycles;
BASE	=	1 if treated granular material (with asphalt, cement) or lean concrete; 0 if untreated granular material; and
SUBGRADE	=	1 if AASHTO classification is A-1, A-2, A-3 (coarse-grained); 0, if AASHTO classification is A-4, A-5, A-6, A-7 (fine-grained).

Statistics:			
	N	=	28 sections
	R^2	=	0.644
	MSE	=	31.29 in./mi (50 cm/km)

A detailed description of the model development is provided in SHRP-P-393. The results from a sensitivity analysis of this equation are shown in Figure 7.10. CESAL has the largest effect, followed closely by PRECIP. FTCYCLE, SUBGRADE, and BASE have significant but lesser effects on the occurrence of roughness for non-doweled JPCP. The form of the equation provides for a linear increase in IRI with increases in predicted CESALs. Two climatic variables were strong enough to be included in the equation. IRI increases with increases in the annual number of air freeze-thaw cycles and with increasing PRECIP, and decreases for pavements having asphalt- or cement-treated bases. Subgrade soil classification affects IRI in that coarse-grained soils result in a lower IRI over time than do fine-grained soils.

The equation includes several variables known to affect roughness from previous studies, and the sense of the effects of these variables are logical. However, several variables that were expected to be significant were not found to be significant for this data set, including joint spacing. The R^2 is only 0.644, and the MSE is 31 in./mi (50 cm/km), which indicates that there is considerable room for improvement.

Roughness (IRI) — JRCP Model

The following equation was developed to predict roughness (IRI) of JRCP, based on data from GPS-4. The current IRIs of the pavements were used rather than increases in IRI, since the initial IRI after construction was not measured.

$$IRI = 141.4 + 0.8488 * AGE + 0.3469 * PRECIP + 1388 * \left(\frac{1}{KSTATIC}\right) + 21.24 * THICK + 15.09 * EDGESUP \quad (7.9)$$

Where:

IR	=	International Roughness Index, inches/mile;
AGE	=	age since construction, years;
THICK	=	concrete slab thickness, inches;
KSTATIC	=	mean backcalculated static k-value, psi/inch;
PRECIP	=	mean annual precipitation, inches; and
EDGESUP	=	1 if tied concrete shoulder; 0 if any other shoulder type.

Statistics: N = 32 sections
R^2 = 0.782
MSE = 9.86 in./mi (15.6 cm/km)

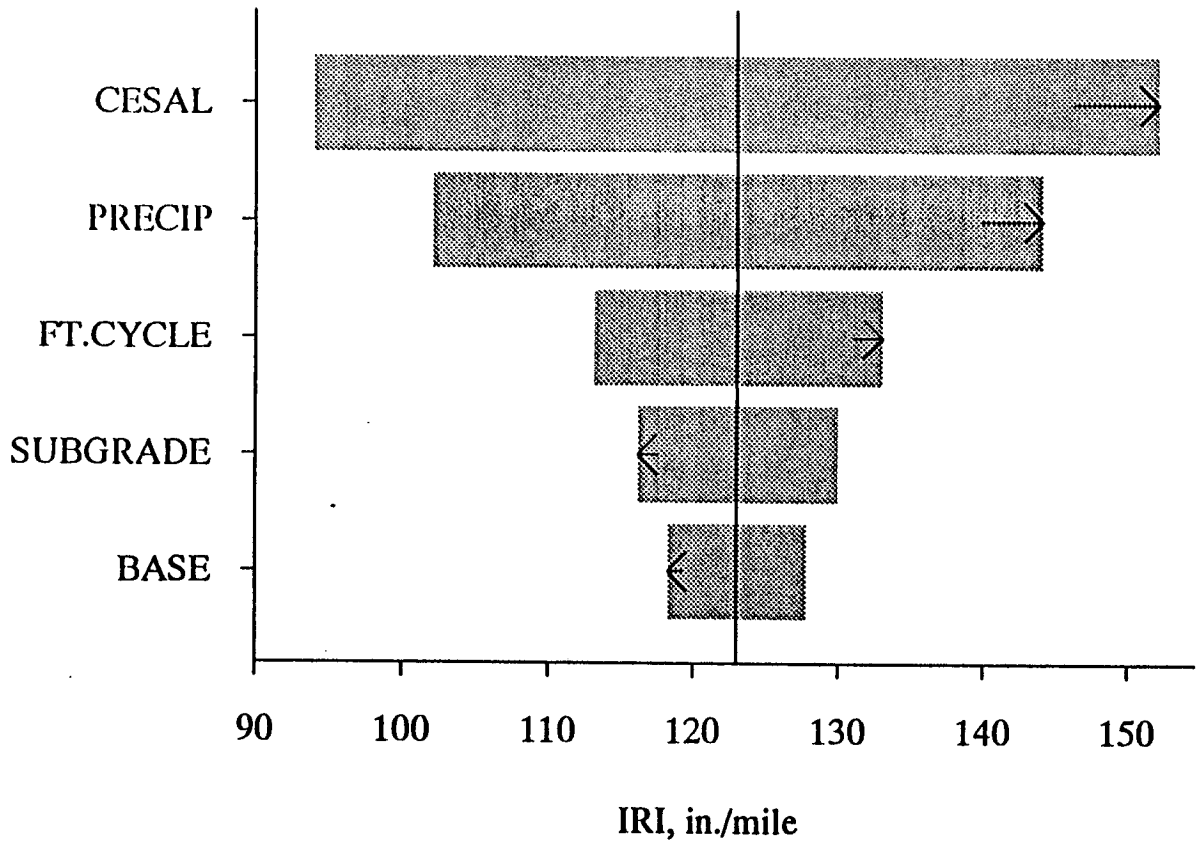

Figure 7.10. Sensitivity Analysis for IRI Roughness for Non-doweled JPCP Joint Model

A detailed description of the development of this equation is provided in SHRP-P-393. The results of a sensitivity analysis for this equation are shown in Figure 7.11. THICK, KSTATIC, and EDGESUP were most significant, followed by AGE and PRECIP. The form of the equation provides for a linear increase in IRI over time. Here, AGE probably represents a combination of factors that include traffic loadings and the effect of cycles of climatic changes: joint opening and closing, thermal curling cycles, cold-hot cycles, etc. Only one climatic variable, PRECIP, was strong enough to be included in the model. As PRECIP increases, IRI also increases. IRI is lower when the subgrade is coarse-grained soil than when it is fine-grained soil. As slab thickness increases, IRI was found to increase for this data set. While this may seem illogical, it may be that the thicker slabs in the GPS-4 data base were constructed rougher originally. The presence of a tied concrete shoulder increases the IRI slightly, which may also be related to the initial construction or other factors.

The equation for prediction of roughness in JRCP includes several variables known to affect roughness from previous studies, and the effects (decrease or increase in roughness) are logical. However, several variables that were expected to be significant were not found to be significant for this data set, including base type (untreated versus treated) and several climatic variables. The R^2 for this equation is 0.78, and the MSE is 10 in./mi (15.6 cm/km); however, data were available for only 32 test sections.

Roughness (IRI) — CRCP Model

The following equation was developed for predicting roughness (IRI) of doweled CRCP based on data from GPS-5. As before, the current IRI of the pavements was used for prediction rather than the increase in IRI:

$$IRI = 262.0 + 1.47 * CESAL - 2.94 * THICK - 232.3 * PSTEEL - 29.79 * WIDENED - 16.82 * SUBGRADE \quad \textbf{(7.10)}$$

Where:

IRI	=	International Roughness Index, inches/mile;
CESAL	=	cumulative 18,000 lbs (80 kN) ESALs in traffic lane, millions;
PSTEEL	=	percentage of steel (longitudinal reinforcement);
THICK	=	concrete slab thickness, inches;
WIDENED	=	1 if widened traffic lane; 0 if normal-width lane; and
SUBGRADE	=	1 if AASHTO classification is A-1, A-2, A-3 (coarse-grained); 0 if AASHTO classification is A-4, A-5, A-6, A-7 (fine-grained).

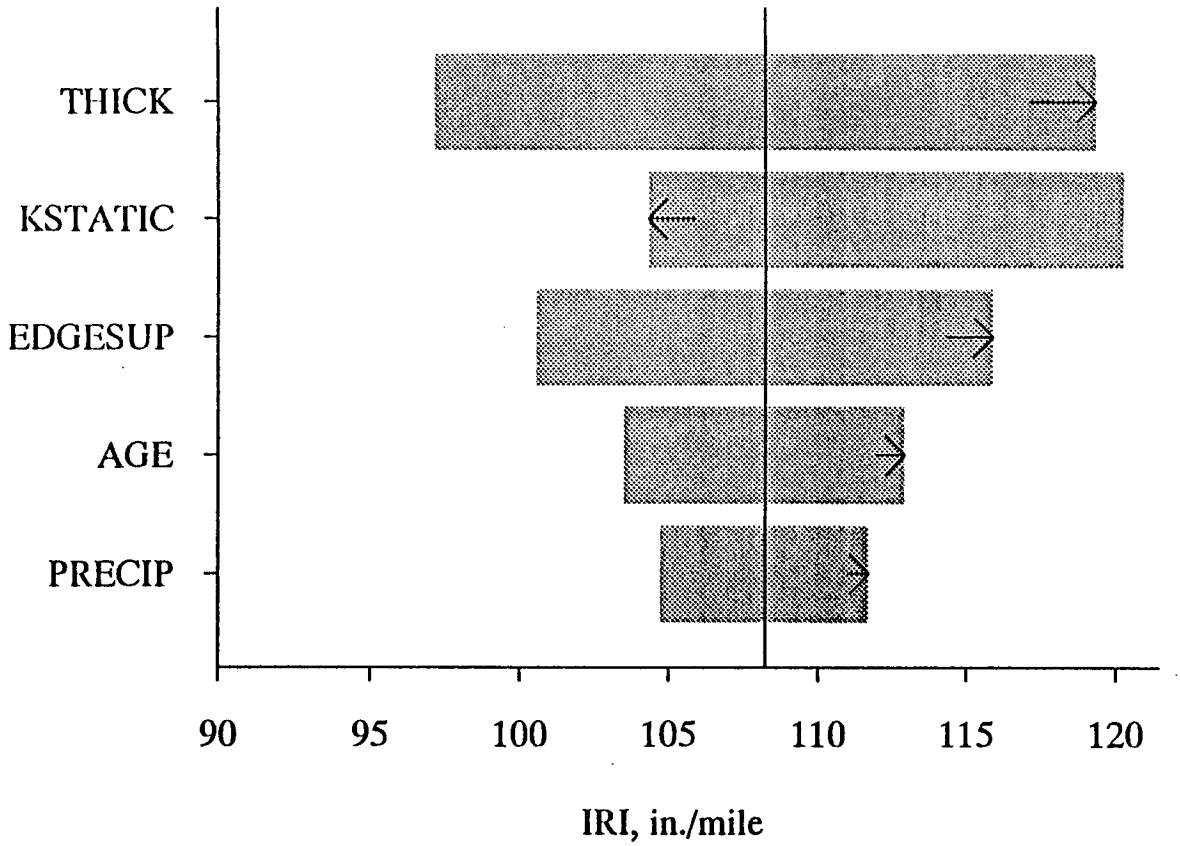

Figure 7.11. Sensitivity Analysis for IRI Roughness for JRCP Model

Statistics: N = 42 sections
R^2 = 0.546
MSE = 17.19 in./mi (27 cm/km)

A detailed description of the model development is provided in SHRP-P-393. The results of a sensitivity analysis for the predictive equation are shown in Figure 7.12. PSTEEL has by far the largest effect on the IRI of CRCP. The form of the model provides for a linear increase in IRI with traffic. No climatic variables were strong enough to be included in the model. A coarse-grained subgrade soil type results in a lower IRI than a fine-grained soil type. As slab thickness increases, the IRI decreases. As the percentage of steel increases, the IRI decreases. The presence of a widened traffic lane reduces the IRI.

The IRI model for CRCP includes several variables known from previous studies to affect roughness and the effects (increases or decreases in roughness) are logical. However, several variables that were expected to be significant were not found to be so for this data set, including base type (untreated versus treated) and several climatic variables. The R^2 is only 0.55 and the MSE is 17 in./mi (27 cm/km), which indicates that there is considerable room for improvement in this predictive equation.

CRCP Failure Model

Adequate data were not available to develop a predictive equation. Only five sections exhibited localized failures such as punchouts. As time and traffic loadings increase and this distress develops on more sections, it is expected that a predictive model can be developed.

Illustration of Use of LTPP Models in Pavement Design Evaluation

The following presentation is intended to illustrate the potential for use of the LTPP models for evaluation or developing pavement designs. This example is for illustration only since the early LTPP prediction models are not adequate for use in design at this time. Future versions of these models should be greatly improved and should be adequate for use in design. A JRCP design has been proposed, based on an agency's standard design procedures and design standards. The values selected for the required design inputs for the LTPP models are summarized below:

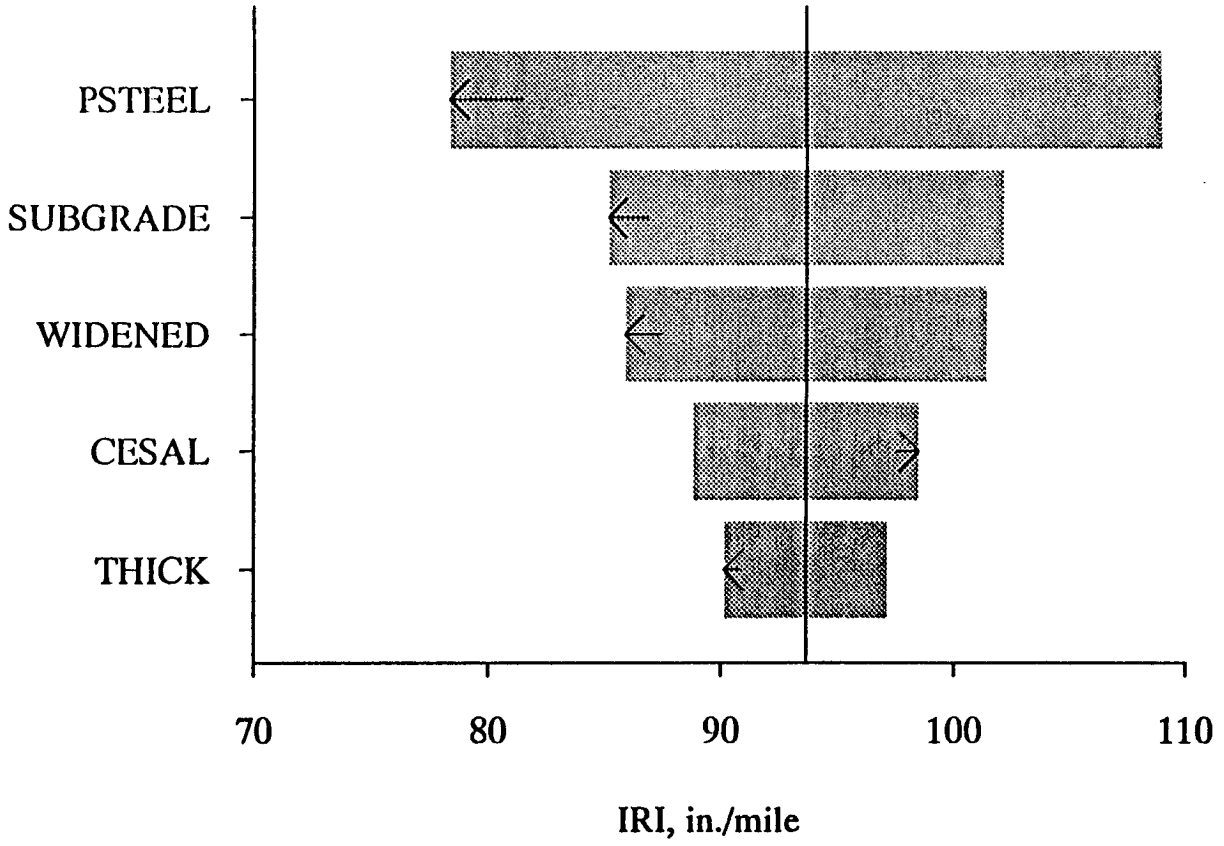

Figure 7.12. Sensitivity Analysis for IRI Roughness for CRCP Model

Design life:	30 years		
Traffic:	30 million ESALs in design lane		
Climate:	PRECIP	=	30 in. (762 mm)
	TRANGE	=	60°F (33.3°C)
Subgrade:	KSTATIC	=	300 psi/in. (82.7 Kpa/mm)
Base:	Treated granular material		
Slab:	THICK	=	9 in. (229 mm)
	PSTEEL	=	0.12 percent area
Joints:	JTSPACE	=	40 ft (12 m)
	DOWDIA	=	1.25 in. (32 mm)
Shoulders:	AC, EDGESUP	=	0

These pavement design inputs and characteristics were used with all the predictive models for JRCP to estimate performance over the 30 year design life and beyond. (Note that prediction beyond about 20 years exceeds the inference space for the current LTPP models.) Joint faulting, joint spalling, transverse crack deterioration, and IRI were predicted. Since some readers may not be familiar with the values of the IRI, the corresponding Present Serviceability Rating (PSR) has been estimated from a recently developed model from user panel data (17). The results are shown in Table 7.1. Some interesting results are summarized below:

- Faulting of only 0.10 in. (2.5 mm) was predicted at 30 years. A level of approximately 0.25 in. (6.4 mm) is critical from a roughness standpoint for a JRCP with long joint spacing. Thus, joint load transfer is adequate over the 30 year period.

- Joint spalling (converted from percentage of joints deteriorated to number of joints per mile) is predicted to increase rapidly after 15 years until at 30 years about 106 joints per mile (67 joints/km) have deteriorated. Joint repair will be required after about 15 to 20 years to keep the pavement in service unless some improvement in joint design is obtained.

- Transverse crack deterioration is relatively low over most of the 30 year design period. However, crack deterioration increases greatly at about 30 years, requiring considerable repair. An increased amount of reinforcement would reduce the amount of crack deterioration as subsequently shown.

- The IRI remains within an acceptable range over the 30 year design period as indicated by the PSR values.

Table 7.1. Use of LTPP Predictive Models to Evaluate a JRCP Design Example

AGE	CESAL	JT Space	K Static	Edge SPRT	Dowel DIA	% Steel	Temp	Pre-cip	THCK	FLT	Spall	CRCK	IRI	PSR
Years	10^6	ft	psi/ in.	*	in.	%	°F	in.	in.	in.	joints /mi	cracks /mi	in./ mi	**
5	5	40.0	300	0	1.25	0.12	60	30	9	0.01	0***	0***	69	3.8
6	6	40.0	300	0	1.25	0.12	60	30	9	0.01	0	0	70	3.8
7	7	40.0	300	0	1.25	0.12	60	30	9	0.01	0	0	71	3.7
8	8	40.0	300	0	1.25	0.12	60	30	9	0.02	0	0	72	3.7
9	9	40.0	300	0	1.25	0.12	60	30	9	0.02	0	0	72	3.7
10	10	40.0	300	0	1.25	0.12	60	30	9	0.02	0	0	73	3.7
15	15	40.0	300	0	1.25	0.12	60	30	9	0.03	21	0	78	3.6
20	20	40.0	300	0	1.25	0.12	60	30	9	0.05	46	7	82	3.6
25	25	40.0	300	0	1.25	0.12	60	30	9	0.07	74	17	86	3.5
30	30	40.0	300	0	1.25	0.12	60	30	9	0.10	106	26	90	3.5
40	40	40.0	300	0	1.25	0.12	60	30	9	0.17	176	45	99	3.3
50	50	40.0	300	0	1.25	0.12	60	30	9	0.28	256	64	107	3.2

* EDGESUP = 1 for tied PCC shoulder, 0 for any other shoulder type.

** $PSR = 5 * e^{(-0.0041*IRI)}$ (1).

*** Values that were negative were set at zero.

Note: 1 in. = 25.4 mm; 1 ft = 0.3 m; 1 psi/in. = 275.6 Pa/mm.

The following results show the effect of percentage of steel varied from 0.06 to 0.15 percent of cross-sectional area on deteriorated transverse cracks per mile at 30 years and 30 million CESALs:

Percentage of Steel	Deteriorated Transverse Cracks/mi
0.06	64 (38 cracks/km)
0.09	36 (22 cracks/km)
0.12	26 (16 cracks/km)
0.15	22 (13 cracks/km)

These results show the strong effect of percentage of steel on crack deterioration. Many sections in the database have less than 0.09 percent steel, and thus have developed considerable crack deterioration.

An important point to note here is that these predictions are all for mean distress and IRI values. No safety factor or reliability considerations have been incorporated into the LTPP models. If models such as these are used in an actual design procedure and for a given level of reliability, then consideration must be given to the formal incorporation of design reliability into the procedure.

Summary and Conclusions

In this chapter the attempts to find improvements to the AASHTO rigid pavement design procedure have been presented. These attempts, which followed an earlier evaluation of the AASHTO rigid pavement design equation, have centered on direct improvements of the equation by the addition of new calibration parameters. Examples of such calibration parameters include the drainage coefficient (Cd), load transfer factor (J), modulus of subgrade reaction (k), the loss of support factor (L), design reliability (R), and others.

In the approach presented in this study improvements to the design equation are offered by supplementing the current design equation with results from the early analysis of the LTPP data. Recommendations are provided for an improved AASHTO design methodology that follows the recommendations in Part IV of the 1993 AASHTO Design Guide (Figure 7.1). Specifically, the approach hinges on the use of IRI and distress prediction models as pavement design checks to ensure that the structural thickness developed with the AASHTO design procedure will meet established performance standards.

The models developed in this study for IRI and the key rigid pavement distress types are presented, and results of sensitivity analyses of these models are given. The models are based on results from early LTPP analysis and have many limitations. However, these LTPP models can be continuously improved in the years to come and used in the recommended improved AASHTO design methodology.

An example illustrates how this improved design methodology would work. The results of this example in Table 7.1 show that this approach could easily be used by a design engineer to predict the performance of a design. The results show that this approach would result in a more comprehensive design that checks specifically for key distress types. Design modifications could then be made to reduce the occurrence of any critical distress.

8

Evaluation of the Overlay Design Procedures

The revised 1993 AASHTO overlay design procedure is intended to provide overlay thicknesses that address a pavement with a structural deficiency. A structural deficiency arises from any conditions that adversely affect the load-carrying capability of the pavement structure. These conditions include inadequate thickness, as well as cracking, distortion, and disintegration. Several types of distress (e.g., distresses caused by poor construction techniques, and low-temperature cracking) will not initially be caused by traffic loads, but can become more severe under traffic to the point that they also detract from the load-carrying capability of the pavement. Part III, Section 4.1.2 of the AASHTO Guide provides descriptions of various structural conditions. If a pavement has only a functional deficiency, procedures in Part II, Chapter 4 and Section 5.3.2 should be used. A functional deficiency arises from any condition that adversely affects the highway user, including poor surface friction and texture, hydroplaning as a result of wheel path rutting, and excess surface distortion (e.g., potholes, corrugation, faulting, blowups, settlements, and heaves).

In the evaluation of the AASHTO overlay design procedures, a matrix of overlay structural capacities were computed based on the AASHTO overlay design procedures for different design periods and reliability levels for the available GPS 6, GPS 7 and GPS 9 test sections. For each reliability level the calculated structural capacities were compared with the actual structural capacity constructed. Since the reliability levels and overlay design periods used for structural design of the overlays are not available from the LTPP Data Base, a direct comparison of the structural capacities was not possible. Hence, a serviceability analysis was carried out to determine the adequacy of the revised AASHTO pavement overlay design procedures. In instances where no information was available on the serviceability of the pavements, the distress condition of the pavement was used to determine the adequacy of the overlay design procedures.

The AASHTO Overlay Design Procedures

The AASHTO pavement overlay design procedures are based on the concept that time and traffic loading reduce a pavement's ability to carry loads. An overlay is designed to increase the pavement's ability to carry loads over a future design period. The required structural capacity for a PCC or AC pavement to successfully carry future traffic is calculated, with the appropriate AASHTO 1993 new pavement design equation. The effective structural capacity of the existing pavement is evaluated with procedures for overlay design presented in the Guide. These procedures can be based on visual survey and material testing results or the remaining life of the pavement in terms of the traffic that can be carried, or by nondestructive testing (NDT) of the existing pavement.

An overlay is then designed based on the structural deficiency represented by the difference between the structural capacity required for future traffic and the effective structural capacity of the existing pavement. Obviously, the required overlay structural capacity can be correct only if the future structural capacity and the effective structural capacity are correct. Therefore, it is important to use the AASHTO rigid and flexible design equations properly to determine the future structural capacity, and to use the appropriate evaluation methods to determine the effective structural capacity of the existing pavement.

The general form of this structural deficiency approach can be written as follows:

$$SC_{overlay} = (SC_{future} - SC_{effective}) \quad \textbf{(8.1)}$$

Where:

$SC_{overlay}$	=	structural capacity of overlay;
SC_{future}	=	structural capacity of pavement for future traffic; and
$SC_{effective}$	=	effective structural capacity of existing pavement.

The structural capacity of overlay is converted to slab thickness, D, for PCC pavement, and to structural number (SN) for flexible pavement. For flexible pavements, with a known structural coefficient of AC, the overlay thickness can be determined from the SN.

Based on this principle, for the design of AC overlay of AC pavement Equation 8.2 can be used to determine pavement overlay thickness according to the AASHTO overlay design procedure. This equation was the basis for the evaluation of the GPS-6 sections.

$$D_{overlay} = \frac{SN_{overlay}}{a_{overlay}} = \frac{SN_{future} - SN_{effective}}{a_{overlay}} \quad \textbf{(8.2)}$$

Where:

$D_{overlay}$	=	thickness of AC overlay,
$SN_{overlay}$	=	structural number of AC overlay,
SN_{future}	=	pavement structural number for future traffic,
$SN_{effective}$	=	effective structural number of existing pavement, and
$a_{overlay}$	=	structural coefficient of AC overlay.

For an AC overlay of PCC pavement and an unbonded PCC overlay of PCC pavement, equations 8.3 and 8.4, respectively, are used to determine overlay thicknesses based on the AASHTO overlay design procedures. These equations were used for the evaluation of the GPS-7 and GPS-9 pavement sections.

$$D_{overlay} = A(D_{future} - D_{effective}) \quad (8.3)$$

$$D_{overlay} = \sqrt{(D^2_{future} - D^2_{effective})} \quad (8.4)$$

Where:

D_{future}	=	structural capacity of pavement for future traffic,
$D_{effective}$	=	effective structural capacity of existing pavement, and
A	=	factor to convert PCC thickness deficiency to AC overlay thickness.

Data Used for Evaluation of the Overlay Design Procedures

In all, the LTPP Data Base consists of 60 GPS-6A, 30 GPS-6B, 33 GPS-7A, 15 GPS-7B, and 28 GPS-9 pavement sections with overlays located throughout the United States and Canada. A variety of information has been collected for each section including climatic data, material properties, traffic loads, profile, and distress data. These data were to be used in the evaluation of the AASHTO overlay design procedures in this study. However, at the time of the evaluation, the overlay layer data required for this analysis were unavailable for most of the newly overlaid GPS-6B and GPS-7B sections. Similarly, some of the data required for the evaluation of the other pavement types were also not available.

In the end, only nine AC overlays of AC pavement, five AC overlays of PCC pavement, and six unbonded PCC overlays of PCC pavement sections had all the data required for the evaluation of the AASHTO overlay procedures. The input data required to compute the future and effective pavement structural capacities for these pavement sections, based on the AASHTO design procedures, were obtained from the LTPP Data Base. Each of the data elements used in the analysis of the GPS-6, GPS-7, and GPS-9 sections is described here.

Initial and Terminal Serviceability

The initial serviceability of the overlays was not available. Therefore, values of 4.2 for flexible pavements and 4.5 for rigid pavements were assumed for use in the AASHTO pavement design models for the calculation of structural capacity for future traffic. The terminal serviceability was set to 2.5 for all overlays. This value was assumed to be the serviceability at the end of the design life of the overlays.

Current Overlay Serviceability

The current overlay serviceability values used for the evaluation of the overlay design procedures were based on a recent relationship developed between the International Roughness Index (IRI) and the Present Serviceability Rating (PSR) for flexible, rigid, and composite pavement types (17). The nonlinear model shown in Equation 8.5 was found to best fit the boundary conditions and the actual data.

$$PSR = 5 * e^{(-\alpha * IRI)} \quad \textbf{(8.5)}$$

Where:

α = 0.0041 if IRI is in units of in./mi or 0.26 if IRI is in units of mm/m.

The regression analysis to develop equation 8.5 included all possible sets of data, based on different states and pavement types. It was determined that there is no significant difference between models for different pavement types.

Future 18 kips ESALs for the Design Period

The expected number of cumulative 18 kip ESALs for the design period after overlay is required for evaluating the overlay design procedures. The historical traffic data furnished initially by the SHAs were generally insufficient to estimate the cumulative ESALs since the pavement was originally opened to traffic or since the overlay was placed. Consequently, the four SHRP Regional Coordination Office (RCO) staffs went back to the SHAs and asked for their best estimates of cumulative ESALs to date for each of the GPS test sections, and these estimates became the historical traffic data available. Therefore, the research staff assumed an average simple annual growth rate for ESALs of 6 percent for all test sections. With Equation 8.6 below (based on a standard financial equation) as a basis, Equation 8.7 was developed to predict the ESALs the pavement experienced during the first year after the pavement was originally opened to traffic. Given this value and the annual growth rate of 6 percent, Equation 8.8 was used to estimate the ESALs the pavement experienced during the year it was overlaid.

$$CESAL = \sum_{t=0}^{n} \omega(1 + .06)^t \quad (8.6)$$

$$\omega = CESAL \frac{1-1.06}{1-(1.06)^{t+1}} = CESAL \frac{-.06}{1 - (1.06)^{t+1}} \quad (8.7)$$

Where:

CESAL	=	cumulative 18 kip (80kN) ESALs since pavement was originally opened to traffic,
t+1	=	years since pavement was originally opened to traffic, and
ω	=	ESALs for the first year after pavement was originally opened to traffic.

With the calculated ESALs for the first year after the original pavement was opened to pavement and a six percent annual traffic growth rate, the annual traffic for the year of the overlay was calculated using Equation 8.8 below:

$$\omega(t_{ovl}) = \omega(1.06)^{t_{ovl}} \quad (8.8)$$

Where:

$\omega(t_{ovl})$	=	annual ESALs for year of overlay, and
t_{ovl}	=	number of years of traffic up to the year of overlay.

With the ESALs for the first year after overlay known, the cumulative ESALs using a 6 percent growth rate were calculated for design periods of 5, 10, 15, and 20 years for use in the analysis.

PCC Modulus of Elasticity

The SHRP LTPP Data Base contains material testing data which includes PCC compressive strength, split cylinder tensile strength, and modulus of elasticity. The moduli of elasticity obtained from the data base were used in the analysis.

Modulus of Subgrade Reaction

Plate load-bearing tests were not conducted on the LTPP sections; therefore, measured deflections from falling weight deflectometer (FWD) testing were used to backcalculate the dynamic modulus of subgrade reaction k for all the sections (2). The dynamic k-value was reduced by a factor of two to estimate the static k-value (3). Since seasonal deflection data planned for the future were not available, no seasonal corrections to the backcalculated k-values were applied. The k-values determined were used directly in the analyses since loss of support (LOS) was set at zero, according to AASHTO recommendations.

Subgrade Resilient Modulus

Subgrade resilient modulus (M_R) values are essential in the AASHTO overlay design procedures for the calculation of structural number for future traffic (SN_f) for an AC overlay of AC pavement. The M_R values for the evaluations were based on pavement layer moduli determined from FWD data, by a backcalculation procedure. To be consistent with the laboratory-measured values used for the AASHO Road Test soil in the development of the flexible pavement design equation, the backcalculated M_R values from deflections were adjusted by multiplying each by a correction factor C = 0.33, as recommended in the 1993 AASHTO Guide, to obtain the final M_R values that were used in the evaluation of the overlay design procedures.

Effective Pavement Modulus

For design of AC overlays of AC pavements, the NDT method of calculating the effective structural number (SN_{eff}) is based on the assumption that the structural capacity of the pavement is a function of its total thickness and overall stiffness. Therefore, an effective pavement modulus, E_P, which characterizes stiffness of the pavement layer, is used in the calculation of the effective pavement structural capacity. For this analysis, a pavement layer moduli backcalculation procedure was used to compute the E_P values from deflection data. Specifically, the deflections under the FWD load plate (D_0) were used to determine the effective pavement moduli. To be consistent with the procedure for new AC overlay design described in Chapter 5, Part II of the 1993 AASHTO Design Guide, the deflections were adjusted to a reference temperature of 68°F (20°C) prior to backcalculation.

PCC Flexural Strength

One input required for the AASHTO model is the mean flexural strength value at 28 days, which is determined from a third-point loading test. Since this value is not available in the LTPP Data Base, it was estimated from splitting tensile strength, with equation 8.9 (7). Since the splitting tensile strengths in the database were not always 28 day strengths, the flexural strengths obtained had to be converted to 28 day flexural strengths.

$$S_c = 1.02\ f_t + 210 \quad (8.9)$$

Where:

f_t = splitting tensile strength of concrete, psi.

To obtain an estimate of the 28 day PCC flexural strength from the flexural strength measured at any other time, the following multiple regression equation developed in a previous study was used[8].

$$F_A = 1.22 + 0.17 \log_{10} T - .05(\log_{10} T)^2 \quad (8.10)$$

Where:

F_A = ratio of the flexural strength at time T to the flexural strength at 28 days, and

T = time since slab construction, years.

The flexural strength was then estimated at 28 days with the following equation:

$$S'_{c-28} = \left(\frac{S_c'}{F_A}\right) \quad (8.11)$$

Where:

S_c' = flexural strength at time T, and

S'_{c-28} = flexural strength at 28 days (third-point loading).

Load Transfer Coefficient, J

The deflection measurements on the test sections considered were taken after the placement of overlay; therefore, load transfer efficiency could not be calculated for the original PCC pavement. Instead, the appropriate load transfer coefficients J, based on the type of load transfer device and type of shoulders for the section, were used. Recommended load transfer coefficients for various pavements and design conditions are given in Table 2.6 of the 1993 AASHTO Design Guide. Table 8.1 shows the load transfer coefficient values used for this analysis.

Table 8.1. Load Transfer Coefficient, J

Shoulder Type		AC	Tied PCC
Pavement Type	Dowels	Load Transfer Coefficient	
JPCP	N	4.10	3.90
	Y	3.20	2.80
JRCP	N	4.10	3.90
	Y	3.20	2.90
CRCP	-	3.05	2.60

Drainage Coefficient, Cd

The environmental region in which a section is located and the quality of the drainage for the section were used to determine the drainage coefficient, Cd. Recommended values of drainage coefficients for concrete pavements are given in Table 2.5 of the 1993 AASHTO Design Guide. Tables 8.2 and 8.3 were developed based on the recommendations in the AASHTO Guide and procedures developed in Selecting AASHTO Drainage Coefficient (9), to best estimate the drainage coefficient for the sections.

Table 8.2. Drainage Coefficient for Pavements With Permeable Blanket Drains

Moisture	Wet	Dry
Type of Drains	Drainage Coefficient	
Permeable Blanket Drains	1.10	1.20
No Permeable Blanket Drains	See Table 8.2	See Table 8.3

Table 8.3. Drainage Coefficient for Pavements Without Permeable Blanket Drains

Moisture	Wet		Dry	
Type of Drains	Drainage Coefficient			
No longitudinal Drains	0.85	0.95	0.83	1.13
Longitudinal Drains	0.90	1.05	1.05	1.18

Reliability Level

As defined by the AASHTO Design Guide, reliability is the probability that a pavement structure will survive the traffic expected during the design period. The reliability levels that were used in the actual designs for each of the overlays were not available. Therefore, a sensitivity analysis was performed for the reliability levels of 50, 90, 95, and 99 percent. The actual overlay structural capacities for the pavements were compared with the overlay structural capacities calculated based on the AASHTO procedure for the different reliability levels.

AC/PCC Interface Condition

For the five GPS-7A pavements that were evaluated, deflection data were only available from measurements after overlay. For backcalculation to determine the subgrade k-value from these deflection measurements, full and continuous contact was assumed to exist between the AC overlay and the original PCC surface of these pavements.

Overall Standard Deviation

The overall standard deviation, S_o, accounts for the variability associated with design and construction, including the variability in material properties, roadbed soil properties, traffic estimates, climatic conditions, and quality of construction. Ideally, these values should be determined locally. However, in the absence of such values, values of 0.49 and 0.39 were assumed, respectively, for the flexible and rigid models used to calculate the structural capacity needed for future traffic.

Using the AASHTO Design Equations to Determine Future Structural Capacity

The current AASHTO design equations for new pavements have their roots in the original prediction equations developed at the AASHO Road Test for AC and jointed PCC pavements. These pavement design equations are used to determine SN_{future} (SN_f) for flexible pavements and D_{future} (D_f) for rigid pavements. SN_f and D_f are used to determine the overlay thickness required to satisfy the structural deficiency of an existing pavement. Therefore, any assumptions and modifications made to the AASHTO model can be important to the overlay design procedures. The procedures for using these equations are given in Part II of the AASHTO Design Guide for new pavement design. Since the AASHTO rigid and flexible design equations were examined in previous chapters of this report, they will not be repeated here.

Determination of Effective Pavement Structural Capacity

The determination of the effective structural capacity prior to overlay was required for this analysis. Since the pavements had already been overlaid before data were collected to evaluate the original pavements, this step presented a unique challenge. The procedures used to determine the effective structural capacity of the original pavements are described below.

AC Overlay of AC Pavement

For AC pavements with AC overlays, the NDT method was used to determine the effective structural capacity of the AC pavements before overlay. Since deflection data after overlay were available, these data were used to determine the effective pavement moduli for the overlaid pavement. Based on these effective pavement moduli determined by a backcalculation procedure, the effective structural number (SN_{eff}) for the pavement *with the overlay* was obtained using Equation 8.12.

$$(SN_{eff})_{w/overlay} = 0.0045 * D * \sqrt[3]{E_p} \quad \textbf{(8.12)}$$

Where:

E_p = backcalculated effective pavement modulus, psi, and
D = thickness of pavement after overlay, in.

With the actual thickness of the overlay known, the structural number for the overlay was calculated as the product of the thickness and the structural coefficient of the overlay material. This structural number of the overlay was subtracted from the effective structural number of the pavement with an overlay to obtain the effective structural number of the pavement prior to overlay. Equations 8.13 and 8.14, respectively, were used for these calculations.

$$SN_{overlay} = a_{overlay} * D_{overlay} \quad \textbf{(8.13)}$$

$$(SN_{eff})_{w/o\ overlay} = (SN_{eff})_{w/overlay} - SN_{overlay} \quad \textbf{(8.14)}$$

Where:

$a_{overlay}$ = overlay structural coefficient (0.44), and
$D_{overlay}$ = overlay thickness, in.

AC Overlay of PCC and Unbonded PCC Overlay of PCC

The condition survey method was used to determine the effective thickness of the original pavement for AC overlay of PCC pavement and unbonded PCC overlay of PCC pavement, respectively, using equations 8.15 and 8.16.

$$D_{eff} = F_{jc} * F_{dur} * F_{fat} * D \quad (8.15)$$

$$D_{eff} = F_{jcu} * D \quad (8.16)$$

Where:

F_{jc} = joint and crack adjustment factor,
F_{dur} = durability adjustment factor,
F_{fat} = fatigue and damage adjustment factor,
F_{jcu} = joint and crack adjustment factor for unbonded overlay, and
D = thickness of pavement before overlay, in.

Since the actual values of the joint and crack adjustment factor F_{jc} (or F_{jcu}), durability adjustment factor F_{dur}, and fatigue and damage adjustment factor F_{fat} were not available; mean values were used in the AASHTO overlay design procedures. A sensitivity analysis was also conducted by varying F_{dur} for AC overlay of PCC pavements and F_{jcu} for unbonded PCC overlay of PCC pavements. Table 8.4 shows the values for the condition adjustment factors used in the analysis.

Table 8.4. Pavement Condition Adjustment Factors

Pavement Condition Adjustment Factor	Range	Value Used
Joints and Cracks Adjustment Factor, Fjc	1.0 - 0.56	0.78
Durability Adjustment Factor, Fdur	1.0 - 0.8	sensitivity
Fatigue Damage Adjustment Factor, Ffat	1.0 - 0.9	0.95
Joints and Cracks Adjustment Factor, Fjcu	1.0 - 0.9	sensitivity

Evaluation of the Overlay Design Procedures

As indicated, the AASHTO overlay design procedures for AC overlay of AC pavements, AC overlay of PCC pavements, and unbonded PCC overlay of PCC pavements were evaluated in this analysis. Essentially, the evaluation comprised a determination of the required overlay structural capacity with use of the appropriate overlay design procedure and a comparison of

this structural capacity to that of the constructed overlay, with consideration given to the current condition of the overlay.

Required Overlay Thickness

In order to successfully perform the comparison, a knowledge of the specific design period and reliability level used for the design of the constructed overlay is required. This information is needed to determine the required structural capacity that has to be compared to the structural capacity of the constructed overlay. Since information on the design period and reliability level were not available in the LTPP Data Base, a sensitivity analysis was conducted which involved determining the overlay structural capacity for several combinations of design period and reliability level. Therefore, based on the appropriate 1993 AASHTO Guide design equations, the required structural capacity for future traffic, SC_f, was obtained for each selected combination of design period and reliability level for the pavement sections.

The effective structural capacity, SC_{eff}, of each pavement prior to overlay was also determined with the procedures outlined previously in this chapter. For the AC overlay of an AC pavement, a single structural capacity or structural number of the original AC pavement was determined. For the AC overlay of a PCC pavement, effective structural capacities of the original pavement were computed for three selected levels of F_{dur}. Correspondingly, for the unbonded PCC overlay of PCC pavement, effective structural capacities were also computed for three selected levels of F_{jcu}.

From these results a matrix of the required overlay structural capacities was computed for each section of the different combinations of design period and reliability level. For the AC overlay of AC pavements, overlay structural capacities were determined in terms of the structural number, as well as the thickness of overlay. For the AC overlay of PCC pavements and the unbonded PCC overlay of PCC pavements, the overlay structural capacities were determined in terms of the overlay thicknesses. The matrix for each of the pavement sections is shown in Appendix C, together with a plot of the results, as well as a summary of the information available on each section.

Evaluation Procedure

To evaluate the overlay design procedures, the required overlay structural capacities in terms of thicknesses were compared to the actual overlay structural capacities, with consideration given to the current serviceability or level of distress. However, since several required thicknesses are possible depending on the design period and reliability level selected, a careful consideration of all the information available on a section is essential before any conclusions can be made. The step-by-step procedure used for the evaluation is described below.

For each section, the constructed overlay thickness will correspond to a thickness for some combination of design period and reliability level. Higher design periods or higher reliability

levels will result in thicker pavements. To begin the evaluation, the location of the constructed overlay thickness is determined on the matrix or plot of required overlay thicknesses developed for the section. Of particular interest is the case where the constructed overlay thickness—and the equal required overlay thickness—is for a design life equal to the age of the overlay.

Where such a case existed, a review of the performance of the overlaid pavement measured at a particular point in time was then conducted to determine the adequacy of the overlay design procedure. Theoretically, an overlay designed with the AASHTO overlay design procedure for a specific design period will reach its terminal serviceability at the end of its design life. Consequently, for these cases the serviceability level of the overlaid pavement compared to the terminal serviceability will indicate the adequacy of the overlay design procedures used.

Based on this same principle, this process was used to evaluate the adequacy of the AASHTO overlay design procedures where possible by comparing the thickness and condition of the constructed overlay to the required overlay, as long as the design period was assumed to equal the age of the overlay. Table 8.5 shows the comparisons that were used for the evaluation based on this principle, as well as the conclusions to be drawn from the comparisons. In cases where information on the current serviceability was not available, an attempt was made to use the pavement's distress information to estimate the current serviceability.

Table 8.5. Approach Used to Evaluate the AASHTO Overlay Design Procedure

Comparison of the Actual Overlay Thickness with the AASHTO-designed Overlay Thickness Based on Design Life Equal to the Actual Age of the Overlay and a Specific Reliability Level	Comparison of Current Overlay Serviceability with the Terminal Serviceability	Comment on the Adequacy of the AASHTO Overlay Design Procedures
Constructed Thickness > Required AASHTO Thickness	Overlay PSR > 2.5	No Conclusion
	Overlay PSR = 2.5	Inadequate Design
	Overlay PSR < 2.5	Inadequate Design
Constructed Thickness = Required AASHTO Thickness	Overlay PSR > 2.5	Conservative Design
	Overlay PSR = 2.5	Adequate Design
	Overlay PSR < 2.5	Inadequate Design
Constructed Thickness < Required AASHTO Thickness	Overlay PSR > 2.5	Conservative Design
	Overlay PSR = 2.5	Conservative Design
	Overlay PSR < 2.5	No Conclusion

It should be noted that current serviceability is not considered the only criteria for evaluating the condition of an overlay. For example, an unbonded PCC overlay may have a low current serviceability because of joint spalling but could be structurally adequate for traffic loading. The results from the evaluations of the AASHTO overlay design procedures conducted for the available GPS-6, GPS-7, and GPS-9 sections and for the different reliability levels, determined by the evaluation process outlined above, are discussed below for each of the 500 ft (152.4 m) sections.

Evaluations for AC Overlay of AC pavement

Section 016012, Alabama

This section was overlaid in 1984 with a 1.1 in. (2.8 cm) AC layer. After 8 years the current serviceability is 3.27. Based on the AASHTO design procedure, a 3.2-in. (8.1 cm) overlay is required for the section to reach the terminal serviceability of 2.5 in 10 years at 50 percent reliability. Distress data collected in 1989 show that there were 322 ft (98.1 m) of low-severity longitudinal cracks and 3 medium- and 26 low-severity transverse cracks. Even though a thin overlay was placed, it performed very well, which suggests the adequacy of the AASHTO overlay procedure in this case.

Section 016109, Alabama

This section was overlaid with a 4 in. (10.1 cm) overlay in 1981. There was no distress after 8 years and the serviceability measured after 11 years was 4.08. This section would require a 2.6 in. (6.6 cm) overlay for a design life of 10 years at a reliability level of 50 percent, or a 5.1 in. (13 cm) overlay at a reliability level of 95 percent. Based on this information, it can be said that the AASHTO design procedure is conservative if a 95 percent reliability level is assumed. However, no conclusion can be made if a 50 percent reliability level is assumed.

Section 351002, New Mexico

The overlay on this section was placed in 1985. No distress was visible when a distress survey was done in 1989. The serviceability measured in 1991 was 4.08. According to the AASHTO overlay design procedure, the actual overlay of 3.5 in. (9 cm) should last for more than 15 years, even at 95 percent reliability. Since serviceability measurement is available only for an overlay age of 6 years, no specific conclusion can be made as to the adequacy of the design procedure at this point.

Section 356033, New Mexico

This section was overlaid with 3 in. (7.6 cm) of AC in 1981. After 8 years of service there were 304 ft (93 m) of low-severity longitudinal cracks and 16 low-severity transverse cracks on the pavement. The serviceability of the pavement after 10 years was 3.47. According to the AASHTO procedure, a 3.14 in (8 cm) overlay is required for a 20 year design life and 99 percent reliability level. Since the pavement is performing adequately after 10 years in service, no conclusion can be made at this time as to the adequacy of the overlay design procedure.

Section 356401, New Mexico

This section was overlaid in 1984 with a 3.5 in. (9 cm) thick AC overlay. A distress survey in 1989 indicated that there were only 54 ft (16.5 m) of longitudinal cracks of low severity and nine transverse cracks of low severity. The serviceability in 1991 was 4.14 after seven years of service. An overlay design based on the AASHTO procedure indicates that, even for a 50 percent reliability level, an overlay thickness of 3.7 in. (9.4 cm) should last 10 years before reaching terminal serviceability. Given the condition of the pavement in 1989 and 1991, it is highly probable that the overlay thickness of 3.5 in. (9 cm) will last for that same period. The data for this pavement, therefore, suggest that the overlay design procedure provides an adequate design.

Section 486079, Texas

This section was overlaid in 1985 with 2.5 in. (6.4 cm) of AC overlay. The distress survey conducted in 1990 indicated that the section had developed a lot of distress. There were 353 ft (107.6 m) of low-severity and 173 ft (52.7 m) of medium-severity longitudinal cracks, in addition to 9 low-, 13 medium-, and 6 high-severity transverse cracks. The serviceability measured in 1991 was 2.55, which is approximately the terminal serviceability. This section is a classic case for the evaluation of the AASHTO overlay design procedure, because it has actually reached terminal serviceability. From the design matrix for this section, it can be seen that 2.4 in. (6.1 cm) of overlay is required for a 5 year design life and 95 percent reliability, which is approximately the same thickness as the actual overlay. Hence, the data from this section suggest that the AASHTO overlay design procedures are adequate with 95 percent reliability, but inadequate with 50 percent reliability.

Section 486086, Texas

This section was overlaid with 1.5 in. (3.8 cm) of AC in 1985. The distress, measured 6 years after overlay, indicated that there were only 134 ft (40.8 m) of low-severity longitudinal cracks. The serviceability measured in the same year was 4.13. Based on the AASHTO design procedure, it was determined that no overlay is required for this section. The thin overlay may have been provided for functional reasons. Therefore, no conclusion

can be made as to the adequacy of the design procedure.

Section 486160, Texas

This section was overlaid with 1.5 in. (3.8 cm) of AC in 1981. After 8 years there were 538 sq ft (50 m^2) of low-severity alligator cracks; 13 ft (4 m) of medium- and 299 ft (91.1 m) of low-severity longitudinal cracks; 3 medium and 55 low-severity transverse cracks; and 876 sq ft (81 m^2) of bleeding area observed. The serviceability observed in 1991 was 3.06. This section had almost reached its terminal serviceability in 10 years. Based on the AASHTO procedures, this section requires at least 4 in. (10.1 cm) of overlay for a design life of 10 years at a 50 percent reliability level, or 6.7 in. (17 cm) of overlay at a 95 percent reliability level. The data observed from this section shows that a much thinner overlay lasted 10 years, which suggests that the overlay design procedure is conservative.

Section 486179, Texas

This section was overlaid in 1975 with a 5 in. (12.7 cm) AC overlay. After 15 years of service, only 80 ft (24.4 m) of longitudinal cracking and 5 ft (1.5 m) of low-severity transverse cracks were observed. The serviceability observed in 1991 was 3.81. This section has performed very well. The required overlay thickness for this section, based on the AASHTO procedure, with a 20 year design life and at a reliability level of 95 percent, would be 3.1 in. (7.9 cm). Therefore, since the overlay provided is much thicker than that required by the design procedure, no conclusion can be made about the adequacy of the design procedure.

AC Overlay of PCC Pavement

Section 87035, Colorado

This section was overlaid with 4.8 in. (12.2 cm) of AC in 1984. By 1990 12.8 ft (3.9 m) of medium-severity and 300.3 ft (91.5 m) of low-severity longitudinal reflective cracking had developed in the pavement. These numbers represent a high level of distress in the pavement in a relatively short 6 year period, which indicates an inadequate thickness may have been applied. A comparison of the overlay thickness applied to that suggested by the AASHTO overlay design procedure bears this finding out. Even for a minimum design period of 5 years and a reliability level of 50 percent, the AASHTO procedure requires a minimum thickness of 6.72 in. (17.1 cm). For this pavement, it appears that a thicker overlay in the order of the thickness required by the AASHTO overlay design procedure was needed. Overlay design procedure bears this finding out.

Section 175453, Illinois

A 2.71 in. (6.9 cm) overlay was placed on this section in 1984. After 5 years of service and over 8 million ESALs, the pavement had developed 20 ft (6.1 m) of low-severity longitudinal cracking and 912 ft (277.9 m) of low-severity longitudinal reflective cracking. This high level of distress is understandable since the AASHTO procedure requires a minimum overlay thickness of 4.57 in. (11.6 cm) for a 5 year design period and this high level of traffic, even for a 50 percent reliability level. Therefore, the AASHTO procedure appears correct in its requirement for a thicker overlay for this sample.

Section 283097, Mississippi

In 1984 a 2.73 in. (6.9 cm) overlay was placed on this section which has experienced relatively low traffic (1 million ESALs in 5 years). The AASHTO overlay design procedure suggests that, even for the high-reliability level of 99 percent, an overlay thickness of only 2.54 in. (6.5 cm) is required to meet the traffic demands for a 5 year design period. Since these thicknesses are practically equal, it is not surprising that the pavement section was showing some distress after 5 years in service with 186 ft (56.7 m) of low-severity longitudinal cracking and one high-severity transverse crack. The AASHTO overlay design procedure appeared to anticipate the actual condition after 5 years reasonably well.

Section 287012, Mississippi

This pavement section has an overlay 3.54 in. (8.9 cm) thick that was placed in 1985. In a distress survey after 4 years, two low-, five medium-, and 11 high-severity transverse reflective cracks were measured, as well as 24 ft^2 (2 m^2) of patches. The pavement had a serviceability level of 3.38 approximately two years later. For a design period of 5 years and a reliability level of 95 percent, the results obtained indicate that a thickness similar to that placed on the pavement would be required to meet traffic needs during that period. Thus, for these conditions, the AASHTO overlay design procedure provided a thickness comparable to that constructed.

Section 467049, South Dakota

This section was overlaid in 1983 with 4.49 in. (11.4 cm) of PCC. This thickness corresponds to thicknesses determined for the following combinations of design period and reliability level or higher, based on the AASHTO pavement overlay design procedure: (1) a 10 year design period and 99 percent reliability, (2) a 15 year design period and 90 percent reliability, and (3) a 20 year design period and 90 percent reliability. In a 1989 distress survey, the following distresses were measured on the pavement: (1) 475 ft (144.8 m) of low-severity longitudinal cracking, (2) six medium- and 56 low-severity transverse cracks, (3) 495 ft (150.9 m) of low-severity longitudinal reflective cracking, and (4) seven medium- and four low-severity transverse reflective cracks. These numbers represent considerable distress for the 500 ft (152.4 m) pavement section in 6 years and approach terminal

serviceability. Since the minimum design period is about 10 years for a 4.49 in. (11.4 cm) thick overlay, according to the AASHTO overlay design procedure, the procedure can be said to be inadequate in this instance.

Unbonded PCC Overlay of PCC Pavement

Section 69049, California

An unbonded PCC overlay 7.5 in. (19.1 cm) thick was placed on this pavement in 1986. After 3 years, there were several distresses manifested on the pavement. These included (1) 21 ft (6.4 m) of high-, 123 ft (37.5 m) of medium-, and 76 ft (23.2 m) of low-severity longitudinal cracking; (2) one medium-severity transverse crack; (3) 13 ft (3.9 m) of high-, 2 ft (0.61 m) of medium-, and 9 ft (2.7 m) of low-severity longitudinal joint spalling; (4) one high-, 6 medium-, and 9 low-severity transverse joint spalls; and (5) 26 sq ft (2.4 m^2) and 21 sq ft (2 m^2), respectively, of medium- and low-severity AC patches.

According to the results obtained, even at 50 percent reliability, the pavement should have lasted for at least 5 years without the provision of an overlay. Since the 7.5 in. (19.0 cm) overlay showed considerable distress after 3 years in service, in the absence of other known reasons, the AASHTO overlay design procedure can be said to be inadequate.

Section 89019, Colorado

This section with 7.9 in. (20.1 cm) of original PCC surface was overlaid with 9 in. (22.9 cm) of unbonded PCC in 1986. During a survey in 1989, the only distress noted on the pavement were transverse joints with spalling. However, there were a high number (16) of these low-severity spalls. Overlay design for the original pavement based on the AASHTO overlay design procedure indicates that a minimum of 3.4 in. (8.6 cm) of overlay should have been adequate for a 5 year design life, even at a 50 percent reliability level. This finding seems to indicate that the AASHTO overlay design procedure does not provide sufficient overlay thickness. However, it is important to note that the occurrence of joint spalls are usually associated with other design and materials features that cannot necessarily be corrected by increasing thickness.

Section 89020, Colorado

This section was overlaid with 8 in. (20.3 cm) of PCC in 1986. A survey in 1989 showed that the pavement had developed one medium-severity transverse crack and 7 ft (2.1 m) of longitudinal joint spalling. A review of the thicknesses calculated with the AASHTO overlay design procedures indicates that, for a reliability of 50 percent, a 6.11 in. (15.5 cm) thick overlay would be adequate for a 5 year design period. Because the 8 in. (20.3 cm) overlay placed does not show considerable damage, no conclusion can be made in this case about the adequacy of the overlay design procedures.

Section 269029, Michigan

This section was overlaid with 7.3 in. (18.5 cm) of PCC in 1984. A survey in 1989 showed the only distress in the pavement 5 years after overlay was 1.3 ft (0.4 m) of low-severity longitudinal joint spalling. For a design period of 5 years, and for 50, 90, 95, and 99 percent reliability, the AASHTO design procedure provides for a maximum overlay thickness of 0, 3.9 in. (9.9 cm), 4.8 in. (12.1 cm), and 6.3 in. (15.8 cm) for this section, respectively. Since the overlay thickness placed on the pavement is thicker than any of the thicknesses required by the AASHTO overlay design procedure, and the pavement is in good condition, no conclusion can be made about the adequacy of the procedure in this instance.

Section 269030, Michigan

A 6.8 in. (17.3 cm) overlay was placed on this section in 1984. This thickness corresponds to the thickness determined from the AASHTO pavement overlay design procedure for a design period of 15 years and a reliability level of 99 percent, and for a design period of 20 years and a reliability level of 95 percent. A distress survey in 1989 showed that the pavement was still performing well, having only 5.15 ft (1.6 m) of low-severity longitudinal cracking and 3.09 ft^2 (0.3 m^2) of low-severity AC patches. Based on these observations, no conclusions can be made about the adequacy of the AASHTO pavement overlay design procedure in this instance.

Section 489167, Texas

This section was overlaid with 10 in. (25.4 cm) of PCC in 1988. This thickness is higher than any thickness determined for this section based on the AASHTO pavement overlay design procedure for the combination of design periods and reliability levels investigated in this study. The thickest PCC overlay determined for a maximum design period of 20 years and a reliability level of 99 percent was 9.8 in. (24.8 cm). However, a distress survey in 1989 showed considerable distress on this 1 year old overlay—19.86 ft (6.1 m) of low-severity longitudinal joint spalling and 11 transverse joints with low-severity spalls. Since joint spalls are more related to materials and construction, the information on this section cannot be used to determine the adequacy of the AASHTO overlay design procedure.

Summary and Conclusions

LTPP data from GPS-6A, GPS 6-B, GPS-7A, GPS-7B, and GPS-9 were used to evaluate the 1993 version of the AASHTO overlay design equations. While data on design life and levels of reliability sought were not available, a limited set of test sections were identified that had sufficient data to support limited evaluations. Even for these test sections, it was necessary to use existing data to estimate values for some of the inputs to the design equations. The procedures used for estimating specific input values are described.

The design equations were then used to predict the overlay thicknesses required, and these thicknesses were compared with the thicknesses of the overlays actually constructed. The results from recent profile measurements and distress surveys were also used to evaluate the adequacy of the AASHTO design equation for establishing an appropriate design overlay thickness. A summary of the results from these comparative evaluations appears in Table 8.6.

Although these evaluations are seriously constrained by data limitations, the equation for this small data set of 5 test sections appears to work quite well for AC overlays of PCC. The evaluations were generally inconclusive for AC overlays of AC and unbonded PCC overlays of PCC.

It is hoped that data regarding design periods and levels of reliability used for the design of overlays to be used for comparative evaluations will be available in the future. Conclusive evaluations are probably not possible without this information because the comparisons should be made on the same design basis.

Table 8.6. Results from Comparative Evaluations of 1993 AASHTO Overlay Equations

Test Section Number	Type of Pavement	Results From Comparisons			
		Conservative	Adequate	Inadequate	Inconclusive
016012	AC/AC		X		
016109	"				X
351002	"				X
356033	"				X
356401	"		X		
486079	"		@95%		
486086	"		Reliability		X
486160	"	X			
486179	"				X
Subtotals for AC/AC:		1	3	0	5
087035	AC/PCC		X		
175453	"		X		
283097	"		X		
287012	"		X		
467049	"			X	
Subtotals for AC/PCC:		0	4	1	0
69049	PCC/PCC			X	
89019	"				X
89020	"				X
269029	"				X
269030	"				X
489167	"				X
Subtotals for PCC/PCC:		0	0	1	5
Overall Subtotals:		1	7	2	10

9

Conclusions

One of the primary objectives of the Strategic Highway Research Program (SHRP) Long-Term Pavement Performance (LTPP) effort is to evaluate existing pavement design methodologies. With the pavement design guidelines developed from the American Association of State Highway Officials (AASHO) Road Test being the most commonly accepted design procedure utilized by State Highway Agencies (SHAs) to date, the American Association of State Highway and Transportation Officials (AASHTO) pavement design equation represented an excellent starting point for early analyses of the SHRP LTPP data base.

Taking into account the fact that rigid and flexible pavements have unique performance characteristics and, in turn, the design equations are unique, the evaluation of AASHTO flexible and rigid pavement equations were addressed separately. Although there are some similarities in the conclusions reached from evaluations of these two design equations, the conclusions will be discussed separately here to maintain the distinctions between the pavement types.

As part of this study, the new AASHTO pavement overlay design procedures were also evaluated. These overlay design procedures were recently introduced in the 1993 AASHTO Design Guide. The conclusions reached from the evaluation of the AASHTO overlay design procedures are also discussed.

Conclusions from the Evaluation of the AASHTO Flexible Pavement Design Equation

With data from 244 General Pavement Studies (GPS)-1 and GPS-2 in-service flexible pavement test sections across the country, the LTPP Data Base offers an unprecedented opportunity for evaluating the ways in which flexible pavements are designed and their associated performance. In these early analyses of the SHRP LTPP Data Base, all efforts were concentrated on evaluating the AASHTO pavement design equation and the suitability

of the data collected from these test sections for use in such evaluations.

From these evaluations, it has been established that the existing AASHTO flexible pavement design equation does not currently predict the pavement performance of the SHRP LTPP test sections very accurately, and, unfortunately, generally predicts many more equivalent single axle loads (ESALs) needed to cause a measured loss of Present Serviceability Index (PSI) than the pavements had actually experienced. Many explanations have been identified. Although modifications have been made over the years to expand the inference space of these design equations, any such modifications cannot be without their own limitations. From the studies conducted here, it is evident that environmental properties such as rainfall, freezing index, and freeze-thaw cycles have a greater impact on pavement performance than that accommodated by the AASHTO flexible pavement design equation.

Similarly, although modifications were made to accommodate the subgrade resilient moduli value in the flexible pavement design equation, these modifications were based on the subgrade resilient modulus measured in the laboratory at the AASHO Road Test (3,000 psi). There is little similarity, however, between the subgrade properties measured as part of the SHRP LTPP program (both laboratory and backcalculated subgrade moduli) and the 3,000 psi value measured at the Road Test. This finding appears to reflect changes in techniques for measurement of subgrade moduli since the Road Test.

The use of the composite PSI also presents some limitations in the use of the AASHTO equation. With composite indices of this type, where all distresses are lumped together, it is difficult to adequately assess to what a change in performance is attributed. That is to say, one cannot tell if the pavement is deteriorating as a result of increased rutting, increased roughness, one of the other distresses that may be present, or some combination of all of the above. This, in turn, makes it difficult to clarify what the cause(s) for this change in performance might be. For the PSI equation in particular, change in performance is very closely associated with roughness. Cracking and patching in the flexible PSI equation have little if any impact on the associated changes in performance.

Similarly, by lumping all the structural properties together, the contribution each specific layer makes to the performance of the pavement structure is also masked. It quickly becomes evident, when comparing the performance of these test sections versus their predicted performance, that one in. of asphalt will not always be equivalent to 3.1 in. of granular base, as the structural number concept would dictate. This relationship will naturally vary, depending on the structural properties of the other layers incorporated in the pavement, the environmental conditions in which the pavement is situated and numerous other factors.

It should be noted that all these conclusions are based on the data currently available for analysis. At the time of these studies, only half the laboratory subgrade moduli tests had been completed. Few of the test sections exhibited a serious loss in PSI, typically displayed a PSI loss less than 0.5. Also, only one round of monitoring data was available for consideration. Despite these limitations, the shortcomings of the AASHTO flexible pavement design equation are sufficiently apparent so that the causes can readily be discerned.

Another observation from these studies is that the 2.5 PSI level, generally considered to represent failure at the Road Test, does not really represent highway practice. It appears from the data that those individuals making maintenance and rehabilitation decisions generally do not allow deterioration to an extent that would result in a 2.5 PSI.

Conclusions from the Evaluation of the AASHTO Rigid Pavement Design Equation

Since the development of the original AASHTO pavement design equation in 1960, following the AASHO Road Test, several changes have been made to the model to improve it. These changes have included the addition of a number of calibration parameters to extend the equation outside of its original inference space. The SHRP LTPP data offered a unique opportunity to evaluate the equation with data from in-service pavements, under diverse traffic and environmental conditions to determine its adequacy. In all, data from 54 jointed plain concrete pavement (JPCP), 34 jointed reinforced concrete pavement (JRCP), and 32 continuously reinforced concrete pavement (CRCP) in-service test sections were available for the evaluation, and the results obtained provide some valuable insights into the adequacy of the AASHTO rigid pavement design equation.

Overall, the results obtained were mixed. An evaluation of the original 1960 AASHTO rigid pavement design equation conducted to provide a benchmark to compare the evaluation of the current 1993 equation proved that the original equation does not accurately predict cumulative ESALs. In all cases, for the two rigid pavement types that the original equation applied to (JPCP and JRCP), the equation overpredicted cumulative ESALs. This finding means that the original AASHTO equation overestimates the traffic loadings required to cause a given drop in the serviceability of a pavement. In fact, 34 out of the 54 JPCP sections and 23 out of the 34 JRCP sections used in this evaluation had ratios of predicted ESALs to actual ESALs in excess of two. This ratio was approximately 10 for 6 of the JPCP and 6 of the JRCP test sections.

The results were also mixed when the original equation was evaluated with the data divided into four groups on the basis of four U.S. environmental regions. The original AASHTO equation proved inadequate for JPCP design in the wet-freeze region (the location of the AASHO Road Test), but was statistically an unbiased predictor of ESALs in the other environmental regions. For JRCP, the original equation was statistically an unbiased predictor of ESALs only in the wet-no freeze region, and was found to be an inadequate predictor of performance in the other three regions. Together, these results lead to the conclusion that the original AASHTO equation is not a good predictor of pavement performance.

The evaluation of the 1993 model provided significantly better results. For the JPCP, JRCP, and CRCP sections evaluated, the results obtained indicate that the current 1993 AASHTO rigid pavement design equation appears to provide more or less unbiased predictions in that the plots of predicted to actual KESALs seem to center on the lines of equality. This finding was true in all cases when the sections for each of the pavement

types were evaluated together, as well as when they were divided into groups based on the four environmental regions of the United States (Table 6.3).

These results initially provided some optimism about the adequacy of the current 1993 AASHTO rigid pavement design equation. However, a closer examination of the results indicated that the scatter was major when viewed arithmetically, instead of in the log-log plots necessary to include all the points. A look at the ratios of predicted ESALs to actual ESALs indicated that 14 out of the 54 JPCPs, 19 out of the 34 JRCPs, and 14 out of the 32 CRCPs still had ratios in excess of two. That is, for 14 JRCPs, 19 CRCPs and 14 CRCPs, the 1993 AASHTO still predicted more than twice the ESALs or traffic loading required to cause a given loss in serviceability. This ratio was approximately 10 for 4 of the JPCP, 5 of the JRCP, and 5 of the CRCP sections.

A sensitivity analysis, conducted to determine how a change in initial serviceability used for the evaluation would affect these results, further reinforced the need for the initial results to be viewed with some caution. An average initial PSI value of 4.25 had been used in the evaluation. When this was changed to 4.5, the value assumed in the original 1960 AASHTO equation, the 1993 AASHTO model overpredicted the number of cumulative ESALs for each of the three pavement types for evaluations with all the data available (Table 6.4).

For evaluations on an environmental regional basis the JPCP model appeared to be an unbiased predictor for all four regions. The model was also an unbiased predictor for the wet-freeze and dry-freeze regions for JRCP (there were no data for the dry-no freeze region). For CRCP, the dry-no freeze region was the only environmental region for which the model was not an unbiased predictor.

These mixed results indicate a need for enhancements to the current AASHTO rigid pavement design equation to improve predictions if design is to continue to be based on serviceability loss. However, distress prediction models were provided for preliminary development of a new methodology recommended for future use. This methodology involves the use of predictive equations for distress and International Roughness Index (IRI) in lieu of the current design model. Because they are preliminary, they are only recommended as design checks to other design procedures at this time. Although the IRI and distress models provided are preliminary in nature, an example given on how they can be used to evaluate or develop pavement design illustrates their applicability.

Conclusions from the Evaluation of the AASHTO Overlay Design Procedures

The overlay design procedures included in the 1993 AASHTO Guide have never been evaluated. This study provided an opportunity for limited evaluation of the procedures with data from the overlaid GPS sections in the SHRP LTPP program. The evaluations were conducted by comparing designs obtained with the procedures to the overlay thicknesses placed, with consideration given to the serviceability and/or state of distress of the overlaid

pavements.

Only limited conclusions were obtained from these evaluations because of a lack of data. Much of the information on the pavements prior to overlay, which was required for a thorough evaluation, could not be obtained. This information included the condition of the pavements prior to overlay and the reliability level and design period ESALs. In addition, the design procedures actually used to design the overlays were not known. As a result, a number of assumptions had to be made and existing data were used to estimate the other inputs required for the evaluations.

In spite of these drawbacks, the evaluation provided a first opportunity for an extensive use of the overlay design procedures. For the small data set available for this study, the results indicated that the overlay design procedures appear to work well for AC overlay of PCC but were inconclusive for AC overlays of AC and unbonded PCC overlays of PCC. Further evaluations will be necessary in order to reach final conclusions on the adequacy of overlay design procedures.

Recommendations for Future Research

With the limited performance data available for these studies, one must be cautious when using the equations established from these early analyses. Based on the conclusions noted above, several data elements warrant further evaluation and consideration for incorporation in future pavement design equations. Similarly, there is a need for additional sections to address gaps noted in the overall sampling plans and/or biases identified during analysis.

Differences in the laboratory and backcalculated subgrade moduli noted in these analyses indicate that either some relationship needs to be established between the two or separate design equations need to be established based on the source of subgrade moduli values utilized in design. As a minimum, future pavement design must incorporate subgrade moduli values more consistent with those generated by contemporary testing methods and representative of the subgrades across North America. Incorporation of environmental properties should also be studied further to establish how best to accommodate these values and their effects on pavement performance.

In the evaluation of the AASHTO rigid pavement design equation, a need for improved guidance on the determination of the inputs necessary for the use of the equation also became evident. A number of the specific factors on which further guidance is required are as follows:

- Drainage coefficient, C_d — Improved guidelines for this factor are required because the current ones are very subjective. These guidelines must recognize that a C_d of 1 represents the poorly drained Road Test pavement in a wet-freeze zone.

- Effective k-value — The procedures for determination of the effective k-value need improvement, especially as to loss of support (LOS).

- Pavement type — The model should consider each of the three pavement types separately and not lump them together.

- Load transfer factor (J) — This factor actually adjusts only for slab corner cracking (stress difference due to protected and unprotected corners). The J factor does not adjust for the effect of load transfer on faulting and erosion. A new factor is needed that will consider doweled versus nondoweled pavements and the diameter and spacing of the dowels.

- Reinforcement effects — A new factor is needed to consider the effects of slab reinforcement, which is not directly considered in the AASHTO model but significantly affects performance for JRCP and CRCP.

- Climate effects — The current AASHTO design model does not seem to provide for an overall factor to accurately adjust for the different climates. Factors such as freeze-thaw (and corrosion from deicing salts) are not considered, which leads to different results in different environmental regions.

It is also recommended that future design equations be structured so that individual layers and their associated properties can be distinguished in the design process. Similarly, future pavement design analysis should provide the ability to consider the specific distresses of concern separately, rather than with composite indices. With modern computer technology and the growing knowledge of how various distress mechanisms manifest themselves, these more detailed analyses will not only become more critical, but considerably less complicated.

Finally, because the current data base is heavily biased toward pavements with coarse subgrades, in order to adequately assess the effects of subgrade soil volume changes, additional test sections with fine-grained subgrades should be sought. In order to effectively evaluate these effects, it may also be necessary to include additional data such as swell rates or heave potential.

References

1. AASHTO Guide for Design of Pavement Structures, AASHTO Task Force on Pavements, Washington, D.C., 1986.

2. The AASHO Road Test, Report 5, Pavement Research, HRB Special Report 61E, National Research Council, Washington, D.C., 1962.

3. McCullough, B. F., C. J. Van Til, and R. G. Hicks. Evaluation of AASHTO Interim Guides for Design of Pavement Structures, NCHRP Report 128, Washington, D.C., 1972.

4. AASHTO Interim Guide for Design of Pavement Structures 1972. AASHTO Subcommittee on Roadway Design, Washington, D.C., revised 1981.

5. Carey, W. N. and P. E. Irick. The Pavement Serviceability Performance Concept. *Highway Research Board Bulletin No. 250.* 1960.

6. Hall, K. T. Backcalculation Solutions for Concrete Pavement. SHRP Long-Term Pavement Performance Data Analysis, Technical Memorandum, May 1992.

7. Foxworthy, P. T. Concepts for the Development of a Nondestructive Testing and Evaluation System for Rigid Airfield Pavements. Ph.D. thesis, University of Illinois at Urbana-Champaign, 1985.

8. Darter, M. I. Design for Zero-Maintenance Plain Jointed Concrete Pavement-Final Report, Report FHWA-RD-77-111, FHWA. U.S. Department of Transportation, Washington, D.C., June 1977.

9. Carpenter, S. H. Selecting AASHTO Drainage Coefficient. Presented at the 67th annual meeting of the Transportation Research Board, January 1989.

10. The AASHTO Road Test, Proceedings of a Conference Held May 16-18, 1962, St. Louis, Mo. HRB Special Report 73, National Research Council, Washington, D.C., 1962.

11. Monismith, C. L., Analytically Based Asphalt Pavement Design and Rehabilitation Theory to Practice, 1962-1992, Transportation Research Record 1354. TRB, National Research Council, Washington, D.C., 1992.

12. *AASHTO Guide for Design of Pavement Structures, 1993.* American Association of State Highway and Transportation Officials. Washington, D.C., 1993.

13. *Microsoft EXCEL™ Version 4.0 User's Guide.* Microsoft Corporation, Redmond, WA, 1992.

14. Darter, M. I., J. M. Becker, M. B. Snyder and R. E. Smith. Portland Cement Concrete Pavement Evaluation System-COPES, NCHRP Report No. 277, Transportation Research Board, Washington, D.C., 1985.

15. Smith, K. D., D. G. Peshkin, M. I. Darter, A. L. Mueller, S. H. Carpenter. Performance of Jointed Concrete Pavements, FHWA-RD-89-136. Federal Highway Administration, Washington D.C., 1990.

16. Lee, Ying-haur and M. I. Darter. Mechanistic Design Models of Loading and Curling in Concrete Pavements, *Proceedings: ASCE Airfield Pavement Specialty Conference.* American Society of Civil Engineers, Vicksburg, Miss., 1993.

17. Al-Omari, Bashar and M. I. Darter, *Relationships Between IRI and PSR*, Transportation Engineering Series No. 69, University of Illinois, Urbana, Ill., 1992.

Appendix A

Sections and Corresponding Data Utilized in Evaluation of the AASHTO Flexible Pavement Equation

Sections and Corresponding Data Utilized in Evaluation of the AASHTO Flexible Pavement Equation

(1) RAIN = AVERAGE ANNUAL RAINFALL
(2) AVG32 = AVERAGE ANNUAL NUMBER OF DAYS BELOW 32 F (0 C)
(3) CALC PSI = 5.03-1.91*LOG(1+AVG SV)-1.38*(AVG RD^2)
(4) OBS PSI LOSS = INIT. PSI. - CALC. PSI

						(1)	(2)		PSI CALCULATIONS:				(3)		(4)	TRAFFIC		
	SHRP ID	EXP	ENV	THAW	FTIN	RAIN	AVG32	DATE OPEN	PROFILE DATE	AVG SV	DATE RUTS MEASURED	AVG RD	CALC. PSI	INIT PSI	OBS PSI LOSS	KESAL /YEAR	TRUCK FACTOR	CUMUL KESAL
AL	11001	1	WNF	42	28	49.8	38	Oct-80	04/03/92	1.74	04/05/89	0.22	4.13	4.4	0.30	174	0.84	2002
AL	11011	2	WNF	70	124	54.3	69	Jun-85	02/11/92	2.60	01/10/90	0.15	3.94	4.2	0.26	64	0.88	430
AL	11019	1	WNF	28	10	63.0	25	Oct-86	07/11/91	3.15	05/15/89	0.36	3.67	4.2	0.53	122	0.83	582
AL	11021	1	WNF	45	22	53.5	39	Jun-85	04/03/92	1.95	04/05/89	0.20	4.08	4.5	0.42	91	0.83	621
AL	14072	2	WNF	24	26	52.5	20	Mar-89	01/29/92	2.05	12/16/89	0.11	4.09	4.2	0.11	111	0.83	324
AL	14073	2	WNF	72	97	66.1	72	Jun-88	04/15/92	5.60	01/10/90	0.10	3.45	4.2	0.74	167	0.84	645
AL	14125	1	WNF	41	20	56.4	38	Jun-72	06/07/90	1.56	02/12/91	0.30	4.13	4.3	0.19	189	0.83	3412
AL	14126	1	WNF	68	93	63.4	65	Jun-88	02/10/92	1.77	06/05/89	0.11	4.17	4.2	0.03	657	0.78	2428
AZ	41001	1	DNF	12	0	9.5	8	Sep-78	03/24/90	3.40	11/20/89	0.81	2.90	4.3	1.37	1923	3.23	22240
AZ	41002	1	DNF	157	97	14.4	149	Feb-80	04/04/90	7.15	11/03/89	0.27	3.19	4.1	0.95	1013	3.24	10310
AZ	41003	1	DNF	15	0	7.7	12	Aug-75	03/25/90	2.22	11/20/89	0.29	3.94	4.4	0.50	1388	3.23	20351
AZ	41006	1	DNF	15	0	8.4	12	Sep-78	03/24/90	2.13	11/20/89	0.20	4.03	4.4	0.38	1624	3.17	18779
AZ	41007	1	DNF	14	0	9.0	11	Sep-78	03/24/90	4.94	11/20/89	0.61	3.04	4	0.97	1787	3.23	20671
AZ	41015	1	DNF	56	3	17.9	47	Jun-79	03/17/90	2.14	11/30/89	0.38	3.88	4.4	0.43	860	12.88	9291
AZ	41017	1	DNF	41	4	21.9	34	Aug-76	03/19/90	2.48	11/30/89	0.26	3.90	4.5	0.64	1007	9.69	13740
AZ	41018	1	DNF	28	4	22.6	22	Aug-76	03/19/90	2.89	11/30/89	0.26	3.81	4.6	0.79	1166	12.74	15902
AZ	41021	1	DNF	53	21	10.9	44	Jun-79	03/30/90	2.85	11/03/89	0.52	3.54	3.9	0.31	1005	2.98	10885
AZ	41022	1	DNF	73	41	11.7	64	Jun-79	03/30/90	0.92	11/03/89	0.51	4.13	4.3	0.19	110	4.68	1194
AZ	41024	1	DNF	147	117	13.9	139	Jun-79	04/03/90	3.58	11/03/89	0.16	3.73	4.1	0.39	1012	3.17	10980
AZ	41025	1	DNF	150	116	14.5	142	Oct-78	04/03/90	4.27	01/09/91	0.16	3.62	3.8	0.20	995	3.24	11456
AZ	41034	1	DNF	7	0	5.3	5	Jul-75	03/26/90	3.26	11/20/89	0.31	3.69	4.3	0.63	559	5.53	8246
AZ	41037	1	DNF	7	0	5.1	5	Jun-85	03/27/90	4.95	11/03/89	0.10	3.54	3.9	0.32	545	9.39	2628
AZ	41062	2	DNF	158	103	14.8	150	Jun-79	04/02/90	7.75	11/03/89	0.14	3.20	3.8	0.59	1001		10853
AZ	41065	2	DNF	136	60	14.1	128	Jun-79	04/02/90	4.26	11/03/89	0.21	3.59	3.9	0.26	992	4.70	10755
AR	52042	2	WNF	69	79	59.8	65	Dec-72	12/11/91	13.12	11/16/89	0.29	2.72	4.7	1.97	70	1.04	1330
AR	53048	2	WNF	45	122	54.9	47	Sep-83	12/10/91	10.54	11/16/89	0.12	2.98	4.7	1.70	35	1.47	291
AR	53071	2	WNF	79	297	46.8	87	Feb-88	08/30/90	1.09	03/15/89	0.14	4.39	4.7	0.29	464	1.62	1196
CA	62002	2	DF	156	143	20.4	146	Dec-80	05/11/91	4.88	09/07/89	0.26	3.47	4.1	0.61	94	0.49	982
CA	62004	2	DNF	11	0	12.5	9	Oct-76	02/20/91	6.29	11/19/89	0.16	3.35	4.1	0.79	628	1.75	9047
CA	62038	2	WNF	10	1	71.3	6	Sep-72	02/11/91	2.59	08/23/89	0.12	3.95	4.3	0.35	161	2.00	2963
CA	62041	2	WNF	14	1	48.0	10	Jul-71	02/11/91	3.34	08/23/89	0.19	3.76	4.3	0.54	211	2.00	4140
CA	62051	2	DNF	18	1	26.5	12	Feb-81	05/04/91	2.07	08/30/89	0.17	4.06	4.1	0.00	266	1.02	2731
CA	62053	2	DNF	22	0	24.6	16	Jun-73	05/03/91	3.62	08/24/89	0.24	3.68	4.3	0.62	588	5.80	10552
CA	62647	2	DNF	54	2	27.0	45	Sep-76	05/02/91	1.99	08/28/89	0.15	4.09	4.3	0.20	914	6.80	13417
CA	67452	2	WNF	68	4	33.0	59	Jun-72	05/04/91	3.60	08/24/89	0.15	3.73	4.3	0.56	18	0.29	332
CA	67491	2	DNF	4	0	5.9	3	Aug-67	03/13/91	9.04	11/12/89	0.21	3.06	4.3	1.24	627	1.93	14817
CA	68151	2	DNF	22	12	12.8	18	Jun-73	01/25/90	1.77	11/12/89	0.22	4.12	4.3	0.18	708	1.82	11803
CA	68153	1	DNF	3	0	18.8	2	Aug-77	02/14/91	5.04	11/16/89	0.16	3.50	4.3	0.30	48	0.49	644
CA	68156	1	DNF	13	0	15.8	9	Sep-74	02/14/91	4.40	11/16/89	0.14	3.60	4.3	0.70	55	1.01	909
CO	81029	1	DF	178	1395	14.7	209	Jun-72	10/29/91	10.51	10/20/89	0.19	2.95	4.2	1.23	22	0.76	422
CO	81047	1	DF	128	1218	11.5	163	Oct-83	04/13/90	3.72	10/20/89	0.24	3.66	4.2	0.54	37	0.58	242
CO	81053	1	DF	146	464	10.0	150	Nov-84	10/27/91	1.86	10/19/89	0.26	4.06	4.2	0.12	59	0.56	415
CO	82008	2	DF	136	471	12.0	146	Oct-72	11/14/91	3.98	10/17/89	0.42	3.45	4.2	0.60	69	0.74	1321
CT	91803	1	WF	90	399	49.6	103	Jul-85	07/26/91	5.86	07/31/89	0.11	3.42	4.2	0.78	26	0.65	157
DL	101450	2	WF	77	241	44.2	83	Jun-76	03/27/90	6.38	10/05/89	0.13	3.35	4.2	0.84	371	1.60	5127
FL	121030	1	WNF	1	0	55.5	1	Jun-71	07/12/90	2.99	04/18/89	0.19	3.83	4.4	0.57	427	1.05	8167
FL	121060	1	WNF	1	0	56.5	0	Dec-79	07/06/90	1.29	04/18/89	0.11	4.33	4.4	0.07	208	1.05	2210
FL	123996	1	WNF	13	2	54.9	11	Jun-74	07/02/90	3.50	04/17/89	0.18	3.74	4.2	0.46	133	1.05	2141
FL	124097	2	WNF	32	14	57.9	29	Nov-85	06/12/90	1.07	04/28/89	0.17	4.39	4.4	0.01	524	1.06	2416
FL	124105	1	WNF	10	4	46.2	7	Dec-84	06/20/90	1.79	04/12/89	0.26	4.08	4.3	0.22	115	1.05	639
FL	124107	1	WNF	2	0	47.7	2	Jan-85	07/12/90	2.42	12/06/89	0.13	3.99	4.4	0.41	103	1.05	568
FL	124154	1	WNF	6	0	5.1	5	Jun-70	07/04/91	7.15	12/09/89	0.24	3.21	4.4	1.19	144	1.05	3039
GA	131001	1	WNF	49	26	44.4	41	Sep-86	05/22/92	2.07	03/20/89	0.17	4.06	4.3	0.19	101	0.94	578
GA	131004	1	WNF	54	47	44.7	49	Jun-83	05/26/92	1.41	01/08/90	0.08	4.29	4.4	0.10	35	0.61	315
GA	131005	1	WNF	37	11	41.3	32	Jun-86	05/27/92	1.99	01/08/90	0.1	4.11	4.3	0.20	173	1.06	1034
GA	131031	1	WNF	74	91	59.8	69	Jun-81	05/20/92	1.55	01/09/90	0.3	4.15	4.2	0.01	58	0.84	637
GA	134096	2	WNF	32	12	49.1	28	Jun-85	06/13/90	3.07	05/10/89	0.07	3.86	4.2	0.34	12	0.65	62
GA	134420	2	WNF	21	7	46.9	18	Apr-84	07/17/90	3.08	04/11/89	0.22	3.80	4.2	0.40	209	1.06	1316

(1) RAIN = AVERAGE ANNUAL RAINFALL
(2) AVG32 = AVERAGE ANNUAL NUMBER OF DAYS BELOW 32 F (0 C)
(3) CALC PSI = 5.03-1.91*LOG(1+AVG SV)-1.38*(AVG RD^2)
(4) OBS PSI LOSS = INIT. PSI. - CALC. PSI

	SHRP ID	EXP	ENV	THAW	FTIN	(1) RAIN	(2) AVG32	DATE OPEN	PSI CALCULATIONS: PROFILE DATE	AVG SV	DATE RUTS MEASURED	AVG RD	(3) CALC PSI	INIT PSI	(4) OBS PSI LOSS	TRAFFIC KESAL /YEAR	TRUCK FACTOR	CUMUL KESAL
ID	161001	1	DF	116	399	26.4	125	Aug-73	11/30/90	2.52	07/17/89	0.18	3.94	4.2	0.26	100	1.04	1727
ID	161005	1	DF	125	923	19.4	152	Aug-75	11/13/90	3.95	09/19/89	0.19	3.65	4.2	0.54	31	1.10	478
ID	161007	1	DF	131	585	10.5	146	Jun-72	10/01/90	2.76	09/20/89	0.24	3.85	4.2	0.35	38	0.53	695
ID	161009	1	DF	139	701	10.2	158	Oct-74	10/02/90	7.00	09/20/89	0.25	3.22	4.2	0.97	117	0.93	1880
ID	161010	1	DF	138	1278	11.9	186	Oct-69	10/05/90	7.21	09/21/89	0.09	3.27	4.2	0.93	76	0.91	1593
ID	161021	1	DF	128	1347	10.9	181	Oct-85	10/05/90	2.62	09/21/89	0.12	3.94	4.2	0.26	105	0.89	526
ID	169032	1	WF	99	461	27.9	117	Oct-87	12/01/90	4.30	07/17/89	0.13	3.62	4.2	0.57	66	1.09	210
ID	169034	1	WF	119	548	31.7	134	Oct-88	11/30/90	4.79	07/17/89	0.05	3.57	4.2	0.63	144	1.10	312
IL	171002	1	WF	108	1065	30.2	153	Jan-86	06/12/90	2.60	09/11/89	0.12	3.95	4.5	0.56	49	0.55	217
IL	171003	1	WF	88	336	40.3	97	Oct-86	03/21/90	1.84	06/23/89	0.12	4.15	4.5	0.30	32	0.40	109
IN	181037	1	WF	72	300	47.6	82	Jan-83	06/12/91	13.18	05/09/91	0.36	2.65	4.2	1.52	83	1.22	701
IN	182008	2	WF	86	773	37.5	123	Jan-80	09/11/91	6.58	10/13/90	0.35	3.18	4.2	0.96	1211	3.59	14173
IA	191044	1	WF	94	1479	33.5	153	Jul-71	05/13/92	12.83	09/21/89	0.10	2.84	4.2	1.27	104	1.13	2168
IA	196150	2	WF	96	1304	30.5	149	Aug-52	06/17/90	4.82	06/01/90	0.25	3.48	4.2	0.64	7	0.28	248
KS	201005	1	DF	82	530	39.3	101	Nov-72	04/10/90	11.50	03/10/89	0.16	2.90	4.2	1.08	38	0.72	668
KS	201006	1	DF					Nov-71	04/19/92	5.06	03/14/89	0.16	3.50	4.2	0.70	62	0.81	1267
KS	201009	1	DF	89	378	26.1	99	Jan-85	04/18/92	6.27	05/02/89	0.20	3.33	4.2	0.87	66	0.80	481
KY	211010	1	WF	109	307	48.9	116	Jan-85	12/05/89	3.90	10/27/89	0.20	3.66	4.2	0.52	18	1.07	86
KY	211014	1	WF	96	225	45.5	99	Jan-84	01/11/91	6.46	10/17/89	0.18	3.32	3.5	0.18	378	5.20	2661
KY	211034	1	WF	72	287	54.7	81	Jan-72	12/04/89	4.17	11/05/89	0.25	3.58	4.2	0.58	24	0.57	433
ME	231001	1	WF	108	1534	44.2	170	Nov-72	08/17/91	10.96	08/11/89	0.31	2.84	4.5	1.66	158	1.14	2973
ME	231009	1	WF	95	1023	47.1	140	Sep-70	08/15/91	3.95	08/10/89	0.20	3.65	4.5	0.85	145	1.14	3033
ME	231012	1	WF	107	981	44.4	146	Nov-85	08/14/91	2.77	08/10/89	0.23	3.86	4.5	0.64	599	1.14	3464
ME	231026	1	WF	117	1522	45.5	172	Jul-73	08/16/91	6.66	08/18/89	0.40	3.12	4.5	1.37	79	1.14	1431
ME	231028	1	WF	108	1585	44.8	171	Nov-72	08/16/91	8.03	08/18/89	0.31	3.07	4.5	1.43	133	1.14	2500
MD	241632	2	WF	67	152	42.5	71	Aug-87	04/08/91	2.95	10/22/89	0.13	3.87	4.2	0.33	93	1.12	341
MD	241634	2	WF	76	185	44.7	78	Jun-76	06/19/91	2.87	10/12/89	0.19	3.86	4.2	0.34	66	1.01	919
MD	242401	2	WF	101	229	52.8	104	Nov-87	08/10/91	2.08	10/11/89	0.11	4.08	4.2	0.10	50	0.47	188
MD	242805	2	WF	86	217	38.1	89	Oct-86	08/10/91	4.43	10/11/89	0.19	3.58	4.2	0.62	1058	1.19	5140
MA	251002	1	WF	112	633	46.3	133	Sep-82	07/28/91	5.23	08/02/89	0.15	3.48	4.5	1.02	160	1.00	1423
MA	251003	1	WF	105	625	47.4	128	Sep-74	07/27/91	22.80	08/04/89	0.13	2.38	4.5	2.12	39	0.99	664
MA	251004	1	WF	73	395	50.0	88	Nov-74	07/26/91	2.60	08/04/89	0.19	3.92	4.5	0.57	185	1.00	3094
MI	261001	1	WF	111	1392	31.0	172	Sep-71	01/09/90	3.72	09/07/89	0.14	3.72	4.2	0.48	16	0.75	296
MI	261004	1	WF	82	1758	36.2	170	Jul-85	12/02/90	5.91	09/13/89	0.11	3.41	4.2	0.79	48	0.68	260
MI	261010	1	WF	91	978	32.4	137	Aug-75	11/29/89	2.42	09/05/89	0.23	3.94	4.2	0.22	123	0.90	1768
MI	261013	1	WF	106	1010	35.1	153	Jan-80	10/09/89	4.60	09/26/89	0.13	3.58	4.2	0.62	146	1.00	1426
MN	271016	1	WF	83	2731	24.5	182	Jan-76	10/26/89	11.02	06/22/89	0.21	2.91	4.2	1.29	20	0.73	278
MN	271018	1	WF	96	2000	26.8	170	Jan-79	08/08/91	23.18	06/22/89	0.18	2.34	4.2	1.85	55	0.91	692
MN	271019	1	WF	104	1919	30.3	173	Jan-80	05/22/90	8.29	06/20/89	0.22	3.11	4.2	1.08	39	0.75	400
MN	271023	1	WF	91	2624	25.9	184	Jan-82	05/23/90	14.63	06/22/89	0.20	2.69	4.2	1.50	124	1.21	1038
MN	271028	1	WF	87	2517	25.4	178	Jan-72	10/25/89	16.73	06/22/89	0.29	2.53	4.2	1.67	76	2.74	1363
MN	271029	1	WF	87	2108	28.7	166	Jan-70	08/07/91	7.97	10/31/90	0.21	3.15	4.2	1.04	47	0.58	1008
MN	271085	1	WF	90	1727	31.1	158	Jan-84	08/05/91	10.44	09/14/89	0.18	2.96	4.2	1.17	40	1.21	305
MN	271087	1	WF	88	1638	31.1	152	Jan-79	08/06/91	5.48	06/09/89	0.14	3.45	4.2	0.72	105	0.83	1322
MN	276251	1	WF					Oct-81	05/23/90	6.18	05/31/90	0.22	3.33	4.2	0.87	65	0.70	564
MS	281001	1	WNF	50	68	52.1	48	Jan-87	02/12/92	1.34	01/10/90	0.21	4.26	4.3	0.03	84	0.69	430
MS	281016	1	WNF	59	45	53.9	56	Nov-86	03/27/92	2.65	05/31/89	0.11	3.94	4.1	0.16	26	0.73	142
MS	281802	1	WNF	37	23	62.3	34	Jun-82	03/27/92	2.72	05/25/89	0.11	3.92	4.2	0.28	61	0.65	597
MS	283083	2	WNF	70	150	56.2	70	Nov-78	02/17/92	4.36	01/10/90	0.08	3.63	3.8	0.17	5	0.62	61
MS	283085	2	WNF	71	148	56.6	71	Nov-78	02/14/92	7.81	01/10/90	0.09	3.21	3.8	0.57	5	0.66	65
MS	283087	2	WNF	67	134	57.0	69	Oct-82	02/13/92	3.21	01/10/90	0.15	3.81	4.1	0.29	47	0.63	445
MO	291002	1	WF	93	382	39.6	103	Jun-86	03/18/90	3.08	06/21/89	0.11	3.85	4.2	0.35	10	0.98	38
MO	291008	1	WF	67	66	55.1	65	May-86	02/16/92	4.67	03/13/89	0.20	3.53	4.2	0.66	148	2.18	856
MO	291010	1	WF	115	396	45.7	123	Sep-80	02/15/92	3.85	06/10/89	0.13	3.70	4.2	0.40	1030	1.92	11806
NE	311030	1	DF	134	716	22.2	154	Jun-82	04/16/90	3.19	05/10/89	0.36	3.66	4.2	0.50	33	0.78	262
NH	331001	1	WF	122				Jun-81	08/13/91	2.07	08/10/89	0.19	4.05	4.3	0.25	138	0.73	1405
NJ	341003	1	WF	116				Jul-74	09/06/91	8.85	07/28/89	0.38	2.93	4.6	1.67	100	0.44	1723
NJ	341011	1	WF	90				Sep-70	09/07/91	6.08	10/05/89	0.25	3.32	4.8	1.48	90	0.32	1893
NJ	341030	1	WF	113				Jul-69	09/06/91	46.54	07/28/89	0.56	1.39	4	2.61	60	0.42	1338
NJ	341031	1	WF	80				Nov-73	09/08/91	6.10	10/05/89	0.37	3.22	4.7	1.48	50	0.50	888
NJ	341033	2	WF	102				Oct-74	09/06/91	15.31	10/05/89	0.21	2.65	4.2	1.55	36	0.29	608
NJ	341034	2	WF	82				Nov-85	11/18/90	3.17	10/05/89	0.13	3.82	4.5	0.68	98	0.28	492
NJ	341638	2	WF	83				Nov-85	09/07/91	2.49	10/05/89	0.13	3.97	4.8	0.83	141	0.41	827

(1) RAIN = AVERAGE ANNUAL RAINFALL
(2) AVG32 = AVERAGE ANNUAL NUMBER OF DAYS BELOW 32 F (0 C)
(3) CALC PSI = 5.03-1.91*LOG(1+AVG SV)-1.38*(AVG RD^2)
(4) OBS PSI LOSS = INIT. PSI. - CALC. PSI

	SHRP ID	EXP	ENV	THAW	FTIN	(1) RAIN	(2) AVG32	DATE OPEN	PSI CALCULATIONS: PROFILE DATE	AVG SV	DATE RUTS MEASURED	AVG RD	(3) CALC. PSI	INIT PSI	(4) OBS PSI LOSS	TRAFFIC KESAL /YEAR	TRUCK FACTOR	CUMUL KESAL
NM	351003	1	DNF	98	107	14.6	95	Apr-83	11/18/91	2.90	12/05/89	0.1	3.87	4.3	0.44	27	0.32	233
NM	351005	1	DF	130	245	15.8	129	Jul-84	11/21/91	1.05	10/31/89	0.3	4.28	4.3	0.05	26	0.65	192
NM	351022	1	DF	131	465	11.1	142	Oct-86	11/20/91	2.36	10/31/89	0.2	3.99	4.3	0.32	33	0.32	170
NM	351112	1	DNF	87	93	16.8	85	Jun-84	10/18/90	1.30	12/05/89	0.14	4.31	4.3	0.02	33	0.32	208
NM	352006	2	DF	170	611	12.2	180	Sep-79	11/20/91	4.54	10/31/89	0.27	3.51	4.3	0.80	24	0.32	298
NM	352118	2	DF	100	195	18.3	101	Sep-77	11/14/91	2.86	01/24/90	0.18	3.86	4.3	0.46	333	0.65	4732
NY	361011	1	WF	89	830	38.7	129	Jun-84	12/14/91	2.76	08/08/89	0.14	3.91	4.7	0.74	166	1.34	1252
NY	361643	2	WF	81	8185	37.2	164	Feb-79	04/19/91	9.65	08/09/89	0.26	2.97	4.2	1.18	1398	6.38	17086
NY	361644	2	WF	109	1757	43.9	174	Aug-80	05/07/91	2.35	08/09/89	0.09	4.02	4.2	0.18	44	2.21	479
NC	371006	1	WNF	57	76	45.1	54	Jul-82	03/14/91	2.08	10/13/89	0.05	4.09	4.2	0.10	387	0.66	3370
NC	371024	1	WNF	96	120	49.4	93	Nov-80	10/31/91	4.37	11/03/89	0.27	3.54	4.2	0.66	18	0.42	203
NC	371028	1	WNF	62	61	47.4	57	May-82	01/30/90	2.35	10/12/89	0.33	3.88	4.2	0.32	61	0.73	475
NC	371030	1	WNF	54	37	45.8	50	Dec-84	12/11/89	2.45	10/12/89	0.20	3.95	4.2	0.25	97	0.70	488
NC	371040	1	WNF	114	289	56.0	117	Sep-78	10/29/91	2.91	11/03/89	0.31	3.77	4.2	0.40	94	0.72	1240
NC	371352	1	WNF	73	68	48.6	67	Jul-80	11/01/91	3.26	03/09/89	0.21	3.77	4.2	0.42	68	0.72	768
NC	371645	2	WNF	60	38	43.6	55	Apr-86	12/13/90	1.77	03/15/89	0.18	4.14	4.2	0.06	116	0.77	546
NC	371801	1	WNF	86	164	41.3	84	May-74	10/30/91	5.13	03/15/89	0.24	3.45	4.2	0.75	220	0.65	3844
NC	371802	1	WNF	63	85	44.0	60	Oct-85	03/16/91	1.99	10/13/89	0.17	4.08	4.2	0.11	54	1.01	294
NC	371803	1	WNF	112	171	51.6	109	Dec-77	10/30/91	3.13	11/03/89	0.23	3.78	4.2	0.40	111	0.71	1545
NC	371814	1	WNF	104	127	53.9	101	Sep-70	10/31/91	2.28	03/13/89	0.14	4.02	4.2	0.17	71	0.70	1505
NC	371817	1	WNF	74	86	44.5	71	Dec-83	12/16/90	3.11	10/15/89	0.26	3.77	4.2	0.43	25	0.74	176
NC	372819	2	WNF	70	86	44.9	65	Aug-81	03/19/91	2.84	10/13/89	0.3	3.80	4.2	0.40	44	0.73	424
NC	372824	2	WNF	70	103	48.9	68	Oct-83	11/01/91	1.88	10/13/89	0.08	4.14	4.2	0.06	101	0.74	607
ND	382001	2	WNF	87	2623	19.3	180	Jul-80	07/20/91	6.40	06/26/89	0.27	3.27	4.2	0.86	144	2.05	1591
OK	404086	2	DNF	73	168	33.6	76	Jun-70	01/30/91	1.95	04/26/89	0.28	4.03	4.2	0.16	183	1.95	3784
OK	404161	1	DNF	48	113	40.8	48	Jun-82	09/28/90	2.93	01/08/90	0.20	3.84	4.2	0.36	103	1.68	856
OK	404164	2	DNF	86	291	28.8	92	May-78	10/02/90	2.88	01/23/90	0.15	3.87	4.2	0.32	135	2.10	1683
OK	404165	2	DNF	84	311	31.6	91	Jun-84	10/02/90	6.12	01/23/90	0.25	3.32	4.2	0.88	242	2.03	1536
PA	421597	1	WF	105	1015	31.5	152	Sep-80	11/20/90	14.26	08/25/89	0.13	2.75	4.5	1.71	17	0.62	176
PA	421599	1	WF	132	903	43.4	165	Aug-87	10/10/91	4.33	07/18/89	0.14	3.62	4.5	0.85	40	0.68	169
PA	421605	1	WF	106	609	43.1	128	Sep-71	11/19/90	6.25	08/29/89	0.57	2.94	4.5	1.54	178	0.83	3415
SC	451008	1	WNF	79	61	36.4	132	May-70	05/21/92	5.42	01/09/90	0.18	3.44	4.1	0.65	22	1.00	482
SC	451011	1	WNF	18	9	49.3	16	Jun-85	04/28/92	4.89	04/11/89	0.26	3.47	4.1	0.63	367	0.68	2533
SC	451024	1	WNF	49	15	45.7	44	Aug-85	04/30/92	7.76	01/09/90	0.13	3.21	4.0	0.79	1	0.60	7
SC	451025	1	WNF	76	59	44.7	72	Feb-80	04/30/92	11.03	03/14/89	0.27	2.87	4.2	1.33	5	0.29	65
TN	471023	1	WNF	90	181	54.0	88	Jun-72	06/13/91	2.54	10/27/89	0.17	3.94	4.7	0.74	820	0.76	15612
TN	471028	2	WNF	87	194	42.5	88	Sep-89	05/15/92	4.35	11/01/89	0.22	3.57	4.5	0.88	90	1.15	243
TN	471029	2	WNF	73	150	60.8	73	Oct-82	05/08/90	1.45	01/10/90	0.10	4.27	4.9	0.62	48	1.29	365
TN	472001	2	WNF	71	256	53.5	78	Jul-89	05/24/90	1.40	11/13/89	0.3	4.17	4.7	0.52	298	1.97	267
TN	472008	2	WNF	72	226	55.7	78	Jun-73	05/24/90	9.62	01/11/89	0.07	3.06	4.8	1.70	130	1.17	2211
TN	473075	1	WNF	87	236	56.8	90	Jun-71	06/17/91	5.95	11/04/89	0.2	3.38	4.4	1.00	30	1.06	604
TN	473101	2	WNF	87	174	52.5	86	Jan-80	06/17/91	6.67	11/04/89	0.13	3.32	4.5	1.09	24	1.26	271
TN	473104	1	WNF	97	161	48.0	95	Jun-86	05/15/92	13.21	11/01/89	0.15	2.80	4.2	1.39	3	1.32	19
TN	479024	2	WNF	85	233	53.4	88	Jun-77	05/17/90	6.53	11/04/89	0.13	3.33	4.7	1.37	15	1.19	199
TN	479025	2	WNF	87	174	52.5	86	Jan-80	05/16/90	6.33	11/04/89	0.14	3.35	4.5	1.15	24	1.26	245
TX	481039	1	WNF	34	63	36.6	32	Jun-82	10/24/91	3.90	03/22/89	0.16	3.68	3.7	0.00	225	1.02	2117
TX	481047	1	DNF	103	253	22.3	106	Jul-71	11/13/91	9.40	04/24/89	0.20	3.03	4.1	1.05	290	1.08	5903
TX	481048	1	DNF	62	46	15.4	58	Nov-74	11/24/91	6.27	12/06/89	0.20	3.33	4.2	0.87	49	0.60	839
TX	481049	2	WNF	31	37	45.9	30	Jun-84	01/23/92	3.73	03/04/90	0.31	3.61	4.2	0.59	429	1.02	3283
TX	481050	1	WNF	20	27	38.0	18	Jul-85	04/04/91	2.86	01/04/90	0.14	3.88	4.5	0.62	71	0.77	407
TX	481056	1	DNF	112	316	19.8	119	Jun-70	10/30/90	5.12	01/11/90	0.18	3.48	4.2	0.72	54	1.13	1098
TX	481060	1	DNF	9	6	33.1	9	Mar-86	04/22/91	3.53	06/18/90	0.18	3.73	4.2	0.47	167	0.96	858
TX	481065	1	DNF	113	301	18.2	120	May-70	10/25/90	14.10	01/24/90	0.24	2.70	4.2	1.49	98	1.24	2014
TX	481068	1	WNF	45	97	50.2	44	Jun-87	10/23/91	2.34	03/23/89	0.11	4.01	4.2	0.18	114	0.90	500
TX	481069	1	WNF	41	69	37.3	39	Jun-77	03/13/90	2.75	01/30/90	0.34	3.77	4.2	0.00	197	0.93	2519
TX	481070	1	WNF	42	72	37.5	40	Jul-77	03/13/90	2.36	03/23/89	0.13	4.00	4.2	0.00	197	0.93	2503
TX	481076	1	DNF	83	145	18.7	84	Nov-77	10/23/90	4.41	12/06/89	0.19	3.58	4.2	0.62	119	1.07	1543
TX	481077	1	DNF	74	182	22.8	75	Jan-82	11/08/91	2.85	04/25/89	0.38	3.71	4.5	0.78	194	0.99	1915
TX	481087	1	WNF	51	65	45.2	49	Dec-73	08/22/90	2.50	03/27/89	0.18	3.95	4.2	0.25	185	0.97	3090
TX	481092	1	DNF	22	17	26.6	20	Sep-83	12/06/91	4.68	04/14/89	0.13	3.57	4.2	0.63	72	0.83	598
TX	481094	1	DNF	29	16	32.0	26	Aug-76	04/11/91	2.47	10/14/90	0.18	3.95	4.5	0.55	10	0.42	142
TX	481096	1	DNF	19	12	25.8	17	Apr-81	12/06/91	6.85	10/14/90	0.30	3.20	3.7	0.50	76	0.75	816
TX	481109	1	WNF	17	35	44.0	17	Jun-84	12/16/91	4.39	01/04/90	0.23	3.56	3.8	0.24	182	0.96	1374

(1) RAIN = AVERAGE ANNUAL RAINFALL
(2) AVG32 = AVERAGE ANNUAL NUMBER OF DAYS BELOW 32 F (0 C)
(3) CALC PSI = 5.03-1.91*LOG(1+AVG SV)-1.38*(AVG RD^2)
(4) OBS PSI LOSS = INIT. PSI. - CALC. PSI

	SHRP ID	EXP	ENV	THAW	FTIN	(1) RAIN	(2) AVG32	DATE OPEN	PSI CALCULATIONS: PROFILE DATE	AVG SV	DATE RUTS MEASURED	AVG RD	(3) CALC. PSI	INIT PSI	(4) OBS PSI LOSS	TRAFFIC KESAL /YEAR	TRUCK FACTOR	CUMUL KESAL
TX	481111	1	DNF	81	139	19.2	81	Sep-72	10/22/90	11.85	12/09/89	0.16	2.88	4.0	1.12	76	0.99	1384
TX	481113	1	WNF	33	38	50.3	31	Jan-86	12/18/91	2.10	03/04/90	0.22	4.02	4.2	0.17	138	0.97	822
TX	481122	1	DNF	29	8	26.9	26	Feb-74	04/10/91	2.48	04/14/89	0.22	3.93	4.2	0.27	42	0.69	729
TX	481130	1	DNF	25	14	35.3	22	Aug-72	03/18/92	17.18	04/11/89	0.45	2.34	4.2	1.72	44	0.79	871
TX	481168	1	WNF	53	73	47.8	52	Sep-85	04/25/90	3.03	03/27/89	0.10	3.86	4.2	0.34	2	0.64	7
TX	481169	1	WNF	44	54	47.4	41	Aug-72	04/23/90	4.50	03/04/90	0.21	3.55	4.2	0.65	84	0.97	1491
TX	481174	1	DNF	8	3	31.1	7	May-75	03/23/92	2.50	10/17/90	0.23	3.92	4.2	0.09	86	0.71	1462
TX	481178	1	WNF	20	54	33.5	22	Jun-89	03/18/92	6.37	04/10/89	0.14	3.35	4.2	0.83	66	0.79	185
TX	481181	1	DNF	13	10	25.8	12	May-80	02/28/92	5.45	04/14/89	0.27	3.38	3.8	0.42	207	0.92	2452
TX	481183	1	DNF	77	140	21.2	77	Feb-75	09/12/90	13.96	12/06/89	0.23	2.71	4.2	1.48	147	1.14	2293
TX	482108	2	WNF	5	6	41.2	4	Aug-85	04/23/91	3.25	03/08/90	0.16	3.80	4.2	0.40	19	0.58	108
TX	482172	2	DNF	55	110	20.5	57	Aug-82	09/13/90	2.83	12/06/89	0.14	3.89	4.0	0.11	404	1.06	3284
TX	483609	1	DNF	71	160	23.7	73	Jun-74	11/08/91	10.47	04/19/89	0.24	2.93	4.2	1.26	45	1.20	786
TX	483669	2	WNF	30	29	44.1	28	May-83	12/17/91	4.10	03/04/90	0.34	3.52	4.1	0.58	73	0.89	628
TX	483679	2	WNF	34	41	45.3	34	Jun-88	12/17/91	13.00	03/04/90	0.10	2.83	3.8	0.97	76	0.83	268
TX	483689	2	WNF	41	36	46.3	40	Apr-87	12/16/91	9.85	03/04/90	0.13	3.03	4.2	1.17	66	0.84	309
TX	483729	1	DNF	4	4	26.5	4	Jun-83	03/19/92	3.20	06/22/90	0.39	3.63	3.7	0.02	216	0.76	1899
TX	483739	1	DNF	7	6	23.9	6	May-82	03/20/92	8.44	06/22/90	0.20	3.11	4.2	1.09	156	0.95	1538
TX	483749	1	DNF	9	10	23.8	9	Mar-81	03/23/92	3.73	10/17/90	0.18	3.70	4.3	0.60	115	0.89	1277
TX	483855	1	WNF	20	19	38.8	18	Oct-79	03/18/92	4.09	06/18/90	0.29	3.56	4.2	0.64	132	0.91	1648
TX	483865	1	DNF	38	43	27.4	36	Jul-69	09/17/90	3.98	10/27/90	0.25	3.61	4.2	0.59	65	0.91	1383
TX	489005	1	DNF	21	13	29.6	18	Sep-86	04/12/91	3.62	10/14/90	0.12	3.74	4.5	0.76	29	0.68	131
UT	491001	1	DF	139	249	8.7	139	Jun-82	08/04/89	2.08	10/30/89	0.29	3.98	4.2	0.22	68	0.93	485
VT	501002	1	WF	99	1379	41.1	157	Aug-84	05/09/91	18.43	08/09/89	0.26	2.48	4.2	1.72	59	0.56	401
VT	501004	1	WF	81	1185	30.6	133	Sep-84	05/08/91	18.12	08/09/89	0.15	2.55	4.2	1.59	37	0.55	246
VA	511002	1	WF	120	305	42.4	126	Oct-79	03/27/91	23.47	10/15/89	0.31	2.25	4.2	1.94	115	0.77	1326
VA	511023	1	WF	86	146	46.3	86	Dec-80	06/23/91	4.73	10/12/89	0.43	3.33	4.5	1.16	626	0.77	6618
VA	512004	2	WF	86	121	44.7	83	Dec-81	11/02/91	5.28	10/13/89	0.13	3.48	4.6	1.11	89	0.77	881
VA	512021	2	WF	94	164	51.8	92	May-85	03/26/91	5.43	10/15/89	0.24	3.41	4.3	0.89	135	0.77	795
WA	531002	1	DF	79	401	18.0	96	Jun-84	10/26/89	7.61	07/18/89	0.17	3.20	4.5	1.29	62	1.14	337
WA	531801	1	WNF	96	76	84.2	85	Oct-73	11/12/89	2.47	07/17/89	0.13	3.98	4.5	0.52	42	1.03	673
WV	541640	2	WF	88	251	43.5	95	Jun-83	11/13/91	9.48	09/28/89	0.18	3.04	4.4	1.36	68	0.69	574
WY	561007	1	DF	147	1066	9.2	175	Jul-80	10/22/90	2.66	09/26/89	0.19	3.90	4.2	0.29	26	1.00	267
WY	562018	2	DF	146	1142	10.5	184	Oct-83	10/24/90	4.64	10/08/89	0.10	3.58	3.9	0.30	79	1.00	556
WY	562019	2	DF	130	1276	13.9	172	Jul-85	10/29/90	3.84	10/08/89	0.15	3.69	4.2	0.50	116	1.00	618
WY	562020	2	DF	158	1155	14.3	188	Jul-85	10/27/90	3.03	09/27/89	0.1	3.85	4.2	0.34	112	1.00	594
WY	562037	2	DF	128	1540	6.3	191	Sep-85	11/08/90	3.68	10/20/89	0.11	3.73	4.2	0.46	44	1.01	230
WY	567773	2	DF	129	1163	9.5	169	Jan-87	10/24/90	2.15	10/08/89	0.13	4.05	4.1	0.04	16	0.99	61
AB	811803	1	DF	100	2763	17.7	203	Oct-84	05/10/90	2.58	07/05/89	0.18	3.93	4.1	0.10	154	1.23	863
AB	811804	1	DF	112	2411	18.8	200	Sep-82	05/10/90	9.73	07/05/89	0.16	3.03	3.6	0.41	74	0.93	565
AB	811805	1	DF	126	1735	15.4	188	Jun-80	05/09/90	8.95	07/07/89	0.25	3.04	3.5	0.42	119	1.00	1185
AB	812812	2	DF	127	1937	16.3	197	Jun-85	05/09/90	37.44	07/07/89	0.14	1.98	3.8	1.75	23	0.95	112
MB	831801	1	DF	89	3012	17.7	197	Jan-84	05/27/90	4.86	06/29/89	0.21	3.50	4.5	0.93	121	1.38	777
MB	836454	2	DF	80	3133	19.1	190	Jun-77	05/27/90	26.95	06/28/89	0.28	2.16	4.6	2.34	173	1.92	2243
MB	841802	1	WF	90	1974	42.1	173	Oct-80	08/20/91	8.74	08/16/89	0.23	3.07	4.1	1.01	199	4.93	2171
ON	871620	1	WF	74	1459	41.8	147	Jun-81	04/25/91	5.33	08/24/89	0.4	3.28	4.6	1.18	115	0.78	1139
ON	871622	1	WF	102	2000	45.5	184	Jun-76	04/26/91	7.28	08/24/89	0.2	3.20	4.8	1.49	115	0.78	1707
ON	871680	2	WF	87	1175	33.8	150	Jun-85	07/10/91	7.92	08/24/89	0.13	3.19	4.2	0.95	177	0.78	1084
ON	871806	1	WF	82	1222	33.9	149	Jun-85	07/10/91	7.60	08/24/89	0.13	3.22	4.2	0.90	177	0.78	1084
ON	872811	2	WF	80	966	35.8	135	Jun-77	07/09/91	4.28	08/31/89	0.13	3.63	4.2	0.49	96	0.79	1356
ON	872812	2	WF	80	1025	40.9	138	Jun-81	05/29/91	2.82	08/31/89	0.17	3.88	4.2	0.22	200	0.78	1994
PEI	881645	1	WF	71	1522	39.5	158	Jul-87	08/21/91	4.54	08/16/89	0.08	3.60	4.3	0.67	132	0.82	545
PEI	881646	1	WF	78	1375	41.5	152	Jun-80	08/21/91	5.49	08/16/89	0.32	3.34	3.6	0.21	36	0.89	408
PEI	881647	2	WF	78	1521	44.9	162	Oct-86	08/22/91	7.35	08/16/89	0.15	3.24	4.3	0.98	60	1.06	295
QE	891021	1	WF	78	2173	40.9	167	Jun-83	07/16/91	5.58	08/14/90	0.34	3.31	4.5	1.19	301	1.30	2448
QE	891125	1	WF	74	2143	44.7	168	Oct-78	09/04/91	12.93	08/14/90	0.40	2.62	4.4	1.75	341	1.30	4404
QE	891127	1	WF	84	2206	42.0	176	Nov-78	09/04/91	17.71	08/22/89	0.51	2.24	4.2	1.93	24	0.13	306
QE	892011	2	WF	73	2208	50.0	171	Oct-79	07/13/91	5.18	08/18/89	0.17	3.48	4.8	1.21	60	1.30	707
SK	901802	1	DF	83	3127	16.9	195	Jul-71	10/21/89	11.24	07/01/89	0.39	2.74	4.2	1.36	115	3.36	2110
SK	906405	1	DF	81	3396	15.1	198	Oct-69	10/22/89	4.29	07/04/89	0.14	3.62	4.4	0.75	39	1.00	779

CODES FOR VARIOUS MATERIAL TYPES:
SEAL COATS (SC): 2,11,71-73
ASPHALT (AC): 1,319,700
BIT BOUND BASE (BBB): 3,9,10,320-330
NON BIT BOUND BASE (NBBB): 331,333,334,339,340,730
UNBOUND BASE (UBB): 302-305,308,337
SUBBASE (SUBB): 201-292,306,307
STAB SUBGRADE (SS): 181-183,333,338

(5) DRAINAGE COEFF(m)=(1.2-.006*avg ann rain)*(1.2-.006*%-200)
(6) SN=.44*AC+.34*BBB+.23*NBBB+m*(.14*UBB+.07*SUBB+.15*SS)
(7) BACKCALCULATED Mr=((FWD Load)*0.2792)/((Defl. at 60")*60)
(8) PREDICTED PSI LOSS = 2.7[(W/p)/S]**B
where: p= 0.64(SN+1)**9.36
S= [10**(-8.07)]*(Mr**2.32)
B= 0.4 + 1094/[(SN+1)**5.19]
(9) PREDICTED KESALS=(S*((SHRP^PSI/2.7)**(1/B)))*p/1000
(10) R = PREDICTED KESALS / SHA ESTIMATE OF TOTAL KESALS

		LAYER THICKNESSES:							(5)	(6)	SUBGRADE:					(7)	PREDICTED: (8)	(9)	RATIOS: (10)
	SHRP ID	SC	AC	BBB	NBBB	UBB	SUBB	SS	m	SN	TYPE	PI	LL	PL	% -200	EST. Mr	PSI LOSS	KESALS	R
AL	11001	0.7	2.6	0.0	0.0	25.4	0.0	0.0	0.95	4.53	SAND	10	30	20	24.1	48183	0.04	67412	33.67
AL	11011	0.0	1.0	5.0	0.0	10.0	0.0	0.0	0.83	3.30	SAND	12	31	19	41.6	78184	0.00	91064	211.66
AL	11019	0.0	6.5	0.0	0.0	5.5	0.0	0.0	0.85	3.51	SAND	1	8	7	28.4	47666	0.01	74430	127.95
AL	11021	0.0	7.6	0.0	0.0	17.4	0.0	0.0	0.69	5.03	SILT	7	28	21	69.0	53226	0.02	238795	384.27
AL	14072	0.0	3.7	4.4	0.0	4.6	8.2	0.0	1.06	4.42	SAND	.	.	0		29622	0.03	3596	11.11
AL	14073	0.0	8.6	0.0	0.0	5.2	0.0	4.9	0.75	4.88	SAND	25	58	33	45.2	81070	0.01	1692194	2623.49
AL	14125	0.0	9.6	0.0	0.0	0.0	6.5	0.0	0.89	4.63	SAND	10	26	16	28.4	58336	0.05	49270	14.44
AL	14126	0.0	13.1	0.0	0.0	18.4	0.0	0.0	0.84	7.92	SAND	1	10	9	29.9	45831	0.02	4701	1.94
AZ	41001	0.6	11.9	0.0	0.0	0.0	0.0	0.0	1.22	5.24	SAND	8	26	18	22.1	40280	0.17	1787225	80.36
AZ	41002	0.7	9.3	0.4	0.0	0.0	0.0	0.0	1.26	4.23	GRAVEL	0	0	0	11.8	75029	0.06	1047945	101.64
AZ	41003	0.5	12.6	0.0	0.0	0.0	6.0	0.0	1.17	6.04	SAND	13	31	18	30.4	48395	0.10	754328	37.06
AZ	41006	0.4	8.2	0.0	0.0	0.0	8.5	0.0	1.18	4.31	SAND	8	25	17	28.4	47394	0.16	84432	4.50
AZ	41007	0.5	6.0	0.0	0.0	0.0	10.8	0.0	1.21	3.56	GRAVEL	9	29	20	23.3	39043	0.26	102696	4.97
AZ	41015	0.5	8.4	0.0	0.0	0.0	9.9	0.0	1.15	4.49	GRAVEL	28	46	18	24.3	107844	0.04	814765	87.69
AZ	41017	0.7	8.2	0.0	0.0	0.0	11.2	0.0	1.15	4.51	GRAVEL	12	28	16	20.3	30629	0.22	89723	6.53
AZ	41018	0.4	8.0	0.0	0.0	0.0	7.2	0.0	1.03	4.04	GRAVEL	10	26	16	38.7	43633	0.17	177656	11.17
AZ	41021	0.5	4.7	0.0	0.0	8.4	0.0	0.0	1.22	3.50	SAND	0	0	0	21.4	40654	0.14	27018	2.48
AZ	41022	0.4	7.9	0.0	0.0	9.5	0.0	0.0	1.23	5.11	SAND	0	23	23	18.9	72840	0.02	105927	88.72
AZ	41024	0.7	10.1	0.0	0.0	0.0	6.3	0.0	1.14	4.95	GRAVEL	22	36	14	29.5	38096	0.14	87335	7.95
AZ	41025	0.8	6.8	0.0	0.0	0.0	7.2	0.0	1.21	3.60	GRAVEL	0	19	19	18.3	92295	0.03	112525	9.82
AZ	41034	0.6	3.3	0.0	0.0	0.0	11.1	0.0	1.28	2.45	SAND	0	9	9	16.9	28093	1.13	6272	0.76
AZ	41037	0.6	2.1	0.0	0.0	10.1	0.0	0.0	1.35	2.83	SAND	0	0	0	8.2	26219	0.09	6292	2.39
AZ	41062	0.3	5.4	11.2	0.0	0.0	0.0	4.5	1.25	7.03	GRAVEL	6	18	12	12.4	59317	0.04	5067581	466.94
AZ	41065	0.4	4.8	13.7	0.0	0.0	0.0	5.5	1.21	7.77	GRAVEL	14	37	23	19.5	30785	0.06	324693	30.19
AR	52042	0.0	5.2	0.0	6.6	0.0	0.0	0.0	0.64	3.81	SILT	2	20	18	73.7	16899	0.14	54443	40.95
AR	53048	0.4	4.7	0.0	7.4	0.0	0.0	0.0	0.56	3.77	CLAY	10	33	23	93.7	25413	0.02	107566	369.69
AR	53071	0.5	15.9	0.0	0.0	0.0	0.0	0.0	0.60	7.00	CLAY	18	35	17	92.1	58819	0.02	879387	735.13
CA	62002	0.2	4.5	0.0	10.4	8.2	0.0	0.0	1.12	5.66	GRAVEL	8	27	19	26.5	33196	0.04	335619	341.78
CA	62004	0.7	3.4	0.0	5.3	0.0	30.6	0.0	1.09	5.06	SILT	2	14	12	37.8	27178	0.18	187296	20.70
CA	62038	0.2	4.2	0.0	6.6	4.7	0.0	0.0	0.81	3.90	SAND	4	20	16	26.2	34966	0.08	27762	9.37
CA	62041	0.2	4.5	0.0	6.5	11.4	0.0	0.0	1.02	5.10	GRAVEL	6	22	16	13.7	60247	0.05	566124	136.75
CA	62051	0.1	4.9	0.0	6.5	3.5	0.0	0.0	1.17	4.22	GRAVEL	16	36	20	12.7	68648	0.03	9	0.00
CA	62053	0.0	4.1	0.0	22.2	0.0	0.0	0.0	0.95	6.91	CLAY	25	43	18	49.3	45718	0.06	2782617	263.72
CA	62647	0.1	3.7	0.0	5.3	0.0	11.9	0.0	1.10	3.76	SAND	14	30	16	23.2	61696	0.08	44857	3.34
CA	67452	0.5	3.4	0.0	6.7	10.2	0.0	0.0	0.87	4.28	CLAY	18	38	20	55.7	39837	0.02	104104	313.19
CA	67491	0.5	3.8	0.0	4.8	0.0	0.0	0.0	1.31	2.78	SAND	0	0	0	13.0	34051	0.51	26817	1.81
CA	68151	0.8	4.1	0.0	6.0	0.0	0.0	0.0	1.27	3.18	SAND	0	0	0	11.3	44853	0.12	16906	1.43
CA	68153	0.3	3.8	0.0	0.0	6.4	15.0	0.0	0.89	3.41	CLAY	44	66	22	63.0	14225	0.10	2151	3.34
CA	68156	0.1	3.8	0.0	0.0	7.5	0.0	0.0	1.23	2.96	GRAVEL	0	0	0	14.9	50511	0.00	59953	65.94
CO	81029	0.1	4.1	0.0	0.0	5.6	13.2	0.0	1.08	3.65	SAND	4	12	8	38.4	17276	0.05	23390	55.45
CO	81047	0.0	3.6	0.0	0.0	18.2	0.0	0.0	1.36	5.04	CLAY	17	31	14		28250	0.03	91218	377.14
CO	81053	0.0	4.6	0.0	0.0	28.5	0.0	0.0	0.74	4.98	CLAY	22	40	18	91.8	28624	0.04	4705	11.33
CO	82008	0.4	3.2	7.7	0.0	5.0	0.0	0.0	0.88	4.65	CLAY	26	41	15	69.3	20917	0.10	38477	29.12
CT	91803	0.0	7.2	0.0	0.0	12.0	0.0	0.0	1.08	4.99	SILT	.	.	0		57546	0.01	959810	6127.58
DL	101450	0.0	9.3	0.0	6.3	0.0	0.0	0.0	0.93	5.54	SAND	0	0	0	33.5	35831	0.09	700806	136.70
FL	121030	0.0	3.3	0.0	0.0	9.8	17.1	0.0	1.03	4.11	SAND	0	0	0	1.3	39330	0.13	89364	10.94
FL	121060	0.0	4.0	0.0	0.0	11.0	0.0	0.0	1.02	3.32	GRAVEL	0	0	0	3.5	64148	0.01	15817	7.16
FL	123996	0.0	1.5	0.0	0.0	8.0	14.2	0.0	1.01	2.81	SAND	0	0	0	5.7	29644	0.05	10460	4.89
FL	124097	0.4	13.6	0.0	6.3	0.0	0.0	0.0	0.92	7.43	SAND	0	0	0	20.5	63908	0.02	701	0.29
FL	124105	0.3	2.0	0.0	0.0	10.1	13.3	0.0	1.09	3.44	SAND	0	0	0	2.95	27698	0.03	7107	11.13
FL	124107	0.6	2.1	0.0	0.0	12.0	0.0	0.0	1.03	2.66	SAND	0	0	0	11.4	34189	0.00	11228	19.77
FL	124154	0.0	1.3	0.0	0.0	0.0	8.8	0.0	1.34	1.40	SAND	0	0	0	8.9	37809	2E+07	762	0.25
GA	131001	0.0	8.1	0.0	0.0	8.6	0.0	0.0	0.82	4.56	SILT	20	50	30	52.9	18115	0.08	3063	5.30
GA	131004	0.0	6.8	0.0	0.0	7.5	0.0	0.0	0.81	3.84	CLAY	13	38	25	55.0	38618	0.01	5356	17.02
GA	131005	0.0	7.7	0.0	0.0	9.1	0.0	0.0	0.93	4.57	SAND	6	23	17	37.2	59965	0.02	56400	54.57
GA	131031	0.6	10.5	0.0	0.0	0.0	8.8	0.0	0.79	5.11	SAND	8	31	23	43.7	16291	0.08	5	0.01
GA	134096	0.0	4.1	0.0	6.3	0.0	0.0	0.0	0.91	3.25	SAND	11	27	16	33.3	63285	0.00	72302	1164.18
GA	134420	0.0	4.9	0.0	7.9	0.0	0.0	0.0	1.00	3.97	SAND	0	0	0	19.4	28073	0.06	21580	16.40

CODES FOR VARIOUS MATERIAL TYPES:
SEAL COATS (SC): 2,11,71-73
ASPHALT (AC): 1,319,700
BIT BOUND BASE (BBB): 3,9,10,320-330
NON BIT BOUND BASE (NBBB): 331,333,334,339,340,730
UNBOUND BASE (UBB): 302-305,308,337
SUBBASE (SUBB): 201-292,306,307
STAB SUBGRADE (SS): 181-183,333,338

(5) DRAINAGE COEFF(m)=(1.2-.006*avg ann rain)*(1.2-.006*%-200)
(6) SN=.44*AC+.34*BBB+.23*NBBB+m*(.14*UBB+.07*SUBB+.15*SS)
(7) BACKCALCULATED Mr=((FWD Load)*0.2792)/((Defl. at 60")*60)
(8) PREDICTED PSI LOSS = 2.7[(W/p)/S]**B
where: p= 0.64(SN+1)**9.36
S= [10**(-8.07)]*(Mr**2.32)
B= 0.4 + 1094/[(SN+1)**5.19]
(9) PREDICTED KESALS=(S*((SHRP^PSI/2.7)**(1/B)))*p/1000
(10) R = PREDICTED KESALS / SHA ESTIMATE OF TOTAL KESALS

	SHRP ID	LAYER THICKNESSES: SC	AC	BBB	NBBB	UBB	SUBB	SS	(5) m	(6) SN	SUBGRADE: TYPE	PI	LL	PL	% -200	(7) EST. Mr	PREDICTED: (8) PSI LOSS	(9) KESALS	RATIOS: (10) R
ID	161001	0.3	3.4	0.0	0.0	9.2	0.0	0.0	1.22	3.06	GRAVEL	1	10	9	5.2	49253	0.01	27495	15.92
ID	161005	0.2	3.6	0.0	0.0	11.3	0.0	0.0	1.18	3.45	GRAVEL	10	36	26	18.2	47353	0.01	70916	148.28
ID	161007	0.2	3.4	0.0	0.0	20.6	0.0	0.0	1.36	5.43	ROCK	0	0	0		70232	0.02	451120	649.02
ID	161009	0.2	10.4	0.0	0.0	0.0	9.2	0.0	1.04	5.25	GRAVEL	0	0	0	47.9	38037	0.05	771725	410.58
ID	161010	0.2	10.7	0.0	0.0	5.4	0.0	0.0	1.28	5.68	SAND	0	0	0	10.7	29418	0.06	638862	401.08
ID	161021	0.3	5.6	0.0	0.0	5.3	0.0	0.0	1.32	3.45	GRAVEL	0	0	0	5.6	81281	0.00	105630	200.97
ID	169032	0.3	5.8	0.0	0.0	23.2	0.0	0.0	0.90	5.49	SILT	14	52	38	54.1	18926	0.04	63905	303.92
ID	169034	0.3	8.9	0.0	0.0	18.8	0.0	0.0	1.08	6.75	GRAVEL	0	0	0	22.3	45273	0.01	2380731	7638.60
IL	171002	0.0	13.2	0.0	0.0	0.0	0.0	0.0	0.90	5.81	SAND	12	28	16	52.6	26791	0.03	198846	917.31
IL	171003	0.0	12.1	0.0	0.0	0.0	0.0	12.0	0.63	6.46	CLAY	14	34	20	90.2	24517	0.02	76739	701.81
IN	181037	0.0	14.4	0.0	0.0	0.0	0.0	0.0	0.75	6.34	CLAY	4	20	16	64.0	23618	0.04	2583964	3684.57
IN	182008	0.0	25.7	12.0	0.0	0.0	0.0	0.0	0.78	15.39	CLAY	10	32	22	67.5	28952	0.01	2.17E+09	153422.73
IA	191044	0.0	16.0	0.0	0.0	0.0	0.0	10.0	0.81	8.25	CLAY	14	30	16	65.2	26770	0.03	17845008	8232.72
IA	196150	0.0	4.8	4.3	0.0	3.0	0.0	0.0	0.84	3.93	CLAY	18	38	20	62.4	16822	0.04	12699	51.28
KS	201005	0.0	13.2	0.0	0.0	0.0	0.0	0.0	0.66	5.81	CLAY	29	48	19	85.8	22035	0.05	536379	802.59
KS	201006	0.0	11.8	0.0	0.0	0.0	0.0	0.0	0.99	5.19	SILT	4	25	21	62.5	65939	0.02	1318192	1040.41
KS	201009	0.0	11.1	0.0	0.0	0.0	0.0	0.0	1.06	4.88	SAND	4	21	17	30.7	33791	0.03	302296	627.93
KY	211010	0.0	6.7	0.0	0.0	9.2	0.0	0.0	0.65	3.78	CLAY	11	34	23	81.2	42644	0.00	70232	814.25
KY	211014	0.0	11.2	0.0	7.3	0.0	0.0	0.0	1.11	6.61	ROCK	.	.	0	.	63501	0.03	247164	92.88
KY	211034	0.0	14.6	0.0	0.0	0.0	0.0	0.0	0.61	6.42	CLAY	22	46	24	83.4	70410	0.01	3879222	8953.57
ME	231001	0.0	8.9	0.0	0.0	0.0	3.0	0.0	1.12	4.15	SAND	0	0	0	.	38018	0.07	484951	163.12
ME	231009	0.0	5.7	0.0	0.0	30.0	0.0	0.0	1.07	6.99	SAND	0	0	0	6.0	34276	0.04	3295017	1086.45
ME	231012	0.0	9.3	0.0	0.0	0.0	34.8	0.0	1.00	6.52	SAND	0	0	0	22.1	34435	0.05	1014618	292.93
ME	231026	0.0	6.4	0.0	0.0	0.0	18.3	0.0	1.05	4.16	SAND	0	0	0	11.9	41182	0.04	429567	300.28
ME	231028	0.0	6.4	0.0	0.0	19.8	0.0	0.0	1.11	5.89	SAND	0	0	0	1.7	35245	0.06	3258313	1303.12
MD	241632	0.0	6.8	0.0	4.2	0.0	0.0	0.0	0.69	3.96	SILT	0	0	0	78.6	21950	0.04	8968	26.29
MD	241634	0.0	3.6	4.8	0.0	0.0	10.9	0.0	1.12	4.07	SILT			0		32232	0.04	23305	25.36
MD	242401	0.0	7.7	0.0	3.6	0.0	6.0	4.8	0.61	4.91	SILT	6	49	43	84.7	29410	0.02	3117	16.62
MD	242805	0.0	9.9	0.0	6.0	0.0	4.8	0.0	0.89	6.04	SILT	3	16	13	46.6	119790	0.02	10167662	1978.24
MA	251002	0.0	7.8	0.0	0.0	0.0	12.4	0.0	1.07	4.36	SAND	0	0	0	7.1	35135	0.05	237876	167.13
MA	251003	0.0	6.6	0.0	0.0	0.0	13.2	0.0	1.06	3.88	SAND	0	0	0	7.1	35690	0.03	391811	590.25
MA	251004	0.0	9.6	0.0	0.0	0.0	24.6	0.0	0.97	5.89	GRAVEL	0	0	0	20.5	45898	0.05	796615	257.45
MI	261001	0.0	2.2	0.0	0.0	10.9	0.0	0.0	1.19	2.79	SAND	0	0	0	4.0	32032	0.00	12612	42.63
MI	261004	0.0	4.2	0.0	0.0	5.0	0.0	0.0	1.17	2.67	SAND	0	0	0	1.5	44188	0.00	30165	115.85
MI	261010	0.0	2.2	0.0	0.0	11.4	19.0	0.0	0.89	3.57	CLAY	6	19	13	52.7	194932	0.00	677461	383.26
MI	261013	0.0	6.7	0.0	0.0	4.8	18.6	0.0	1.16	5.24	SAND	0	0	0	4.4	38195	0.05	305400	214.11
MN	271016	0.0	3.0	0.0	0.0	6.5	0.0	0.0	1.22	2.43	SAND	0	0	0	7.5	34465	0.00	13354	48.12
MN	271018	0.0	4.4	0.0	0.0	5.2	0.0	0.0	1.21	2.82	SAND	0	0	0	5.7	32762	0.01	35074	50.66
MN	271019	0.0	4.9	0.0	0.0	6.4	0.0	0.0	1.16	3.19	SAND	0	0	0	10.8	23540	0.02	21053	52.61
MN	271023	0.0	10.5	0.0	0.0	4.0	6.8	0.0	1.21	5.88	SAND	0	0	0	6.4	43893	0.03	6012355	5793.52
MN	271028	0.0	9.6	0.0	0.0	0.0	0.0	0.0	1.22	4.22	SAND	0	0	0	6.2	29689	0.06	307127	225.36
MN	271029	0.0	8.4	0.0	0.0	0.0	0.0	0.0	1.17	3.70	SAND	0	0	0	11.0	26365	0.05	54139	53.70
MN	271085	0.0	11.3	0.0	0.0	0.0	0.0	0.0	0.90	4.97	CLAY	12	26	14	52.6	19974	0.05	179928	589.62
MN	271087	0.0	15.7	0.0	0.0	0.0	0.0	0.0	1.06	6.91	SAND	0	0	0	26.4	31100	0.04	1650866	1248.63
MN	276251	0.0	7.4	0.0	0.0	10.2	0.0	0.0	1.39	5.24	SAND	0	0	0	7.0	33940	0.03	469296	831.81
MS	281001	0.0	9.7	0.0	0.0	0.0	8.2	0.0	0.67	4.66	CLAY	14	32	18	73.3	17856	0.07	105	0.24
MS	281016	0.0	7.9	0.0	0.0	0.0	19.5	0.0	0.89	4.70	SAND	2	20	18	30.1	24323	0.02	4718	33.15
MS	281802	0.0	7.9	0.0	0.0	0.0	2.0	0.0	0.97	3.61	SAND	2	9	7	4.25	34074	0.02	16400	27.47
MS	283083	0.5	1.6	0.0	6.8	0.0	0.0	0.0	1.03	2.27	SAND	0	0	0	1.35	20386	0.00	1294	21.22
MS	283085	0.6	1.1	0.0	4.5	0.0	0.0	0.0	0.75	1.52	SAND	10	24	14	54.9	59467	0.00	3139	48.63
MS	283087	0.0	6.0	0.0	5.9	0.0	0.0	0.0	1.02	4.00	SAND	0	0	0	1.65	21587	0.05	7409	16.66
MO	291002	0.0	6.8	0.0	0.0	6.0	0.0	0.0	0.97	3.80	GRAVEL	10	26	16	32.5	29688	0.00	17900	471.39
MO	291008	0.0	11.4	0.0	0.0	4.8	0.0	0.0	0.85	5.58	GRAVEL	11	27	16	37.8	32717	0.04	355599	415.66
MO	291010	0.0	13.9	0.0	0.0	4.2	0.0	0.0	0.92	6.66	SAND	26	43	17	34.2	40403	0.08	575505	48.75
NE	311030	0.0	7.2	0.0	0.0	0.0	0.0	0.0	0.66	3.17	SILT	8	32	24	97.5	28031	0.01	14639	55.88
NH	331001	0.0	8.4	0.0	0.0	0.0	32.2	0.0	1.36	6.76	SAND	0	0	0	11.4	44652	0.03	271713	193.40
NJ	341003	0.0	7.5	0.0	0.0	33.4	0.0	0.0	1.44	10.03	ROCK	.	.	0	.	54325	0.01	917804478	532711.88
NJ	341011	0.0	9.0	0.0	0.0	37.8	0.0	0.0	1.37	11.23	SAND	0	0	0	9.1	42801	0.01	1.03E+09	543356.47
NJ	341030	0.0	6.0	0.0	0.0	6.8	23.4	0.0	1.37	6.20	SAND	0	0	0	9.2	105631	0.01	239777384	179139.57
NJ	341031	0.0	7.3	0.0	0.0	11.0	0.0	0.0	1.39	5.35	SAND	0	0	0	6.9	37031	0.04	2011739	2266.57
NJ	341033	0.0	7.4	0.0	0.0	15.0	0.0	0.0	1.27	5.93	GRAVEL	4	26	22	23.4	76855	0.01	24956763	41037.50
NJ	341034	0.0	12.1	0.0	0.0	0.0	0.0	0.0	1.36	5.32	SAND	0	0	0	10.6	24502	0.05	142939	290.34
NJ	341638	0.0	9.2	0.0	7.0	0.0	0.0	0.0	1.37	5.66	SAND	0	0	0	9.5	32118	0.04	603108	729.62

CODES FOR VARIOUS MATERIAL TYPES:
SEAL COATS (SC): 2,11,71-73
ASPHALT (AC): 1,319,700
BIT BOUND BASE (BBB): 3,9,10,320-330
NON BIT BOUND BASE (NBBB): 331,333,334,339,340,730
UNBOUND BASE (UBB): 302-305,308,337
SUBBASE (SUBB): 201-292,306,307
STAB SUBGRADE (SS): 181-183,333,338

(5) DRAINAGE COEFF(m)=(1.2-.006*avg ann rain)*(1.2-.006*%-200)
(6) SN=.44*AC+.34*BBB+.23*NBBB+m*(.14*UBB+.07*SUBB+.15*SS)
(7) BACKCALCULATED Mr=((FWD Load)*0.2792)/((Defl. at 60")*60)
(8) PREDICTED PSI LOSS = 2.7[(W/p)/S]**B
where: p= 0.64(SN+1)**9.36
S= [10**(-8.07)]*(Mr**2.32)
B= 0.4 + 1094/[(SN+1)**5.19]
(9) PREDICTED KESALS=(S*((SHRP^PSI/2.7)**(1/B)))*p/1000
(10) R = PREDICTED KESALS / SHA ESTIMATE OF TOTAL KESALS

	SHRP ID	LAYER THICKNESSES: SC	AC	BBB	NBBB	UBB	SUBB	SS	(5) m	(6) SN	SUBGRADE: TYPE	PI	LL	PL	% -200	(7) EST. Mr	PREDICTED: (8) PSI LOSS	(9) KESALS	RATIOS: (10) R
NM	351003	0.6	6.7	0.0	0.0	6.9	0.0	0.0	1.15	4.06	GRAVEL	6	24	18	27.7	101088	0.00	506768	2172.77
NM	351005	0.6	8.3	0.0	0.0	8.3	0.0	0.0	1.29	5.15	SAND	3	22	19	5.3	48048	0.01	3067	15.95
NM	351022	0.8	5.5	0.0	0.0	10.8	0.0	0.0	1.30	4.39	SAND	2	20	18	8.45	30641	0.02	23551	138.85
NM	351112	0.8	5.5	0.0	0.0	6.0	0.0	0.0	1.30	3.51	SAND	0	0	0	3.15	51002	0.00	1366	6.56
NM	352006	0.7	4.6	4.8	0.0	0.0	6.0	0.0	1.18	4.15	SAND	0	0	0	25.6	14430	0.07	15702	52.68
NM	352118	0.8	10.3	0.0	0.0	19.0	0.0	0.0	1.17	7.64	SAND	0	0	0	21.4	35945	0.04	1694357	358.04
NY	361011	0.0	9.9	0.0	0.0	15.6	0.0	0.0	0.91	6.35	GRAVEL	6	22	16	42.6	69548	0.02	6148063	4912.18
NY	361643	0.0	2.2	8.2	0.0	0.0	6.0	0.0	1.11	4.22	SAND	0	0	0	11.3	30562	0.28	184439	10.79
NY	361644	0.0	2.3	6.3	0.0	13.8	0.0	0.0	1.10	5.27	SAND	0	0	0	5.1	40401	0.03	27859	58.20
NC	371006	0.0	9.3	0.0	0.0	9.4	0.0	0.0	0.83	5.19	SILT	0	0	0	50.6	19369	0.15	1411	0.42
NC	371024	0.0	4.8	0.0	0.0	0.0	12.0	0.0	0.90	2.86	SAND	6	19	13	34.9	26709	0.00	11418	56.26
NC	371028	0.0	9.4	0.0	0.0	0.0	0.0	0.0	1.05	4.14	SAND	0	0	0	8.7	22832	0.05	10571	22.24
NC	371030	0.0	8.7	0.0	0.0	0.0	0.0	0.0	1.08	3.83	SAND	0	0	0	4.6	21966	0.04	5757	11.80
NC	371040	0.0	5.3	0.0	0.0	14.4	0.0	0.0	0.64	3.61	SILT	0	0	0	77.4	21857	0.08	9422	7.60
NC	371352	0.0	6.3	0.0	0.0	6.0	0.0	0.0	0.67	3.33	SILT	16	45	29	77.3	81096	0.00	170941	222.72
NC	371645	0.0	7.9	0.0	7.0	0.0	0.0	0.0	1.10	5.09	SAND	0	0	0	4.5	32351	0.04	1461	2.68
NC	371801	0.0	7.2	0.0	0.0	12.0	0.0	0.0	0.90	4.67	SILT	0	24	24	43.3	35838	0.09	204424	53.18
NC	371802	0.0	4.5	0.0	0.0	8.2	0.0	0.0	0.80	2.90	SAND	16	44	28	56.7	29818	0.00	4174	14.22
NC	371803	0.0	5.2	0.0	0.0	0.0	13.2	0.0	0.65	2.89	SILT	0	0	0	77.5	31765	0.02	12300	7.96
NC	371814	0.0	5.1	0.0	0.0	0.0	13.8	0.0	0.83	3.05	SAND	6	32	26	41.3	29225	0.04	5791	3.85
NC	371817	0.0	4.3	0.0	0.0	0.0	12.0	0.0	0.86	2.62	SILT	0	0	0	45.6	35932	0.00	12161	69.03
NC	372819	0.0	4.9	0.0	8.2	7.2	0.0	0.0	0.80	4.85	SiltyClay	12	39	27	56.1	26989	0.04	37608	88.71
NC	372824	0.0	4.7	0.0	6.0	0.0	0.0	0.0	1.09	3.45	SILT			0		24679	0.03	1164	1.92
ND	382001	0.2	4.8	0.0	12.6	5.6	0.0	0.0	0.99	5.78	SAND	14	30	16	48.4	12303	0.14	82211	51.67
OK	404086	0.3	5.2	7.9	0.0	0.0	0.1	0.0	0.63	4.98	SILT	0	0	0	95.2	24433	0.13	5406	1.43
OK	404161	0.9	9.7	0.0	0.0	0.0	0.0	0.0	0.96	4.27	SAND	0	0	0	33.0	19828	0.08	9745	11.38
OK	404164	0.0	4.6	7.6	0.0	0.0	0.0	0.0	1.06	4.61	SAND	2	10	8	28.4	32705	0.06	32518	19.32
OK	404165	0.0	8.1	0.0	0.0	0.0	0.0	0.0	1.04	3.56	SAND	0	0	0	29.1	34771	0.04	70127	45.65
PA	421597	0.0	6.4	0.0	0.0	16.2	0.0	0.0	0.93	4.93	CLAY	6	28	22	46.6	83605	0.01	9991264	56812.41
PA	421599	0.0	12.3	0.0	0.0	12.0	0.0	0.0	0.85	6.85	GRAVEL	6	26	20	48.4	54444	0.01	8296450	49039.48
PA	421605	0.0	8.1	0.0	0.0	0.0	16.8	0.0	0.96	4.69	GRAVEL	8	26	18	30.6	62860	0.04	2994304	876.84
SC	451008	0.0	3.7	0.0	0.0	7.8	0.0	0.0	0.91	2.62	SAND	4	32	28	45.4	29917	0.00	10124	21.01
SC	451011	0.0	3.2	0.0	0.0	10.1	0.0	0.0	1.00	2.83	SAND	0	0	0	14.8	38384	0.02	24500	9.67
SC	451024	0.0	1.6	0.0	0.0	4.8	0.0	0.0	0.96	1.35	SAND	15	36	21	27.2	69319	0.00	2505	371.05
SC	451025	0.0	1.1	0.0	0.0	8.3	0.0	0.0	0.86	1.49	SAND	0	0	0	45.3	22885	0.00	336	5.18
TN	471023	0.0	5.4	6.1	0.0	6.0	0.0	0.0	0.74	5.07	CLAY	20	40	20	59.7	58671	0.10	984710	63.07
TN	471028	0.8	11.3	0.0	0.0	3.8	0.0	0.0	0.73	5.36	CLAY	32	60	28	70.8	78314	0.01	3802580	15624.70
TN	471029	0.0	2.8	12.9	0.0	6.1	0.0	0.0	0.80	6.30	SAND	12	33	21	41.1	76633	0.01	4787752	13109.99
TN	472001	0.9	6.8	0.0	4.5	0.0	0.0	0.0	0.59	4.03	CLAY	12	32	20	87.9	26232	0.02	28401	106.25
TN	472008	0.0	11.6	0.0	9.3	0.0	0.0	0.0	0.56	7.24	CLAY	6	28	22	92.9	39527	0.03	31442537	14222.89
TN	473075	0.0	5.0	0.0	0.0	9.2	0.0	0.0	0.83	3.27	GRAVEL	4	34	30	39.3	12961	0.11	5489	9.09
TN	473101	0.6	8.9	0.0	0.0	5.5	0.0	0.0	0.65	4.42	CLAY	26	52	26	77.6	51485	0.01	702963	2597.87
TN	473104	0.0	1.3	0.0	0.0	8.7	0.0	0.0	0.78	1.52	CLAY	10	30	20	58.0	64399	0.00	4139	213.73
TN	479024	0.6	5.1	7.1	0.0	0.0	0.0	0.0	0.99	4.66	GRAVEL	6	20	14	11.7	126954	0.00	11766962	58983.98
TN	479025	0.8	3.7	2.3	0.0	12.0	0.0	0.0	1.06	4.19	ROCK	6	20	14	.	162048	0.00	8184753	33417.69
TX	481039	0.0	7.4	0.0	0.0	14.0	0.0	7.8	0.64	5.26	CLAY	32	56	24	90.9	26397	0.09	0	0.00
TX	481047	0.0	10.0	0.0	0.0	15.3	0.0	14.4	0.77	7.71	CLAY	22	40	18	79.6	29732	0.05	8482389	1437.05
TX	481048	0.0	11.0	0.0	0.0	0.0	0.0	0.0	1.20	4.84	SAND	0	0	0	19.9	26963	0.06	171542	204.52
TX	481049	0.5	4.6	0.0	11.2	0.0	0.0	7.8	0.84	5.58	SAND	14	48	34	49.2	42949	0.06	514537	156.74
TX	481050	0.8	1.0	0.0	0.0	9.6	0.0	6.5	0.81	2.31	CLAY	20	40	20	61.4	25375	0.00	3773	9.28
TX	481056	0.4	1.8	0.0	0.0	14.4	0.0	0.0	1.18	3.16	CLAY	19	34	15	18.7	21361	0.06	10951	9.97
TX	481060	0.0	7.5	0.0	0.0	12.3	0.0	6.0	1.00	5.92	SAND	4	20	16	34.0	20622	0.06	80339	93.64
TX	481065	0.3	8.3	0.0	0.0	4.8	0.0	0.0	0.70	4.12	CLAY	22	40	18	93.2	24972	0.10	146271	72.63
TX	481068	0.0	10.9	0.0	0.0	6.0	0.0	8.0	0.68	6.18	CLAY	20	38	18	74.0	29460	0.03	27356	54.73
TX	481069	0.0	9.5	0.0	0.0	0.0	0.0	6.5	0.63	4.79	CLAY	41	72	31	93.1	29945	0.09	0	0.00
TX	481070	0.0	10.5	0.0	0.0	0.0	0.0	10.0	0.64	5.59	CLAY	41	66	25	89.9	33698	0.07	0	0.00
TX	481076	0.0	5.4	0.0	0.0	8.4	0.0	0.0	1.19	3.78	SAND	0	0	0	17.7	38053	0.04	69127	44.80
TX	481077	0.0	5.1	0.0	0.0	10.4	0.0	0.0	0.88	3.52	SILT	0	0	0	62.7	26725	0.08	31248	16.32
TX	481087	0.3	6.9	0.0	0.0	7.2	0.0	0.0	1.06	4.11	SAND	0	0	0	9.1	57242	0.04	59379	19.22
TX	481092	0.4	2.0	0.7	0.0	12.5	0.0	0.0	0.82	2.55	SILT	12	39	27	68.6	34306	0.00	12133	20.30
TX	481094	0.0	1.9	0.0	0.0	8.4	0.0	0.0	1.01	2.02	SAND	12	29	17	33.4	70128	0.00	19760	139.39
TX	481096	0.0	7.1	0.0	0.0	8.1	0.0	0.0	0.76	3.99	CLAY	22	50	28	78.5	23264	0.06	19748	24.21
TX	481109	0.0	6.3	0.0	0.0	0.0	0.0	6.5	0.73	3.48	CLAY	25	52	27	70.7	29599	0.05	9347	6.80

CODES FOR VARIOUS MATERIAL TYPES:
SEAL COATS (SC): 2,11,71-73
ASPHALT (AC): 1,319,700
BIT BOUND BASE (BBB): 3,9,10,320-330
NON BIT BOUND BASE (NBBB): 331,333,334,339,340,730
UNBOUND BASE (UBB): 302-305,308,337
SUBBASE (SUBB): 201-292,306,307
STAB SUBGRADE (SS): 181-183,333,338

(5) DRAINAGE COEFF(m)=(1.2-.006*avg ann rain)*(1.2-.006*%-200)
(6) SN=.44*AC+.34*BBB+.23*NBBB+m*(.14*UBB+.07*SUBB+.15*SS)
(7) BACKCALCULATED Mr=((FWD Load)*0.2792)/((Defl. at 60")*60)
(8) PREDICTED PSI LOSS = 2.7[(W/p)/S]**B
where: p= 0.64(SN+1)**9.36
S= [10**(-8.07)]*(Mr**2.32)
B= 0.4 + 1094/[(SN+1)**5.19]
(9) PREDICTED KESALS=(S*((SHRP^PSI/2.7)**(1/B)))*p/1000
(10) R = PREDICTED KESALS / SHA ESTIMATE OF TOTAL KESALS

	SHRP ID	LAYER THICKNESSES: SC	AC	BBB	NBBB	UBB	SUBB	SS	(5) m	(6) SN	SUBGRADE: TYPE	PI	LL	PL	% -200	(7) EST. Mr	PREDICTED: (8) PSI LOSS	(9) KESALS	RATIOS: (10) R
TX	481111	0.5	6.9	0.0	0.0	8.4	0.0	0.0	1.02	4.23	SAND	10	25	15	44.0	33225	0.05	208330	150.47
TX	481113	0.7	0.8	0.0	0.0	11.5	0.0	0.0	0.77	1.59	CLAY	14	35	21	57.1	65181	0.00	4276	5.20
TX	481122	0.4	3.0	0.0	0.0	15.6	8.4	0.0	1.13	4.44	SAND	6	13	7	19.3	76273	0.01	152688	209.53
TX	481130	0.4	2.3	0.0	0.0	17.9	0.0	8.0	0.70	3.61	CLAY	30	53	23	81.7	24692	0.05	77947	89.52
TX	481168	0.4	0.8	0.0	0.0	10.4	0.0	0.0	0.86	1.60	SAND	3	12	9	43.8	36955	0.00	1267	170.39
TX	481169	0.8	1.1	0.0	0.0	0.0	11.3	0.0	1.08	1.34	SAND	0	0	0	2.65	28817	*********	313	0.21
TX	481174	0.0	4.7	0.0	0.0	13.2	0.0	0.0	0.83	3.60	CLAY	34	55	21	64.0	14323	0.20	521	0.36
TX	481178	0.0	8.5	0.0	0.0	10.8	0.0	4.5	0.76	5.41	CLAY	26	49	23	72.6	25779	0.03	274628	1487.54
TX	481181	0.6	6.3	0.0	0.0	9.6	0.0	5.9	0.85	4.66	CLAY	18	44	26	65.0	19679	0.15	16877	6.88
TX	481183	0.4	5.3	0.0	0.0	0.0	8.4	0.0	0.88	2.85	CLAY	12	27	15	63.3	29417	0.05	24930	10.87
TX	482108	0.0	3.0	0.0	14.2	0.0	0.0	6.5	0.76	5.33	CLAY	18	39	21	67.0	26228	0.02	56832	527.68
TX	482172	0.9	10.0	6.8	0.0	0.0	8.8	0.0	0.99	7.32	SAND	10	24	14	47.5	32026	0.04	28508	8.68
TX	483609	0.3	3.9	0.0	0.0	6.6	0.0	0.0	0.68	2.35	CLAY	22	42	20	92.6	22539	0.02	4083	5.19
TX	483669	0.0	4.3	0.0	8.0	0.0	0.0	7.9	0.82	4.70	CLAY	16	33	17	54.6	28068	0.05	74094	118.00
TX	483679	0.0	1.6	0.0	8.4	0.0	0.0	0.0	0.74	2.64	CLAY	16	30	14	66.4	18306	0.01	4156	15.53
TX	483689	0.4	2.7	0.0	7.9	0.0	0.0	6.0	0.83	3.75	CLAY	6	20	14	49.7	86122	0.00	1067459	3449.62
TX	483729	0.0	10.0	0.0	0.0	10.5	0.0	5.4	0.65	5.89	CLAY	26	46	20	95.4	20074	0.09	41	0.02
TX	483739	0.3	1.5	0.0	0.0	11.4	0.0	7.4	1.23	4.00	SAND	0	0	0	5.3	20123	0.12	45983	29.89
TX	483749	0.3	1.5	0.0	0.0	8.1	0.0	8.8	0.96	3.01	SAND	20	38	18	49.0	23634	0.05	9781	7.66
TX	483855	0.5	0.9	0.0	0.0	16.8	0.0	6.0	1.03	3.75	GRAVEL	7	25	18	22.1	111401	0.01	847123	513.88
TX	483865	0.4	1.9	0.0	0.0	17.5	0.0	0.0	0.89	3.02	CLAY	6	21	15	56.7	54800	0.01	67860	49.07
TX	489005	0.4	1.1	0.0	0.0	0.0	9.4	0.0	0.84	1.03	CLAY	21	38	17	63.7	35726	0.04	146	1.11
UT	491001	0.4	5.1	0.0	0.0	5.8	0.0	0.0	1.24	3.25	SAND	0	0	0	20.4	24190	0.02	4972	10.25
VT	501002	0.0	8.3	0.0	0.0	25.8	0.0	0.0	1.10	7.64	GRAVEL	0	0	0	6.9	24379	0.02	16215542	40466.79
VT	501004	0.0	8.0	0.0	0.0	0.0	47.1	0.0	0.82	6.23	SILT	17	28	11	65.3	44037	0.01	10544047	42822.24
VA	511002	0.0	5.7	0.0	0.0	0.0	6.0	0.0	0.87	2.87	GRAVEL	0	0	0	46.8	40537	0.01	67021	50.55
VA	511023	0.0	10.1	0.0	0.0	6.0	0.0	8.4	0.57	5.64	SILT	5	16	11	97.2	37382	0.09	1731023	261.58
VA	512004	0.0	7.4	0.0	5.3	0.0	0.0	0.0	0.82	4.48	SAND	0	0	0	53.1	13142	0.15	32777	37.21
VA	512021	0.0	7.5	0.0	0.0	3.6	0.0	0.0	0.76	3.68	SILT	0	24	24	58.2	14988	0.11	11580	14.57
WA	531002	0.3	4.3	0.0	0.0	8.0	0.0	0.0	0.90	2.90	SILT	6	24	18	63.1	87908	0.00	312736	928.16
WA	531801	0.0	9.2	0.0	0.0	5.0	0.0	0.0	0.76	4.58	GRAVEL	4	14	10	18.7	69989	0.01	453771	674.70
WV	541640	0.0	15.3	4.1	0.0	0.0	5.1	0.0	0.93	8.46	GRAVEL	8	24	16	34.9	37399	0.01	55958007	97424.73
WY	561007	0.0	2.8	0.0	0.0	6.2	0.0	0.0	1.19	2.26	SAND	0	0	0	27.3	33985	0.00	5070	18.98
WY	562018	0.9	4.9	0.0	14.4	0.8	0.0	0.0	0.92	5.57	SAND	20	36	16	64.9	27194	0.04	40543	72.97
WY	562019	0.8	3.4	0.0	10.6	8.5	16.3	0.0	1.25	6.84	SAND	9	17	8	14.0	33919	0.02	800353	1294.12
WY	562020	0.8	4.2	0.0	12.5	0.0	0.0	0.0	1.25	4.72	GRAVEL	17	30	13	12.9	37271	0.03	54528	91.74
WY	562037	0.2	3.4	0.0	16.4	0.0	0.0	0.0	1.12	5.27	SAND	6	22	16	39.6	40778	0.02	196080	852.35
WY	567773	0.6	4.0	0.0	5.2	19.9	0.0	0.0	1.21	6.33	SAND	0	0	0	23.6	42073	0.01	2805	45.97
AB	811803	0.0	4.5	0.0	0.0	11.0	0.0	0.0	0.98	3.50	SAND	0	0	0	50.0	27443	0.04	2716	3.15
AB	811804	0.3	3.2	0.0	0.0	22.4	0.0	0.0	0.72	3.67	CLAY	24	40	16	89.5	15526	0.08	4487	7.93
AB	811805	0.3	6.8	0.0	0.0	8.4	2.0	0.0	0.94	4.23	SiltyClay	13	28	15	58.6	17782	0.12	9591	8.09
AB	812812	0.0	5.6	0.0	0.0	0.0	0.0	6.5	1.02	3.46	GRAVEL	19	34	15	46.3	29332	0.01	90312	808.97
MB	831801	0.0	4.4	0.0	0.0	18.8	0.0	0.0	1.15	4.95	SAND	0	0	0	25.4	21779	0.07	136301	175.37
MB	836454	0.0	10.7	0.0	0.0	0.0	0.0	0.0	1.04	4.71	SAND	0	0	0	40.0	23658	0.11	702621	313.30
MB	841802	0.0	10.9	2.1	0.0	18.6	0.0	0.0	1.05	8.25	GRAVEL	0	0	0	15.2	31018	0.03	14343894	6607.59
ON	871620	0.0	5.0	0.0	0.0	0.0	29.6	0.0	0.69	3.62	CLAY	4	24	20	79.6	17831	0.11	23199	20.37
ON	871622	0.0	5.6	0.0	0.0	6.6	26.3	0.0	0.84	4.80	SILT	0	0	0	48.2	40949	0.05	1215292	711.88
ON	871680	0.0	10.3	0.0	0.0	3.0	24.3	0.0	0.80	6.23	SILT	0	8	8	66.5	46170	0.03	3615125	3335.47
ON	871806	0.0	5.6	0.0	0.0	7.1	38.2	0.0	0.74	5.19	SILT	0	0	0	75.6	44588	0.03	889565	820.75
ON	872811	0.0	3.2	0.0	13.4	0.0	0.0	0.0	0.71	4.49	CLAY	8	26	18	79.2	41790	0.04	113857	83.97
ON	872812	0.0	2.8	0.0	11.7	0.0	0.0	0.0	0.69	3.92	CLAY	14	28	14	78.7	30430	0.07	10568	5.30
PEI	881645	0.0	6.4	14.2	0.0	3.3	0.0	0.0	0.96	8.09	SAND	0	0	0	33.5	49695	0.01	13456994	24703.78
PEI	881646	0.0	9.6	11.2	0.0	0.0	0.0	0.0	0.93	8.03	SAND	0	0	0	37.6	39444	0.01	437658	1073.86
PEI	881647	0.0	6.9	6.9	0.0	5.5	0.0	0.0	0.82	6.02	SILT	4	24	20	52.6	61608	0.01	5927829	20082.13
QE	891021	0.0	5.2	0.0	0.0	15.0	0.0	0.0	1.11	4.62	SAND	0	0	0	6.1	23875	0.12	178872	73.06
QE	891125	0.0	5.2	0.0	0.0	14.1	30.0	0.0	1.04	6.53	SAND	0	0	0	13.7	29598	0.07	7624609	1731.25
QE	891127	0.0	4.9	0.0	0.0	16.4	23.4	0.0	1.03	6.22	GRAVEL	1	8	7	18.3	34956	0.02	9543024	31181.53
QE	892011	0.0	3.0	3.3	0.0	40.7	0.0	0.0	0.86	7.36	SAND	0	0	0	40.3	37704	0.02	14050995	19864.49
SK	901802	0.0	7.3	0.0	0.0	0.0	0.0	0.0	0.92	3.21	CLAY	16	32	16	60.8	16028	0.25	11159	5.29
SK	906405	0.0	2.8	1.2	0.0	9.0	0.0	0.0	1.18	3.13	SAND	2	10	8	22.6	29086	0.02	22295	28.62

Appendix B

Sections and Corresponding Data Utilized in Evaluation of the AASHTO Rigid Pavement Equation

Evaluation of AASHTO rigid pavement design equation - General Information

st_shrp	exp#	new exp#	cell	region	construction date	traffic open date	distress date	SV date	traffic count start	traffic count end	years of count	KESAL	KESAL/yr	pavement age	years of traffic	estimated KESAL
183002	3		2	W-F	8/1/76	8/1/76	6/28/89	9/10/91	1976	1989	14	2303	165	14	14	2289
273003	3		2	W-F	10/1/86	10/1/86	5/19/89	8/10/91	1985	1989	5	401	80	4	4	291
193055	3		3	W-F	11/1/68	8/1/69	6/14/89	6/18/90	1972	1989	18	1892	105	22	21	2195
233013	3		4	W-F	11/1/73	11/1/73	8/10/89	8/15/91	1973	1989	17	3170	186	17	17	3130
393013	3		5	W-F	3/1/70	7/1/70	9/27/89	8/16/90	1970	1989	20	1654	83	21	20	1675
183030	3		6	W-F	1/1/81	1/1/81	9/25/89	9/11/91	1981	1989	9	3584	398	10	10	3877
393801	3		6	W-F	6/1/83	1/1/84	6/30/89	8/15/90	1984	1989	6	1527	255	7	6	1654
183031	3		8	W-F	7/1/77	7/1/77	6/28/89	12/3/89	1977	1989	13	5246	404	13	13	5246
193033	3		8	W-F	8/1/83	10/1/83	9/21/89	5/13/92	1984	1989	6	819	137	7	7	953
553009	3		9	W-F	10/1/84	10/1/84	9/12/89	6/19/92	1984	1989	6	1878	313	6	6	1863
893015	3		10	W-F	9/1/84	10/1/85	8/23/89	7/16/91	1985	1989	5	1701	340	6	5	1666
893016	3		10	W-F	11/1/82	9/1/84	8/23/89	9/4/91	1985	1989	5	1555	311	8	6	1859
553008	3		11	W-F	12/1/75	12/1/75	9/12/89	6/20/92	1975	1989	15	9093	606	15	15	8967
553010	3		11	W-F	10/1/78	10/1/78	9/12/89	6/20/92	1978	1989	12	2535	211	12	12	2526
423044	3		12	W-F	9/1/85	12/1/85	2/8/90	10/8/91	1985	1989	5	4774	955	5	5	4957
193006	3		14	W-F	10/1/75	11/1/75	9/22/89	5/14/92	1976	1989	14	2097	150	15	15	2232
193028	3		16	W-F	11/1/84	6/1/86	9/21/89	5/13/92	1986	1989	4	1052	263	6	4	1133
843803	3		17	W-F	6/1/80	6/1/80	8/16/89	9/28/89	1981	1989	9	1920	213	10	10	2179
263069	3		18	W-F	1/1/74	1/1/74	9/7/89	7/9/91	1974	1989	16	975	61	17	17	1017
273013	3		18	W-F	10/1/85	10/1/85	6/9/89	8/5/91	1985	1989	5	888	178	5	5	833
553014	3		19	W-F	10/1/76	10/1/76	9/11/89	6/20/92	1976	1989	14	4529	324	14	14	4514
233014	3		20	W-F	11/1/73	11/1/73	8/10/89	8/15/91	1973	1989	17	3203	188	17	17	3162
893001	3		21	W-F	6/1/77	6/1/78	8/23/89	10/25/90	1982	1989	8	1403	175	13	12	2146
553015	3		25	W-F	9/1/84	10/1/84	9/14/89	6/19/92	1984	1989	6	2081	347	6	6	2066
193009	3		32	W-F	12/1/75	6/1/76	9/21/89	6/26/90	1976	1989	14	2731	195	15	14	2792
133007	3		34	W-N-F	12/1/81	12/1/81	3/28/89	5/19/92	1987	1989	3	95	32	8	8	264
133019	3		34	W-N-F	12/1/81	12/1/81	3/27/89	5/20/92	1988	1989	2	424	212	8	8	1765
373008	3		38	W-N-F	6/1/84	6/1/84	3/9/89	3/22/91	1984	1989	6	473	79	6	6	455
373044	3		42	W-N-F	8/1/66	8/1/66	10/13/89	3/15/91	1966	1989	24	18510	771	24	24	18677
13028	3		44	W-N-F	6/1/71	6/1/71	5/23/89	2/7/92	1971	1989	19	2917	154	19	19	2915
133016	3		44	W-N-F	12/1/77	12/1/77	3/29/89	4/6/92	1987	1989	3	3205	1068	12	12	13174
373807	3		45	W-N-F	8/1/80	8/1/80	10/15/89	3/25/91	1980	1989	10	1465	147	10	10	1496
373816	3		46	W-N-F	4/1/73	4/1/73	10/13/89	3/15/91	1975	1989	15	3827	255	18	18	4476
483010	3		48	W-N-F	9/1/84	10/1/84	3/8/90	4/24/91	1984	1989	6	875	146	7	6	939

Evaluation of AASHTO rigid pavement design equation - General Information

st_shrp	exp#	new exp#	cell	region	construction date	traffic open date	distress date	SV date	traffic count start	traffic count end	years of count	KESAL	KESAL/yr	pavement age	years of traffic	estimated KESAL
124109	3		49	W-N-F	3/1/89	3/1/89	12/2/89	7/13/90	1989	1989	1	169	169	2	2	297
124000	3		53	W-N-F	11/1/74	11/1/74	4/13/89	7/4/91	1974	1989	16	4312	270	15	15	4166
124138	3		53	W-N-F	11/1/74	11/1/74	4/13/89	6/29/90	1974	1989	16	4312	270	15	15	4166
133020	3		56	W-N-F	9/1/85	9/1/85	12/16/89	6/14/90	1986	1989	4	256	64	5	5	339
123811	3		61	W-N-F	2/1/76	6/1/76	4/28/89	5/16/91	1989	1989	1	798	798	14	14	11104
283019	3		62	W-N-F	10/1/84	11/1/84	6/6/89	2/11/92	1984	1989	6	413	69	6	6	385
123804	3		64	W-N-F	7/1/85	9/1/85	5/3/89	7/3/90	1989	1989	1	904	904	5	5	4223
463013	3		67	D-F	10/1/76	10/1/76	10/8/89	11/28/90	1976	1989	14	331	24	14	14	332
203013	3		71	D-F	1/1/84	1/1/84	3/9/89	4/16/92	1984	1989	6	627	105	6	6	647
463010	3		83	D-F	9/1/83	9/1/83	5/16/89	8/11/91	1984	1989	6	155	26	7	7	173
163023	3		89	D-F	10/1/83	12/1/83	9/19/89	11/12/90	1983	1989	7	4079	583	7	7	3966
563027	3		91	D-F	6/1/81	6/1/81	10/21/89	11/9/90	1981	1989	9	4553	506	9	9	4753
63005	3		93	D-F	11/1/73	8/1/74	9/7/89	5/10/91	1975	1989	15	14753	984	17	16	15847
63010	3		109	D-N-F	4/1/78	4/1/78	11/19/89	3/9/91	1978	1989	12	3137	261	13	13	3305
63013	3		111	D-N-F	7/1/82	7/1/82	11/19/89	2/20/91	1986	1989	4	2699	675	8	8	5662
63019	3		117	D-N-F	12/1/79	12/1/79	11/19/89	2/20/91	1986	1989	4	2902	726	11	11	7963
63024	3		119	D-N-F	11/1/80	11/1/80	11/19/89	2/20/91	1985	1989	5	2625	525	10	10	5279
67493	3		127	D-N-F	6/1/83	6/1/83	11/19/89	2/20/91	1983	1989	7	3238	463	7	7	3457
264015	4		2	W-F	1/1/85	1/1/85	8/31/89	6/27/91	1985	1989	5	938	188	6	6	1063
364017	4		2	W-F	6/1/73	6/1/73	8/25/89	7/31/91	1975	1989	15	13719	915	17	17	15771
204054	4		5	W-F	1/1/85	11/1/85	5/4/89	5/29/91	1985	1989	5	1865	373	5	5	1681
274082	4		5	W-F	1/1/69	10/1/69	6/15/89	4/14/92	1969	1989	21	5804	276	21	21	5726
295000	4		6	W-F	7/1/77	12/1/77	5/9/89	3/10/91	1978	1989	12	8483	707	13	12	8797
295091	4		6	W-F	7/1/77	12/1/77	5/9/89	3/10/91	1978	1989	12	8483	707	13	12	8797
174074	4		7	W-F	10/1/86	10/1/86	6/25/89	6/12/90	1986	1989	4	387	97	4	4	361
214025	4		8	W-F	1/1/73	1/1/73	10/26/89	1/12/91	1973	1989	17	5587	329	18	18	5859
544004	4		8	W-F	6/1/81	6/1/84	9/28/89	11/14/91	1984	1989	6	4308	718	9	6	4544
274033	4		9	W-F	1/1/81	1/1/84	6/9/89	8/6/91	1981	1989	9	1866	207	9	6	1335
104002	4		10	W-F	6/1/77	6/1/77	10/5/89	3/27/90	1977	1989	13	444	34	13	13	456
364018	4		10	W-F	6/1/74	6/1/74	8/8/89	7/29/91	1976	1989	14	14295	1021	16	16	16539
394018	4		11	W-F	1/1/75	1/1/75	9/27/89	8/16/90	1975	1989	15	2670	178	16	16	2803
544003	4		11	W-F	10/1/82	10/1/82	9/28/89	11/13/91	1982	1989	8	765	96	8	8	765
101201	4		12	W-F	6/1/66	6/1/66	10/5/89	3/27/90	1966	1989	24	2806	117	24	24	2848
204063	4		13	W-F	6/1/81	6/1/81	5/4/89	4/16/92	1981	1989	9	551	61	9	9	547
274054	4		13	W-F	10/1/72	10/1/72	9/14/89	8/4/91	1972	1989	18	5821	323	18	18	5809
94008	4		15	W-F	12/1/86	12/1/86	7/31/89	7/25/91	1988	1989	2	1300	650	4	4	2383
294069	4		16	W-F	10/1/74	10/1/74	3/9/89	2/12/92	1975	1989	15	4142	276	15	15	4265
484146	4		19	W-N-F	8/1/81	10/1/81	3/8/90	4/24/91	1981	1989	9	1025	114	10	9	1075
484152	4		19	W-N-F	12/1/81	12/1/81	3/8/90	4/13/90	1981	1989	9	703	78	9	9	724
224001	4		20	W-N-F	6/1/70	6/1/71	5/26/89	12/12/91	1971	1989	19	6952	366	20	19	6951

Evaluation of AASHTO rigid pavement design equation - General Information																
		new			construction	traffic open	distress	SV	traffic count	traffic count	years of			pavement	years of	estimated
st_shrp	exp#	exp#	cell	region	date	date	date	date	start	end	count	KESAL	KESAL/yr	age	traffic	KESAL
484143	4		20	W-N-F	10/1/70	12/1/70	3/7/90	4/8/91	1970	1989	20	1873	94	20	20	1899
54021	4		22	W-N-F	10/1/70	10/1/70	11/14/89	11/19/90	1970	1989	20	4081	204	20	20	4108
484142	4		22	W-N-F	9/1/76	5/1/77	3/5/90	4/19/90	1977	1989	13	2111	162	15	14	2249
14007	4		23	W-N-F	6/1/70	6/1/70	5/23/89	1/30/92	1977	1989	13	2420	186	20	20	3721
14084	4		24	W-N-F	6/1/70	6/1/70	5/23/89	2/7/92	1976	1989	14	12021	859	20	20	17163
483699	4		24	W-N-F	4/1/73	4/1/73	3/8/90	4/23/91	1973	1989	17	21476	1263	18	18	22670
53059	4		30	W-N-F	2/1/79	2/1/79	3/15/89	8/30/90	1979	1989	11	1133	103	11	11	1146
54019	4		30	W-N-F	3/1/73	4/1/73	11/16/89	11/16/90	1973	1989	17	1696	100	18	18	1760
204052	4		33	D-F	6/1/83	6/1/83	5/9/89	4/16/92	1983	1989	7	704	101	7	7	698
204016	4		34	D-F	6/1/79	6/1/79	5/4/89	4/1/91	1979	1989	11	795	72	11	11	790
314019	4		38	D-F	1/1/76	1/1/76	8/18/89	11/19/89	1981	1989	9	2675	297	15	15	4351
185043	5		1	W-F	1/1/69	1/1/69	6/22/89	6/13/91	1969	1989	21	289	14	21	21	296
175020	5		2	W-F	5/1/86	10/1/86	6/23/89	3/6/91	1986	1989	4	188	47	4	4	175
175854	5		3	W-F	9/1/80	12/1/82	6/24/89	6/16/91	1982	1989	8	637	80	10	8	603
195042	5		5	W-F	9/1/75	12/1/75	9/21/89	5/12/92	1976	1989	14	5306	379	15	15	5615
555040	5		6	W-F	11/1/80	11/1/80	9/12/89	6/20/92	1980	1989	10	4932	493	10	10	4867
195046	5		13	W-F	9/1/75	11/1/75	6/14/89	5/12/92	1976	1989	14	5306	379	15	15	5544
95001	5		15	W-F	7/1/81	11/1/81	7/31/89	7/25/91	1980	1989	10	7970	797	9	9	6974
105004	5		15	W-F	6/1/77	6/1/77	10/5/89	3/28/90	1977	1989	13	9514	732	13	13	9773
285006	5		17	W-N-F	7/1/79	4/1/79	1/10/90	2/12/92	1980	1989	10	1477	148	12	12	1741
485026	5		19	W-N-F	11/1/85	6/1/88	6/13/90	4/23/91	1988	1989	2	214	107	6	3	325
483719	5		21	W-N-F	9/1/64	1/1/65	3/7/90	12/16/91	1965	1989	25	7992	320	27	26	8374
485035	5		21	W-N-F	9/1/79	9/1/79	1/25/89	3/12/90	1979	1989	11	8393	763	10	10	7941
375037	5		22	W-N-F	10/1/72	10/1/72	11/3/89	10/30/91	1973	1989	17	5742	338	18	18	6114
455017	5		23	W-N-F	2/1/79	3/1/79	1/9/89	4/29/92	1979	1989	11	3894	354	11	11	3847
485024	5		23	W-N-F	7/1/81	1/1/82	4/11/89	4/25/91	1982	1989	8	1109	139	9	8	1148
285803	5		25	W-N-F	12/1/79	9/1/79	1/10/90	2/13/92	1979	1989	11	3222	293	11	11	3330
485154	5		29	W-N-F	7/1/71	8/1/71	4/11/89	4/9/91	1971	1989	19	8136	428	19	19	8010
415022	5		32	W-N-F	10/1/84	10/1/84	9/8/89	11/18/89	1984	1989	6	10879	1813	6	6	10770
465025	5		33	D-F	11/1/74	11/1/74	10/6/89	11/27/90	1974	1989	16	555	35	16	16	553
165025	5		41	D-F	9/1/72	9/1/72	9/20/89	10/3/90	1972	1989	18	13536	752	18	18	13583
417081	5		48	D-F	9/1/88	9/1/88	9/18/89	10/21/89	1988	1989	2	879	440	2	2	899
485287	5		49	D-N-F	8/1/73	8/1/73	3/21/89	10/18/91	1973	1989	17	3115	183	17	17	3050
485301	5		51	D-N-F	2/1/82	2/1/82	3/21/89	10/17/91	1982	1989	8	1389	174	8	8	1413
485336	5		51	D-N-F	8/1/83	12/1/86	1/11/90	10/26/90	1986	1989	4	1061	265	7	4	1092
67455	5		53	D-N-F	5/1/71	12/1/71	8/28/89	5/1/91	1972	1989	18	7207	400	19	19	7509
485328	5		53	D-N-F	9/1/75	9/1/75	3/21/89	11/1/90	1975	1989	15	6652	443	15	15	6458
485310	5		55	D-N-F	7/1/87	7/1/87	3/21/89	10/18/91	1987	1989	3	1398	466	3	3	1269
485323	5		55	D-N-F	5/1/79	10/1/80	4/24/89	11/13/91	1980	1989	10	5471	547	11	10	5234
485335	5		55	D-N-F	5/1/79	10/1/80	4/24/89	11/12/91	1980	1989	10	5560	556	11	10	5319

Evaluation of AASHTO rigid pavement design equation - General Information

st_shrp	exp#	new exp#	cell	region	construction date	traffic open date	distress date	SV date	traffic count start	traffic count end	years of count	KESAL	KESAL/yr	pavement age	years of traffic	estimated KESAL
485274	5		57	D-N-F	3/1/73	3/1/73	3/21/89	10/17/91	1973	1989	17	4421	260	17	17	4438
485317	5		57	D-N-F	4/1/82	4/1/82	4/24/89	10/17/91	1982	1989	8	3169	396	8	8	3196
485284	5		59	D-N-F	10/1/87	3/1/88	3/22/89	10/22/91	1988	1989	2	439	220	2	2	452

Evaluation of AASHTO rigid pavement design equation - Distress Data

		new			lane	longitudinal cracking			transverse cracking			AC patch			PCC patch		
st_shrp	exp#	exp#	cell	region	width	H	M	L	H	M	L	H	M	L	H	M	L
183002	3		2	W-F	12	0	0	0	0	0	0	0	0	0	0	0	0
273003	3		2	W-F	14	0	0	0	0	0	0	0	0	0	0	0	0
193055	3		3	W-F	12	0	0	0	0	0	0	0	0	0	0	0	0
233013	3		4	W-F	12	0	0	0	0	0	0	0	0	0	0	0	0
393013	3		5	W-F	12	0	0	0	0	0	0	0	7.24	6.2	0	0	0
183030	3		6	W-F	12	0	0	0	0	0	0	0	0	0	0	0	0
393801	3		6	W-F	12	0	0	0	0	0	0	0	0	0	0	0	0
183031	3		8	W-F	12	0	0	0	0	0	0	0	0	0	0	0	0
193033	3		8	W-F	12	0	0	0	0	0	0	0	0	0	0	0	0
553009	3		9	W-F	12	0	0	0	0	0	0	0	0	1.04	0	0	0
893015	3		10	W-F	12	0	183.99	41.35	0	0	4.13	0	5.17	42.38	0	0	0
893016	3		10	W-F	12	0	0	0	0	0	0	0	0	0	0	0	0
553008	3		11	W-F	12	0	0	0	13.51	0	0	0	0	0	0	0	0
553010	3		11	W-F	12	0	0	0	0	0	0	0	0	0	0	0	0
423044	3		12	W-F	12	0	0	0	0	0	0	0	0	0	0	0	0
193006	3		14	W-F	12	0	0	0	0	13.29	26.58	0	0	0	0	0	0
193028	3		16	W-F	12	0	0	0	0	0	0	0	0	0	0	0	0
843803	3		17	W-F	12	13.63	0	0	4.19	0	0	0	0	3.15	0	25.17	0
263069	3		18	W-F	12	0	0	0	0	0	0	0	0	0	0	0	0
273013	3		18	W-F	14	0	0	0	0	0	0	0	0	0	0	0	0
553014	3		19	W-F	12	0	0	0	0	0	0	0	0	0	0	0	0
233014	3		20	W-F	12	0	0	0	0	0	0	0	0	0	0	0	0
893001	3		21	W-F	12	0	11.35	5.16	0	0	0	0	0	0	0	0	0
553015	3		25	W-F	12	0	0	0	0	0	0	0	0	0	0	0	0
193009	3		32	W-F	12	0	0	0	0	0	0	0	0	0	0	0	0
133007	3		34	W-N-F	12	0	0	0	0	0	0	0	0	0	0	0	0
133019	3		34	W-N-F	12	0	0	0	0	0	0	0	0	0	0	0	2.05
373008	3		38	W-N-F	14	0	0	0	0	0	0	0	0	0	0	0	0
373044	3		42	W-N-F	12	0	0	10.37	0	0	0	0	0	0	0	0	0
13028	3		44	W-N-F	12	0	0	0	0	0	0	0	0	0	0	0	0
133016	3		44	W-N-F	12	0	0	0	0	0	0	0	0	0	0	0	0
373807	3		45	W-N-F	12	0	0	0	0	0	12.4	0	0	0	0	0	0
373816	3		46	W-N-F	12	0	0	0	0	0	0	0	0	0	0	0	0
483010	3		48	W-N-F	12	0	0	0	0	0	0	0	0	0	0	0	0

Evaluation of AASHTO rigid pavement design equation - Distress Data																		
		new			lane	longitudinal cracking			transverse cracking			AC patch			PCC patch		
st_shrp	exp#	exp#	cell	region	width	H	M	L	H	M	L	H	M	L	H	M	L
124109	3		49	W-N-F	12	0	0	0	0	0	0	0	0	0	0	0	0
124000	3		53	W-N-F	12	0	0	0	0	0	0	0	0	0	0	0	0
124138	3		53	W-N-F	12	0	0	4.23	25.39	11.64	0	0	0	0	0	0	0
133020	3		56	W-N-F	12	0	0	0	0	0	0	0	0	0	0	0	0
123811	3		61	W-N-F	12	0	0	0	0	27.14	94.98	0	0	1.04	0	0	0
283019	3		62	W-N-F	12	0	0	0	0	0	0	0	0	0	0	0	0
123804	3		64	W-N-F	12	0	0	0	26.79	112.33	40.19	0	0	0	0	0	0
463013	3		67	D-F	12	0	0	0	0	0	0	0	0	0	0	0	0
203013	3		71	D-F	12	0	0	0	0	9.52	0	0	0	0	0	0	0
463010	3		83	D-F	12	0	0	0	0	0	0	0	0	0	0	0	0
163023	3		89	D-F	12	0	0	0	0	0	0	0	0	0	0	0	0
563027	3		91	D-F	12	0	0	0	0	0	0	0	0	0	0	0	0
63005	3		93	D-F	12	0	88.04	32.11	232	100.46	42.46	0	0	0	0	0	500.25
63010	3		109	D-N-F	12	0	0	0	0	0	0	0	0	0	0	0	214.14
63013	3		111	D-N-F	12	0	0	0	0	0	0	0	0	0	0	0	0
63019	3		117	D-N-F	12	0	0	0	0	0	0	0	0	0	0	0	0
63024	3		119	D-N-F	12	0	0	0	0	0	0	0	0	0	0	0	0
67493	3		127	D-N-F	12	0	0	5.2	0	0	0	0	0	1.04	0	0	0
264015	4		2	W-F	12	0	0	0	0	0	0	0	0	0	0	0	0
364017	4		2	W-F	12	0	0	0	62.02	163.31	73.39	0	0	0	0	0	0
204054	4		5	W-F	12	0	0	0	0	0	135.3	0	0	0	0	0	0
274082	4		5	W-F	12	0	0	0	0	0	13.47	0	71.51	100.53	0	0	0
295000	4		6	W-F	12	0	0	0	0	13.44	13.44	0	0	0	0	0	0
295091	4		6	W-F	12	0	0	0	0	0	12.25	0	0	0	0	0	0
174074	4		7	W-F	12	0	0	0	0	54.18	54.18	0	0	0	0	0	0
214025	4		8	W-F	12	0	0	0	76.68	39.88	133.9	0	7.16	6.13	0	0	0
544004	4		8	W-F	12	0	0	0	187	5.16	12.39	0	0	0	0	0	0
274033	4		9	W-F	12	0	0	0	0	13.54	0	0	0	0	0	0	0
104002	4		10	W-F	12	0	0	0	0	0	0	0	7.13	28.52	0	0	0
364018	4		10	W-F	12	0	0	19.55	0	0	0	0	0	0	0	0	0
394018	4		11	W-F	12	0	0	0	0	24.54	245.4	0	0	0	0	0	0
544003	4		11	W-F	12	0	0	0	0	0	0	0	0	0	0	0	0
101201	4		12	W-F	12	0	0	0	0	13.29	0	0	2.04	0	0	0	0
204063	4		13	W-F	12	0	0	0	0	27.01	188.1	0	0	0	0	0	0
274054	4		13	W-F	12	0	0	3.1	0	0	0	0	0	11.38	0	0	0
94008	4		15	W-F	12	0	0	0	0	13.35	0	0	0	0	0	0	0
294069	4		16	W-F	12	0	0	16.58	0	13.47	296.3	0	0	24.87	0	0	0
484146	4		19	W-N-F	12	0	0	0	0	0	0	0	0	0	0	0	0
484152	4		19	W-N-F	12	0	0	0	0	120.91	13.43	0	4.13	0	0	0	0
224001	4		20	W-N-F	12	0	0	0	0	13.53	46.84	0	0	0	0	0	0

Evaluation of AASHTO rigid pavement design equation - Distress Data

		new			lane	longitudinal cracking			transverse cracking			AC patch			PCC patch		
st_shrp	exp#	exp#	cell	region	width	H	M	L	H	M	L	H	M	L	H	M	L
484143	4		20	W-N-F	12	0	0	0	0	0	25.18	0	0	0	0	0	0
54021	4		22	W-N-F	12	0	0	0	0	0	0	0	0	0	0	0	0
484142	4		22	W-N-F	12	0	0	0	0	0	0	0	0	0	0	0	0
14007	4		23	W-N-F	12	0	0	0	0	13.46	0	0	1.04	0	0	0	0
14084	4		24	W-N-F	12	0	0	0	54.48	81.72	40.86	0	0	0	0	0	0
483699	4		24	W-N-F	12	0	0	0	0	25.03	5.21	0	0	8.34	0	0	0
53059	4		30	W-N-F	12	0	0	0	0	0	0	0	0	1.05	0	0	0
54019	4		30	W-N-F	12	0	0	0	0	0	0	0	0	2.06	0	0	0
204052	4		33	D-F	12	0	0	0	0	0	0	0	0	0	0	0	0
204016	4		34	D-F	12	0	0	0	0	13.56	27.13	0	0	0	0	0	0
314019	4		38	D-F	12	0	0	0	0	0	212.9	0	0	0	0	1.04	0
185043	5		1	W-F	12	0	0	0	0	1229.6	170.9	0	0	0	0	0	0
175020	5		2	W-F	12	0	0	0	0	0	169.7	0	0	0	0	0	0
175854	5		3	W-F	12	0	0	0	0	1094	489.5	0	0	0	0	0	0
195042	5		5	W-F	12	0	0	0	0	510.97	1057	0	0	0	0	0	0
555040	5		6	W-F	12	0	0	9.33	0	134.8	1085	0	0	0	0	0	0
195046	5		13	W-F	12	0	0	0	0	12.57	100.6	0	0	0	0	0	6.28
95001	5		15	W-F	12	0	0	0	0	691.96	504.4	0	0	0	0	0	0
105004	5		15	W-F	12	14.02	28.04	82.94	0	387.83	732.4	0	0	0	0	0	0
285006	5		17	W-N-F	12	0	0	0	0	831.47	691.4	0	0	0	0	0	0
485026	5		19	W-N-F	12	0	0	0	0	254.91	849.7	0	0	0	0	0	0
483719	5		21	W-N-F	12	0	0	0	13.62	908.29	340.5	0	0	0	0	0	0
485035	5		21	W-N-F	12	0	0	0	0	889.76	385.9	0	0	0	0	0	0
375037	5		22	W-N-F	12	0	0	0	0	878.74	304.5	0	0	0	0	0	0
455017	5		23	W-N-F	12	0	0	0	0	66.84	1122	0	0	0	0	0	0
485024	5		23	W-N-F	12	0	0	0	12.44	472.87	510.2	0	0	0	0	0	0
285803	5		25	W-N-F	12	0	0	0	0	905.02	147.7	0	0	0	0	0	0
485154	5		29	W-N-F	12	0	0	0	0	1063	265	0	0	0	0	0	0
415022	5		32	W-N-F	13	0	0	0	0	1112.5	0	0	0	0	0	0	0
465025	5		33	D-F	12	0	0	0	0	2926	0	0	0	0	0	0	0
165025	5		41	D-F	12	0	0	0	0	280.78	1310	0	0	0	0	0	0
417081	5		48	D-F	12	0	0	0	0	0	27.2	0	0	0	0	0	0
485287	5		49	D-N-F	12	0	0	0	0	742.3	673.4	0	0	0	0	0	0
485301	5		51	D-N-F	12	0	0	0	0	680	507.4	0	0	4.18	0	0	0
485336	5		51	D-N-F	12	0	0	0	0	1125.6	13.59	0	0	0	0	0	0
67455	5		53	D-N-F	12	0	0	0	0	25.03	1745	0	0	0	0	0	0
485328	5		53	D-N-F	12	0	0	0	0	663.33	903.3	0	0	0	0	0	0
485310	5		55	D-N-F	12	0	0	0	0	579.25	304.3	0	0	0	0	0	0
485323	5		55	D-N-F	12	0	0	0	0	1873.5	329	0	0	0	0	0	0
485335	5		55	D-N-F	12	0	0	0	0	1980.3	117.5	0	0	0	0	0	0

Evaluation of AASHTO rigid pavement design equation - Distress Data

		new			lane	longitudinal cracking			transverse cracking			AC patch			PCC patch		
st_shrp	exp#	exp#	cell	region	width	H	M	L	H	M	L	H	M	L	H	M	L
485274	5		57	D-N-F	12	0	0	0	0	711.28	189.8	0	0	0	0	0	0
485317	5		57	D-N-F	12	0	0	0	0	502.99	302.2	0	0	0	0	0	0
485284	5		59	D-N-F	12	0	0	0	0	38.46	256.4	0	0	0	0	0	0

Evaluation of AASHTO rigid pavement design equation - Calculated PSI														
		new			Cracks	Patch	C	P	SV	SV	SV	Calculated	initial	Loss
st_shrp	exp#	exp#	cell	region	ft/sect	ft2/sect	ft/1000ft2	ft2/1000ft2	left	right	average	PSI	PSI	PSI
183002	3		2	W-F	0	0	0.00	0.00	3.97	4.95	4.46	4.10	4.25	0.15
273003	3		2	W-F	0	0	0.00	0.00	5.94	5.71	5.82	3.93	4.25	0.32
193055	3		3	W-F	0	0	0.00	0.00	4.8	4.3	4.55	4.09	4.25	0.16
233013	3		4	W-F	0	0	0.00	0.00	5.01	8.74	6.87	3.82	4.25	0.43
393013	3		5	W-F	0	13.44	0.00	2.24	18.67	18.42	18.54	2.98	4.25	1.27
183030	3		6	W-F	0	0	0.00	0.00	4.37	3.14	3.75	4.21	4.25	0.04
393801	3		6	W-F	0	0	0.00	0.00	4.87	6.26	5.56	3.96	4.25	0.29
183031	3		8	W-F	0	0	0.00	0.00	3.72	3.28	3.5	4.25	4.25	0.00
193033	3		8	W-F	0	0	0.00	0.00	5.54	4.38	4.96	4.03	4.25	0.22
553009	3		9	W-F	0	1.04	0.00	0.17	18.38	12.34	15.36	3.21	4.25	1.04
893015	3		10	W-F	183.99	47.55	30.67	7.93	3.02	11.42	7.22	3.22	4.25	1.03
893016	3		10	W-F	0	0	0.00	0.00	8.69	12.53	10.61	3.51	4.25	0.74
553008	3		11	W-F	13.51	0	2.25	0.00	28.8	23.2	26	2.73	4.25	1.52
553010	3		11	W-F	0	0	0.00	0.00	8.11	6.47	7.29	3.77	4.25	0.48
423044	3		12	W-F	0	0	0.00	0.00	5.75	8.67	7.21	3.78	4.25	0.47
193006	3		14	W-F	13.29	0	2.22	0.00	12.38	12.46	12.42	3.27	4.25	0.98
193028	3		16	W-F	0	0	0.00	0.00	4.8	5.65	5.22	4.00	4.25	0.25
843803	3		17	W-F	17.82	28.32	2.97	4.72	15.02	11.09	13.06	3.12	4.25	1.13
263069	3		18	W-F	0	0	0.00	0.00	3.48	3.87	3.67	4.22	4.25	0.03
273013	3		18	W-F	0	0	0.00	0.00	4	4.28	4.14	4.14	4.25	0.11
553014	3		19	W-F	0	0	0.00	0.00	25.9	19.03	22.46	2.97	4.25	1.28
233014	3		20	W-F	0	0	0.00	0.00	4.33	5.12	4.72	4.06	4.25	0.19
893001	3		21	W-F	11.35	0	1.89	0.00	12.14	7.16	9.65	3.46	4.25	0.79
553015	3		25	W-F	0	0	0.00	0.00	7.58	5.63	6.6	3.84	4.25	0.41
193009	3		32	W-F	0	0	0.00	0.00	7.83	8.22	8.03	3.71	4.25	0.54
133007	3		34	W-N-F	0	0	0.00	0.00	4.76	5.02	4.89	4.04	4.25	0.21
133019	3		34	W-N-F	0	2.05	0.00	0.34	3.66	3.79	3.72	4.16	4.25	0.09
373008	3		38	W-N-F	0	0	0.00	0.00	5.65	5.52	5.58	3.95	4.25	0.30
373044	3		42	W-N-F	0	0	0.00	0.00	6.07	6.23	6.15	3.89	4.25	0.36
13028	3		44	W-N-F	0	0	0.00	0.00	14.94	17.63	16.29	3.21	4.25	1.04
133016	3		44	W-N-F	0	0	0.00	0.00	3.84	3.23	3.54	4.24	4.25	0.01
373807	3		45	W-N-F	0	0	0.00	0.00	5.62	7.27	6.45	3.86	4.25	0.39
373816	3		46	W-N-F	0	0	0.00	0.00	8.19	6.9	7.55	3.75	4.25	0.50
483010	3		48	W-N-F	0	0	0.00	0.00	9.14	5.01	7.07	3.80	4.25	0.45

Evaluation of AASHTO rigid pavement design equation - Calculated PSI														
		new			Cracks	Patch	C	P	SV	SV	SV	Calculated	initial	Loss
st_shrp	exp#	exp#	cell	region	ft/sect	ft2/sect	ft/1000ft2	ft2/1000ft2	left	right	average	PSI	PSI	PSI
124109	3		49	W-N-F	0	0	0.00	0.00	6.42	9.96	8.19	3.70	4.25	0.55
124000	3		53	W-N-F	0	0	0.00	0.00	3.95	3.65	3.8	4.20	4.25	0.05
124138	3		53	W-N-F	37.03	0	6.17	0.00	11.54	16.68	14.11	3.09	4.25	1.16
133020	3		56	W-N-F	0	0	0.00	0.00	3.59	4.02	3.81	4.20	4.25	0.05
123811	3		61	W-N-F	27.14	1.04	4.52	0.17	5.62	5.75	5.69	3.75	4.25	0.50
283019	3		62	W-N-F	0	0	0.00	0.00	5.8	5.78	5.79	3.93	4.25	0.32
123804	3		64	W-N-F	139.12	0	23.19	0.00	4.09	4.09	4.09	3.72	4.25	0.53
463013	3		67	D-F	0	0	0.00	0.00	4.22	4.16	4.19	4.14	4.25	0.11
203013	3		71	D-F	9.52	0	1.59	0.00	4.27	3.96	4.12	4.03	4.25	0.22
463010	3		83	D-F	0	0	0.00	0.00	23.88	5.07	14.47	3.29	4.25	0.96
163023	3		89	D-F	0	0	0.00	0.00	3.92	3.77	3.85	4.19	4.25	0.06
563027	3		91	D-F	0	0	0.00	0.00	13.11	8.86	10.98	3.49	4.25	0.76
63005	3		93	D-F	420.5	500.25	70.08	83.38	15.03	8.16	11.59	2.34	4.25	1.91
63010	3		109	D-N-F	0	214.14	0.00	35.69	3.1	2.6	2.85	3.83	4.25	0.42
63013	3		111	D-N-F	0	0	0.00	0.00	4.24	4.42	4.33	4.12	4.25	0.13
63019	3		117	D-N-F	0	0	0.00	0.00	3.87	3.32	3.59	4.23	4.25	0.02
63024	3		119	D-N-F	0	0	0.00	0.00	4.06	4.45	4.26	4.13	4.25	0.12
67493	3		127	D-N-F	0	1.04	0.00	0.17	4.16	3.59	3.87	4.15	4.25	0.10
264015	4		2	W-F	0	0	0.00	0.00	4.06	3.32	3.69	4.22	4.25	0.03
364017	4		2	W-F	225.33	0	37.56	0.00	6.32	10.01	8.17	3.15	4.25	1.10
204054	4		5	W-F	0	0	0.00	0.00	5.28	3.78	4.53	4.09	4.25	0.16
274082	4		5	W-F	0	172.04	0.00	28.67	18.35	7.1	12.72	2.90	4.25	1.35
295000	4		6	W-F	13.44	0	2.24	0.00	7.64	6.17	6.9	3.68	4.25	0.57
295091	4		6	W-F	0	0	0.00	0.00	4.84	3.74	4.29	4.12	4.25	0.13
174074	4		7	W-F	54.18	0	9.03	0.00	4.17	4.79	4.48	3.82	4.25	0.43
214025	4		8	W-F	116.56	13.29	19.43	2.22	12.98	10.64	11.81	3.02	4.25	1.23
544004	4		8	W-F	192.16	0	32.03	0.00	16.87	25.6	21.23	2.50	4.25	1.75
274033	4		9	W-F	13.54	0	2.26	0.00	5.9	4.5	5.2	3.86	4.25	0.39
104002	4		10	W-F	0	35.65	0.00	5.94	7.74	11.49	9.61	3.36	4.25	0.89
364018	4		10	W-F	0	0	0.00	0.00	5.7	5.63	5.66	3.94	4.25	0.31
394018	4		11	W-F	24.54	0	4.09	0.00	3.95	3.73	3.84	4.01	4.25	0.24
544003	4		11	W-F	0	0	0.00	0.00	6.04	11.23	8.64	3.66	4.25	0.59
101201	4		12	W-F	13.29	2.04	2.22	0.34	7	8.71	7.86	3.58	4.25	0.67
204063	4		13	W-F	27.01	0	4.50	0.00	5.23	5.04	5.13	3.82	4.25	0.43
274054	4		13	W-F	0	11.38	0.00	1.90	5.63	5.12	5.38	3.85	4.25	0.40
94008	4		15	W-F	13.35	0	2.23	0.00	5.12	6.77	5.94	3.78	4.25	0.47
294069	4		16	W-F	13.47	24.87	2.25	4.15	4.09	4.06	4.07	3.93	4.25	0.32
484146	4		19	W-N-F	0	0	0.00	0.00	10.5	6.71	8.61	3.66	4.25	0.59
484152	4		19	W-N-F	120.91	4.13	20.15	0.69	12	8.15	10.08	3.14	4.25	1.11
224001	4		20	W-N-F	13.53	0	2.26	0.00	6.58	7.12	6.85	3.68	4.25	0.57

Evaluation of AASHTO rigid pavement design equation - Calculated PSI														
		new			Cracks	Patch	C	P	SV	SV	SV	Calculated	initial	Loss
st_shrp	exp#	exp#	cell	region	ft/sect	ft2/sect	ft/1000ft2	ft2/1000ft2	left	right	average	PSI	PSI	PSI
484143	4		20	W-N-F	0	0	0.00	0.00	6.53	6.61	6.57	3.85	4.25	0.40
54021	4		22	W-N-F	0	0	0.00	0.00	6.29	5.82	6.06	3.90	4.25	0.35
484142	4		22	W-N-F	0	0	0.00	0.00	6.43	7.6	7.02	3.80	4.25	0.45
14007	4		23	W-N-F	13.46	1.04	2.24	0.17	4.2	4.64	4.42	3.96	4.25	0.29
14084	4		24	W-N-F	136.2	0	22.70	0.00	14.88	18.25	16.56	2.77	4.25	1.48
483699	4		24	W-N-F	25.03	8.34	4.17	1.39	4.86	6.57	5.71	3.73	4.25	0.52
53059	4		30	W-N-F	0	1.05	0.00	0.18	4.08	3.94	4.01	4.13	4.25	0.12
54019	4		30	W-N-F	0	2.06	0.00	0.34	4.77	4.09	4.43	4.05	4.25	0.20
204052	4		33	D-F	0	0	0.00	0.00	4.06	12.66	8.36	3.68	4.25	0.57
204016	4		34	D-F	13.56	0	2.26	0.00	3.31	3.04	3.17	4.17	4.25	0.08
314019	4		38	D-F	0	1.04	0.00	0.17	5.33	4.21	4.77	4.02	4.25	0.23
185043	5		1	W-F	1229.6	0	204.93	0.00	6.54	6.14	6.34	3.87	4.25	0.38
175020	5		2	W-F	0	0	0.00	0.00	3.57	3.47	3.52	4.24	4.25	0.01
175854	5		3	W-F	1094	0	182.33	0.00	6.24	5.98	6.11	3.89	4.25	0.36
195042	5		5	W-F	510.97	0	85.16	0.00	4.01	4.62	4.31	4.12	4.25	0.13
555040	5		6	W-F	134.8	0	22.47	0.00	8.34	6.29	7.32	3.77	4.25	0.48
195046	5		13	W-F	12.57	6.28	2.10	1.05	4.24	3.88	4.06	4.16	4.25	0.09
95001	5		15	W-F	691.96	0	115.33	0.00	7.37	6.35	6.86	3.82	4.25	0.43
105004	5		15	W-F	429.89	0	71.65	0.00	5.56	5.14	5.35	3.98	4.25	0.27
285006	5		17	W-N-F	831.47	0	138.58	0.00	4.86	4.56	4.71	4.06	4.25	0.19
485026	5		19	W-N-F	254.91	0	42.49	0.00	4.31	3.22	3.76	4.20	4.25	0.05
483719	5		21	W-N-F	921.91	0	153.65	0.00	6.28	7.26	6.77	3.83	4.25	0.42
485035	5		21	W-N-F	889.76	0	148.29	0.00	4.54	4.84	4.69	4.07	4.25	0.18
375037	5		22	W-N-F	878.74	0	146.46	0.00	4.27	4.47	4.37	4.11	4.25	0.14
455017	5		23	W-N-F	66.84	0	11.14	0.00	5.85	5.12	5.49	3.96	4.25	0.29
485024	5		23	W-N-F	485.31	0	80.89	0.00	8.54	11.03	9.78	3.57	4.25	0.68
285803	5		25	W-N-F	905.02	0	150.84	0.00	4.57	4.16	4.36	4.11	4.25	0.14
485154	5		29	W-N-F	1063	0	177.17	0.00	4.4	3.5	3.95	4.17	4.25	0.08
415022	5		32	W-N-F	1112.5	0	171.15	0.00	8.59	1.44	5.01	4.02	4.25	0.23
465025	5		33	D-F	2926	0	487.67	0.00	6.46	2.86	4.66	4.07	4.25	0.18
165025	5		41	D-F	280.78	0	46.80	0.00	6.09	6.9	6.49	3.85	4.25	0.40
417081	5		48	D-F	0	0	0.00	0.00	9.58	7.56	8.57	3.66	4.25	0.59
485287	5		49	D-N-F	742.3	0	123.72	0.00	4.52	5.02	4.77	4.06	4.25	0.19
485301	5		51	D-N-F	680	4.18	113.33	0.70	5.29	5.88	5.58	3.95	4.25	0.30
485336	5		51	D-N-F	1125.6	0	187.60	0.00	11.45	3.18	7.31	3.77	4.25	0.48
67455	5		53	D-N-F	25.03	0	4.17	0.00	3.23	3.9	3.56	4.24	4.25	0.01
485328	5		53	D-N-F	663.33	0	110.56	0.00	4.06	4.52	4.29	4.12	4.25	0.13
485310	5		55	D-N-F	579.25	0	96.54	0.00	5.66	8.16	6.91	3.81	4.25	0.44
485323	5		55	D-N-F	1873.5	0	312.25	0.00	6.1	5.26	5.68	3.94	4.25	0.31
485335	5		55	D-N-F	1980.3	0	330.05	0.00	7.37	6.44	6.9	3.81	4.25	0.44

Evaluation of AASHTO rigid pavement design equation - Calculated PSI														
		new			Cracks	Patch	C	P	SV	SV	SV	Calculated	initial	Loss
st_shrp	exp#	exp#	cell	region	ft/sect	ft2/sect	ft/1000ft2	ft2/1000ft2	left	right	average	PSI	PSI	PSI
485274	5		57	D-N-F	711.28	0	118.55	0.00	4.53	19.62	12.07	3.42	4.25	0.83
485317	5		57	D-N-F	502.99	0	83.83	0.00	6.96	7.13	7.04	3.80	4.25	0.45
485284	5		59	D-N-F	38.46	0	6.41	0.00	7.9	7.63	7.77	3.73	4.25	0.52

Evaluation of AASHTO rigid pavement design equation - Load Transfer and Drainage Coefficient												
st_shrp	exp#	new exp#	cell	region	shoulder material	dowels	J	subgrade	base	drain type	drain loc	Cd
183002	3		2	W-F	JPCP	Yes	2.80	fine	crush stone	none	continuous	0.70
273003	3		2	W-F	Sand AC	No	4.10	fine	crush stone	none	none	0.70
193055	3		3	W-F	Sand AC	No	4.10	fine	crush stone	none	none	0.70
233013	3		4	W-F	Sand AC	Yes	3.20	fine	crush stone	none	none	0.70
393013	3		5	W-F	JRCP	No	3.90	fine	cement-aggregate	none	none	0.80
183030	3		6	W-F	Sand AC	Yes	3.20	fine	other		intermittent	0.70
393801	3		6	W-F	JPCP	Yes	2.80	fine	cement-aggregate	longitudinal	continuous	0.90
183031	3		8	W-F	CRCP	Yes	2.80	fine	none	longitudinal	continuous	0.80
193033	3		8	W-F	Open AC	Yes	3.20	fine	cement-aggregate	longitudinal	intermittent	0.90
553009	3		9	W-F	Sand AC	No	4.10	fine	crush stone	none	none	0.70
893015	3		10	W-F	Open AC	Yes	3.20	fine	crush stone	none	none	0.70
893016	3		10	W-F	Open AC	Yes	3.20	fine	crush stone	transverse		0.70
553008	3		11	W-F	Sand AC	No	4.10	fine	crush stone		continuous	0.70
553010	3		11	W-F	JPCP	No	3.90	fine	crush stone	none	none	0.70
423044	3		12	W-F	JPCP	Yes	2.80	fine	crush stone	longitudinal	intermittent	0.80
193006	3		14	W-F	Open AC	Yes	3.20	fine	cement-aggregate	none	none	0.80
193028	3		16	W-F	Open AC	Yes	3.20	fine	lean concrete	longitudinal	intermittent	0.90
843803	3		17	W-F	JPCP	Yes	2.80	coarse	gravel	none	none	0.90
263069	3		18	W-F	Sand AC	Yes	3.20	coarse	sand	none	none	0.90
273013	3		18	W-F	Sand AC	No	4.10	coarse	crush stone	none	none	0.90
553014	3		19	W-F	Sand AC	No	4.10	coarse	crush stone		continuous	0.90
233014	3		20	W-F	Sand AC	Yes	3.20	coarse	crush stone	none	none	0.90
893001	3		21	W-F	Sand AC	No	4.10	coarse	soil cement	none	none	1.00
553015	3		25	W-F	Sand AC	No	4.10	coarse	crush stone	none	none	0.90
193009	3		32	W-F	JPCP	Yes	2.80	fine	soil cement	longitudinal	intermittent	0.90
133007	3		34	W-N-F	Sand AC	Yes	3.20	fine	crush stone	none	none	0.80
133019	3		34	W-N-F	CRCP	Yes	2.80	fine	crush stone	none	none	0.80
373008	3		38	W-N-F	Dense AC	Yes	3.20	fine	lean concrete	none	none	0.80
373044	3		42	W-N-F	Sand AC	Yes	3.20	fine	crush stone	other	continuous	0.80
13028	3		44	W-N-F	JRCP	No	3.90	fine	crush stone	blanket	continuous	1.10
133016	3		44	W-N-F	JPCP	Yes	2.80	fine	crush stone	longitudinal	continuous	0.90
373807	3		45	W-N-F	JPCP	No	3.90	fine	lean concrete	none	none	0.90
373816	3		46	W-N-F	Sand AC	Yes	3.20	fine	cement-aggregate	none	none	0.90
483010	3		48	W-N-F	JRCP	Yes	2.80	fine	cement-aggregate	none	none	0.90

Evaluation of AASHTO rigid pavement design equation - Load Transfer and Drainage Coefficient

st_shrp	exp#	new exp#	cell	region	shoulder material	dowels	J	subgrade	base	drain type	drain loc	Cd
124109	3		49	W-N-F	Sand AC	Yes	3.20	coarse	lime rock	longitudinal	continuous	1.10
124000	3		53	W-N-F	Dense AC	No	4.10	coarse	soil cement	none	none	1.10
124138	3		53	W-N-F	Dense AC	No	4.10	coarse	soil cement	none	none	1.10
133020	3		56	W-N-F	Sand AC	Yes	3.20	coarse	soil cement	none	none	1.10
123811	3		61	W-N-F	Sand AC	No	4.10	coarse	soil cement	longitudinal	intermittent	1.20
283019	3		62	W-N-F	Open AC	Yes	3.20	coarse	cement-aggregate	none	none	1.10
123804	3		64	W-N-F	JPCP	Yes	2.80	coarse	lean concrete	none	none	1.10
463013	3		67	D-F	Sand AC	No	4.10	fine	crush stone	none	none	0.90
203013	3		71	D-F	JPCP	No	3.90	fine	cement-aggregate	none	none	1.00
463010	3		83	D-F	JPCP	No	3.90	coarse	crush stone	none	none	1.10
163023	3		89	D-F	JPCP	No	3.90	coarse	crush stone	none	none	1.10
563027	3		91	D-F	JPCP	No	3.90	fine	crush stone	none	none	0.90
63005	3		93	D-F	Sand AC	No	4.10	coarse	cement-aggregate	longitudinal	continuous	1.15
63010	3		109	D-N-F	JPCP	No	3.90	fine	cement-aggregate	none	none	1.10
63013	3		111	D-N-F	JPCP	No	3.90	fine	lean concrete	longitudinal	continuous	1.20
63019	3		117	D-N-F	Sand AC	No	4.10	coarse	cement-aggregate	longitudinal	continuous	1.25
63024	3		119	D-N-F	JPCP	No	3.90	coarse	cement-aggregate	longitudinal	continuous	1.25
67493	3		127	D-N-F	Sand AC	No	4.10	coarse	cement-aggregate	none	none	1.25
264015	4		2	W-F	JPCP	Yes	2.80	fine	crush stone	longitudinal	continuous	0.80
364017	4		2	W-F	Sand AC	Yes	3.20	fine	crush stone	none	none	0.70
204054	4		5	W-F	JPCP	Yes	2.80	fine	cement-aggregate	none	none	0.80
274082	4		5	W-F	Sand AC	Yes	3.20	fine	crush stone	none	none	0.70
295000	4		6	W-F	JRCP	Yes	2.80	fine	crush stone	none	none	0.70
295091	4		6	W-F	JRCP	Yes	2.80	fine	cement-aggregate	none	none	0.80
174074	4		7	W-F	JPCP	Yes	2.80	fine	cement-aggregate	longitudinal	intermittent	0.90
214025	4		8	W-F	Sand AC	Yes	3.20	fine	crush stone		continuous	0.70
544004	4		8	W-F	JPCP	Yes	2.80	fine	crush stone	none	none	0.70
274033	4		9	W-F	Sand AC	Yes	3.20	fine	crush stone	none	none	0.70
104002	4		10	W-F	Sand AC	Yes	3.20	coarse	coarse soil	none	none	0.90
364018	4		10	W-F	Sand AC	Yes	3.20	coarse	crush stone		continuous	0.90
394018	4		11	W-F	Sand AC	Yes	3.20	coarse	none	none	none	0.90
544003	4		11	W-F	JRCP	Yes	2.80	coarse	crush stone	none	none	0.90
101201	4		12	W-F	JRCP	Yes	2.80	coarse	coarse soil	none	none	0.90
204063	4		13	W-F	JPCP	Yes	2.80	coarse	cement-aggregate	none	none	1.00
274054	4		13	W-F	Sand AC	Yes	3.20	coarse	crush stone	none	none	0.90
94008	4		15	W-F	Sand AC	Yes	3.20	coarse	gravel	longitudinal	continuous	1.00
294069	4		16	W-F	Sand AC	Yes	3.20	coarse	none	none	none	0.90
484146	4		19	W-N-F	JRCP	Yes	2.80	fine	cement-aggregate	none	none	0.90
484152	4		19	W-N-F	JRCP	Yes	2.80	fine	cement-aggregate	none	none	0.90
224001	4		20	W-N-F	Sand AC	Yes	3.20	fine	cement treated soil	none	none	0.90

Evaluation of AASHTO rigid pavement design equation - Load Transfer and Drainage Coefficient												
st_shrp	exp#	new exp#	cell	region	shoulder material	dowels	J	subgrade	base	drain type	drain loc	Cd
484143	4		20	W-N-F	JRCP	Yes	2.80	fine	cement-aggregate	none	none	0.90
54021	4		22	W-N-F	JRCP	Yes	2.80	fine	crush stone	none	none	0.80
484142	4		22	W-N-F	JRCP	Yes	2.80	coarse	sand	none	none	1.00
14007	4		23	W-N-F	Sand AC	Yes	3.20	fine	crush stone	blanket	continuous	1.10
14084	4		24	W-N-F	Sand AC	Yes	3.20	fine	crush stone	none	none	0.80
483699	4		24	W-N-F	Sand AC	Yes	3.20	fine	cement-aggregate	none	none	0.90
53059	4		30	W-N-F	JRCP	Yes	2.80	coarse	cement treated soil	none	none	1.10
54019	4		30	W-N-F	Sand AC	Yes	3.20	coarse	cement-aggregate	none	none	1.10
204052	4		33	D-F	Sand AC	Yes	3.20	fine	none	none	none	0.90
204016	4		34	D-F	Open AC	Yes	3.20	fine	crush stone	transverse	intermittent	0.90
314019	4		38	D-F	Sand AC	Yes	3.20	fine	cement-aggregate	none	none	1.00
185043	5		1	W-F	Sand AC	No	3.05	fine	crush stone	longitudinal	continuous	0.80
175020	5		2	W-F	JPCP	No	2.60	fine	cement-aggregate	longitudinal	continuous	0.90
175854	5		3	W-F	Sand AC	No	3.05	fine	cement-aggregate	longitudinal	continuous	0.90
195042	5		5	W-F	Sand AC	No	3.05	fine	other	longitudinal	continuous	0.80
555040	5		6	W-F	JPCP	No	2.60	fine	crush stone	none	none	0.70
195046	5		13	W-F	Sand AC	Yes	3.05	coarse	cement-aggregate	none	none	1.00
95001	5		15	W-F	Sand AC	No	3.05	coarse	gravel	none	none	0.90
105004	5		15	W-F	Sand AC	No	3.05	coarse	soil cement	none	none	1.00
285006	5		17	W-N-F	Open AC	No	3.05	fine	cement-aggregate	none	none	0.90
485026	5		19	W-N-F	JPCP	No	2.60	fine	cement-aggregate	none	none	0.90
483719	5		21	W-N-F	JRCP	No	2.60	fine	cement-aggregate	none	none	0.90
485035	5		21	W-N-F	JPCP	No	2.60	fine	lime treated soil	longitudinal	intermittent	1.00
375037	5		22	W-N-F	Sand AC	No	3.05	fine	crush stone	other	continuous	0.80
455017	5		23	W-N-F	Sand AC	No	3.05	fine	cement-aggregate	none	none	0.90
485024	5		23	W-N-F	JPCP	No	2.60	fine	lime treated soil	none	none	0.90
285803	5		25	W-N-F	Open AC	No	3.05	coarse	soil cement	none	none	1.10
485154	5		29	W-N-F	Sand AC	No	3.05	coarse	lime treated soil	none	none	1.10
415022	5		32	W-N-F	Sand AC	No	3.05	coarse	crush stone	none	none	1.00
465025	5		33	D-F	Sand AC	No	3.05	fine	crush stone	none	none	0.90
165025	5		41	D-F	Sand AC	No	3.05	fine	cement-aggregate	none	none	1.00
417081	5		48	D-F	Sand AC	No	3.05	coarse	lean concrete	none	none	1.15
485287	5		49	D-N-F	Sand AC	No	3.05	fine	lime treated soil	none	none	1.10
485301	5		51	D-N-F	JPCP	No	2.60	fine	lime treated soil	none	none	1.10
485336	5		51	D-N-F	JPCP	No	2.60	fine	lime treated soil	transverse	continuous	1.10
67455	5		53	D-N-F	Sand AC	No	3.05	fine	cement-aggregate	none	none	1.10
485328	5		53	D-N-F	JRCP	No	2.60	fine	crush stone	none	none	1.00
485310	5		55	D-N-F	JRCP	No	2.60	fine	lime treated soil	none	none	1.10
485323	5		55	D-N-F	JPCP	No	2.60	fine	lime treated soil	none	none	1.10
485335	5		55	D-N-F	JPCP	No	2.60	fine	lime treated soil	none	none	1.10

Evaluation of AASHTO rigid pavement design equation - Load Transfer and Drainage Coefficient												
		new			shoulder							
st_shrp	exp#	exp#	cell	region	material	dowels	J	subgrade	base	drain type	drain loc	Cd
485274	5		57	D-N-F	Sand AC	No	3.05	coarse	lime treated soil	none	none	1.25
485317	5		57	D-N-F	JRCP	No	2.60	coarse	lime treated soil	none	none	1.25
485284	5		59	D-N-F	JPCP	No	2.60	coarse	lime treated soil	none	none	1.25

Evaluation of AASHTO rigid pavement design equation - PCC modulus of rupture and Backcalculation													
		new			compressive	split	Testing			backcalculation			
st_shrp	exp#	exp#	cell	region	strength	strength	Epcc	S'c	S'c-28	lk	k-dynamic	Epcc	S'c
183002	3		2	W-F	9.19E+03	682	5.68E+06	1028	762	37.80	251	7.01E+06	794
273003	3		2	W-F	8.03E+03	587	5.00E+06	914	704	35.98	126	5.51E+06	728
193055	3		3	W-F	8.55E+03	581	3.48E+06	907	668	40.15	179	5.66E+06	735
233013	3		4	W-F	7.33E+03	753	4.55E+06	1114	823	43.62	148	5.65E+06	734
393013	3		5	W-F	1.24E+04	699	6.00E+06	1049	773	40.65	125	7.21E+06	802
183030	3		6	W-F	8.41E+03	702	5.03E+06	1052	786	31.60	381	8.64E+06	864
393801	3		6	W-F	8.59E+03	476	3.75E+06	781	588	34.01	356	7.41E+06	811
183031	3		8	W-F	8.08E+03	520	4.88E+06	834	619	43.65	184	7.54E+06	817
193033	3		8	W-F	7.52E+03	519	4.33E+06	833	627	45.23	210	1.18E+07	1003
553009	3		9	W-F	7.95E+03	653	6.28E+06	994	752	39.59	203	9.24E+06	890
893015	3		10	W-F	6.11E+03	512	4.30E+06	824	624	40.51	109	6.22E+06	759
893016	3		10	W-F	9.06E+03	526	4.58E+06	841	632	42.17	132	7.59E+06	818
553008	3		11	W-F	1.05E+04	681	6.80E+06	1027	761	45.27	186	7.73E+06	825
553010	3		11	W-F	1.03E+04	879	6.65E+06	1265	940	29.85	693	4.93E+06	703
423044	3		12	W-F	4.80E+03	515	3.35E+06	828	628	30.48	1070	4.89E+06	701
193006	3		14	W-F	8.48E+03	517	4.58E+06	830	615	41.90	147	7.52E+06	816
193028	3		16	W-F	7.04E+03	556	4.40E+06	877	664	54.70	127	1.52E+07	1151
843803	3		17	W-F	1.03E+04	570	4.75E+06	894	667	36.04	188	6.49E+06	771
263069	3		18	W-F	7.48E+03	471	4.75E+06	775	573	34.97	300	6.79E+06	784
273013	3		18	W-F	8.27E+03	791	5.45E+06	1159	884	40.17	120	6.54E+06	773
553014	3		19	W-F	9.86E+03	593	6.20E+06	922	683	44.65	257	1.06E+07	949
233014	3		20	W-F	7.14E+03	691	3.38E+06	1039	768	44.82	184	8.03E+06	838
893001	3		21	W-F	9.06E+03	607	5.68E+06	938	696	48.78	149	1.08E+07	960
553015	3		25	W-F	8.93E+03	575	6.18E+06	900	681	51.82	138	1.30E+07	1054
193009	3		32	W-F	6.88E+03	587	4.53E+06	914	677	48.29	188	1.02E+07	930
133007	3		34	W-N-F	7.59E+03	576	5.43E+06	901	676	53.09	97	1.05E+07	946
133019	3		34	W-N-F	6.74E+03	512	3.75E+06	824	618	36.32	190	5.18E+06	714
373008	3		38	W-N-F	8.89E+03	668	4.03E+06	1012	766	34.69	341	1.19E+07	1004
373044	3		42	W-N-F	5.79E+03	549	3.73E+06	869	639	37.36	227	6.37E+06	766
13028	3		44	W-N-F	7.22E+03	610	5.53E+06	942	695	34.12	478	7.25E+06	804
133016	3		44	W-N-F	8.15E+03	697	4.05E+06	1046	777	40.39	270	6.01E+06	750
373807	3		45	W-N-F	7.35E+03	545	3.95E+06	864	644	33.05	363	6.31E+06	763
373816	3		46	W-N-F	6.80E+03	520	4.03E+06	834	616	45.01	203	1.24E+07	1028
483010	3		48	W-N-F	7.19E+03	706	5.10E+06	1057	798	62.57	180	1.62E+07	1194

Evaluation of AASHTO rigid pavement design equation - PCC modulus of rupture and Backcalculation

		new			compressive	split	Testing			backcalculation			
st_shrp	exp#	exp#	cell	region	strength	strength	Epcc	S'c	S'c-28	lk	k-dynamic	Epcc	S'c
124109	3		49	W-N-F	8.28E+03	618	4.23E+06	952	756	30.58	368	1.13E+07	978
124000	3		53	W-N-F	5.92E+03	457	3.58E+06	758	561	33.02	280	7.26E+06	804
124138	3		53	W-N-F	5.77E+03	436	3.33E+06	733	543	32.83	306	8.42E+06	855
133020	3		56	W-N-F	8.97E+03	773	3.58E+06	1138	864	32.45	632	8.09E+06	841
123811	3		61	W-N-F	5.96E+03	446	3.05E+06	745	552	30.89	757	9.77E+06	913
283019	3		62	W-N-F	7.50E+03	605	4.18E+06	936	709	31.94	614	7.39E+06	810
123804	3		64	W-N-F	6.10E+03	506	3.95E+06	817	622	28.85	542	3.13E+06	625
463013	3		67	D-F	8.56E+03	534	3.98E+06	851	631	30.69	382	4.61E+06	689
203013	3		71	D-F	6.92E+03	472	4.33E+06	776	587	33.20	497	6.43E+06	768
463010	3		83	D-F	7.92E+03	679	5.80E+06	1025	773	37.54	220	6.36E+06	765
163023	3		89	D-F	8.39E+03	799	3.98E+06	1169	880	33.18	324	6.36E+06	765
563027	3		91	D-F	7.55E+03	779	4.53E+06	1145	856	28.64	401	2.68E+06	605
63005	3		93	D-F		701	2.83E+06	1051	777	30.15	270	5.29E+06	719
63010	3		109	D-N-F	5.73E+03	661	3.55E+06	1003	745	33.26	444	9.05E+06	882
63013	3		111	D-N-F	5.92E+03	725	4.18E+06	1080	809	44.47	218	1.15E+07	990
63019	3		117	D-N-F	4.73E+03	827	3.35E+06	1202	895	37.12	268	9.19E+06	888
63024	3		119	D-N-F	6.58E+03	777	4.38E+06	1142	852	38.57	347	8.51E+06	859
67493	3		127	D-N-F	7.15E+03	696	4.35E+06	1045	786	42.21	322	1.35E+07	1075
264015	4		2	W-F	8.58E+03	585	4.90E+06	912	691	41.59	186	7.28E+06	805
364017	4		2	W-F	5.47E+03	722	3.63E+06	1076	795	29.28	330	4.25E+06	673
204054	4		5	W-F	6.91E+03	515	4.20E+06	828	629	35.58	329	7.12E+06	798
274082	4		5	W-F	8.10E+03	551	4.93E+06	871	642	36.93	164	6.78E+06	784
295000	4		6	W-F	7.61E+03	676	4.05E+06	1021	758	38.75	150	5.95E+06	747
295091	4		6	W-F	6.67E+03	463	5.18E+06	766	568	43.15	172	8.87E+06	874
174074	4		7	W-F	8.45E+03	667	5.98E+06	1010	777	35.92	444	8.28E+06	849
214025	4		8	W-F	7.59E+03	550	4.73E+06	870	642	32.34	414	5.51E+06	728
544004	4		8	W-F	7.96E+03	671	5.45E+06	1015	759	29.85	435	4.54E+06	686
274033	4		9	W-F	9.29E+03	1024	4.95E+06	1439	1075	40.89	170	6.99E+06	793
104002	4		10	W-F	6.16E+03	780	3.63E+06	1146	850	33.24	245	6.72E+06	781
364018	4		10	W-F	8.68E+03	551	3.93E+06	871	644	38.19	232	7.02E+06	794
394018	4		11	W-F	5.76E+03	664	4.13E+06	1007	745	34.00	460	6.71E+06	780
544003	4		11	W-F	8.90E+03	569	4.48E+06	893	670	32.33	400	6.02E+06	750
101201	4		12	W-F	7.28E+03	637	3.85E+06	974	717	38.32	192	6.11E+06	754
204063	4		13	W-F	7.47E+03	561	4.70E+06	883	661	47.15	183	1.23E+07	1024
274054	4		13	W-F	8.31E+03	570	5.55E+06	894	660	42.07	219	9.57E+06	905
94008	4		15	W-F	8.08E+03	640	4.95E+06	978	752	45.72	144	6.65E+06	778
294069	4		16	W-F	7.88E+03	635	3.50E+06	972	719	42.39	188	7.24E+06	803
484146	4		19	W-N-F	6.73E+03	712	4.63E+06	1064	795	56.82	159	1.71E+07	1230
484152	4		19	W-N-F	6.01E+03	635	4.83E+06	972	727	52.60	204	1.31E+07	1060
224001	4		20	W-N-F	1.14E+04	756	5.48E+06	1117	824	44.86	194	1.09E+07	961

Evaluation of AASHTO rigid pavement design equation - PCC modulus of rupture and Backcalculation													
		new			compressive	split	Testing			backcalculation			
st_shrp	exp#	exp#	cell	region	strength	strength	Epcc	S'c	S'c-28	lk	k-dynamic	Epcc	S'c
484143	4		20	W-N-F	8.15E+03	943	5.63E+06	1342	989	50.56	213	1.47E+07	1128
54021	4		22	W-N-F	8.64E+03	664	4.35E+06	1007	742	38.52	233	6.71E+06	780
484142	4		22	W-N-F	7.13E+03	687	5.13E+06	1034	766	43.73	207	1.02E+07	933
14007	4		23	W-N-F	7.45E+03	791	6.35E+06	1159	855	40.29	254	6.65E+06	778
14084	4		24	W-N-F	7.67E+03	716	6.15E+06	1069	788	51.91	95	6.81E+06	785
483699	4		24	W-N-F	8.02E+03	804	6.18E+06	1175	867	46.48	193	1.02E+07	930
53059	4		30	W-N-F	6.60E+03	652	3.83E+06	992	739	35.13	264	5.74E+06	738
54019	4		30	W-N-F	6.80E+03	566	5.53E+06	889	657	39.39	276	9.31E+06	893
204052	4		33	D-F	7.31E+03	462	4.43E+06	764	576	42.25	222	1.09E+07	962
204016	4		34	D-F	6.28E+03	559	4.30E+06	881	656	42.79	139	7.05E+06	795
314019	4		38	D-F	6.57E+03	635	4.78E+06	972	720	43.53	127	7.02E+06	794
185043	5		1	W-F	7.96E+03	711	5.20E+06	1063	783	29.02	273	5.27E+06	718
175020	5		2	W-F	6.97E+03	682	3.43E+06	1028	787	36.00	190	6.14E+06	756
175854	5		3	W-F	8.12E+03	670	4.98E+06	1014	757	44.04	186	8.41E+06	854
195042	5		5	W-F	8.15E+03	684	4.35E+06	1031	763	36.31	197	7.70E+06	823
555040	5		6	W-F	7.97E+03	846	6.20E+06	1225	915	38.87	163	7.35E+06	808
195046	5		13	W-F	7.50E+03	664	4.53E+06	1007	746	34.94	326	1.01E+07	927
95001	5		15	W-F	9.13E+03	707	5.33E+06	1058	792	36.71	218	8.56E+06	861
105004	5		15	W-F	6.12E+03	606	3.18E+06	937	695	36.61	167	4.92E+06	703
285006	5		17	W-N-F	9.40E+03	730	5.03E+06	1086	808	33.23	440	1.16E+07	993
485026	5		19	W-N-F	9.10E+03	702	5.48E+06	1052	798	50.17	176	1.29E+07	1050
483719	5		21	W-N-F	7.53E+03	619	6.40E+06	953	700	42.51	157	1.21E+07	1013
485035	5		21	W-N-F	5.84E+03	569	4.33E+06	893	666	23.28	1677	9.76E+06	913
375037	5		22	W-N-F	8.06E+03	691	3.10E+06	1039	767	31.92	231	5.86E+06	743
455017	5		23	W-N-F	6.50E+03	810	3.03E+06	1182	880	30.16	356	4.25E+06	673
485024	5		23	W-N-F	7.62E+03	633	5.38E+06	970	726	41.92	397	1.15E+07	988
285803	5		25	W-N-F	7.79E+03	670	4.58E+06	1014	755	34.34	278	9.18E+06	888
485154	5		29	W-N-F	6.70E+03	582	4.55E+06	908	670	34.85	401	1.24E+07	1028
415022	5		32	W-N-F	7.73E+03	843	3.53E+06	1222	924	44.43	201	4.38E+06	679
465025	5		33	D-F	8.24E+03	771	4.33E+06	1135	840	37.82	145	6.57E+06	774
165025	5		41	D-F	7.19E+03	588	4.30E+06	916	676	26.65	517	5.38E+06	722
417081	5		48	D-F		848	3.78E+06	1228	968	35.74	459	8.16E+06	844
485287	5		49	D-N-F	4.86E+03	512	3.60E+06	824	609	31.07	252	4.93E+06	703
485301	5		51	D-N-F	8.05E+03	752	5.05E+06	1112	834	32.30	548	6.94E+06	790
485336	5		51	D-N-F	6.68E+03	564	4.43E+06	887	667	35.82	339	9.25E+06	891
67455	5		53	D-N-F	7.66E+03	749	4.65E+06	1109	818	35.74	459	8.16E+06	844
485328	5		53	D-N-F	7.33E+03	641	4.38E+06	979	725	33.07	317	8.92E+06	877
485310	5		55	D-N-F	8.85E+03	607	5.03E+06	938	731	38.73	423	7.65E+06	821
485323	5		55	D-N-F	8.27E+03	657	4.25E+06	998	744	37.28	198	7.87E+06	831
485335	5		55	D-N-F	9.28E+03	761	5.08E+06	1123	836	37.29	236	6.75E+06	782

Evaluation of AASHTO rigid pavement design equation - PCC modulus of rupture and Backcalculation													
		new			compressive	split	Testing			backcalculation			
st_shrp	exp#	exp#	cell	region	strength	strength	Epcc	S'c	S'c-28	lk	k-dynamic	Epcc	S'c
485274	5		57	D-N-F	8.71E+03	694	5.48E+06	1043	770	33.66	345	7.86E+06	830
485317	5		57	D-N-F	7.66E+03	679	5.68E+06	1025	769	36.04	211	8.14E+06	843
485284	5		59	D-N-F	5.64E+03	648	4.53E+06	988	772	40.32	350	8.19E+06	845

Evaluation of AASHTO rigid pavement design equation - Effective k-value

st_shrp	exp#	new exp#	cell	region	k-static	Subgrade MR	base	LOS	Ebase	base thickness	Effective k-value	LOS correct k-value
183002	3		2	W-F	126	2439	crush stone	0.5	20000	6.00	126	76
273003	3		2	W-F	63	1220	crush stone	0.5	20000	5.00	63	40
193055	3		3	W-F	89	1736	crush stone	0.5	20000	4.00	89	56
233013	3		4	W-F	74	1436	crush stone	0.5	20000	3.00	74	47
393013	3		5	W-F	62	1212	cement-aggregate	0.75	1000000	4.00	117	57
183030	3		6	W-F	191	3696	other	0	0	24.00	191	191
393801	3		6	W-F	178	3450	cement-aggregate	0.75	1000000	4.00	293	128
183031	3		8	W-F	92	1785	none	0	0	0.00	92	92
193033	3		8	W-F	105	2032	cement-aggregate	0.75	1000000	4.00	184	85
553009	3		9	W-F	102	1971	crush stone	0.5	20000	8.00	102	63
893015	3		10	W-F	54	1055	crush stone	0.5	20000	9.00	54	35
893016	3		10	W-F	66	1283	crush stone	0.5	20000	9.00	66	42
553008	3		11	W-F	93	1802	crush stone	0.5	20000	6.00	93	58
553010	3		11	W-F	347	6725	crush stone	0.5	20000	9.00	347	194
423044	3		12	W-F	535	10377	crush stone	0.5	20000	8.00	535	290
193006	3		14	W-F	73	1424	cement-aggregate	0.75	1000000	4.00	135	65
193028	3		16	W-F	63	1229	lean concrete	0.25	1500000	4.00	124	95
843803	3		17	W-F	94	1822	gravel	0.5	20000	4.00	94	58
263069	3		18	W-F	150	2905	sand	1	20000	10.00	150	56
273013	3		18	W-F	60	1163	crush stone	0.5	20000	5.00	60	39
553014	3		19	W-F	128	2488	crush stone	0.5	20000	6.00	128	78
233014	3		20	W-F	92	1786	crush stone	0.5	20000	3.00	92	57
893001	3		21	W-F	74	1444	soil cement	0.75	1000000	6.00	188	87
553015	3		25	W-F	69	1334	crush stone	0.5	20000	6.00	69	44
193009	3		32	W-F	94	1828	soil cement	0.75	1000000	4.00	168	78
133007	3		34	W-N-F	48	936	crush stone	0.5	20000	10.00	48	32
133019	3		34	W-N-F	95	1847	crush stone	0.5	20000	6.00	95	59
373008	3		38	W-N-F	171	3308	lean concrete	0.25	1500000	5.00	348	257
373044	3		42	W-N-F	113	2202	crush stone	0.5	20000	4.00	113	69
13028	3		44	W-N-F	239	4640	crush stone	0.5	20000	6.00	252	145
133016	3		44	W-N-F	135	2615	crush stone	0.5	20000	5.00	135	81
373807	3		45	W-N-F	181	3518	lean concrete	0.25	1500000	4.00	313	232
373816	3		46	W-N-F	101	1964	cement-aggregate	0.75	1000000	4.00	179	83
483010	3		48	W-N-F	90	1748	cement-aggregate	0.75	1000000	6.00	221	100

Evaluation of AASHTO rigid pavement design equation - Effective k-value

st_shrp	exp#	new exp#	cell	region	k-static	Subgrade MR	base	LOS	Ebase	base thickness	Effective k-value	LOS correct k-value
124109	3		49	W-N-F	184	3570	lime rock	0.5	20000	8.80	184	108
124000	3		53	W-N-F	140	2720	soil cement	0.75	1000000	4.00	238	107
124138	3		53	W-N-F	153	2970	soil cement	0.75	1000000	4.00	257	114
133020	3		56	W-N-F	316	6134	soil cement	0.75	1000000	6.00	622	249
123811	3		61	W-N-F	379	7346	soil cement	0.75	1000000	6.00	722	284
283019	3		62	W-N-F	307	5951	cement-aggregate	0.75	1000000	5.00	540	220
123804	3		64	W-N-F	271	5253	lean concrete	0.25	1500000	6.00	587	424
463013	3		67	D-F	191	3704	crush stone	0.5	20000	3.30	191	112
203013	3		71	D-F	248	4816	cement-aggregate	0.75	1000000	4.00	393	166
463010	3		83	D-F	110	2131	crush stone	0.5	20000	3.50	110	67
163023	3		89	D-F	162	3142	crush stone	0.5	20000	4.80	162	96
563027	3		91	D-F	201	3890	crush stone	0.5	20000	8.00	201	117
63005	3		93	D-F	135	2623	cement-aggregate	0.75	1000000	5.40	285	125
63010	3		109	D-N-F	222	4307	cement-aggregate	0.75	1000000	5.40	432	181
63013	3		111	D-N-F	109	2114	lean concrete	0.25	1500000	4.80	230	173
63019	3		117	D-N-F	134	2604	cement-aggregate	0.75	1000000	4.80	260	115
63024	3		119	D-N-F	173	3365	cement-aggregate	0.75	1000000	5.40	351	150
67493	3		127	D-N-F	161	3121	cement-aggregate	0.75	1000000	4.50	290	127
264015	4		2	W-F	93	1800	crush stone	0.5	20000	4.00	93	58
364017	4		2	W-F	165	3198	crush stone	0.5	20000	12.00	165	98
204054	4		5	W-F	165	3195	cement-aggregate	0.75	1000000	4.00	274	121
274082	4		5	W-F	82	1590	crush stone	0.5	20000	6.00	82	51
295000	4		6	W-F	75	1450	crush stone	0.5	20000	4.00	75	47
295091	4		6	W-F	86	1664	cement-aggregate	0.75	1000000	4.00	154	73
174074	4		7	W-F	222	4307	cement-aggregate	0.75	1000000	4.50	383	162
214025	4		8	W-F	207	4016	crush stone	0.5	20000	6.00	207	121
544004	4		8	W-F	217	4219	crush stone	0.5	20000	6.00	217	127
274033	4		9	W-F	85	1652	crush stone	0.5	20000	5.00	85	53
104002	4		10	W-F	122	2373	coarse soil	1	20000	6.00	122	47
364018	4		10	W-F	116	2250	crush stone	0.5	20000	12.00	116	71
394018	4		11	W-F	230	4465	none	0	0	0.00	230	230
544003	4		11	W-F	200	3880	crush stone	0.5	20000	6.00	200	117
101201	4		12	W-F	96	1863	coarse soil	1	20000	6.00	96	39
204063	4		13	W-F	91	1774	cement-aggregate	0.75	1000000	4.00	163	76
274054	4		13	W-F	110	2124	crush stone	0.5	20000	6.00	110	67
94008	4		15	W-F	72	1401	gravel	0.5	20000	18.00	72	46
294069	4		16	W-F	94	1822	none	0	0	0.00	94	94
484146	4		19	W-N-F	79	1539	cement-aggregate	0.75	1000000	5.40	182	84
484152	4		19	W-N-F	102	1978	cement-aggregate	0.75	1000000	6.00	244	109
224001	4		20	W-N-F	97	1883	cement treated soil	0.75	1000000	6.00	97	48

Evaluation of AASHTO rigid pavement design equation - Effective k-value												
		new				Subgrade				base	Effective	LOS correct
st_shrp	exp#	exp#	cell	region	k-static	MR	base	LOS	Ebase	thickness	k-value	k-value
484143	4		20	W-N-F	106	2065	cement-aggregate	0.75	1000000	4.00	187	86
54021	4		22	W-N-F	117	2263	crush stone	0.5	20000	4.00	117	71
484142	4		22	W-N-F	104	2008	sand	1	20000	6.00	104	41
14007	4		23	W-N-F	127	2463	crush stone	0.5	20000	6.00	127	77
14084	4		24	W-N-F	48	925	crush stone	0.5	20000	6.00	48	31
483699	4		24	W-N-F	97	1873	cement-aggregate	0.75	1000000	6.00	234	105
53059	4		30	W-N-F	132	2560	cement treated soil	0.75	1000000	6.00	302	132
54019	4		30	W-N-F	138	2677	cement-aggregate	0.75	1000000	8.00	395	167
204052	4		33	D-F	111	2151	none	0	0	0.00	111	111
204016	4		34	D-F	69	1345	crush stone	0.5	20000	4.00	69	44
314019	4		38	D-F	63	1232	cement-aggregate	0.75	1000000	3.00	96	48
185043	5		1	W-F	136	2645	crush stone	0.5	20000	8.00	136	82
175020	5		2	W-F	95	1846	cement-aggregate	0.75	1000000	4.00	169	79
175854	5		3	W-F	93	1801	cement-aggregate	0.75	1000000	4.00	165	77
195042	5		5	W-F	99	1915	other	0	0	24.00	99	99
555040	5		6	W-F	81	1576	crush stone	0.5	20000	6.00	81	51
195046	5		13	W-F	163	3167	cement-aggregate	0.75	1000000	4.00	272	120
95001	5		15	W-F	109	2118	gravel	0.5	20000	10.00	109	67
105004	5		15	W-F	84	1623	soil cement	0.75	1000000	4.00	151	71
285006	5		17	W-N-F	220	4268	cement-aggregate	0.75	1000000	6.00	461	191
485026	5		19	W-N-F	88	1708	cement-aggregate	0.75	1000000	6.00	88	44
483719	5		21	W-N-F	78	1518	cement-aggregate	0.75	1000000	4.00	142	68
485035	5		21	W-N-F	838	16264	lime treated soil	1	20000	6.00	711	209
375037	5		22	W-N-F	116	2243	crush stone	0.5	20000	4.00	116	71
455017	5		23	W-N-F	178	3455	cement-aggregate	0.75	1000000	6.00	387	164
485024	5		23	W-N-F	198	3850	lime treated soil	1	20000	6.00	216	77
285803	5		25	W-N-F	139	2693	soil cement	0.75	1000000	6.00	315	137
485154	5		29	W-N-F	201	3891	lime treated soil	1	20000	7.00	226	80
415022	5		32	W-N-F	101	1950	crush stone	0.5	20000	20.00	101	62
465025	5		33	D-F	73	1410	crush stone	0.5	20000	3.00	73	46
165025	5		41	D-F	258	5012	cement-aggregate	0.75	1000000	4.00	407	171
417081	5		48	D-F	230	4457	lean concrete	0.25	1500000	8.00	643	463
485287	5		49	D-N-F	126	2445	lime treated soil	1	20000	6.00	149	56
485301	5		51	D-N-F	274	5313	lime treated soil	1	20000	6.00	282	96
485336	5		51	D-N-F	170	3289	lime treated soil	1	20000	6.00	190	69
67455	5		53	D-N-F	230	4457	cement-aggregate	0.75	1000000	5.40	444	185
485328	5		53	D-N-F	159	3079	crush stone	0.5	20000	4.40	159	95
485310	5		55	D-N-F	212	4107	lime treated soil	1	20000	6.00	228	80
485323	5		55	D-N-F	99	1925	lime treated soil	1	20000	6.00	122	47
485335	5		55	D-N-F	118	2287	lime treated soil	1	20000	6.00	141	53

Evaluation of AASHTO rigid pavement design equation - Effective k-value												
		new				Subgrade				base	Effective	LOS correct
st_shrp	exp#	exp#	cell	region	k-static	MR	base	LOS	Ebase	thickness	k-value	k-value
485274	5		57	D-N-F	172	3343	lime treated soil	1	20000	24.00	341	113
485317	5		57	D-N-F	106	2050	lime treated soil	1	20000	18.00	209	74
485284	5		59	D-N-F	175	3399	lime treated soil	1	20000	8.00	211	75

Evaluation of AASHTO rigid pavement design equation - Actual vs. Predicted ESALs (1993 AASHTO)												
		new			PCC		calculated	calculated	estimated	psi		
st_shrp	exp#	exp#	cell	region	thick	pt	ESALs	KESALs	KESALs	loss	diff	ratio
183002	3		2	W-F	9.48	4.10	1074918	1075	2289	0.15	-1214	0.47
273003	3		2	W-F	7.58	3.93	155429	155	291	0.32	-136	0.53
193055	3		3	W-F	9.87	4.09	342416	342	2195	0.16	-1853	0.16
233013	3		4	W-F	10.23	3.82	3791658	3792	3130	0.43	662	1.21
393013	3		5	W-F	8.23	2.98	1664711	1665	1675	1.27	-10	0.99
183030	3		6	W-F	8.01	4.21	150462	150	3877	0.04	-3727	0.04
393801	3		6	W-F	9.06	3.96	1873134	1873	1654	0.29	219	1.13
183031	3		8	W-F	10.16	4.25	27546	28	5246	0.00	-5218	0.01
193033	3		8	W-F	9.56	4.03	1379932	1380	953	0.22	427	1.45
553009	3		9	W-F	8.58	3.21	940683	941	1863	1.04	-922	0.51
893015	3		10	W-F	8.25	3.22	859692	860	1666	1.03	-806	0.52
893016	3		10	W-F	8.63	3.51	922333	922	1859	0.74	-937	0.50
553008	3		11	W-F	10.72	2.73	5347253	5347	8967	1.52	-3620	0.60
553010	3		11	W-F	10.88	3.77	6175186	6175	2526	0.48	3649	2.44
423044	3		12	W-F	12.70	3.78	25763839	25764	4957	0.47	20807	5.20
193006	3		14	W-F	8.91	3.27	2166502	2167	2232	0.98	-66	0.97
193028	3		16	W-F	9.56	4.00	1907146	1907	1133	0.25	774	1.68
843803	3		17	W-F	8.30	3.12	4482998	4483	2179	1.13	2304	2.06
263069	3		18	W-F	9.17	4.22	119418	119	1017	0.03	-898	0.12
273013	3		18	W-F	7.95	4.14	295341	295	833	0.11	-538	0.35
553014	3		19	W-F	10.28	2.97	6094557	6095	4514	1.28	1581	1.35
233014	3		20	W-F	10.27	4.06	3230055	3230	3162	0.19	68	1.02
893001	3		21	W-F	9.03	3.46	2723984	2724	2146	0.79	578	1.27
553015	3		25	W-F	9.60	3.84	1283158	1283	2066	0.41	-783	0.62
193009	3		32	W-F	10.59	3.71	11399919	11400	2792	0.54	8607	4.08
133007	3		34	W-N-F	9.42	4.04	861350	861	264	0.21	598	3.27
133019	3		34	W-N-F	9.07	4.16	430632	431	1765	0.09	-1334	0.24
373008	3		38	W-N-F	7.87	3.95	1215949	1216	455	0.30	761	2.67
373044	3		42	W-N-F	9.00	3.89	1139568	1140	18677	0.36	-17537	0.06
13028	3		44	W-N-F	10.23	3.21	13685886	13686	2915	1.04	10771	4.69
133016	3		44	W-N-F	11.08	4.24	430255	430	13174	0.01	-12744	0.03
373807	3		45	W-N-F	9.35	3.86	1688094	1688	1496	0.39	192	1.13
373816	3		46	W-N-F	9.22	3.75	2305267	2305	4476	0.50	-2171	0.51
483010	3		48	W-N-F	12.53	3.80	48646021	48646	939	0.45	47707	51.83

Evaluation of AASHTO rigid pavement design equation - Actual vs. Predicted ESALs (1993 AASHTO)

st_shrp	exp#	new exp#	cell	region	PCC thick	pt	calculated ESALs	calculated KESALs	estimated KESALs	psi loss	diff	ratio
124109	3		49	W-N-F	6.97	3.70	2287893	2288	297	0.55	1991	7.71
124000	3		53	W-N-F	8.08	4.20	113840	114	4166	0.05	-4052	0.03
124138	3		53	W-N-F	7.98	3.09	1399757	1400	4166	1.16	-2766	0.34
133020	3		56	W-N-F	10.08	4.20	2998238	2998	339	0.05	2659	8.85
123811	3		61	W-N-F	9.38	3.75	3281541	3282	11104	0.50	-7823	0.30
283019	3		62	W-N-F	9.37	3.93	5917081	5917	385	0.32	5532	15.36
123804	3		64	W-N-F	11.97	3.72	54596927	54597	4223	0.53	50374	12.93
463013	3		67	D-F	9.33	4.14	342870	343	332	0.11	11	1.03
203013	3		71	D-F	10.16	4.03	1433446	1433	647	0.22	787	2.22
463010	3		83	D-F	9.30	3.29	8040460	8040	173	0.96	7867	46.39
163023	3		89	D-F	8.95	4.19	795284	795	3966	0.06	-3170	0.20
563027	3		91	D-F	10.55	3.49	12520320	12520	4753	0.76	7768	2.63
63005	3		93	D-F	8.23	2.34	10758807	10759	15847	1.91	-5088	0.68
63010	3		109	D-N-F	8.82	3.83	3491533	3492	3305	0.42	186	1.06
63013	3		111	D-N-F	9.55	4.12	2774962	2775	5662	0.13	-2887	0.49
63019	3		117	D-N-F	8.60	4.23	307845	308	7963	0.02	-7655	0.04
63024	3		119	D-N-F	10.17	4.13	4618332	4618	5279	0.12	-660	0.87
67493	3		127	D-N-F	9.50	4.15	1682625	1683	3457	0.10	-1775	0.49
264015	4		2	W-F	9.58	4.22	297434	297	1063	0.03	-765	0.28
364017	4		2	W-F	8.75	3.15	3755404	3755	15771	1.10	-12016	0.24
204054	4		5	W-F	9.43	4.09	1096665	1097	1681	0.16	-584	0.65
274082	4		5	W-F	8.05	2.90	1040686	1041	5726	1.35	-4685	0.18
295000	4		6	W-F	8.70	3.68	2154152	2154	8797	0.57	-6643	0.24
295091	4		6	W-F	9.23	4.12	494581	495	8797	0.13	-8302	0.06
174074	4		7	W-F	9.97	3.82	10187009	10187	361	0.43	9826	28.20
214025	4		8	W-F	9.90	3.02	4372312	4372	5859	1.23	-1487	0.75
544004	4		8	W-F	9.93	2.50	16013395	16013	4544	1.75	11469	3.52
274033	4		9	W-F	9.22	3.86	3955493	3955	1335	0.39	2620	2.96
104002	4		10	W-F	8.03	3.36	4252931	4253	456	0.89	3797	9.33
364018	4		10	W-F	9.35	3.94	1760302	1760	16539	0.31	-14778	0.11
394018	4		11	W-F	10.22	4.01	4820443	4820	2803	0.24	2017	1.72
544003	4		11	W-F	9.45	3.66	6440107	6440	765	0.59	5675	8.42
101201	4		12	W-F	9.20	3.58	6165860	6166	2848	0.67	3318	2.16
204063	4		13	W-F	9.52	3.82	5886004	5886	547	0.43	5339	10.77
274054	4		13	W-F	9.43	3.85	2348169	2348	5809	0.40	-3461	0.40
94008	4		15	W-F	10.35	3.78	9701456	9701	2383	0.47	7319	4.07
294069	4		16	W-F	9.93	3.93	4028162	4028	4265	0.32	-237	0.94
484146	4		19	W-N-F	10.53	3.66	19698119	19698	1075	0.59	18623	18.33
484152	4		19	W-N-F	11.35	3.14	48579258	48579	724	1.11	47855	67.08
224001	4		20	W-N-F	9.75	3.68	7518326	7518	6951	0.57	567	1.08

Evaluation of AASHTO rigid pavement design equation - Actual vs. Predicted ESALs (1993 AASHTO)												
		new			PCC		calculated	calculated	estimated	psi		
st_shrp	exp#	exp#	cell	region	thick	pt	ESALs	KESALs	KESALs	loss	diff	ratio
484143	4		20	W-N-F	10.30	3.85	21704954	21705	1899	0.40	19806	11.43
54021	4		22	W-N-F	9.63	3.90	3745622	3746	4108	0.35	-363	0.91
484142	4		22	W-N-F	9.48	3.80	8142839	8143	2249	0.45	5893	3.62
14007	4		23	W-N-F	10.47	3.96	12866242	12866	3721	0.29	9145	3.46
14084	4		24	W-N-F	10.43	2.77	16150328	16150	17163	1.48	-1013	0.94
483699	4		24	W-N-F	10.15	3.73	11830927	11831	22670	0.52	-10839	0.52
53059	4		30	W-N-F	9.33	4.13	3352501	3353	1146	0.12	2207	2.93
54019	4		30	W-N-F	9.45	4.05	2688315	2688	1760	0.20	929	1.53
204052	4		33	D-F	9.13	3.68	2096649	2097	698	0.57	1398	3.00
204016	4		34	D-F	9.13	4.17	403728	404	790	0.08	-386	0.51
314019	4		38	D-F	9.13	4.02	1988013	1988	4351	0.23	-2363	0.46
185043	5		1	W-F	7.53	3.87	985938	986	296	0.38	690	3.33
175020	5		2	W-F	8.52	4.24	98775	99	175	0.01	-76	0.56
175854	5		3	W-F	9.92	3.89	5280106	5280	603	0.36	4678	8.76
195042	5		5	W-F	8.03	4.12	523521	524	5615	0.13	-5092	0.09
555040	5		6	W-F	8.40	3.77	3079744	3080	4867	0.48	-1787	0.63
195046	5		13	W-F	8.30	4.16	823975	824	5544	0.09	-4720	0.15
95001	5		15	W-F	8.23	3.82	2346381	2346	6974	0.43	-4628	0.34
105004	5		15	W-F	8.97	3.98	2541441	2541	9773	0.27	-7231	0.26
285006	5		17	W-N-F	8.15	4.06	1478266	1478	1741	0.19	-263	0.85
485026	5		19	W-N-F	10.03	4.20	1263033	1263	325	0.05	939	3.89
483719	5		21	W-N-F	7.93	3.83	2049818	2050	8374	0.42	-6324	0.24
485035	5		21	W-N-F	8.10	4.07	1894150	1894	7941	0.18	-6047	0.24
375037	5		22	W-N-F	7.77	4.11	497448	497	6114	0.14	-5617	0.08
455017	5		23	W-N-F	8.88	3.96	4797715	4798	3847	0.29	950	1.25
485024	5		23	W-N-F	10.90	3.57	25822713	25823	1148	0.68	24675	22.50
285803	5		25	W-N-F	7.88	4.11	1348334	1348	3330	0.14	-1981	0.40
485154	5		29	W-N-F	8.24	4.17	581809	582	8010	0.08	-7429	0.07
415022	5		32	W-N-F	12.78	4.02	43939429	43939	10770	0.23	33170	4.08
465025	5		33	D-F	8.10	4.07	1126297	1126	553	0.18	573	2.04
165025	5		41	D-F	8.32	3.85	2647175	2647	13583	0.40	-10936	0.19
417081	5		48	D-F	10.38	3.66	90255790	90256	899	0.59	89356	100.34
485287	5		49	D-N-F	8.23	4.06	995022	995	3050	0.19	-2055	0.33
485301	5		51	D-N-F	10.02	3.95	18875950	18876	1413	0.30	17463	13.36
485336	5		51	D-N-F	8.87	3.77	7180378	7180	1092	0.48	6089	6.58
67455	5		53	D-N-F	8.88	4.24	332957	333	7509	0.01	-7176	0.04
485328	5		53	D-N-F	7.92	4.12	1258889	1259	6458	0.13	-5199	0.19
485310	5		55	D-N-F	11.40	3.81	42350936	42351	1269	0.44	41082	33.37
485323	5		55	D-N-F	8.28	3.94	4168535	4169	5234	0.31	-1066	0.80
485335	5		55	D-N-F	9.25	3.81	15465120	15465	5319	0.44	10146	2.91

Evaluation of AASHTO rigid pavement design equation - Actual vs. Predicted ESALs (1993 AASHTO)

st_shrp	exp#	new exp#	cell	region	PCC thick	pt	calculated ESALs	calculated KESALs	estimated KESALs	psi loss	diff	ratio
485274	5		57	D-N-F	8.32	3.42	13021944	13022	4438	0.83	8584	2.93
485317	5		57	D-N-F	7.98	3.80	8309961	8310	3196	0.45	5114	2.60
485284	5		59	D-N-F	10.98	3.73	69051574	69052	452	0.52	68600	152.89

Evaluation of AASHTO rigid pavement design equation - Actual vs. Predicted ESALs (1960 AASHTO)									
		new			calculated	estimated	psi		
st_shrp	exp#	exp#	cell	region	KESALs	KESALs	loss	diff	ratio
183002	3		2	W-F	3966	2289	0.15	1677	1.73
273003	3		2	W-F	1604	291	0.32	1313	5.51
193055	3		3	W-F	5246	2195	0.16	3052	2.39
233013	3		4	W-F	10754	3130	0.43	7625	3.44
393013	3		5	W-F	5871	1675	1.27	4196	3.50
183030	3		6	W-F	1174	3877	0.04	-2704	0.30
393801	3		6	W-F	4026	1654	0.29	2372	2.43
183031	3		8	W-F	3880	5246	0.00	-1366	0.74
193033	3		8	W-F	4853	953	0.22	3901	5.10
553009	3		9	W-F	6500	1863	1.04	4638	3.49
893015	3		10	W-F	5086	1666	1.03	3421	3.05
893016	3		10	W-F	5254	1859	0.74	3395	2.83
553008	3		11	W-F	37244	8967	1.52	28277	4.15
553010	3		11	W-F	17009	2526	0.48	14484	6.73
423044	3		12	W-F	47382	4957	0.47	42425	9.56
193006	3		14	W-F	7873	2232	0.98	5641	3.53
193028	3		16	W-F	5182	1133	0.25	4049	4.57
843803	3		17	W-F	5667	2179	1.13	3488	2.60
263069	3		18	W-F	2309	1017	0.03	1292	2.27
273013	3		18	W-F	1336	833	0.11	503	1.60
553014	3		19	W-F	24390	4514	1.28	19876	5.40
233014	3		20	W-F	7120	3162	0.19	3958	2.25
893001	3		21	W-F	7311	2146	0.79	5165	3.41
553015	3		25	W-F	6894	2066	0.41	4829	3.34
193009	3		32	W-F	15521	2792	0.54	12728	5.56
133007	3		34	W-N-F	4349	264	0.21	4086	16.50
133019	3		34	W-N-F	2610	1765	0.09	845	1.48
373008	3		38	W-N-F	1848	455	0.30	1393	4.06
373044	3		42	W-N-F	4316	18677	0.36	-14361	0.23
13028	3		44	W-N-F	20044	2915	1.04	17129	6.88
133016	3		44	W-N-F	6948	13174	0.01	-6226	0.53
373807	3		45	W-N-F	5717	1496	0.39	4221	3.82
373816	3		46	W-N-F	6072	4476	0.50	1595	1.36
483010	3		48	W-N-F	42456	939	0.45	41517	45.24

Evaluation of AASHTO rigid pavement design equation - Actual vs. Predicted ESALs (1960 AASHTO)									
		new			calculated	estimated	psi		
st_shrp	exp#	exp#	cell	region	KESALs	KESALs	loss	diff	ratio
124109	3		49	W-N-F	1421	297	0.55	1124	4.79
124000	3		53	W-N-F	1253	4166	0.05	-2913	0.30
124138	3		53	W-N-F	4563	4166	1.16	397	1.10
133020	3		56	W-N-F	4426	339	0.05	4087	13.06
123811	3		61	W-N-F	6803	11104	0.50	-4301	0.61
283019	3		62	W-N-F	5170	385	0.32	4785	13.42
123804	3		64	W-N-F	34595	4223	0.53	30372	8.19
463013	3		67	D-F	3263	332	0.11	2932	9.84
203013	3		71	D-F	7058	647	0.22	6411	10.91
463010	3		83	D-F	10121	173	0.96	9948	58.39
163023	3		89	D-F	2205	3966	0.06	-1761	0.56
563027	3		91	D-F	19246	4753	0.76	14493	4.05
63005	3		93	D-F	8053	15847	1.91	-7794	0.51
63010	3		109	D-N-F	4174	3305	0.42	869	1.26
63013	3		111	D-N-F	3964	5662	0.13	-1699	0.70
63019	3		117	D-N-F	1540	7963	0.02	-6422	0.19
63024	3		119	D-N-F	5719	5279	0.12	440	1.08
67493	3		127	D-N-F	3526	3457	0.10	69	1.02
264015	4		2	W-F	3029	1063	0.03	1966	2.85
364017	4		2	W-F	7691	15771	1.10	-8080	0.49
204054	4		5	W-F	3931	1681	0.16	2250	2.34
274082	4		5	W-F	5355	5726	1.35	-371	0.94
295000	4		6	W-F	4662	8797	0.57	-4135	0.53
295091	4		6	W-F	3178	8797	0.13	-5618	0.36
174074	4		7	W-F	8991	361	0.43	8630	24.89
214025	4		8	W-F	18448	5859	1.23	12589	3.15
544004	4		8	W-F	25190	4544	1.75	20646	5.54
274033	4		9	W-F	5192	1335	0.39	3856	3.89
104002	4		10	W-F	3904	456	0.89	3448	8.56
364018	4		10	W-F	4975	16539	0.31	-11564	0.30
394018	4		11	W-F	7716	2803	0.24	4913	2.75
544003	4		11	W-F	7920	765	0.59	7155	10.36
101201	4		12	W-F	7293	2848	0.67	4445	2.56
204063	4		13	W-F	6780	547	0.43	6233	12.40
274054	4		13	W-F	6064	5809	0.40	254	1.04
94008	4		15	W-F	12213	2383	0.47	9831	5.13
294069	4		16	W-F	7458	4265	0.32	3193	1.75
484146	4		19	W-N-F	15848	1075	0.59	14773	14.74
484152	4		19	W-N-F	41976	724	1.11	41251	57.96
224001	4		20	W-N-F	9393	6951	0.57	2442	1.35

Evaluation of AASHTO rigid pavement design equation - Actual vs. Predicted ESALs (1960 AASHTO)									
		new			calculated	estimated	psi		
st_shrp	exp#	exp#	cell	region	KESALs	KESALs	loss	diff	ratio
484143	4		20	W-N-F	10756	1899	0.40	8857	5.66
54021	4		22	W-N-F	6441	4108	0.35	2333	1.57
484142	4		22	W-N-F	6760	2249	0.45	4510	3.01
14007	4		23	W-N-F	9834	3721	0.29	6113	2.64
14084	4		24	W-N-F	30367	17163	1.48	13204	1.77
483699	4		24	W-N-F	11520	22670	0.52	-11150	0.51
53059	4		30	W-N-F	3352	1146	0.12	2207	2.93
54019	4		30	W-N-F	4341	1760	0.20	2581	2.47
204052	4		33	D-F	6223	698	0.57	5525	8.91
204016	4		34	D-F	2613	790	0.08	1823	3.31
314019	4		38	D-F	3760	4351	0.23	-591	0.86
185043	5		1	W-F	1680	296	0.38	1384	5.68
175020	5		2	W-F	1406	175	0.01	1231	8.02
175854	5		3	W-F	7838	603	0.36	7235	13.01
195042	5		5	W-F	1489	5615	0.13	-4126	0.27
555040	5		6	W-F	3391	4867	0.48	-1476	0.70
195046	5		13	W-F	1604	5544	0.09	-3939	0.29
95001	5		15	W-F	2856	6974	0.43	-4118	0.41
105004	5		15	W-F	3627	9773	0.27	-6145	0.37
285006	5		17	W-N-F	1813	1741	0.19	73	1.04
485026	5		19	W-N-F	4178	325	0.05	3854	12.88
483719	5		21	W-N-F	2309	8374	0.42	-6065	0.28
485035	5		21	W-N-F	1747	7941	0.18	-6194	0.22
375037	5		22	W-N-F	1298	6114	0.14	-4816	0.21
455017	5		23	W-N-F	3522	3847	0.29	-325	0.92
485024	5		23	W-N-F	21968	1148	0.68	20821	19.14
285803	5		25	W-N-F	1382	3330	0.14	-1948	0.42
485154	5		29	W-N-F	1477	8010	0.08	-6534	0.18
415022	5		32	W-N-F	32875	10770	0.23	22106	3.05
465025	5		33	D-F	1733	553	0.18	1180	3.13
165025	5		41	D-F	2885	13583	0.40	-10699	0.21
417081	5		48	D-F	14374	899	0.59	13475	15.98
485287	5		49	D-N-F	1940	3050	0.19	-1111	0.64
485301	5		51	D-N-F	7549	1413	0.30	6136	5.34
485336	5		51	D-N-F	4662	1092	0.48	3571	4.27
67455	5		53	D-N-F	1803	7509	0.01	-5706	0.24
485328	5		53	D-N-F	1383	6458	0.13	-5074	0.21
485310	5		55	D-N-F	22026	1269	0.44	20757	17.36
485323	5		55	D-N-F	2458	5234	0.31	-2776	0.47
485335	5		55	D-N-F	5711	5319	0.44	391	1.07

Evaluation of AASHTO rigid pavement design equation - Actual vs. Predicted ESALs (1960 AASHTO)									
		new			calculated	estimated	psi		
st_shrp	exp#	exp#	cell	region	KESALs	KESALs	loss	diff	ratio
485274	5		57	D-N-F	4583	4438	0.83	145	1.03
485317	5		57	D-N-F	2469	3196	0.45	-727	0.77
485284	5		59	D-N-F	19139	452	0.52	18687	42.38

Appendix C

Sections and Corresponding Data Utilized in Evaluation of the AASHTO Overlay Design Procedures

Evaluation of AASHTO Overlay Design Procedure

AC Overlay of AC Pavement

General Information

Section ID Alabama	16012
Pavement Functional Classification	Interstate
Date of Overlay	1984
Total Pavement Thickness (in)	15.1
Original AC Layer Thickness (in)	9.16
Overlay AC Layer Thickness(in)	1.1

Future Structural Capacity

Traffic	
ESAL 5 years	4965000
ESAL 10 years	10656747
ESAL 15 years	18273589
ESAL 20 years	28466641
Initial Serviceability	4.2
Terminal Serviceability	2.5
Overall Standard Deviation	0.49
Subgrade Resilient Modulus (psi)	7381

Existing Structural Capacity

Effective Pavement Modulus (psi)	106471
Existing SN with Overlay	3.21
Existing SN without Overlay	2.73

Overlay SN Design Matrix

Reliability	Design Period (years) 5	10	15	20
50%	0.93 (2.11)+	1.4 (3.18)	1.75 (3.98)	2.06 (4.68)
90%	1.85 (4.20)	2.39 (5.43)	2.78 (6.32)	3.12 (7.09)
95%	2.13 (4.84)	2.69 (6.11)	3.1 (7.05)	3.45 (7.84)
99%	2.69 (6.11)	3.28 (7.45)	3.72 (8.45)	4.09 (9.30)

+ Corresponding thickness

Overlay Structural Capacity

Overlay structural coefficient	0.44
Existing Overlay SN	0.48

Overlay Serviceability

Mean IRI (in/mile)	103.31
Date of IRI measurement	1992
Age of Overlay (years)	8
PSR	3.27

Overlay Condition

Date	1989
Age of Overlay (years)	7

Distress	H	M	L
Alligator Cracking (sq. ft)	0	0	0
Block Cracking (sq. ft)	0	0	0
Longitudinal Cracking (ft)	0	0	322
Transverse Cracking (no)	0	3	26
Patches (no)	0	0	0
Potholes (no)	0	0	0

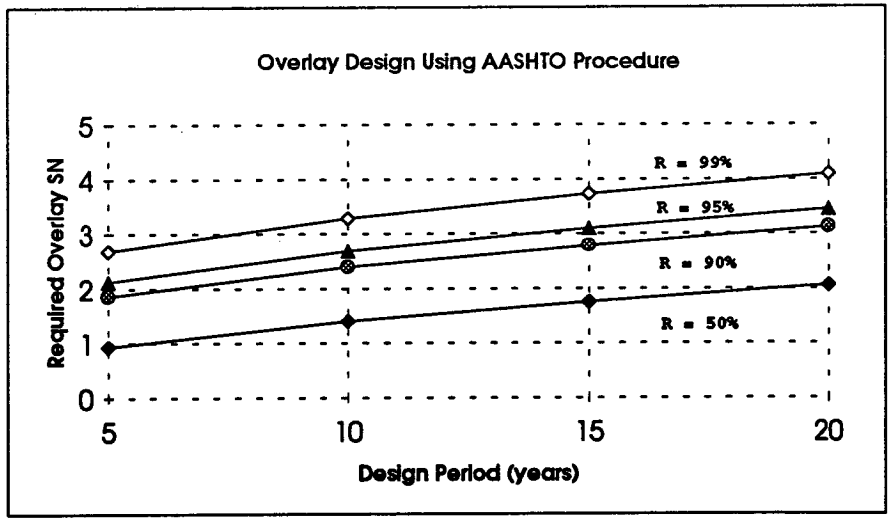

Evaluation of AASHTO Overlay Design Procedure

AC Overlay of AC Pavement

General Information

Section ID Alabama	16109
Pavement Functional Classification	Interstate
Date of Overlay	1981
Total Pavement Thickness (in)	17.2
Original AC Layer Thickness (in)	8.04
Overlay AC Layer Thickness(in)	4

Future Structural Capacity

Traffic	
ESAL 5 years	1636493
ESAL 10 years	3512526
ESAL 15 years	6023082
ESAL 20 years	9382771
Initial Serviceability	4.2
Terminal Serviceability	2.5
Overall Standard Deviation	0.49
Subgrade Resilient Modulus (psi)	8799

Existing Structural Capacity

Effective Pavement Modulus (psi)	116515
Existing SN with Overlay	3.77
Existing SN without Overlay	2.1

Overlay SN Design Matrix

Reliability	Design Period (years) 5	10	15	20
50%	0.75 (1.70)+	1.13 (2.57)	1.43 (3.25)	1.69 (3.84)
90%	1.51 (3.43)	1.98 (4.50)	2.34 (5.32)	2.64 (6.00)
95%	1.76 (4.00)	2.25 (5.11)	2.61 (5.93)	2.93 (6.66)
99%	2.25 (5.11)	2.77 (6.30)	3.16 (7.18)	3.49 (7.93)

+ Corresponding thickness

Overlay Structural Capacity

Overlay structural coefficient	0.44
Existing Overlay SN	1.76

Overlay Serviceability

Mean IRI (in/mile)	49.85
Date of IRI measurement	1992
Age of Overlay (years)	11
PSR	4.08

Overlay Condition

Date	1989		
Age of Overlay (years)	8		
Distress	H	M	L
Alligator Cracking (sq. ft)	0	0	0
Block Cracking (sq. ft)	0	0	0
Longitudinal Cracking (ft)	0	0	0
Transverse Cracking (no)	0	0	0
Patches (no)	0	0	0
Potholes (no)	0	0	0

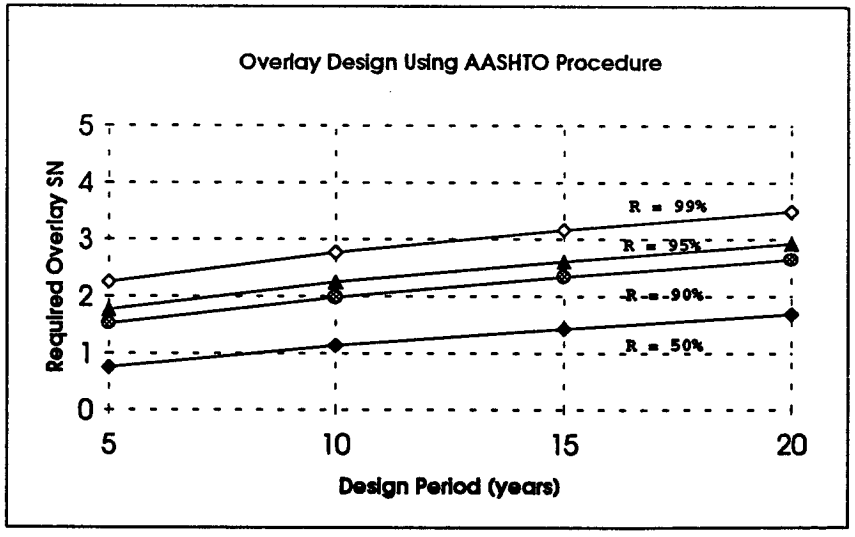

Evaluation of AASHTO Overlay Design Procedure

AC Overlay of AC Pavement

General Information

Section ID	New Mexico	351002
Pavement Functional Classification		Principal Arterial
Date of Overlay		1985
Total Pavement Thickness (in)		14.1
Original AC Layer Thickness (in)		4.42
Overlay AC Layer Thickness(in)		3.5

Future Structural Capacity

Traffic	
ESAL 5 years	172206
ESAL 10 years	369618
ESAL 15 years	633800
ESAL 20 years	987336
Initial Serviceability	4.2
Terminal Serviceability	2.5
Overall Standard Deviation	0.49
Subgrade Resilient Modulus (psi)	8319

Existing Structural Capacity

Effective Pavement Modulus (psi)	194964
Existing SN with Overlay	3.66
Existing SN without Overlay	2.12

Overlay SN Design Matrix

Reliability	Design Period (years) 5	10	15	20
50%	0 (0.00)+	0.14 (0.32)	0.36 (0.82)	0.55 (1.25)
90%	0.42 (0.95)	0.76 (1.73)	1.03 (2.34)	1.27 (2.89)
95%	0.59 (1.34)	0.96 (2.18)	1.25 (2.84)	1.5 (3.41)
99%	0.96 (2.18)	1.38 (3.14)	1.7 (3.86)	1.97 (4.48)

+ Corresponding thickness

Overlay Structural Capacity

Overlay structural coefficient	0.44
Existing Overlay SN	1.54

Overlay Serviceability

Mean IRI (in/mile)	52.26
Date of IRI measurement	1991
Age of Overlay (years)	6
PSR	4.04

Overlay Condition

Date	1989		
Age of Overlay (years)	4		
Distress	H	M	L
Alligator Cracking (sq. ft)	0	0	0
Block Cracking (sq. ft)	0	0	0
Longitudinal Cracking (ft)	0	0	0
Transverse Cracking (no)	0	0	0
Patches (no)	0	0	0
Potholes (no)	0	0	0

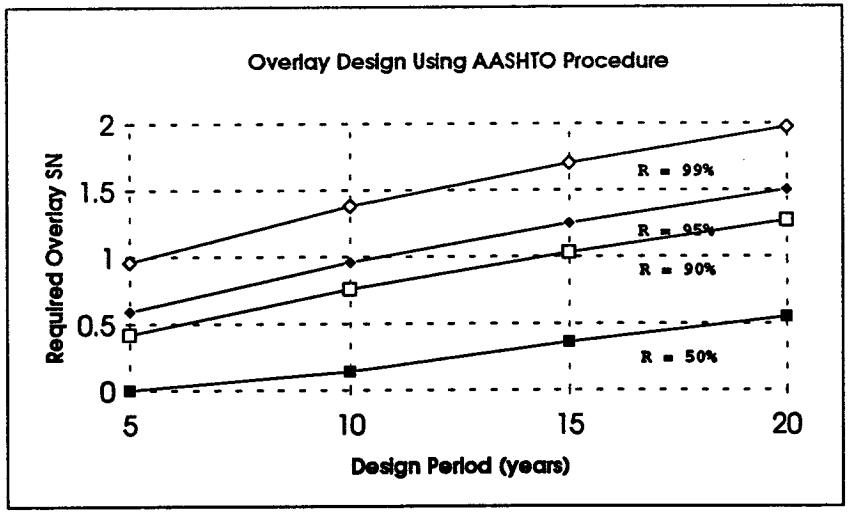

Evaluation of AASHTO Overlay Design Procedure

AC Overlay of AC Pavement

General Information

Section ID	New Mexico	356033
Pavement Functional Classification		Interstate
Date of Overlay		1981
Total Pavement Thickness (in)		19.9
Original AC Layer Thickness (in)		3.71
Overlay AC Layer Thickness(in)		3

Future Structural Capacity

Traffic	
ESAL 5 years	541959
ESAL 10 years	1163246
ESAL 15 years	1994669
ESAL 20 years	3107300
Initial Serviceability	4.2
Terminal Serviceability	2.5
Overall Standard Deviation	0.49
Subgrade Resilient Modulus (psi)	9833

Existing Structural Capacity

Effective Pavement Modulus (psi)	132606
Existing SN with Overlay	4.55
Existing SN without Overlay	3.23

Overlay SN Design Matrix

Reliability	Design Period (years) 5	10	15	20
50%	0 (0.00)+	0 (0.00)	0 (0.00)	0 (0.00)
90%	0 (0.00)	0.05 (0.11)	0.35 (0.80)	0.61 (1.39)
95%	0 (0.00)	0.27 (0.61)	0.59 (1.34)	0.87 (1.98)
99%	0.28 (0.64)	0.74 (1.68)	1.08 (2.45)	1.38 (3.14)

+ Corresponding thickness

Overlay Structural Capacity

Overlay structural coefficient	0.44
Existing Overlay SN	1.32

Overlay Serviceability

Mean IRI (in/mile)	83.02
Date of IRI measurement	1991
Age of Overlay (years)	10
PSR	3.56

Overlay Condition

Date	1989		
Age of Overlay (years)	8		
Distress	H	M	L
Alligator Cracking (sq. ft)	0	0	0
Block Cracking (sq. ft)	0	0	0
Longitudinal Cracking (ft)	0	0	304
Transverse Cracking (no)	0	0	16
Patches (no)	0	0	0
Potholes (no)	0	0	0

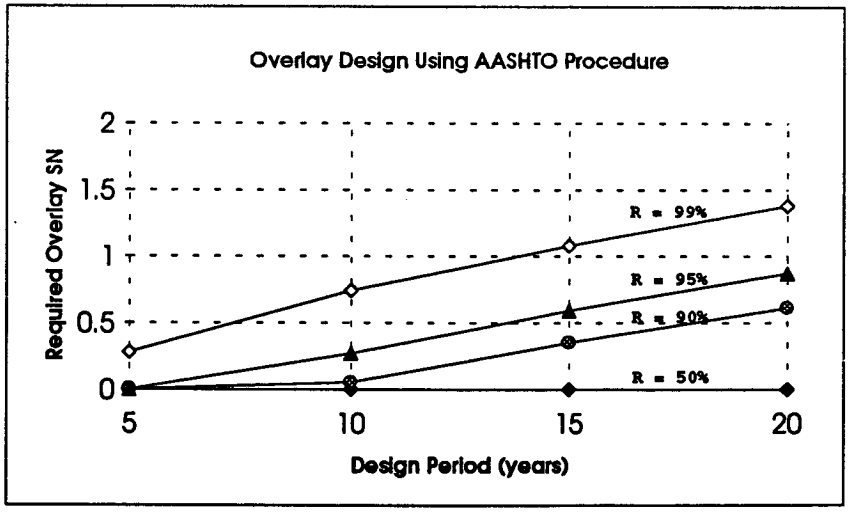

Evaluation of AASHTO Overlay Design Procedure

AC Overlay of AC Pavement

General Information

Section ID	New Mexico	356401
Pavement Functional Classification		Interstate
Date of Overlay		1984
Total Pavement Thickness (in)		19.2
Original AC Layer Thickness (in)		4.75
Overlay AC Layer Thickr		3.5

Future Structural Capacity

Traffic	
ESAL 5 years	2041704
ESAL 10 years	4382261
ESAL 15 years	7514453
ESAL 20 years	11706033
Initial Serviceability	4.2
Terminal Serviceability	2.5
Overall Standard Deviation	0.49
Subgrade Resilient Modulus (psi)	5745

Existing Structural Capacity

Effective Pavement Modulus (psi)	97735
Existing SN with Overlay	3.96
Existing SN without Overlay	2.32

Overlay SN Design Matrix

Reliability	Design Period (years) 5	10	15	20
50%	1.16 (2.64)+	1.61 (3.66)	1.96 (4.45)	2.26 (5.14)
90%	1.86 (4.23)	2.37 (5.39)	2.75 (6.25)	3.07 (6.98)
95%	2.07 (4.70)	2.6 (5.91)	2.99 (6.80)	3.32 (7.55)
99%	2.49 (5.66)	3.04 (6.91)	3.45 (7.84)	3.8 (8.64)

+ Corresponding thickness

Overlay Structural Capacity

Overlay structural coefficient	0.44
Existing Overlay SN	1.54

Overlay Serviceability

Mean IRI (in/mile)	46.03
Date of IRI measurement	1991
Age of Overlay (years)	7
PSR	4.14

Overlay Condition

Date	1989		
Age of Overlay (years)	5		
Distress	H	M	L
Alligator Cracking (sq. ft)	0	0	0
Block Cracking (sq. ft)	0	0	0
Longitudinal Cracking (ft)	0	0	53.9
Transverse Cracking (no)	0	0	9
Patches (no)	0	0	0
Potholes (no)	0	0	0

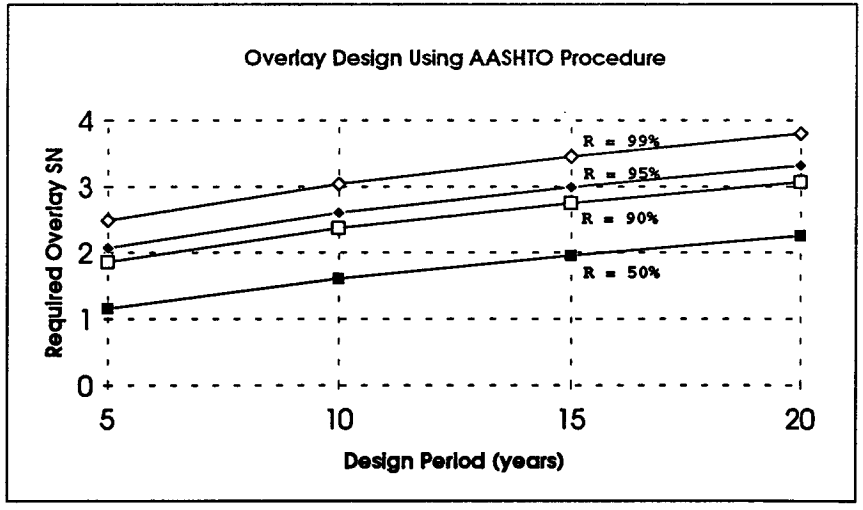

Evaluation of AASHTO Overlay Design Procedure

AC Overlay of AC Pavement

General Information

Section ID Texas	486086
Pavement Functional Classification	Interstate
Date of Overlay	1985
Total Pavement Thickness (in)	28.5
Original AC Layer Thickness (in)	8.65
Overlay AC Layer Thickness(in)	1.5

Future Structural Capacity

Traffic	
ESAL 5 years	1409395
ESAL 10 years	3025088
ESAL 15 years	2187250
ESAL 20 years	8080710
Initial Serviceability	4.2
Terminal Serviceability	2.5
Overall Standard Deviation	0.49
Subgrade Resilient Modulus (psi)	11149

Existing Structural Capacity

Effective Pavement Modulus (psi)	125920
Existing SN with Overlay	6.4
Existing SN without Overlay	5.74

Overlay SN Design Matrix

Reliability	Design Period (years) 5	10	15	20
50%	0 (0)+	0 (0)	0 (0)	0 (0)
90%	0 (0)	0 (0)	0 (0)	0 (0)
95%	0 (0)	0 (0)	0 (0)	0 (0)
95%	0 (0)	0 (0)	0 (0)	0 (0)

+ Corresponding thickness

Overlay Structural Capacity

Overlay structural coefficient	0.44
Existing Overlay SN	0.66

Overlay Serviceability

Mean IRI (in/mile)	46.48
Date of IRI measurement	1991
Age of Overlay (years)	6
PSR	4.13

Overlay Condition

Date	1991		
Age of Overlay (years)	5		
Distress	H	M	L
Alligator Cracking (sq. ft)	0	0	0
Block Cracking (sq. ft)	0	0	0
Longitudinal Cracking (ft)	0	0	134
Transverse Cracking (no)	0	0	0
Patches (no)	0	0	0
Potholes (no)	0	0	0

Evaluation of AASHTO Overlay Design Procedure

AC Overlay of AC Pavement

General Information

Section ID Texas	486079
Pavement Functional Classification	Interstate
Date of Overlay	1985
Total Pavement Thickness (in)	17
Original AC Layer Thickness (in)	7.72
Overlay AC Layer Thickness(in)	2.5

Future Structural Capacity

Traffic	
ESAL 5 years	2437671
ESAL 10 years	5232154
ESAL 15 years	8971802
ESAL 20 years	13976295
Initial Serviceability	4.2
Terminal Serviceability	2.5
Overall Standard Deviation	0.49
Subgrade Resilient Modulus (psi)	4706

Existing Structural Capacity

Effective Pavement Modulus (psi)	310981
Existing SN with Overlay	5.16
Existing SN without Overlay	4.06

Overlay SN Design Matrix

Reliability	Design Period (years) 5	10	15	20
50%	0 (0.00)+	0.29 (0.66)	0.65 (1.48)	0.96 (2.18)
90%	0.75 (1.70)	1.3 (2.95)	1.71 (3.89)	2.06 (4.68)
95%	1.04 (2.36)	1.61 (3.66)	2.03 (4.61)	2.39 (5.43)
99%	1.61 (3.66)	2.22 (5.05)	2.67 (6.07)	3.06 (6.95)

+ Corresponding thickness

Overlay Structural Capacity

Overlay structural coefficient	0.44
Existing Overlay SN	1.1

Overlay Serviceability

Mean IRI (in/mile)	164.26
Date of IRI measurement	1991
Age of Overlay (years)	6
PSR	2.55

Overlay Condition

Date	1990		
Age of Overlay (years)	5		
Distress	H	M	L
Alligator Cracking (sq. ft)	0	0	0
Block Cracking (sq. ft)	0	0	0
Longitudinal Cracking (ft)	0	173	353
Transverse Cracking (no)	6	13	9
Patches (no)	0	0	0
Potholes (no)	0	0	0

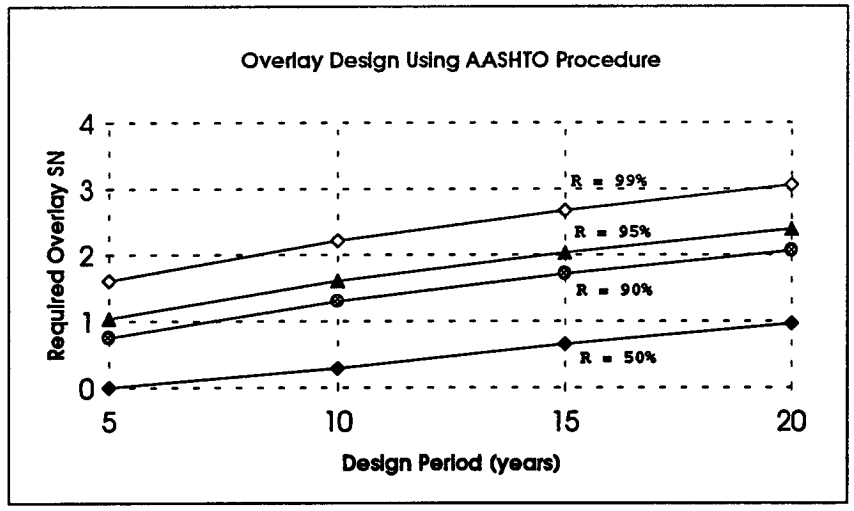

Evaluation of AASHTO Overlay Design Procedure

AC Overlay of AC Pavement

General Information

Section ID Texas	486160
Pavement Functional Classification	Principal Arterial
Date of Overlay	1981
Total Pavement Thickness (in)	16.7
Original AC Layer Thickness (in)	2.58
Overlay AC Layer Thickness(in)	1.5

Future Structural Capacity

Traffic	
ESAL 5 years	786682
ESAL 10 years	1688514
ESAL 15 years	2895369
ESAL 20 years	4510412
Initial Serviceability	4.2
Terminal Serviceability	2.5
Overall Standard Deviation	0.49
Subgrade Resilient Modulus (psi)	4702

Existing Structural Capacity

Effective Pavement Modulus (psi)	39667
Existing SN with Overlay	2.55
Existing SN without Overlay	1.89

Overlay SN Design Matrix

Reliability	Design Period (years) 5	10	15	20
50%	1.32 (3.00)+	1.75 (3.98)	2.07 (4.70)	2.36 (5.36)
90%	2.16 (4.91)	2.67 (6.07)	3.04 (6.91)	3.36 (7.64)
95%	2.43 (5.52)	2.95 (6.70)	3.34 (7.59)	3.67 (8.34)
99%	2.95 (6.70)	3.51 (7.98)	3.92 (8.91)	4.27 (9.70)

+ Corresponding thickness

Overlay Structural Capacity

Overlay structural coefficient	0.44
Existing Overlay SN	0.66

Overlay Serviceability

Mean IRI (in/mile)	119.93
Date of IRI measurement	1991
Age of Overlay (years)	10
PSR	3.06

Overlay Condition

Date	1989		
Age of Overlay (years)	8		
Distress	H	M	L
Alligator Cracking (sq. ft)	0	0	538
Block Cracking (sq. ft)	0	0	0
Longitudinal Cracking (ft)	0	13	299
Transverse Cracking (no)	0	3	55
Patches (no)	0	0	0
Potholes (no)	0	0	0
Bleeding (sq. ft)	0	0	876

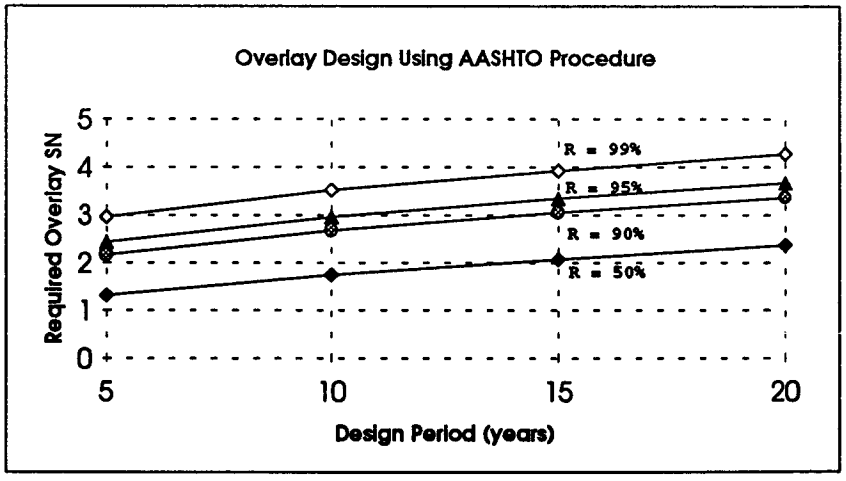

Evaluation of AASHTO Overlay Design Procedure

AC Overlay of AC Pavement

General Information

Section ID Texas	486179
Pavement Functional Classification	Principal Arterial
Date of Overlay	1975
Total Pavement Thickness (in)	19.1
Original AC Layer Thickness (in)	0.89
Overlay AC Layer Thickness(in)	5

Future Structural Capacity

Traffic	
ESAL 5 years	334142
ESAL 10 years	717194
ESAL 15 years	1229803
ESAL 20 years	1915791
Initial Serviceability	4.2
Terminal Serviceability	2.5
Overall Standard Deviation	0.49
Subgrade Resilient Modulus (psi)	10457

Existing Structural Capacity

Effective Pavement Modulus (psi)	149476
Existing SN with Overlay	4.54
Existing SN without Overlay	2.34

Overlay SN Design Matrix

Reliability	Design Period (years) 5	10	15	20
50%	0 (0.00)+	0 (0.00)	0.2 (0.45)	0.39 (0.89)
90%	0.26 (0.59)	0.61 (1.39)	0.89 (2.02)	1.13 (2.57)
95%	0.44 (1.00)	0.82 (1.86)	1.11 (2.52)	1.37 (3.11)
99%	0.82 (1.86)	1.25 (2.84)	1.57 (3.57)	1.85 (4.20)

+ Corresponding thickness

Overlay Structural Capacity

Overlay structural coefficient	0.44
Existing Overlay SN	2.2

Overlay Serviceability

Mean IRI (in/mile)	66.28
Date of IRI measurement	1991
Age of Overlay (years)	16
PSR	3.81

Overlay Condition

Date	1990		
Age of Overlay (years)	15		
Distress	H	M	L
Alligator Cracking (sq. ft)	0	0	0
Block Cracking (sq. ft)	0	0	0
Longitudinal Cracking (ft)	0	0	80
Transverse Cracking (no)	0	0	5
Patches (no)	0	0	0
Potholes (no)	0	0	0

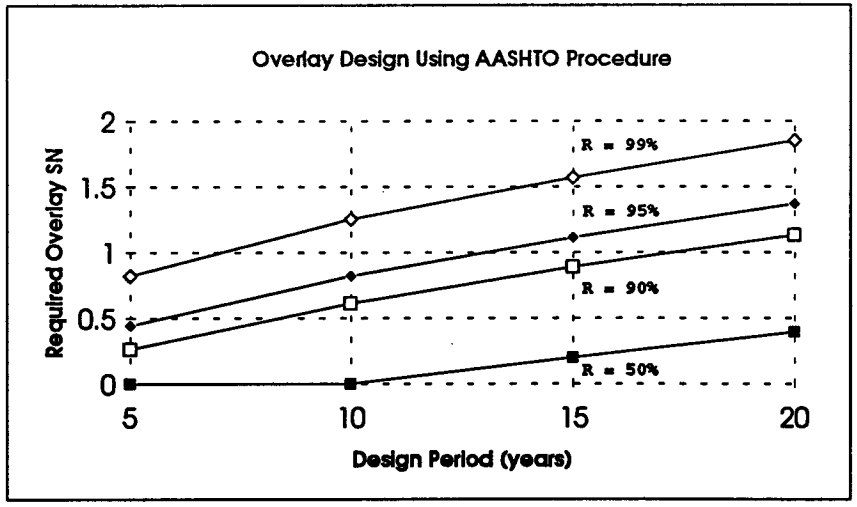

Evaluation of AASHTO Overlay Design Procedure

AC Overlay of PCC Pavement

General Information

Section ID	Colorado	87035
Pavement Functional Classification		Rural Interstate
Date of Overlay		1984
Original PCC Layer Thickness (in)		8.42

Future Structural Capacity

Traffic	
ESAL 5 years	3024000
ESAL 10 years	6490635
ESAL 15 years	11129775
ESAL 20 years	17337990
Initial Serviceability	4.5
Terminal Serviceability	2.5
Overall Standard Deviation	0.39
Load Transfer Coefficient	4.1
Drainage Coefficient	0.825
28-day PCC Resilient Modulus (psi)	531
PCC Elastic Modulus (psi)	3750000
Static k-value (pci)	132.5

Existing Structural Capacity

Fat (range 1.0 - 0.9)	0.95
Fjc (range 1.0 - 0.56)	0.78

Overlay Thickness Design Matrix

Reliability	Fdur	Design Period (years) 5	10	15	20
50%	1.00	6.72	8.53	9.93	11.71
	0.90	7.64	9.44	10.85	12.14
	0.80	8.53	10.34	11.8	13.15
90%	1.00	9.52	11.69	13.51	15.31
	0.90	10.44	12.69	14.63	16.58
	0.80	11.37	13.74	15.82	17.94
95%	1.00	10.41	12.76	14.8	16.86
	0.90	11.35	13.82	16.03	18.26
	0.80	12.32	14.95	17.33	19.77
99%	1.00	12.24	15.12	17.76	20.5
	0.90	13.27	16.37	19.24	22.54
	0.80	14.36	17.71	20.84	24.1

Overlay Structural Capacity

Existing Overlay AC Thickness (in)	4.83

Overlay Serviceability

Mean IRI (in/mile)	N.A.
Date of IRI measurement	
Age of Overlay (years)	
PSR	

Overlay Condition

Date	1990		
Age of Overlay (years)	6		
Distress	**H**	**M**	**L**
Longitudinal Cracking (ft)	0	0	0
Transverse Cracking (no)	0	0	2
Long. Reflect Cracking (ft)	0	12.83	300.27
Tran. Reflect Cracking (no)	0	5	3
Patches (no)	0	0	0
Potholes (no)	0	0	0

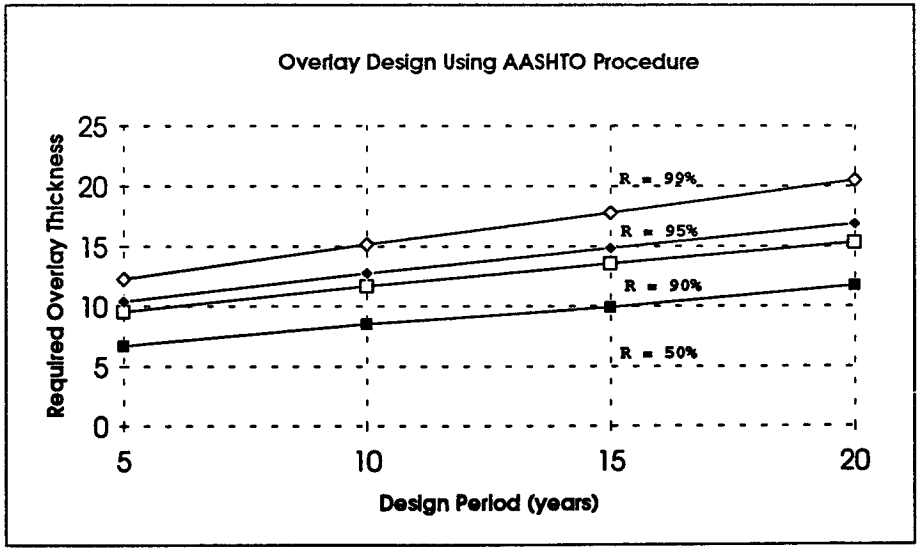

Evaluation of AASHTO Overlay Design Procedure

AC Overlay of PCC Pavement

General Information

Section ID	Illinois	175453
Pavement Functional Classification		Rural Interstate
Date of Overlay		1984
Original PCC Layer Thickness (in)		8.25

Future Structural Capacity

Traffic	
ESAL 5 years	8858000
ESAL 10 years	19012581
ESAL 15 years	32601720
ESAL 20 years	50787010
Initial Serviceability	4.5
Terminal Serviceability	2.5
Overall Standard Deviation	0.39
Load Transfer Coefficient	3.05
Drainage Coefficient	0.9
28-day PCC Resilient Modulus (psi)	695
PCC Elastic Modulus (psi)	5125000
Static k-value (pci)	115

Existing Structural Capacity

Fat (range 1.0 - 0.9)	0.95
Fjc (range 1.0 - 0.56)	0.78

Overlay Thickness Design Matrix

Reliability	Fdur	Design Period (years) 5	10	15	20
50%	1.00	4.57	6.3	7.53	8.58
	0.90	5.56	7.2	8.4	9.45
	0.80	6.49	8.09	9.28	10.34
90%	1.00	7.18	8.98	10.38	11.64
	0.90	8	8.85	11.29	12.61
	0.80	8.93	10.75	12.24	13.63
95%	1.00	7.93	9.81	11.29	12.67
	0.90	8.81	10.7	12.24	13.7
	0.80	9.68	11.63	13.24	14.8
99%	1.00	9.42	11.5	13.26	14.97
	0.90	10.31	12.46	14.32	16.17
	0.80	11.21	13.48	15.47	17.47

Overlay Structural Capacity

Existing Overlay AC Thickness (in)	2.71

Overlay Serviceability

Mean IRI (in/mile)	N.A.
Date of IRI measurement	
Age of Overlay (years)	
PSR	

Overlay Condition

Date	1989		
Age of Overlay (years)	5		
Distress	H	M	L
Longitudinal Cracking (ft)	0	0	20
Transverse Cracking (no)	0	0	0
Long. Reflect Cracking (ft)	0	0	912
Tran. Reflect Cracking (no)	0	0	0
Patches (no)	0	0	0
Potholes (no)	0	0	1

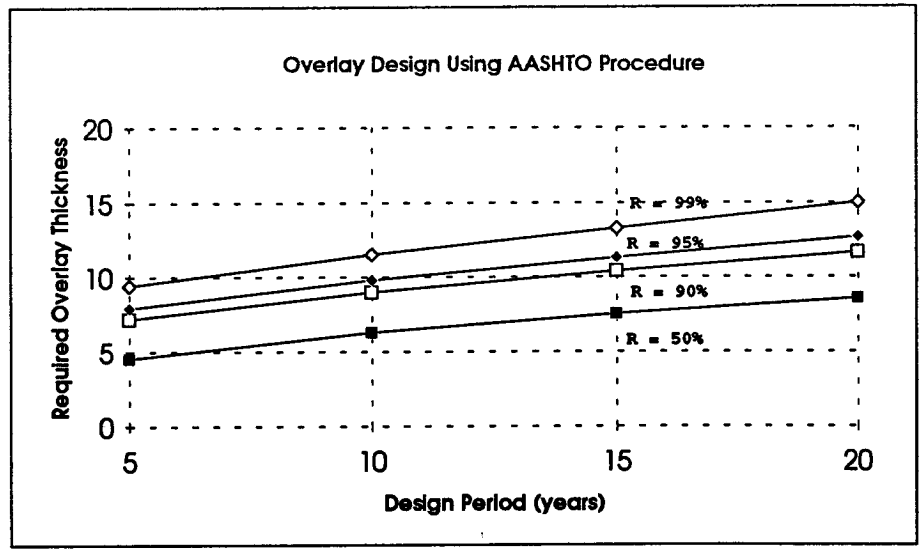

Evaluation of AASHTO Overlay Design Procedure

AC Overlay of PCC Pavement

General Information

Section ID	Mississippi	283097
Pavement Functional Classification		Rural Interstate
Date of Overlay		1984
Original PCC Layer Thickness (in)		8.32

Future Structural Capacity

Traffic	
ESAL 5 years	1076296
ESAL 10 years	2310134
ESAL 15 years	3961287
ESAL 20 years	6170902
Initial Serviceability	4.5
Terminal Serviceability	2.5
Overall Standard Deviation	0.39
Load Transfer Coefficient	2.6
Drainage Coefficient	0.95
28-day PCC Resilient Modulus (psi)	859
PCC Elastic Modulus (psi)	4825000
Static k-value (pci)	242.5

Existing Structural Capacity

Fat (range 1.0 - 0.9)	0.95
Fjc (range 1.0 - 0.56)	0.78

Overlay Thickness Design Matrix

Reliability	Fdur	Design Period (years) 5	10	15	20
50%	1.00	0	0	0	0
	0.90	0	0	0	0.44
	0.80	0	0	0.67	1.73
90%	1.00	0	0	1.01	2.18
	0.90	0	0.87	2.23	3.31
	0.80	0.33	2.12	3.38	4.39
95%	1.00	0	0.44	1.88	3
	0.90	0	1.71	3.04	4.08
	0.80	1.1	2.89	4.14	5.11
99%	1.00	0.02	2.06	3.42	4.51
	0.90	1.32	3.21	4.47	5.49
	0.80	2.54	4.29	5.48	6.45

Overlay Structural Capacity

Existing Overlay AC Thickness (in)	2.73

Overlay Serviceability

Mean IRI (in/mile)	64.19
Date of IRI measurement	1992
Age of Overlay (years)	8
PSR	3.84

Overlay Condition

Date	1989		
Age of Overlay (years)	5		
Distress	H	M	L
Longitudinal Cracking (ft)	0	0	186
Transverse Cracking (no)	0	0	1
Long. Reflect Cracking (ft)	0	0	0
Tran. Reflect Cracking (no)	0	0	0
Patches (no)	0	0	0
Potholes (no)	0	0	0

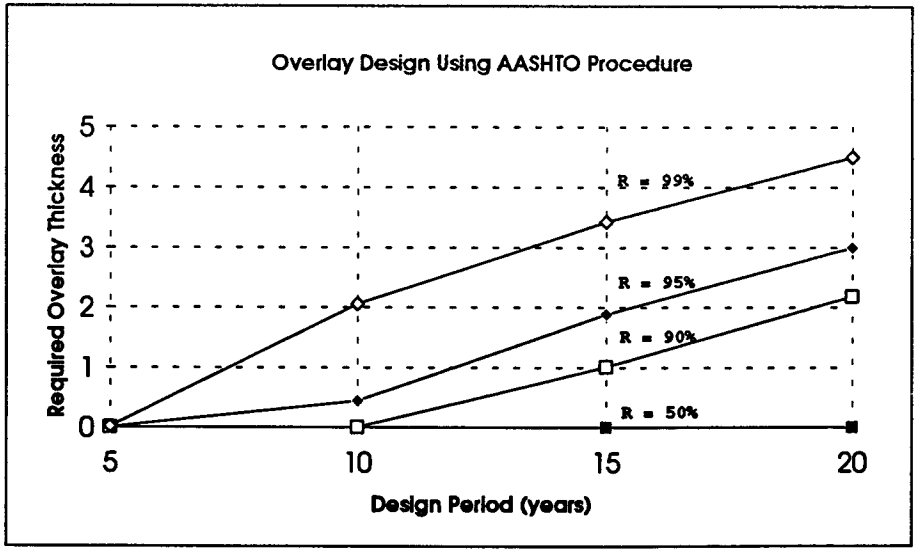

Evaluation of AASHTO Overlay Design Procedure

AC Overlay of PCC Pavement

General Information

Section ID	Mississippi	287012
Pavement Functional Classification		Rural Interstate
Date of Overlay		1985
Original PCC Layer Thickness (in)		9.43

Future Structural Capacity

Traffic	
ESAL 5 years	1630888
ESAL 10 years	3500497
ESAL 15 years	6002454
ESAL 20 years	9350638
Initial Serviceability	4.5
Terminal Serviceability	2.5
Overall Standard Deviation	0.39
Load Transfer Coefficient	3.2
Drainage Coefficient	0.95
28-day PCC Resilient Modulus (psi)	829
PCC Elastic Modulus (psi)	5100000
Static k-value (pci)	74

Existing Structural Capacity

Fat (range 1.0 - 0.9)	0.95
Fjc (range 1.0 - 0.56)	0.78

Overlay Thickness Design Matrix

Reliability	Fdur	Design Period (years) 5	10	15	20
50%	1.00	0	0	0.78	1.92
	0.90	0	0.91	2.2	3.24
	0.80	0.57	2.31	3.49	4.46
90%	1.00	0.4	2.35	3.67	4.74
	0.90	1.84	3.63	4.85	5.85
	0.80	3.17	4.82	5.96	6.91
95%	1.00	1.24	3.15	4.46	5.51
	0.90	2.62	4.37	5.59	6.58
	0.80	3.88	5.51	6.66	7.61
99%	1.00	2.78	4.64	5.91	6.97
	0.90	4.03	5.76	6.97	7.99
	0.80	5.19	6.82	7.99	8.99

Overlay Structural Capacity

Existing Overlay AC Thickness (in)	3.54

Overlay Serviceability

Mean IRI (in/mile)	95.41
Date of IRI measurement	1990
Age of Overlay (years)	6
PSR	3.38

Overlay Condition

Date	1989		
Age of Overlay (years)	4		
Distress	H	M	L
Longitudinal Cracking (ft)	0	0	0
Transverse Cracking (no)	0	0	0
Long. Reflect Cracking (ft)	0	0	0
Tran. Reflect Cracking (no)	2	5	11
Patches (sq. ft)	0	0	24
Potholes (no)	0	0	0

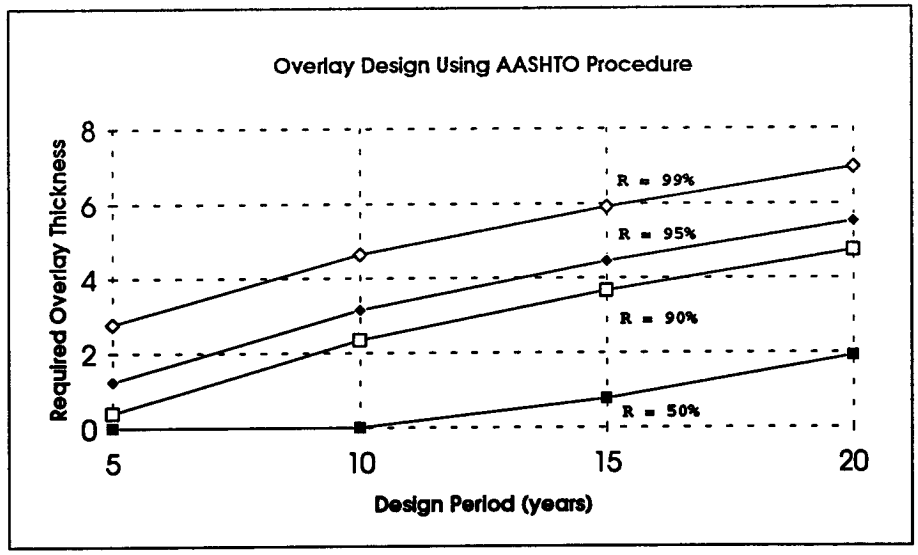

Evaluation of AASHTO Overlay Design Procedure

AC Overlay of PCC Pavement

General Information

Section ID	South Dakota	467049
Pavement Functional Classification		Rural Minor Arterial
Date of Overlay		1983
Original PCC Layer Thickness (in)		7.37

Future Structural Capacity

Traffic	
ESAL 5 years	61917
ESAL 10 years	132897
ESAL 15 years	227884
ESAL 20 years	354997
Initial Serviceability	4.5
Terminal Serviceability	2.5
Overall Standard Deviation	0.39
Load Transfer Coefficient	4.1
Drainage Coefficient	0.825
28-day PCC Resilient Modulus (psi)	756
PCC Elastic Modulus (psi)	5950000
Static k-value (pci)	95.5

Existing Structural Capacity

Fat (range 1.0 - 0.9)	0.95
Fjc (range 1.0 - 0.56)	0.78

Overlay Thickness Design Matrix

Reliability	Fdur	Design Period (years) 5	10	15	20
50%	1.00	0	0	0.04	1.03
	0.90	0	0.15	1.22	2.14
	0.80	0	1.32	2.31	3.17
90%	1.00	0	1.4	2.62	3.6
	0.90	0.91	2.48	3.62	4.54
	0.80	2.02	3.49	4.56	5.43
95%	1.00	0.44	2.41	3.35	4.3
	0.90	1.59	3.17	4.3	5.21
	0.80	2.65	4.14	5.21	6.07
99%	1.00	1.8	3.49	4.66	5.6
	0.90	2.86	4.44	5.54	6.45
	0.80	3.84	5.54	6.39	7.26

Overlay Structural Capacity

Existing Overlay AC Thickness (in)	4.49

Overlay Serviceability

Mean IRI (in/mile)	N/A
Date of IRI measurement	
Age of Overlay (years)	
PSR	

Overlay Condition

Date	1989		
Age of Overlay (years)	6		
Distress	H	M	L
Longitudinal Cracking (ft)	0	0	475
Transverse Cracking (no)	0	6	56
Long. Reflect Cracking (ft)	0	0	495
Tran. Reflect Cracking (no)	0	7	4
Patches (no)	0	0	0
Potholes (no)	0	0	0

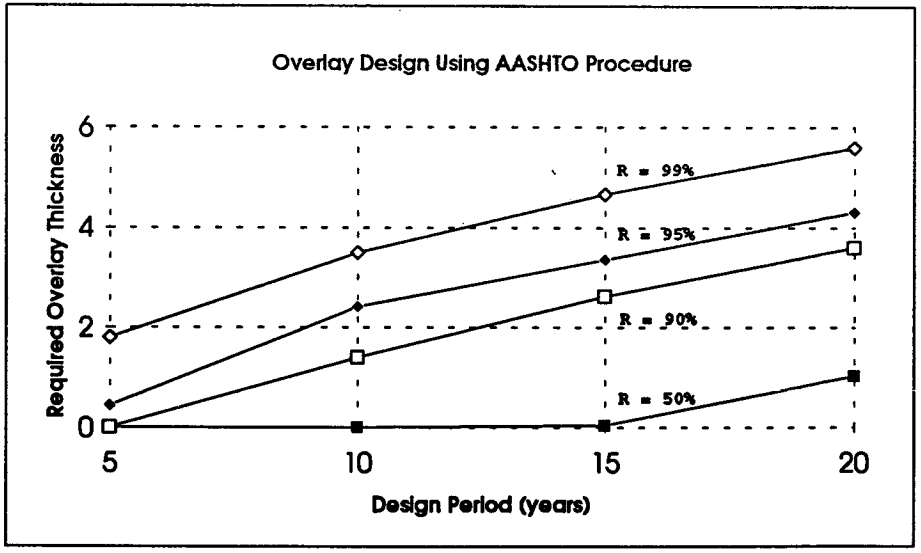

Evaluation of AASHTO Overlay Design Procedure

Unbonded PCC Overlay of PCC Pavement

General Information

Section ID	California	69049
Pavement Functional Classification		Urban Expressway
Date of Overlay		1986
Original PCC Layer Thickness (in)		7.67

Future Structural Capacity

Traffic	
ESAL 5 years	2504942
ESAL 10 years	5376544
ESAL 15 years	9219393
ESAL 20 years	14361994
Initial Serviceability	4.5
Terminal Serviceability	2.5
Overall Standard Deviation	0.39
Load Transfer Coefficient	4.1
Drainage Coefficient	1.125
28-day PCC Resilient Modulus (psi)	700
PCC Elastic Modulus (psi)	4250000
Static k-value (pci)	134.5

Existing Structural Capacity

Fjcu(range 1.0 - 0.9)

Overlay Structural Capacity

Existing Overlay PCC Thickness (in)	7.48

Overlay Serviceability

Mean IRI (in/mile)	N.A.
Date of IRI measurement	
Age of Overlay (years)	
PSR	

Overlay Condition

Date	1989		
Age of Overlay (years)	3		
Distress	H	M	L
Longitudinal Cracking (ft)	21	123	76
Transverse Cracking (no)	0	1	0
Long. Joint Spall (ft)	13	2	9
Tran. Joint Spall (no)	1	6	9
AC Patches (sq. ft)	0	26	21
PCC Patches (sq. ft)	0	0	0

Overlay Thickness Design Matrix

Reliability	Fjcu	Design Period (years) 5	10	15	20
50%	0.90	0	3.77	5.16	6.17
	0.95	0	3.04	4.65	5.75
	1.00	0	1.72	3.92	5.18
90%	0.90	4.78	6.54	7.72	8.69
	0.95	4.23	6.15	7.39	8.4
	1.00	3.4	5.61	6.96	8.02
95%	0.90	5.55	7.26	8.43	9.41
	0.95	5.08	6.91	8.13	9.14
	1.00	4.42	6.44	7.74	8.79
99%	0.90	6.93	8.59	9.78	10.79
	0.95	6.56	8.3	9.52	10.56
	1.00	6.06	7.91	9.19	10.26

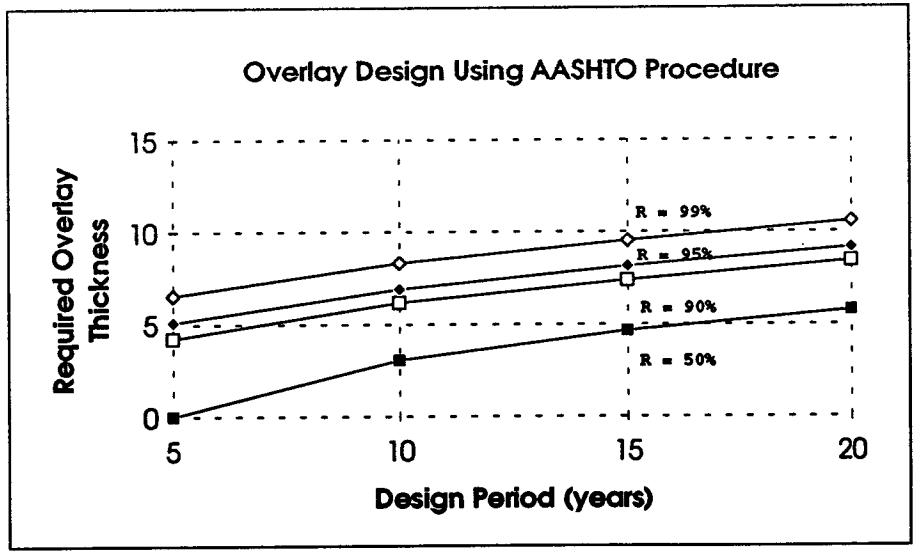

Evaluation of AASHTO Overlay Design Procedure

Unbonded PCC Overlay of PCC Pavement

General Information

Section ID	Colorado	89019
Pavement Functional Classification		Rural Interstate
Date of Overlay		1986
Original PCC Layer Thickness (in)		7.9

Future Structural Capacity

Traffic	
ESAL 5 years	4321019
ESAL 10 years	9274677
ESAL 15 years	15903693
ESAL 20 years	24774812
Initial Serviceability	4.5
Terminal Serviceability	2.5
Overall Standard Deviation	0.39
Load Transfer Coefficient	3.9
Drainage Coefficient	0.825
28-day PCC Resilient Modulus (psi)	530
PCC Elastic Modulus (psi)	4050000
Static k-value (pci)	137.5

Existing Structural Capacity

Fjcu(range 1.0 - 0.9)

Overlay Structural Capacity

Existing Overlay PCC Thickness (in) 9.02

Overlay Serviceability

Mean IRI (in/mile)	N.A.
Date of IRI measurement	
Age of Overlay (years)	
PSR	

Overlay Condition

Date	1989		
Age of Overlay (years)	3		
Distress	H	M	L
Longitudinal Cracking (ft)	0	0	0
Transverse Cracking (no)	0	0	0
Long. Joint Spall (ft)	0	0	0
Tran. Joint Spall (no)	0	0	16
AC Patches (sq. ft)	0	0	0
PCC Patches (sq. ft)	0	0	0

Overlay Thickness Design Matrix

Reliability	Fjcu	Design Period (years) 5	10	15	20
50%	0.90	4.84	7.1	8.54	9.69
	0.95	4.26	6.72	8.22	9.42
	1.00	3.4	6.21	7.81	9.06
90%	0.90	8.13	10.31	11.57	12.77
	0.95	7.8	9.87	11.34	12.57
	1.00	7.36	9.53	11.06	12.3
95%	0.90	8.99	11	12.45	13.69
	0.95	8.69	10.76	12.24	13.5
	1.00	8.3	10.45	11.97	13.25
99%	0.90	10.6	12.66	14.18	15.47
	0.95	10.34	12.45	13.99	15.3
	1.00	10.02	12.18	13.75	15.09

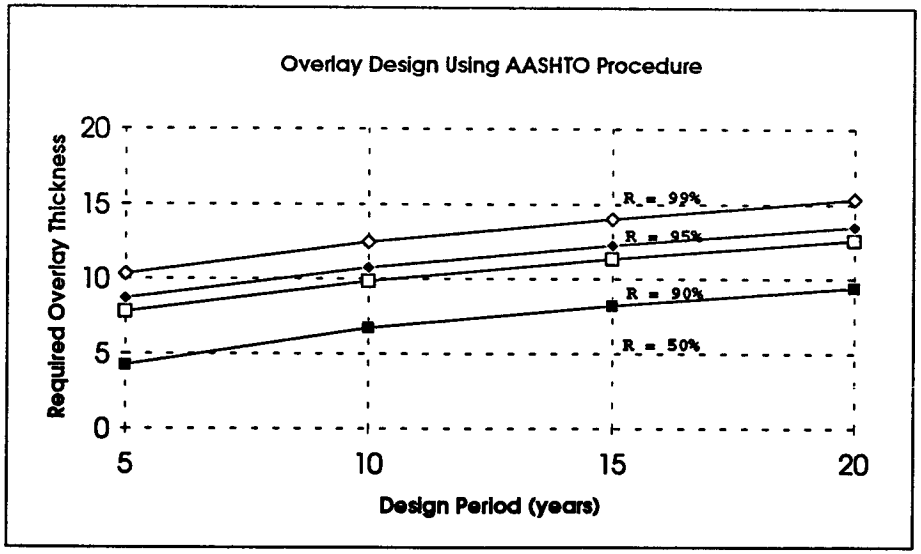

Evaluation of AASHTO Overlay Design Procedure

Unbonded PCC Overlay of PCC Pavement

General Information

Section ID	Colorado	89020
Pavement Functional Classification		Rural Interstate
Date of Overlay		1986
Original PCC Layer Thickness (in)		7.72

Future Structural Capacity

Traffic	
ESAL 5 years	4478946
ESAL 10 years	9613494
ESAL 15 years	16484677
ESAL 20 years	25679870
Initial Serviceability	4.5
Terminal Serviceability	2.5
Overall Standard Deviation	0.39
Load Transfer Coefficient	3.9
Drainage Coefficient	0.825
28-day PCC Resilient Modulus (psi)	511
PCC Elastic Modulus (psi)	4150000
Static k-value (pci)	340

Existing Structural Capacity

Fjcu(range 1.0 - 0.9)

Overlay Structural Capacity

Existing Overlay PCC Thickness (in) 8.02

Overlay Serviceability

Mean IRI (in/mile)	
Date of IRI measurement	
Age of Overlay (years)	
PSR	

Overlay Condition

Date	1989		
Age of Overlay (years)	3		
Distress	**H**	**M**	**L**
Longitudinal Cracking (ft)	0	0	0
Transverse Cracking (no)	0	1	0
Long. Joint Spall (ft)	0	0	7
Tran. Joint Spall (no)	0	0	0
AC Patches (sq. ft)	0	0	0
PCC Patches (sq. ft)	0	0	0

Overlay Thickness Design Matrix

Reliability	Fjcu	Design Period (years) 5	10	15	20
50%	0.90	7.11	8.89	10.17	11.24
	0.95	6.72	8.58	9.9	11
	1.00	6.19	8.17	9.55	10.68
90%	0.90	9.8	11.65	13.02	14.2
	0.95	9.52	11.42	12.82	14.01
	1.00	9.15	11.12	12.55	13.76
95%	0.90	10.58	12.47	13.89	15.09
	0.95	10.33	12.26	13.69	14.91
	1.00	9.99	11.97	13.44	14.68
99%	0.90	12.09	14.08	15.57	16.85
	0.95	11.87	13.89	15.4	16.69
	1.00	11.57	13.64	15.17	16.48

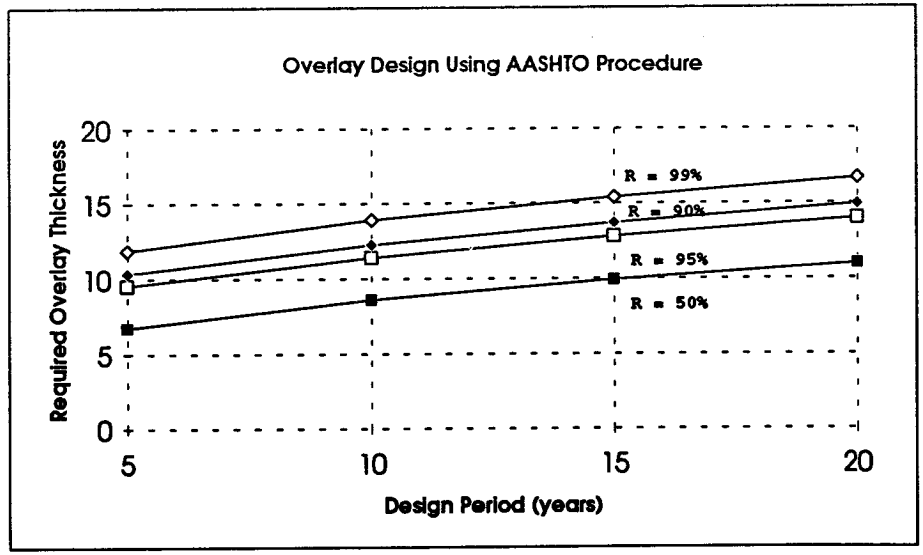

Evaluation of AASHTO Overlay Design Procedure

Unbonded PCC Overlay of PCC Pavement

General Information

Section ID	Michigan	269029
Pavement Functional Classification		Rural Interstate
Date of Overlay		1984
Original PCC Layer Thickness (in)		7.99

Future Structural Capacity

Traffic	
ESAL 5 years	3573000
ESAL 10 years	7668994
ESAL 15 years	13150359
ESAL 20 years	20485661
Initial Serviceability	4.5
Terminal Serviceability	2.5
Overall Standard Deviation	0.39
Load Transfer Coefficient	2.8
Drainage Coefficient	1.05
28-day PCC Resilient Modulus (psi)	595
PCC Elastic Modulus (psi)	4925000
Static k-value (pci)	204

Existing Structural Capacity

Fjcu(range 1.0 - 0.9)

Overlay Structural Capacity

Existing Overlay PCC Thickness (in)	7.29

Overlay Serviceability

Mean IRI (in/mile)	N.A.
Date of IRI measurement	
Age of Overlay (years)	
PSR	

Overlay Condition

Date	1989		
Age of Overlay (years)	5		
Distress	**H**	**M**	**L**
Longitudinal Cracking (ft)	0	0	0
Transverse Cracking (no)	0	0	0
Long. Joint Spall (ft)	0	0	1.3
Tran. Joint Spall (no)	0	0	0
AC Patches (sq. ft)	0	0	0
PCC Patches (sq. ft)	0	0	0

Overlay Thickness Design Matrix

Reliability	Fjcu	Design Period (years) 5	10	15	20
50%	0.90	0	2.61	4.3	5.45
	0.95	0	1.23	3.64	4.94
	1.00	0	0	2.53	4.19
90%	0.90	3.88	5.85	7.09	8.09
	0.95	3.12	5.38	6.71	7.75
	1.00	1.71	4.7	6.18	7.3
95%	0.90	4.77	6.6	7.83	8.82
	0.95	4.18	6.19	7.48	8.51
	1.00	3.26	5.61	7.01	8.1
99%	0.90	6.25	7.99	9.2	10.23
	0.95	5.82	7.65	8.91	9.96
	1.00	5.19	7.19	8.52	9.61

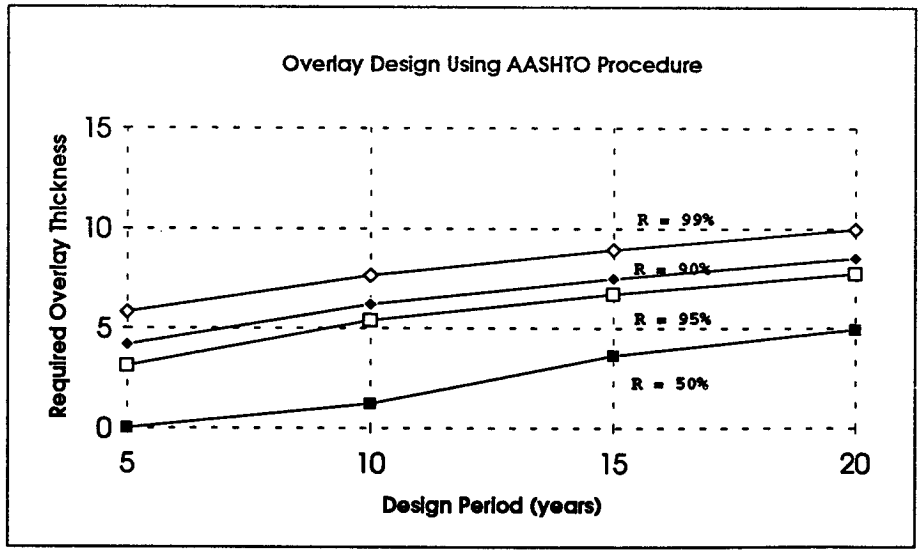

Evaluation of AASHTO Overlay Design Procedure

Unbonded PCC Overlay of PCC Pavement

General Information

Section ID	Michigan	269030
Pavement Functional Classification		Rural Principal Arterial
Date of Overlay		1984
Original PCC Layer Thickness (in)		9.03

Future Structural Capacity

Traffic	
ESAL 5 years	3617000
ESAL 10 years	7763435
ESAL 15 years	13312300
ESAL 20 years	20737934
Initial Serviceability	4.5
Terminal Serviceability	2.5
Overall Standard Deviation	0.39
Load Transfer Coefficient	2.8
Drainage Coefficient	1.05
28-day PCC Resilient Modulus (psi)	661
PCC Elastic Modulus (psi)	5400000
Static k-value (pci)	219

Existing Structural Capacity

Fjcu(range 1.0 - 0.9)

Overlay Structural Capacity

Existing Overlay PCC Thickness (in)	6.8

Overlay Serviceability

Mean IRI (in/mile)	N.A.
Date of IRI measurement	
Age of Overlay (years)	
PSR	

Overlay Condition

Date	1989		
Age of Overlay (years)	5		
Distress	H	M	L
Longitudinal Cracking (ft)	0	0	5.15
Transverse Cracking (no)	0	0	0
Long. Joint Spall (ft)	0	0	0
Tran. Joint Spall (no)	0	0	0
AC Patches (sq. ft)	0	0	3.09
PCC Patches (sq. ft)	0	0	0

Overlay Thickness Design Matrix

Reliability	Fjcu	Design Period (years) 5	10	15	20
50%	0.90	0	0	0	2.58
	0.95	0	0	0	0
	1.00	0	0	0	0
90%	0.90	0	3.29	5.05	6026
	0.95	0	2.04	4.34	5.7
	1.00	0	0	3.17	4.87
95%	0.90	0.57	4.41	5.94	7.11
	0.95	0	3.58	5.35	6.62
	1.00	0	2.01	4.46	5.92
99%	0.90	3.91	6.14	7.53	8.63
	0.95	2.93	5.57	7.07	8.24
	1.00	0	4.72	6.42	7.69

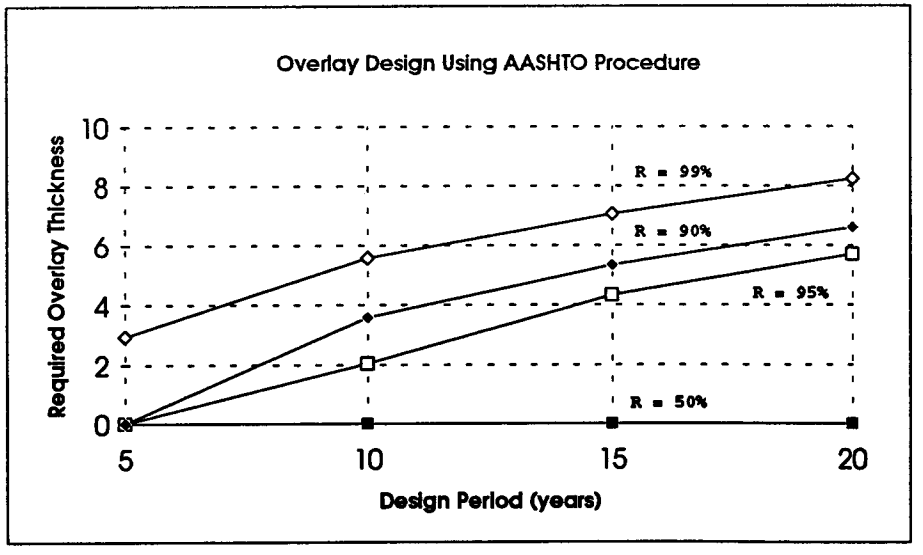

Evaluation of AASHTO Overlay Design Procedure

Unbonded PCC Overlay of PCC Pavement

General Information

Section ID	Texas	489167
Pavement Functional Classification		Rural Interstate
Date of Overlay		1988
Original PCC Layer Thickness (in)		8.3

Future Structural Capacity

Traffic	
ESAL 5 years	4662628
ESAL 10 years	10007744
ESAL 15 years	17160714
ESAL 20 years	2633002
Initial Serviceability	4.5
Terminal Serviceability	2.5
Overall Standard Deviation	0.39
Load Transfer Coefficient	2.8
Drainage Coefficient	0.95
28-day PCC Resilient Modulus (psi)	733
PCC Elastic Modulus (psi)	5200000
Static k-value (pci)	214

Existing Structural Capacity

Fjcu(range 1.0 - 0.9)

Overlay Structural Capacity

Existing Overlay PCC Thickness (in)	10.03

Overlay Serviceability

Mean IRI (in/mile)	116.11
Date of IRI measurement	1991
Age of Overlay (years)	3
PSR	3.11

Overlay Condition

Date	1989		
Age of Overlay (years)	1		
Distress	H	M	L
Longitudinal Cracking (ft)	0	0	0
Transverse Cracking (no)	0	0	0
Long. Joint Spall (ft)	0	0	19.86
Tran. Joint Spall (no)	0	0	11
AC Patches (sq. ft)	0	0	0
PCC Patches (sq. ft)	0	0	0

Overlay Thickness Design Matrix

Reliability	Fjcu	Design Period (years) 5	10	15	20
50%	0.90	0	0.77	3.48	4.78
	0.95	0	0	2.54	4.15
	1.00	0	0	0	3.13
90%	0.90	2.95	5.21	6.54	7.59
	0.95	1.74	4.64	6.09	7.21
	1.00	0	3.76	5.45	6.67
95%	0.90	4.01	6.03	7.32	8.35
	0.95	3.23	5.54	6.92	8
	1.00	1.74	4.82	6.37	7.52
99%	0.90	5.66	7.49	8.74	9.77
	0.95	5.13	7.1	8.41	9.48
	1.00	4.35	6.56	7.96	9.08